CLIMATE CHANGE AND ISLAND AND COASTAL VULNERABILITY

Springer

Edited by: J. Sundaresan • S. Sreekesh • AL. Ramanathan • L. Sonnenschein • R. Boojh

Climate Change and Island and Coastal Vulnerability

Climate Change and Island and Coastal Vulnerability

Edited by

J. Sundaresan

Council of Scientific and Industrial Research, Ministry of Science and Technology, Government of India New Delhi, India

S. Sreekesh

Centre for Study of Regional Development, School of Social Sciences, Jawaharlal Nehru University, New Delhi, India

AL. Ramanathan

School of Environmental Sciences Jawaharlal Nehru University, New Delhi, India

L. Sonnenschein

World Aquarium and Conservation for the Ocean Foundation, St. Louis, MO, USA

R. Boojh

Ecological and Earth Sciences, UNESCO, New Delhi, India

Springer

CP

A C.I.P. Catalogue record for this book is available from the Library of Congress.

ISBN 978-94-007-6015-8 (HB)
ISBN 978-94-007-6016-5 (e-book)

Copublished by Springer,
P.O. Box 17, 3300 AA Dordrecht, The Netherlands
with Capital Publishing Company, New Delhi, India.

Sold and distributed in North, Central and South America by Springer,
233 Spring Street, New York 10013, USA.

In all other countries, except SAARC countries—Afghanistan, Bangladesh, Bhutan, India, Maldives, Nepal, Pakistan and Sri Lanka—sold and distributed by Springer, Haberstrasse 7, D-69126 Heidelberg, Germany.

In SAARC countries—Afghanistan, Bangladesh, Bhutan, India, Maldives, Nepal, Pakistan and Sri Lanka—sold and distributed by Capital Publishing Company, 7/28, Mahaveer Street, Ansari Road, Daryaganj, New Delhi, 110 002, India.

www.springer.com

Cover photo credit: Lakshadweep Administration.

Printed on acid-free paper

Printed in India.

Foreword

In the 21st century, the coastal zone is increasingly becoming very significant due to growing world population living near coasts. They are continually changing because of the dynamic interaction between the oceans and the land. In recent years they get degraded by multiple stresses arising from local to global scale changes in water use, influx of sediments and pollutants, ecosystem degradation, river flooding, shoreline erosion, storms, tsunamis, relative sea level rise, aggregate extraction etc. The islands near coastal environs are fragile and highly vulnerable to some of the most devastating hydro meteorological and geological disasters. Islands experience long-term, more chronic vulnerabilities such as maintaining adequate water and energy supplies, preventing emigration which depletes the population and removes a needed skill base, maintaining self-sufficient economies, and preserving their culture.

Changing sea level and tropical cyclones in their destructive power can engulf entire island groups and cause devastation on a proportional scale on agricultural and occupational lands unknown in large and sub-continental countries. Climate change predictions show the shift in rainfall patterns causing prolonged droughts in severe allocations near coastal regions. The potential socio-economic impacts of climate change on the smaller island countries mainly due to sea level rise has shown negative impacts on tourism, freshwater availability and quality, aquaculture, agriculture, human settlements, financial services and human health. Storm surges are likely to have a harmful impact on low-lying islands. In this context more than 200 scientists and professionals from all over the globe came together for this International Conference on 28-31st October 2010 to discuss all aspects of climate change impact on coastal and island issues for making these regions more sustainable. Each of the paper in this book discusses the contemporary issue which needs urgent attention of the planners.

This book explicitly discusses the impact of climate change on coastal and island ecosystem which will affect all components of ecosystem in totality. The book captures the reality and the climate change issues daunting this sector's traditional ecosystem through the ecosystem management approach. This book brings out integrated articles covering the real time issues of this vast region involved with multifaceted ecosystem. This book is an asset to all academic and research libraries and will be of great benefit to researchers, policymakers and administrators.

(Prof. K.V. Thomas)
Minister of State (Independent Charge)
for Consumer Affairs, Food and Public
Distribution, Government of India
New Delhi-110 001

Preface

In recent times climate change is believed to play a major role in modifying the coastal/marine ecosystems with implications on their ecological and economical aspects that also support the high density populations living there. Thus the coastal and marine environments are closely linked to climate in numerous ways. The resultant sea-level rise is expected to increase at an alarming rate in the 21^{st} century with severe impacts on low-lying regions where salt water inundation/intrusion, soil salinity, coastal ecosystem biodiversity, subsidence and erosion and host of problems get enhanced. Added to these are the impacts of increasing pollution load; and the GHGs increase also have major impact on mangroves, lagoons, coral reefs, etc.

In the last decade, the various reports and research works identified several small island nations that are in a vulnerable position due to climate change. India has around eleven hundred islands and islets in the Arabian Sea and the Bay of Bengal. Hence, there is an urgent need for an integrated attempt to address these issues systematically along with a strategy to develop adaptation and mitigation in islands and with islander's aspects to combat with climate change. The IWCCI conference was organised and the recommendations for specific action plans based on the research submissions in various sessions brought out this edited volume. We hope it will be highly beneficial to the researchers on climate change especially on islands and coast as well as the public who are interested in Climate Change Science.

The book consists of four parts viz. Hydrological Regime Changes and Water Woes; Biotic Changes and Responses (Stresses and Vulnerability); Coastal Dynamics; and Livelihood Options. The chapters are arranged in the sequence of the occurrence of climate change in a system. The status of coastal and island hydrological regimes are examined, followed by the biotic changes and their responses to coastal dynamics and the vulnerability due to sea level rise—the most conspicuous aspects of climate change. The last part, the impact of climate change on livelihood options, incorporates mitigation and adaptation scenarios of these regions.

Many researchers from various national and international institutions have contributed to this volume which reflects their own views and ideas. The editors thank all the contributors, reviewers and the publisher for their support. Peer reviewers of the volume helped greatly in improving the quality of the articles. The articles in this volume will be very useful to managers, researchers and stake-holders belonging to these regions. It will be a great asset to all the libraries of colleges, universities, institutions and also useful for individual collections as well.

J. Sundaresan
S. Sreekesh
AL. Ramanathan
L. Sonnenschein
R. Boojh

About the Editors

J. Sundaresan

Head, Climate Change Informatics in CSIR-NISCAIR, an autonomous institution under Council of Scientific and Industrial Research (CSIR), Ministry of Science & Technology, Govt of India. He is the Editor of Indian Journal of Geo-Marine Sciences, a publication of CSIR. He is a PhD in Oceanography from Cochin University of Science & Technology, India. Has thirty years research experience in coastal oceanography and twenty two years experience in island studies. Associated with science education, science popularisation and ecological activities for the last 36 years. Actively associated with scientists' associations to sustain ethics, truth and scientific temper in scientific institutions. Published more than fifty publications, an examiner for doctoral thesis evaluation and member of national and international committees. Invited for key note address and invited talk in many universities. Travelled in many countries.

S. Sreekesh

S. Sreekesh has about 18 years of experience in teaching and research. He obtained his PhD in land degradation in Periyar river basin from the Jawaharlal Nehru University, New Delhi and worked with The Energy and Resources Institute, New Delhi. He is currently working as an Associate Professor in the Centre for the Study of Regional Development, Jawaharlal Nehru University, New Delhi, India. He is actively engaged in teaching and research in the field of climate, climate change and water resources management. He has expertise in application of geospatial techniques in resource and environment management. He has published many research papers in the national and international journals and written several chapters in books. He also has vast experience in collaborative research with the support from the national and international funding agencies.

AL. Ramanathan

AL. Ramanathan is a Professor in School of Environmental Sciences, Jawaharlal Nehru University, New Delhi, India. He is leading the group working on coastal biogeochemistry and hydro geochemistry and has worked extensively on mangroves, estuaries and coastal ground waters of India for the past two decades. He is actively engaged in coastal research with different institutions in India and from various parts of the world such as Australia, Russia, USA, on nutrient dynamics, biomarkers, paleo environment, nutrient source identification etc. He has guided two dozen PhDs in these aspects and published more than seven dozen papers in referred reputed journals like Estuaries, Wetland Ecology and Management, Estuarine, Coastal and Shelf Science, Journal of Coastal Research, Bull of Marine Sciences, Indian Journal of Marine Sciences, Marine Pollution Bulletin, Hydrogeology Journal, Water Soil and Air Pollution, Hydrological Process, Geofluids Applied Geochemistry, Journal of Geochemical Exploration etc. He has also published five books and written several chapters in books of national and international repute. He was a post-doc fellow under STA Japan program, UGC Russian Academy of Science Program, CSIR, INSA, DST, etc. He was a member of editorial board in Indian Journal of Marine Sciences and is a referee for many national and international journals.

Leonard Sonnenschein

Forty-six years experience in keeping fish, 35 years experience in scientific research, 23 years experience in science education innovation, over 100 publications, and extensive performance in conservation collaboration, climate change issues and public awareness. Leonard Sonnenschein opened St. Louis Children's Aquarium in 1993 and on June 8, 2004 (World Ocean Day) opened its expansion facility, the World Aquarium. Leonard regularly supervises students from over 45 universities which collaborate with the research component of the aquarium in facility development, exhibit design, fisheries, aquatic sciences, ecology, aquariology, legal frameworks, consumer awareness, cultural comprehension of environmental issues, and public understanding through field, conference and inter-governmental work. In 2006, Sonnenschein founded the Conservation for the Oceans Foundation to expand the World Aquarium's focus. The mission of the Conservation for the Oceans Foundation (CFTO) is to support grassroots-level conservation, education and research projects that bring about positive changes to ecosystems worldwide through local and multi-stakeholder actions. In 2009, Youth Voices in Conservation was developed for additional youth engagement opportunities (ages 3-50). In 2011, based upon the Low Carbon Lifestyles' campaign, the Youth Voices in Conservation's GreenLeaf Program was developed to allow for raising capital for residual support mechanism based upon the carbon offset credit from worldwide projects' actions. Leonard regularly collaborates with international agencies such as UNESCO, UNEP, WHO, International Ocean Institute, and the Global Forum on Ocean, Coasts and Islands and is a co-founder of the World Ocean Network. Leonard recently started innovative drug manufacturing, LLC to bring new patented technology to the pharmaceutical, nutraceutical, cosmetic and aquaculture industries.

Ram Boojh

Programme specialist at the UNESCO Office in New Delhi, responsible for Ecological and Earth Sciences, World Heritage Biodiversity and Natural Heritage Programmes and is also the focal point for the UN Decade for Education for Sustainable Development (DESD). He has over 30 years of working experience with the academic institutions, voluntary sector, government and international organizations. He has a distinguished academic career with Doctorate in Ecology and recipient of many awards and honours including the Indian National Science Academy Medal presented by Mrs Indira Gandhi, the then Prime Minister of India in January 1984. He has travelled widely and has been visiting fellow at many European and US universities and academic institutions. He has published over 100 research/technical papers/popular articles and 11 books.

Contents

Foreword *v*
Preface *vii*
About the Editors *ix*

Part I: Hydrological Regime Changes and Water Woes

1. Projected Precipitation Changes over Malaysia by the End of the 21st Century Using PRECIS Regional Climate Model 3
Fredolin T. Tangang, Liew Juneng, Ester Salimun, Meng Sei Kwan and Jui Le Loh
2. Monsoonal Fluctuations vs Marine Productivity during Past 10,000 Years — A Study Based on Sediment Core Retrieved from Southeastern Arabian Sea 21
V. Yoganandan, C. Krishnaiah, K. Selvaraj, G.V. Ravi Prasad and Koushik Dutta
3. Prediction of Rain on the Basis of Cloud Liquid Water, Precipitation Water and Latent Heat in the Perspective of Climate Change over Two Coastal Stations 31
Rajasri Sen Jaiswal, Neela V.S., Sonia R. Fredrick, Rasheed M. and Leena Zaveri
4. Inter-annual Variability of Sea Surface Temperature in the Arabian Sea 53
C. Shaji, M.P. Sudev and M.V. Martin
5. Paleoclimate of Peninsular India 78
R. Ramesh, S.R. Managave and M.G. Yadava

Part II: Biotic Changes and Responses (Stresses and Vulnerability)

6. Marine Biodiversity: Climate Impact and Conservation Planning 101
Leonard Sonnenschein

7. Inventory and Monitoring of Coral Reefs of United Arab Emirates (UAE), Arabian Gulf, Using Remote Sensing Techniques 114
Dimpal Sanghvi, Richa Tiwari, Nandini Ray Chaudhury, Alpana Shukla and Ajai

8. Impact of Climate Change in the Sundarban Aquatic Ecosystems: Phytoplankton as Proxies 126
Dola Bhattacharjee, Brajagopal Samanta, Anurag Danda and Punyasloke Bhadury

9. Elevated CO_2 and Temperature Affect Leaf Anatomical Characteristics in Coconut (*Cocos nucifera* L.) 141
Muralikrishna K.S., S. Naresh Kumar and V.S. John Sunoj

10. Biochemical Composition of Seaweeds after the Influence of Oil Spill from 'Tasman Spirit' at the Coast of Karachi 154
Qaisar Abbas, Rashida Qari and Fozia Khan

11. Distribution of Ostracoda in the Mullipallam Lagoon, near Muthupet, Tamil Nadu, Southeast Coast of India – Implications on Microenvironment 166
S.M. Hussain and A. Kalaiyarasi

Part III: Coastal Dynamics

12. Influence of Suspended Solid on in situ and ex situ Chlorophyll-*a:* A Case Study of Indian Sundarbans 179
Atanu Kumar Raha, Kakoli Banerjee, Susmita Das and Abhijit Mitra

13. Climate and Sea Level Changes in a Holocene Bay Head Delta, Kerala, Southwest Coast of India 191
D. Padmalal, K.M. Nair, K.P.N. Kumaran, K. Sajan, S. Vishnu Mohan, K. Maya, V. Santhosh, S. Anooja and Ruta B. Limaye

14. Role of Sea Level Rise on the Groundwater Quality in Coastal Areas of Sri Lanka 209
Ranjana U.K. Piyadasa, K.D.N. Weerasinghe, J.A. Liyanage and L.M.J.R. Wijayawardhana

15. Mangrove Responses to Climate Change along the Southwestern Coast of India during Holocene: Evidence from Palynology and Geochronology 217
K.P.N. Kumaran, Ruta B. Limaye and D. Padmalal

16. Predicted Recurrence of Coral Bleaching Events along Lakshadweep Reef Region 239
M. Hussain Ali, B. Jasper and E. Vivekanandan

Part IV: Livelihood Options

17. Hatchery Production of Marine Ornamental Fishes: An Alternate Livelihood Option for the Island Community at Lakshadweep 253
K.V. Dhaneesh, R. Vinoth, Swagat Ghosh, M. Gopi, T.T. Ajith Kumar and T. Balasubramanian

18. Living in Harmony with Nature: Complication of Climate Change and Governance 266
H.A. Karl

Index 283

Part I

Hydrological Regime Changes and Water Woes

CHAPTER

1

Projected Precipitation Changes over Malaysia by the End of the 21st Century Using PRECIS Regional Climate Model

Fredolin T. Tangang, Liew Juneng, Ester Salimun, Meng Sei Kwan and Jui Le Loh

Research Centre for Tropical Climate Change System
Faculty of Science and Technology, Universiti Kebangsaan Malaysia
43600 Bangi Selangor, Malaysia
ftangang@gmail.com

INTRODUCTION

Malaysia is situated at the western part of the Maritime Continent. The surface climate and weather fluctuation over the Maritime Continent is modulated mainly by the Asian-Australian monsoon. This large scale circulation is reported to be weakened by the elevated global temperature in numerous observational and modelling studies (e.g. Gong and Ho, 2004; Wu et al., 2007; Xu et al., 2006; Yu and Zhou, 2007; Hu et al., 2000; Hori and Ueda, 2006). Juneng and Tangang (2010) indicated possible association between the weakened winter monsoon and the synoptic circulations changes over the southern South China Sea. Future changes associated with the monsoon circulation are expected to incur modification of precipitation regimes over the Malaysia regions (Juneng and Tangang, 2010).

The changes of precipitation regimes can have a substantial impact on nation's water resources availability. Proper addressing of the issue requires quantitative assessment of the sensitivity, adaptive capacity and vulnerability to climate change in order to support formulation of sustainable water resource

J. Sundaresan et al. (eds.), *Climate Change and Island and Coastal Vulnerability*,
DOI 10.1007/978-94-007-6016-5_1, © 2013 Capital Publishing Company

management strategies. To systematically pursue such assessments, the most fundamental requirement is the availability of future climate information on regional and local scales.

The Global Circulation Models (GCMs) are important tools in the study of climate change and climate variability. They model the responses of the climate system to scenarios of greenhouse gas and aerosol concentrations or some other hypothetical forcings. Current version of GCMs can generally simulate well the large and continental scale present-day climate (Houghton et al., 2001; McGuffie and Henderson-Sellers, 1997; McCarthy et al., 2001). Over the decades, there have been considerable improvements in GCMs performance to simulate the climatic consequences of increasing atmospheric concentrations of greenhouse gases (Kumar et al., 2006). However, their application to regional studies is restricted by their coarse resolutions and limited capability in capturing local and regional scales dynamic. Hence, direct utilization of GCMs output to assess climate change at regional and local scale, which is crucial at national level, is rather infeasible. These impact assessment applications often require detail climate projection information (Robinson and Finkelstein, 1991) in order to capture fine scale climate variations, particularly in the regions with complex topography, coastal or island locations, and in areas of highly heterogeneous land-cover and irregular landmasses (Wilby et al., 2004) such as the Southeast Asia maritime continent.

A possible approach to bridge the scale gap is by a technique called downscaling, which uses either dynamical or statistical approaches to relate the large-scale information from GCMs to reproduce regional or local climate (Karl et al., 1990; Giorgi and Mearns, 1991; Joubert et al., 1999; Zorita and von Storch, 1999). While the historical data-based statistical approaches link large scale climatic field (usually called predictor) to the local climate variables using empirical relationship (Benesterd et al., 2008), the dynamic approaches require the use of regional climate models (RCM) nested within a GCM simulation. These RCM simulations are conditioned at the boundaries by the GCMs output (Georgi and Hewitson, 2001; Jones et al., 2004b). Although it requires higher computational cost, RCM downscaling provides local climate information taking in account physical interaction between various local features and is more favourable over areas without observational data.

The present work examines projected changes of seasonal precipitation by the end of 21st century over the Malaysia region based on the IPCC SRES A1B emission scenario. The Hadley Centre regional climate model known as PRECIS (Providing Regional Climate for Impacts Studies) nested within the UKMO HadCM3 were used to produce the rainfall projection at resolution of $0.22° \times 0.22°$. This paper also describes briefly the model, data and analysis methods employed in the study. Following section elaborates and discusses the simulation results and the last section summarizes the study.

MATERIALS AND METHODS

Model Description and Simulation Experiment Design

PRECIS (Providing Regional Climate for Impacts Studies) is a regional climate modelling system developed by the Hadley Centre. The regional climate model component, HadRM3P, is a land-atmosphere coupled model similar to the HadRM3H described by Hudson and Jones (2002). The atmospheric model is based on hydrostatic primitive equations discretized on a regular longitude-latitude grid (Arakawa B grid) of 0.22° × 0.22° (a coarser resolution of 0.44° × 0.44° is also available) and configured with 19 levels of hybrid vertical coordinates set from ground up to 0.5 hPa (Simon et al., 2004). In current study, the model has been configured for a domain extending from about 95°E to 123°E and 7.5°S to 14°N (Fig. 1.1), covering both Peninsular Malaysia and East Malaysia. The convective scheme used is the mass flux penetrative scheme with an explicit downdraught (Gregory and Rowntree, 1990; Gregory and Allen, 1991). The Met Office Surface Exchange

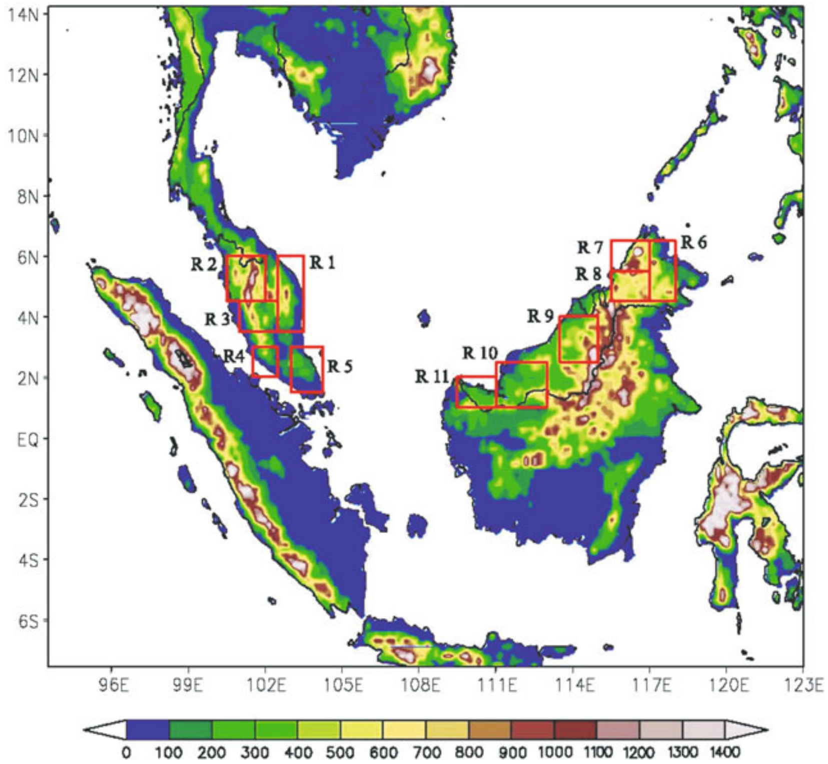

Fig. 1.1: The geographical extend of the domain used for HadCM3/PRECIS simulations. The topography within the domain is also provided (unit in m). The red boxes represent the 11 regions selected for area-averaged analysis. Refer text for further information.

Scheme (MOSES) (Cox et al., 1999) is used as the land surface model component. A detail description of the model is given in Jones et al. (2004b).

For current simulation experiment, the HadRM3P is forced at its lateral boundaries by the Hadley Centre Coupled Model version 3, HadCM3 running for the IPCC SRES A1B emission scenario. A relaxation method implemented across four points buffer zone are used to drive the RCM (Davies and Turner, 1977). The lateral boundary conditions are updated every six hours whilst the surface boundary conditions were updated every 24 hours. The simulation was integrated for 141 years from 1960-2100. However for the climate change analysis in current study, the baseline climate is calculated from the 30 years period of 1961-1990 allowing one year of spin up integration. The end of 21st century climate was defined from a 30-year period of 2071-2100. To facilitate discussion, the downscaled product is referred to as HadCM3/PRECIS throughout the subsequent text.

Data and Analysis Method

The first part of study evaluates the performance of 19 IPCC coupled ocean-atmosphere GCMs in reproducing large scale rainfall characteristics over the Malaysia region for the baseline climate simulation experiments (20C3M). These GCMs-simulated rainfall were obtained from the multi-model output archive of the Third Climate Models Inter-comparison Project (CMIP3) of the World Climate Research Program (WRCP) (Meehl et al., 2007). The selected GCMs are shown in Table 1.1 with their respective IPCC ID along with the key references and respective atmospheric resolutions. The rainfall spanning 1950-2000 reproduced from these GCMs were compared to the gridded product of Climate Prediction Center Merged Analysis Precipitation (CMAP) (Xie and Arkin, 1997). The resolution of the CMAP precipitation is $2.5° \times 2.5°$. The CMAP and the GCMs simulations are compared on the basis of the area-averaged precipitation annual cycle and the seasonal spatial pattern of rainfall.

To evaluate the HadCM3/PRECIS downscaling simulation of the baseline climate, gridded precipitation product of Climate Research Unit (CRU), University of East Anglia (Mitchell and Jones, 2005) were used as rainfall observation. The CRU data set is available at $0.5° \times 0.5°$ grid resolution. A total of 11 regions covering both Peninsular and East Malaysia were defined (Fig. 1.1). The model validation and climate change analysis were performed on the basis of rainfall annual cycles of the area averaged values. The selection of these areas was based on the topography setting in the Peninsular Malaysia as well as the East Malaysia, covering the northern Borneo. In addition, the spatial maps of rainfall were also used for clearer picture of the rainfall spatial variations. Seasonal averaged rainfall (DJF, MAM, JJA and SON) was considered for all spatial comparisons. To overcome the difference in grid resolutions, the PRECIS simulation output of $0.22° \times 0.22°$ was interpolated to the coarser CRU precipitation grids before comparisons.

Table 1.1: The 19 GCMs used in current study together with their versions, resolution and key reference

No.	*IPCC ID*	*Approximate resolution*	*Country*	*Key reference*
1	BCCR-BCM2.0	2.8 × 2.8	Norway	Furevik et al. (2003)
2	CGCM3.1	3.7 × 3.7	Canada	Flato et al. (2000)
3	CNRM-CM3	2.8 × 2.8	France	Salas-Melia et al. (2006)
4	CSIRO-MK3.0	1.9 × 1.9	Australia	Gordon et al. (2002)
5	GFDL-CM2.0	2.5 × 2.0	USA	Delworth et al. (2006)
6	GFDL-CM2.1	2.5 × 2.0	USA	Delworth et al. (2006)
7	GISS-AOM	4.0 × 3.0	USA	Russell et al. (1995)
8	GISS-EH	5.0 × 4.0	USA	Schmidt et al. (2006)
9	GISS-ER	5.0 × 4.0	USA	Schmidt et al. (2006)
10	FGOALS-g1.0	2.8 × 3.0	China	Yu et al. (2004)
11	INM-CM3.0	5.0 × 4.0	Russia	Diansky and Volodon (2002)
12	IPSL-CM4	3.7 × 2.5	France	Marti et al. (2005)
13	MIROC3.2 (hires)	1.1 × 1.1	Japan	K-1 Model Developers (2004)
14	MIROC3.2 (medres)	2.8 × 2.8	Japan	K-1 Model Developers (2004)
15	ECHO-G	3.7 × 3.7	Germany/ Korea	Legutke and Voss (1999)
16	ECHAM5/MPI-OM	1.9 × 1.9	Germany	Jungclaus et al. (2006)
17	MRI-CGCM2.3.2	2.8 × 2.8	Japan	Yukimoto et al. (2001, 2002)
18	UKMO-HadCM3	3.7 × 2.5	UK	Jones et al. (2004a)
19	UKMO-HadGEM1	1.9 × 1.2	UK	Johns et al. (2005)

RESULTS AND DISCUSSION

Large Scale Rainfall Simulated by GCMs

Figure 1.2 depicts the seasonal march of the CMAP precipitation (observation) and the 19 GCMs-simulated precipitation averaged over the Malaysia region (95°E to 120°E and 5°S to 7°N). Generally, the performance of the GCMs in simulating the annual cycle of precipitation over the region shows large inter-model variations. Based on the curve of the annual cycles, the performance of the GCMs is intuitively grouped into six different patterns. The GCMs in group 1 (UKMO-HadCM3, UKMO-HadGEM1 and IPSL-CM4) and group 2 (GFDL-CM2.0 and GFDL-CM2.1) generally over-estimates the rainfall in the region. However the group 1 GCMs show consistency in terms of the shape of the seasonal curves. The GFDL's climate models (group 2), on the other hand, depict large positive biases in the summer and fall. The GCMs in group 3 (MRI-CGCM2.3.2, CSIRO-MK3.0, CGCM3.1, ECHO-G and ECHAM5/MPI-OM), group 4 (CNRM-CM3, GISS-ER and FGOALS-g1.0) and group 5 (MIROC3.2(medres), MIROC3.2(hires) and BCCR-BCM2.0) show a strong bi-modal precipitation distribution with a secondary peak during the summer months. These groups of models usually produce weaker winter and spring rainfall but higher summer rainfall. This is inconsistent with the observation which shows minimum rainfall during the summer over the region. On the other hand, GCMs in group 6 (GISS-AOM, GISS-EH and INM-CM3.0) are generally more consistent with the observation which the simulated precipitation annual cycles show minimum rainfall during the summer and maximum during winter with less biases.

Generally, most of the GCMs have difficulties in simulating the rainfall satisfactorily over the Malaysia region. This is partly due to the convective nature of the rainfall as well as complex topography and coastlines over the

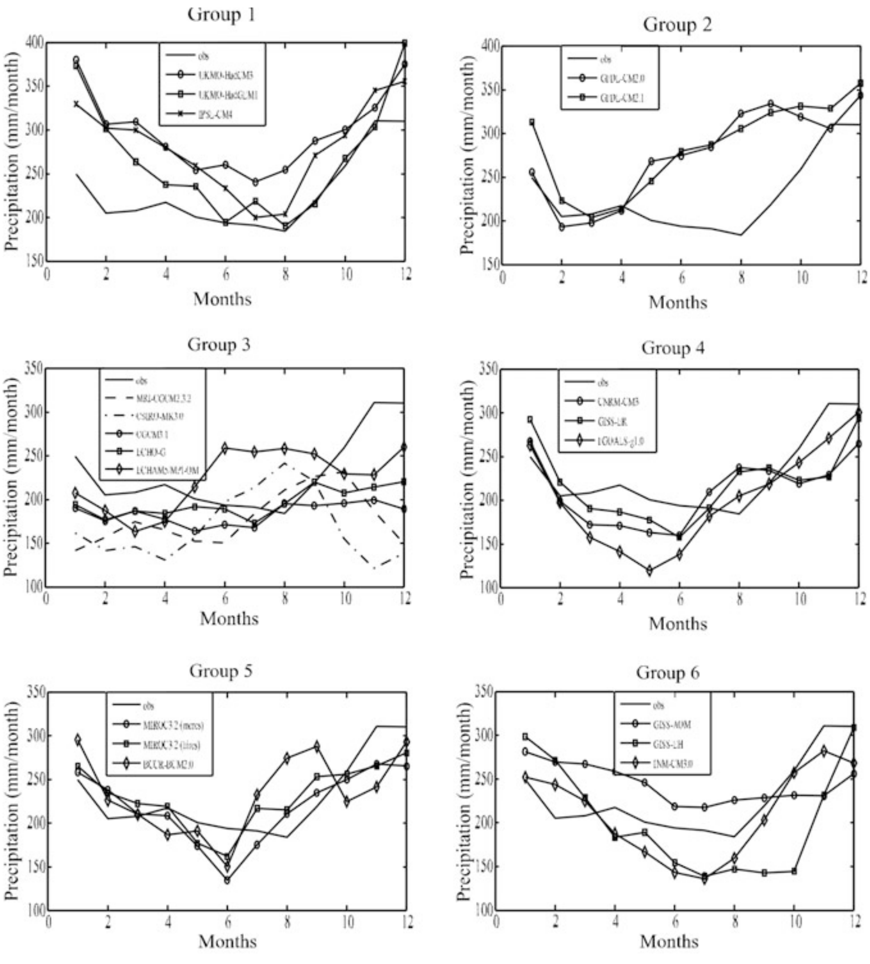

Fig. 1.2: The annual cycle of the averaged monthly rainfall (mm/month) for the CMAP observation (obs: solid line in each group) and the 19 GCMs simulations. Annual cycles are grouped according to their general patterns.

Southeast Asia maritime continent which plays crucial role in the rainfall processes (e.g. Salimun et al., 2010). Among the GCMs, UKMO-HadCM3 is of particular interest because the model data is readily to be used in the PRECIS modelling system for climate downscaling experiments. Despite producing higher rainfall over the considered region, the annual cycle curve and the spatial distribution of rainfall are generally consistent with the observation (CMAP). Figure 1.3 compares the rainfall spatial distribution between the CMAP and the GFDL-CM2.1 as well as UKMO-HadCM3 on seasonal basis. The GFDL-CM2.1 simulates a strong rainfall band over the equatorial region during summer which is inconsistent with the observation. On the other hand, the UKMO-HadCM3 simulated rainfall is spatially more consistent with CMAP except generally higher rainfall over the southern South China Sea area. The report shows consistently higher rainfall over the annual cycle (Fig. 1.2a). The PRECIS modelling system was then used for downscaling experiments using the UKMO-HadCM3 output as boundary conditions. An interesting question is whether the downscaling is able to improve the positive biases from the driving GCMs.

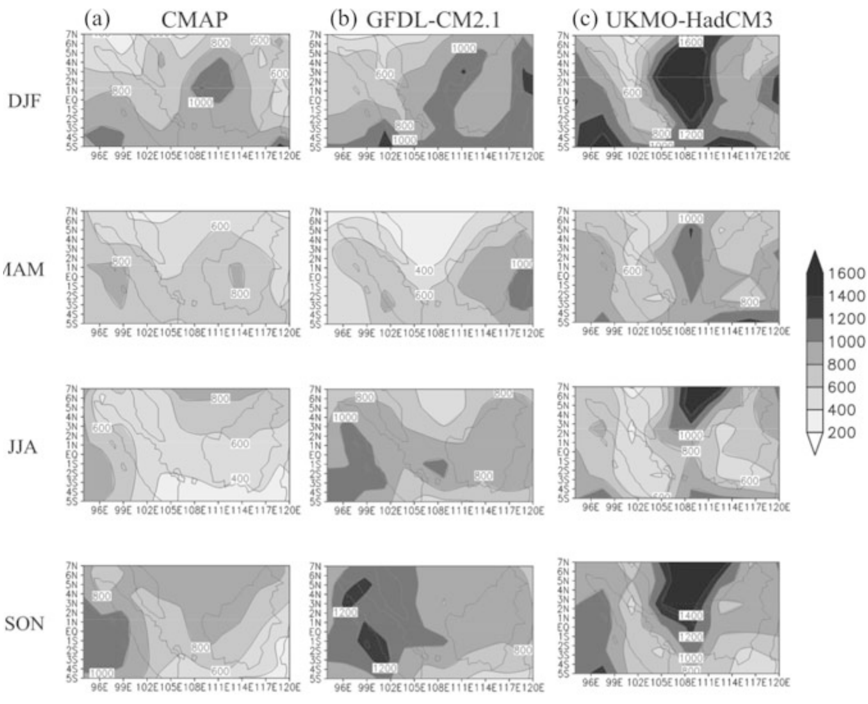

Fig. 1.3: Spatial patterns of seasonal precipitation (DJF, MAM, JJA and SON) of the (a) observation (CMAP), (b) GFDL-CM2.1 simulation and (c) UKMO-HadCM3 simulation.

Baseline Climate from HadCM3/PRECIS Simulation

Figure 1.4 shows the seasonal cycles of averaged precipitation of the CMAP, UKMO-HadCM3 and the HadCM3/PRECIS downscaling simulation. It is noted that the HadCM3/PRECIS improves the overall magnitude of the area-averaged rainfall while maintaining the shape of the seasonal curve. Substantial improvement is attained for spring, summer and fall seasons. There are however still noticeable positive biases during the winter months. These positive biases are probably inherited from the driving HadCM3. During the winter months, the regional rainfall is largely influenced by the northeast monsoon winds when the dynamic and moisture information from northern boundary dominates the climate of the RCM simulations.

Figure 1.5 compares the baseline observed monthly rainfall (CRU) climatology (1961-1990) to those of the HadCM3/PRECIS downscaling simulation averaged over the 11 regions defined in Fig. 1.1. Generally, the HadCM3/PRECIS simulates well the seasonal march of area averaged rainfall over Malaysia. In particular, the simulation reproduces the maximum rainfall during the winter months and minimum during the summer over the northeastern part of Peninsular Malaysia (R1) and western part of Sarawak (R10 and R11). The winter northeast monsoon (Nov(0)-Feb(1)) is an important feature over Malaysia. The strong northeasterly cold surge winds are associated to large amount of rainfall over Malaysia region, particularly over the northeastern coast of Peninsular Malaysia and western coast of Borneo. However, there appears to be consistent negative biases across the seasons over most parts of the western Borneo. Negative biases are also simulated over the northwest regions (R2 and R3) of Peninsular Malaysia during the beginning of the monsoon. Overall, the results indicate slightly drier tendency of the HadCM3/PRECIS simulating rainfall climate over the land. Given that the area averaged rainfall (Fig. 1.4) across the region shows overestimation of rainfall in the winter months, the excessive rainfall is largely produced over the South China Sea.

Figure 1.5 also compares the observed rainfall interannual variability structure to those of the HadCM3/PRECIS simulations. In general, the results indicate maximum interannual variability occurrence during the winter northeast monsoon season with minimum variability during the dry seasons of summer monsoon. This suggests that the precipitation in Malaysia varies the most during the northeast monsoon. Tangang and Juneng (2004) reported that the largest interannual variability of the Malaysia precipitation always coincides with the wet seasons. Overall, the HadCM3/PRECIS simulated the interannual variations reasonably well throughout the Malaysian regions except over the northern Borneo. Over the northern Borneo (R6, R7 and R8) the model simulated weaker interannual variability. Generally speaking, HadCM3/PRECIS performs satisfactorily in simulating the rainfall climatology and the interannual variations over the Malaysian regions.

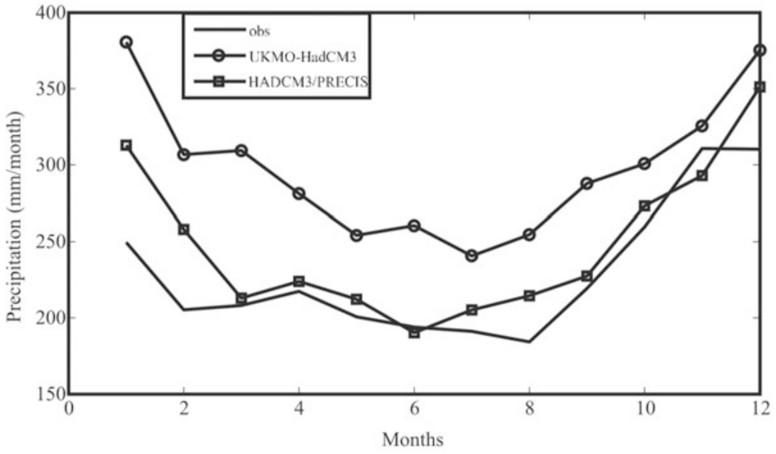

Fig. 1.4: Monthly rainfall climatology (unit in mm/month) of the observation, HadCM3 simulation and HadCM3/PRECIS downscaling simulation.

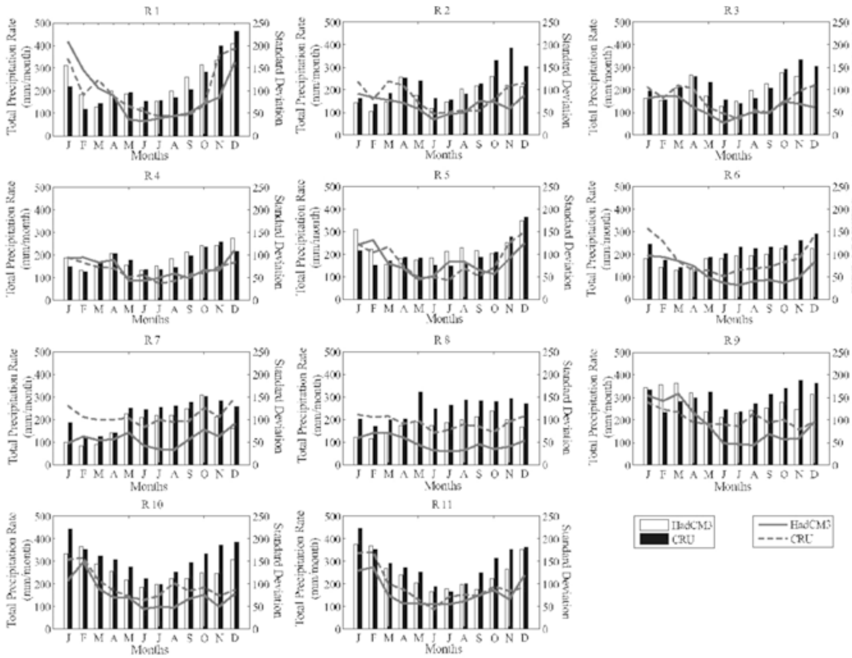

Fig. 1.5: Comparison between baseline monthly rainfall climatology (left ordinates) of the observation (CRU) (black bars) and the HadCM3/PRECIS downscaling simulation (white bars), averaged over the 11 regions (refer Fig. 1.1). The observed (dashed line) and simulated (solid line) interannual variability as indicated by the year-to-year standard deviations (right ordinates) are also plotted.

Figure 1.6 shows the seasonal comparison between the CRU gridded precipitation and the downscaled HadCM3/PRECIS precipitation. For better visual comparison, the HadCM3/PRECIS data was interpolated to the CRU grids and the result is shown in the third column of Fig. 1.6. The HadCm3/PRECIS reproduced the spatial distribution of the seasonal precipitation reasonably well. Generally, better simulation results were attained for MAM and SON when the monsoon influence is minimal. During MAM, HadCm3/PRECIS reproduced the maximum rainfall over the inland of Sarawak consistent with the observation. Over the Peninsular Malaysia, maximum rainfall during MAM over the northwestern region was also reproduced. Although the SON rainfall maximum over the inland Sarawak was generally reproduced, the HadCM3/PRECIS simulated a more concentrated rainfall area slightly eastward to the mountainous area of the central Borneo mountain range. The rainfall peak over the northeastern coast of Peninsular Malaysia during SON was also simulated well by HadCM2/PRECIS.

During DJF and JJA, the simulation shows noticeable spatial and magnitude biases. During DJF, the maximum rainfall over the east coast of Peninsular Malaysia shifted slightly northward in the HadCM3/PRECIS simulation. Although wetter region over the western Borneo was simulated well, there appears to be higher rainfall spread over the central region of Borneo. However, the maximum peak over the western tip of Borneo is well

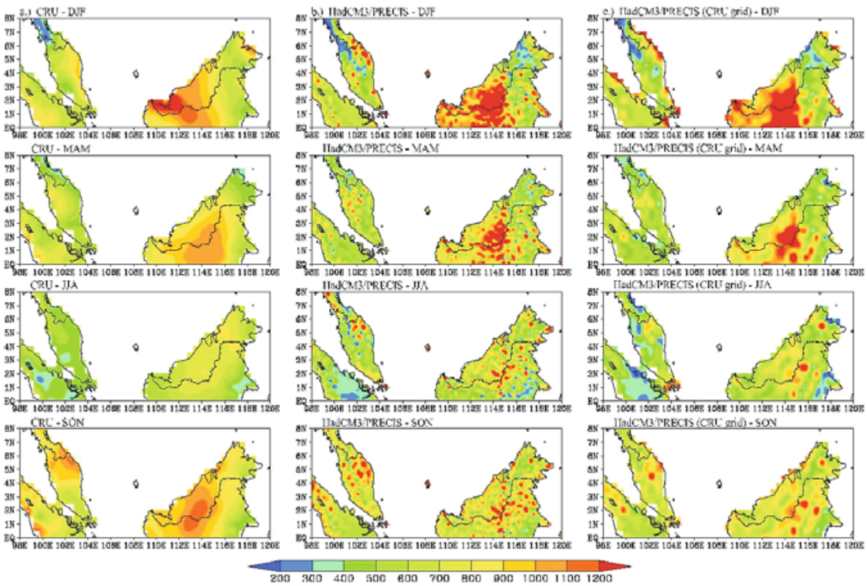

Fig. 1.6: Spatial distributions of seasonal averaged rainfall (unit: mm/month) of the observation (CRU) (left panels), downscaled HadCM3/PRECIS data (centre panels) and the downscaled HadCM3/PRECIS interpolated to the CRU grid resolution (right panels).

simulated by the model. During JJA, the model fails to simulate the predominantly dry pattern over Peninsular Malaysia. The model simulates high precipitation at the northeastern region Peninsular Malaysia which is inconsistent with the CRU precipitation. Over the northern Borneo, HadCM3/PRECIS simulated overall wetter climate despite strong positive biases over the inland Sarawak at the central Borneo.

During the monsoon periods (DJF and JJA), the regional climate is largely dominated by the southwest and northeast monsoon winds and the associated moisture processes. Hence, the quality of the simulation can depend more on the northern and southern boundary conditions as compared to other seasons (MAM and SON). The weaker performance of HadCM3/PRECIS during DJF and JJA may indicate poorer performance of driving HadCM3 during these seasons. Also, there is a general overestimation of rainfall, dominant over the inland areas, where topography is complex such as the central inland Borneo. The biases may be due to inadequate model grid resolution to properly resolve the complex local topographic features that are important to rainfall processes. It is also worth to mention that the CRU dataset were produced from the interpolation of station observations. In the mountainous area of the central Borneo and inland Peninsular Malaysia, the rainfall observations are sparse. These regions are particularly prone to interpolation errors because of the complex topographic forcing and the low-elevation bias to the station network (New et al., 2002). Hence, the gridded CRU rainfall data may not have a good representation of the actual rainfall field. This may also reflect the discrepancies shown in the inland areas of central Borneo (Fig. 1.6). This possible issue related to using CRU dataset is also recognized by Kotroni et al. (2008).

Rainfall Projection by the End of 21st Century

Figure 1.7 shows the comparison of rainfall annual cycle for baseline and projected precipitation over the 11 regions. By the end of the century, the annual precipitation pattern at both Peninsular Malaysia and East Malaysia are not expected to vary much from the present precipitation climatology. However, the HadCM3/PRECIS simulation results suggest an overall drier climate over the Malaysia regions except during the end of summer and fall. A clearer comparison is provided in Fig. 1.8 which shows spatial variations of the percentage of projected rainfall changes. The largest change in the precipitation climate are projected during the month of February (not shown) with a reduction of ~40% over the eastern and southeastern regions of Peninsular Malaysia and inland of Borneo (Fig. 1.8d). This indicates a possibility of shorter and weaker winter monsoon seasons under the SRES A1B emission forcing and hence, produces less monsoon rainfall during the season. Several GCMs studies have indicated possible weaker East Asian winter monsoon due to the weakening of Siberian High and shrinking of the

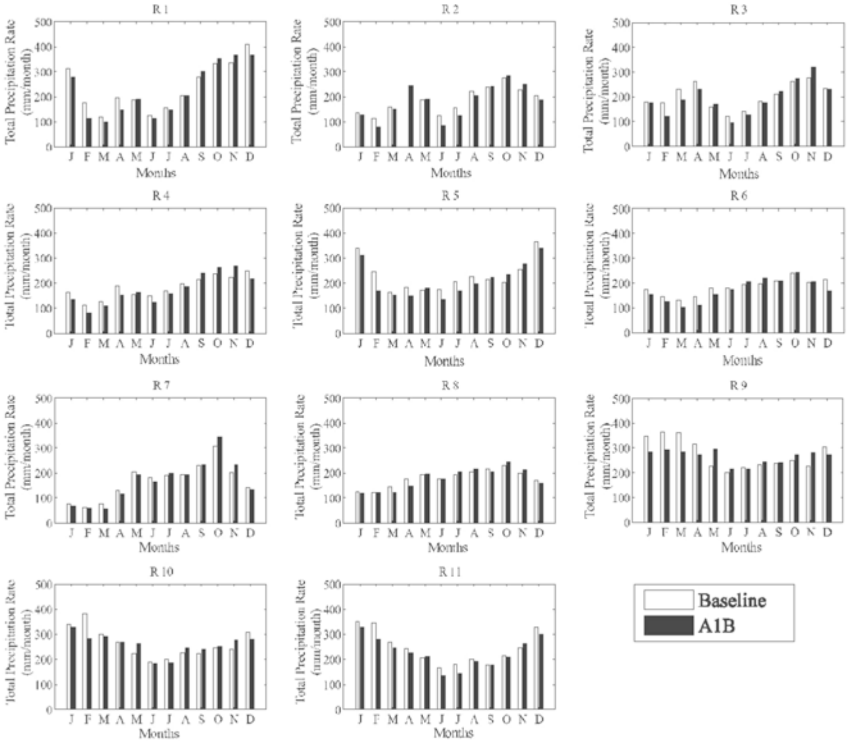

Fig. 1.7: The comparison of rainfall climatology between the HadCM3/PRECIS baseline (1961-1990) (white) and the future projection by the end of the 21^{st} century (2071-2099) (black).

Aleutian Low in a warmer climate (Hu et al., 2000; Hori and Ueda, 2006). Juneng and Tangang (2010) has also reported weakening of the winter monsoon cold surge wind over the South China Sea during the last decades. The overall summer southwest monsoon rainfall shows a maximum decrease of about 20-30%.

Over the inland of central Borneo, wetter condition is expected to start during the spring and persists through the fall with ~30% rainfall surplus compared to that of the baseline climate. Over the seasons, the eastern Borneo regions was projected to be overall drier with considerable spatial variations and changes magnitude, while the regions west of the central Borneo mountain range was projected to be wetter (Figs 1.8b, c and d). This indicates strong climate modulation by the regional topography. The largest rainfall increase was detected during May (not shown). In fact, most of the sub-regions, including those over the Peninsular Malaysia (~10-20%) were predicted to experience an increase in rainfall during SON (Fig. 1.8d) under the SRES A1B emission forcing. On the other hand, regions over the Peninsular Malaysia remain drier throughout the spring and summer.

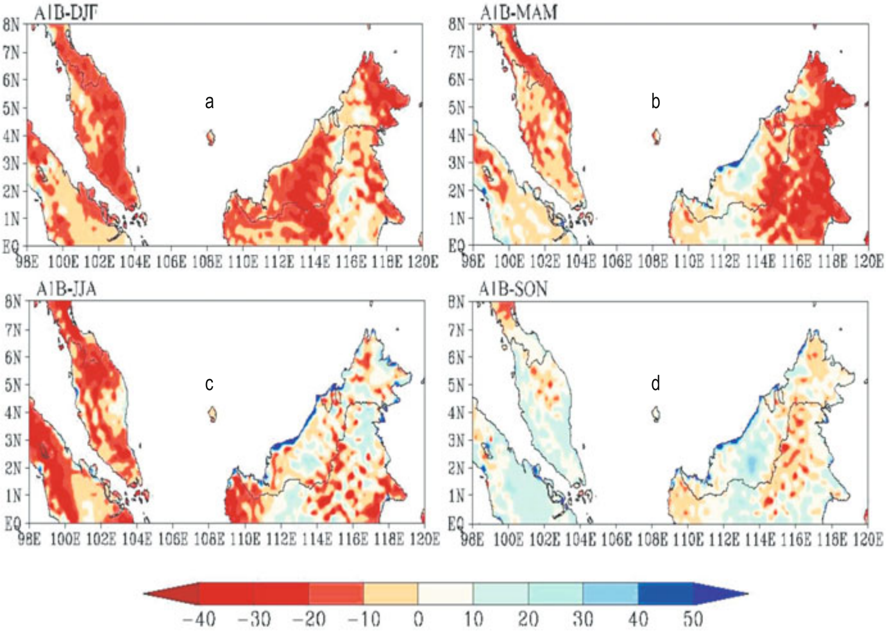

Fig. 1.8: Spatial patterns of the seasonal rainfall changes (unit: %) as simulated by the HadCM3/PRECIS.

CONCLUSION

This study examined the impact of climate change to the Malaysian rainfall climatology under the IPCC SRES A1B emission scenario. Generally, the GCMs performance is unsatisfactory over the region where most of them produce fallacious curves of rainfall annual cycle. A few of them simulated reasonable annual curves with substantial biases. Result suggests that dynamical downscaling using PRECIS model nested within the HadCM3 simulation improves the annual cycle simulations and removes the large scale biases substantially. At local and regional scale, the HadCM3/PRECIS downscaling produces reasonable simulation of rainfall climate over the Malaysia region when compared to CRU gridded precipitation. In addition, the interannual variations of the rainfall were also reasonably simulated. However, the skills of the HadCM3/PRECIS downscaling show considerable spatial variation. Remarkable biases are simulated over the Peninsular Malaysia during the summer months.

The climate change analysis using the HadCM3/PRECIS downscaled output suggests a generally drier tendency over the Malaysia regions by the end of the 21st century based on the SRES A1B emission forcing. The largest decrease appears to be expected during the winter monsoon months. In certain areas the monsoon rainfall reduction may access 30-40%. This is associated likely to the weakening of East Asian winter monsoon as suggested by many GCM studies. The analysis results also suggested possible shorter winter monsoon period when rainfall decreased dramatically during the month of February. Despite the overall drying tendencies, slightly higher rainfall is expected in large areas of Malaysia during the SON, particularly over the inland of central Borneo where the increment is expected to access 40% of the baseline climate.

The model is considered effective in producing the rainfall climate and the inter-annual variations over the study region. The changing of future rainfall is expected to incur greater challenges to the nation's water resource management. Better simulation results are required for better and more sustainable adaptation and mitigation strategies design. Future research towards reducing the climate model systematic errors is needed in order to reproduce a more reliable future climate projection. Also, climate change analysis based on other driving GCMs as well different scenarios are required to produce robust error estimation which is crucial for better water resource risk assessment and management.

ACKNOWLEDGEMENT

This research is funded by UKM Research Grant UKM-GUP-ASPL-08-05-218, UKM-AP-PI-18-2009/2 and MOHE Grant LRGS-TD/2011/UKM/PG/01. The authors wish to thank the Hadley Centre for providing the PRECIS modelling system to the Research Centre for Tropical Climate Change System, Universiti Kebangsaan Malaysia. Also, the availability of the CRU gridded precipitation data from the Climate Research Unit, University of East Anglia is acknowledged.

REFERENCES

Benesterd, R.E., Hanssen-Bauer, I. and Chen, D.L. (2008). Empirical-statistical downscaling. World Scientific Publishing, Singapore.

Cox, P.M., Betts, R.A., Bunton, C.B., Essery, R.L.H., Rowntree, P.R. and Smith, J. (1999). The impact of new land surface physics on the GCM simulation of climate and climate sensitivity. *Climate Dynamics*, **15:** 189-203.

Davies, H.C. and Turner, R.E. (1977). Updating prediction models by dynamical relaxation: An examination of the technique. *Quart. J. Roy. Meteor. Soc.*, **103:** 225-245.

Delworth, T.L., Broccoli, A.J., Rosati, A., Stouffer, R.J., Balaji, V., Beesley, J.A., Cooke, W.F., Dixon, K.W., Dunne, J., Dunne, K.A., Durachta, J.W., Findell, K.L., Ginoux, P., Gnanadesikan, A., Gordon, C.T., Grif?es, S.M., Gudgil, R., Harrison, M.J., Held, I.M., Hemler, R.S., Horowitz, L.W., Klein, S.A., Knutson, T.R., Kushner, P.J., Langenhorst, A.R., Lee, H.C., Lin, S.J., Lu, J., Malyshev, S.L., Milly, P.C.D., Ramaswamy, V., Russel, J., Schwarzkopf, M.D., Shevliakova, E., Sirutis, J.J., Spelman, M.J., Stern, W.F., Winton, M., Wittenberg, A.T., Wyman, B., Zeng, F. and Zhang, R. (2006). GFDL's CM2 global climate models. Part 1: Formulation and simulation characteristics. *J Clim.*, **19:** 643-674.

Diansky, N.A. and Volodin, E.M. (2002). Simulation of present-day climate with a coupled Atmosphere-Ocean general circulation model. *Izv. Atmos. Ocean Phys.* (Engl. Transl.), **38:** 732-747.

Flato, G.M., Boer, G.J., Lee, W.G., McFarlane, N.A., Ramsden, D., Reader, M.C. and Weaver, A.J. (2000). The Canadian Centre for Climate Modeling and Analysis of Global Coupled Model and its climate. *Clim. Dyn.*, **16:** 451-467.

Furevik, T., Bentsen, M., Drange, H., Kindem, I.K.T., Kvamsto, N.G. and Sorteberg, A. (2003). Description and evaluation of the Bergen Climate Model: ARPEGE coupled with MICOM. *Clim. Dyn.*, **21:** 27-51.

Georgi, F. and Hewitson, B. (2001). Regional climate Information – Evaluation and projections. *In:* Climate Change 2001: The Scientific Basis, Contribution of Working Group I to the Third Assessment Report of the Intergovernmental Panel on Climate Change. Houghton, J.T., Ding, Y., Griggs, D.J., Noguer, M., van der Linden, P.J., and Xiaosu, D. (eds). Cambridge University Press, Cambridge

Giorgi, F. and Mearns, M.R. (1991). Approaches to the simulation of regional climate change: A review. *Rev Geophys*, **29:** 191-216.

Gong, D.Y. and Ho, C.H. (2004). Intra-seasonal variability of wintertime temperature over East Asia. *International Journal of Climatology*, **24:** 131-144.

Gordon, H.B., Rotstayn, L.D., McGregor, J.L., Dix, M.R., Kowalczyk, O'Farrell, S.P., Waterman, L.J., Hirst, A.C., Wilson, S.G., Collier, M.A., Watterson, I.G. and Elliott, T.I. (2002). The CSIRO Mk3 Climate System Model, Asoendale: CSIRO Atmospheric Research Technical Paper No. 60. Available from http://www.dar.csiro.au/publications/gordon_2002a.pdf.

Gregory, D. and Allen, S. (1991). The Effect of Convective Scale Downdrafts upon NWP and Climate Simulations. Paper presented in Ninth Conference on Numerical Weather Prediction, Denver, Colo, 14-18 October 1991.

Gregory, D. and Rowntree, P.R. (1990). A mass flux convection scheme with representation of cloud ensemble characteristics and stability-dependent closure. *Mon. Weather Rev.*, **118:** 1483-1506.

Hori, M.E. and Ueda, H. (2006). Impact of global warming on the East Asian winter monsoon as revealed by coupled atmosphere-ocean GCMs. *Geophysical Research Letters,* **33:** L03713.

Houghton, J.T., Ding, Y., Griggs, D.J., Noguer, M., van der Linden, P.J. and Xiaosu, D. (eds) (2001). Climate Change 2001: The Scientific Basis, Contribution of Working Group I to the Third Assessment Report of the Intergovernmental Panel on Climate Change. Cambridge University Press, Cambridge.

Hu, Z.Z., Bengtsson, L. and Arpe, K. (2000). Impact of global warming on the Asian winter monsoon in a coupled GCM. *Journal of Geophysical Research*, **105:** 4607-4624.

Hudson, D.A. and Jones, R.G. (2002). Regional Climate Model Simulations of Present-Day and Future Climates of Southern Africa. Met Office Hadley Centre, Exeter.

Johns, T., Durman, C., Banks, H., Roberts, M., McLaren, A., Ridley, J., Senior, C., Williams, K., Jones, A., Keen, A., Rickard, G., Cusack, S., Joshi, M., Ringer, M., Dong, B., Spencer, H., Hill, R., Gregory, J., Pardaens, A., Lowe, J., Bodas-Salcedo, A., Start, S. and Searl, Y. (2005). HadGEM1-Model description and analysis of preliminary experiments for the IPCC Fourth Assessment Report. Hadley Centre Technical Note 55, UK Met Of?ce. Available from www.metof?ce.com=research=hadleycentre=pubs=HCTN=HCTN_55.pdf.

Jones, C., Gregory, J., Thorpe, R., Cox, P., Murphy, J., Sexton, D. and Valdes, H. (2004a). Systematic optimization and climate simulation of FAMOUS, a fast version of HADCM3, Hadley Centre Technical Note 60. Available at http://www.metof?ce.gov.uk/research/hadleycentre/pubs/HCTN/HCTN_60.pdf.

Jones, R.G., Noguer, M., Hassell, D.C., Hudson, D., Wilson, S.S., Jenkins, G.J. and Mitchell, J.F.B. (2004b). Generating High Resolution Climate Change Scenarios Using PRECIS. Met Office Hadley Centre, Exeter.

Joubert, A.M., Katzfey, J.J., Mcgregor, J.L. and Nguyen, K.C. (1999). Simulating mid-summer climate over Southern Africa using a nested regional climate model. *J. Phys. Geog.*, **21:** 51-78.

Juneng, L. and Tangang, F.T. (2010). Long-term trends of winter monsoon synoptic circulations over the maritime continent: 1962–2007. *Atmospheric Science Letter*, **11(3):** 199-203.

Jungclaus, J.H., Keenlyside, N., Botzet, M., Haak, H., Luo, J.J., Latif, M., Marotzke, J., Mikolajewicz, U. and Roeckner, E. (2006). Ocean circulation and tropical variability in the AOGCM ECHAM5/MPI-OM. *J. Clim.*, **19:** 3952-3972.

K-1 Model Developers (2004). K-1 Coupled GCM (MIROC) description, K-1 Tech Report No. 1. Center for Climate System Research, University of Tokyo, National Institute for Environmental Studies, Frontier Research Center for Global Change. Hasumi and Emori (eds). Available at http://www.ccsr.u-tokyo.ac.jp/kyosei/hasumi/MIROC/tech-repo.pdf).

Karl, T.R., Wang, W.C., Schlesinger, M.E., Knight, R.W. and Portman, D. (1990). A method of relating general circulation model simulated climate to the observed local climate. Part I: Seasonal statistics. *J. Clim.*, **3:** 1053-1079.

Kripalani, R.H., Oh, J.H. and Chaudhari, H.S. (2007). Response of the East Asian summer monsoon to doubled atmospheric CO_2: Coupled climate model simulations and projections under IPCC AR4. *Theor. Appl. Climatol.*, **87:** 1-28.

Kripalani, R.H., Oh, J.H., Kulkarni, A., Sabade, S.S. and Chaudhari, H.S. (2007). South Asian summer monsoon precipitation variability: Coupled climate model simulations and projections under IPCC AR4. *Theor. Appl. Climatol.*, **90:** 133-159.

Kotroni, V., Lykoudis, S., Lagouvardos, K. and Lalas, D. (2008). A fine resolution regional climate change experiment for the Eastern Mediterranean: Analysis of the present climate simulations. *Global and Planetary Change*, **64:** 93-104.

Legutke, S. and Voss, R. (1999). The Hamburg atmosphere-ocean coupled circulation model ECHO-G. DKRZ Technical Report No. 18, Deutsches Klimarechenzentrum, Hamburg, Germany.

Marti, O., Braconnot, P., Bellier, J., Benshile, R., Bony, S., Brockmann, P., Cadulle, P., Caubel, A., Denvil, S., Dufresne, J.L., Fairhead, L., Filiberti, M.A., Fichefet, T., Friedlingstein, P., Grandpeix, J.Y., Hourdin, F., Krinner, G., Levy, C., Musat, I. and Talandier, C. (2005). The new IPSL climate system model: IPSL-CM4. Institut Pierre Simon Laplace, Paris. Available at http://dods.ipsl.jussieu.fr/omamce/IPSLCM4/DocIPSLCM4/FILES/DocIPSLCM4.pdf.

McCarthy, J.J., Canziani, O.F., Leary, N.A., Dokken, D.J. and White, K.S. (eds) (2001). Climate Change 2001: Impacts, Adaptation, and Vulnerability. Inter-

Governmental Panel on Climate Change (IPCC), Work Group II Input to the Third Assessment Report. Cambridge University Press, Cambridge.

McGuffie, K. and Henderson-Sellers, A. (1997). A Climate Modelling Primer. John Wiley and Sons, New York.

Meehl, G.A., Covey, C., Delworth, T., Latif, M., McAvaney, B., Mitchell, J.F.B., Stouffer, R.J. and Taylor, K.E. (2007). The WCRP CMIP3 Multimodel Dataset: A New Era in Climate Change Research. *Bulletin of the American Meteorological Society*, **88(9):** 1383-1394.

Mitchell, T.D. and Jones (2005). An improved method of constructing a database of monthly climate observations and associated high-resolution grids. *International Journal of Climatology*, Royal Meteorological Society, **25:** 693-712.

Neale, R. and Slingo, J. (2003). The Maritime Continent and Its Role in the Global Climate: A GCM Study. *J. Climate*, **16:** 834-848.

New, M., Lister, D., Hulme, M. and Makin, L. (2002). A high-resolution data set of surface climate over global land areas. *Clim. Res.*, **21:** 1-25.

Robinson, P.J. and Finkelstein, P.L. (1991). The development of impact oriented climate scenarios. *Bulletin of the American Meteorological Society*, 72: 481-490.

Rupa Kumar, K., Sahai, A.K., Krishna Kumar, K., Patwardhan, S.K., Mishra, P.K., Revadekar, J.V., Kamala, K. and Pant, G.B. (2006). High-resolution climate change scenarios for India for the 21st century. *India Institute of Tropical Meteorology*, **90:** 334-345.

Russell, G.L., Miller, J.R. and Rind, D. (1995). A coupled atmosphere-ocean model for transient climate change studies. *Atmos-Ocean*, **33:** 683-730.

Salas-Melia, D., Chauvin, F., Deque, M., Douville, H., Gueremy, J.F., Marquet, P., Planton, S., Royer, J.F. and Tyteca, S. (2006). Description and validation of the CNRM-CM3 global coupled model. *Clim. Dyn.*

Salimun, E., Tangang, F.T. and Juneng, L. (2010). Simulation of heavy precipitation episode over eastern Peninsular Malaysia using MM5: Sensitivity to cumulus parameterization schemes. *Meteorology and Atmospheric Physics*, **107(1-2):** 33-49.

Schmidt, G.A., Ruedy, R., Hansen, J.E., Aleinov, I., Bell, N., Bauer, M., Bauer, S., Cairns, B., Canuto, V., Cheng, Y., DelGenio, A., Faluvegi, G., Friend, A.D., Hall, T.M., Hu, Y., Kelley, M., Kiang, N.Y., Koch, D., Lacis, A.A., Lerner, J., Lo, K.K., Miller, R.L., Nazarenko, L., Oinas, V., Perlwitz Jan, Perlwitz Judith, Rind, D., Romanou, A., Russel, G.L., Sato, M., Shindell, D.T., Stone, P.H., Sun, S., Tausnev, N., Thresher, D. and Yao, M.S. (2006). Present day atmospheric simulations using GISS Model E: Comparison to in-situ, satellite and reanalysis data, *J. Clim*.

Simon, W., Hassel, D., Hein, D., Jones, R. and Taylor, R. (2004). Installing and Using the Hadley Centre Regional Climate Modelling System, PRECIS, Version 1.1. Met Office Hadley Centre: Exeter.

Tangang, F.T. and Juneng, L. (2004). Mechanisms of Malaysia rainfall anomalies. *Journal of Climate*, **17(18):** 3615-3621.

Wilby, R.L., Charles, S.P., Zorita, E., Timbal, B., Whetton, P. and Mearns, L.O. (2004). Guidelines for use of climate scenarios developed from statistical downscaling methods. Supporting material of the Intergovernmental Panel on Climate Change (DDC of IPCC TGCIA, 27).

Wu, M.C., Yeung, K.H. and Leung, Y.K. (2007). Changes in the East Asian winter atmospheric circulation, paper presented in International Conference on Climate Change, Hong Kong, China, 29-31 May 2007.

Xie, P. and Arkin, P.A. (1997). Global Precipitation: A 17-year monthly analysis based on gauge observations, satellite estimates, and numerical model outputs. *Bulletin of the American Meteorological Society*, **78:** 2539-2558.

Xu, M., Chang, C.P., Fu, C., Qi, Y., Robock, A., Robinson, D. and Zhang, H. (2006). Steady decline of East Asian monsoon winds, 1969-2000: evidence from direct ground measurements of wind speed. *Journal of Geophysical Research*, **111:** D24111, DOI:10.1029/2006D007337.

Yukimoto, S., Noda, A., Kitoh, A., Sugi, M., Kitamura, Y., Hosaka, M., Shibata, K., Maeda, S. and Uchiyama, T. (2001). The new Meteorological Research Institute Coupled GCM (MRI-CGCM2)-Model climate and variability. *Meteorology and Geophysics*, **51:** 47-88. Available at http://www.mri-jma.go.jp/Dep/cl/c14/publications/publications/ yukimoto_pap2001.pdf.

Yukimoto, S. and Noda, A. (2002). Improvements of the Meteorological Research Institute global ocean-atmosphere coupled GCM (MRI-CGCM2) and its climate sensitivity. CGER's Supercomputer Activity Report No. 10, 37-44, NIES, Japan. Available at http://www.mri-jma.go.jp/Dep/cl/c14/publications/yukimoto_CGER2002.pdf.

Yu, R. and Zhou, T. (2007). Seasonality and three-dimensional structure of the interdecadal change in East Asian monsoon. *Journal of Climate*, **20:** 5344-5355.

Yu, Y., Zhang, X. and Guo, Y. (2004). Global coupled ocean-atmosphere general circulation models in LASG/IAP. *Adv. Atmos. Sc.*, **21:** 444-455.

Zorita, E. and von Storch, H. (1999). The analog method as a simple statistical downscaling technique: Comparison with more complicated methods. *Journal of Climate*, **12:** 2474-2489.

CHAPTER

2

Monsoonal Fluctuations vs Marine Productivity during Past 10,000 Years — A Study Based on Sediment Core Retrieved from Southeastern Arabian Sea

V. Yoganandan, C. Krishnaiah[1], K. Selvaraj[2], G.V. Ravi Prasad and Koushik Dutta[3]

Department of Marine Science, Bharathidasan University
Tiruchirappalli – 620024, India
[1]Ocean and Atmospheric Science & Technology Cell
Department of Marine Geology, Mangalore University
Mangalagangotri – 574199, India
[2]Institute of Marine Geology and Chemistry
National Sun Yat-sen University
Kaohsiung 804, Taiwan, R.O.C.
[3]Institute of Physics, Bhubaneswar – 751005, India
yoganandan1@rediffmail.com

INTRODUCTION

The intensity of the Indian monsoon has varied greatly over the past glacial-interglacial cycles as well as on shorter time scales (Duplessy, 1982; Van Campo, 1986; Clemens et al., 1991; Sirocko et al., 1993; Reichart et al., 1998; Von Red et al., 1999). It is well known that seasonal variation in the heating of the southern Asian continent produces a semiannual reversal in wind direction over the northern Indian Ocean (Wyrtki, 1973). In summer (June-September), the intense SW monsoon winds cause strong mixing of the water column and upwelling which eventually promotes high productivity

J. Sundaresan et al. (eds.), *Climate Change and Island and Coastal Vulnerability*,
DOI 10.1007/978-94-007-6016-5_2, © 2013 Capital Publishing Company

in the Arabian Sea. In contrast, during winter, reversal of weak and NW wind direction relatively lowers the productivity in the Arabian Sea (Quasim, 1977). It was demonstrated that biological productivity and terrigenous supply in the Arabian Sea is strongly linked to the intensity of the monsoon, although the lowest biological productivity was noticed during inter-monsoon period in the Arabian Sea. These strong seasonal contrasts during summer, winter and inter-monsoons also reflect in water column productivity in the Arabian Sea and therefore, considered as an excellent natural laboratory to study the paleomonsoon and associated productivity fluctuations. So carbonate and organic matter percentage of the undisturbed marine sediment core can be used to unravel the paleomonsoon and paleoproductivity fluctuation of the particular region.

Detailed studies have been carried out in the western and northeastern Arabian Sea to understand the productivity variation and terrigenous supply in relation to the strength of the SW monsoon during the Late Quaternary (Shimmield et al., 1990; Clemens et al., 1991; Anderson et al., 1993; Naidu et al., 1995). Nonetheless, limited studies have been made from the western continental margin of India with a main focus on the solid phase productivity indicators, calcium carbonate and organic matter, especially in terms of paleomonsoon fluctuations (Naidu, 1991; Paropkari et al., 1991; Thamban et al., 2001; Sarkar et al., 2000; Bhushan et al., 2001; Pattan et al., 2003).

In this paper we present the paleproductivity and paleomonsoon fluctuations based on the sedimentary calcium carbonate and organic carbon down sediment core variations (4.2 m long gravity core raised from the upper continental slope of southeastern Arabian Sea). Down-core variations of both parameters as well as textural parameters show productivity changes from late glacial through Holocene period.

MODERN CLIMATE AND OCEANOGRAPHY

The Arabian Sea experiences extremes in atmospheric forcing that lead to the greatest seasonal variability. Modern surface circulation in the Arabian Sea is modulated by the seasonal variation of the monsoonal wind system. This seasonal reversal of wind direction drives a strong southwest (SW) monsoon during the summer (June-September) and a moderate, dry northeast (NE) monsoon during the winter (December-February). Much of the intensity of the SW monsoon is derived from direct heating of the troposphere above Asia and through latent heat collected over southern subtropical Indian Ocean, which is transported across the equator and released by precipitation over South Asia (Clemens et al., 1991). The precipitation pattern over the Indian peninsula is controlled by the Western Ghats, the major physiographic feature along the west coast of India with elevations above 1000 m.

The region off southwestern India is characterized by a weak upwelling system during the summer monsoon. It has been observed that the upwelling along this coast begins as early as February, well before the onset of favourable

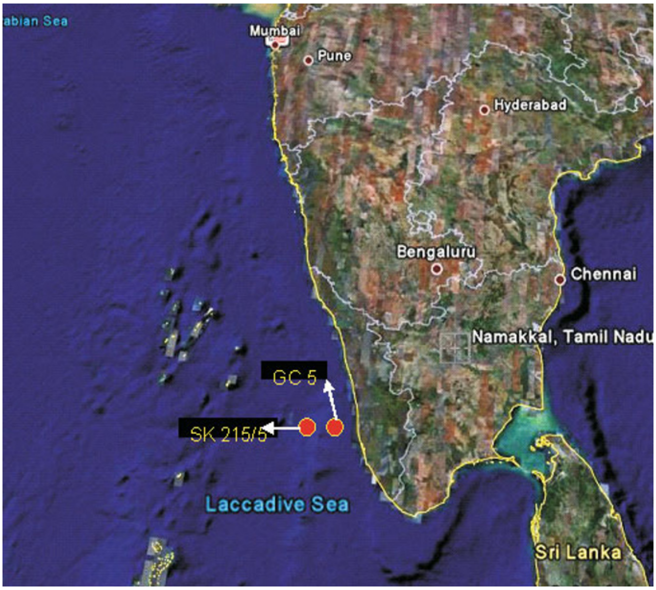

Fig. 2.1: Study area and location of the sediment core SK-215/5 and the Core GC5.

southwest monsoon winds (Shetye, 1984). Recent studies have demonstrated that this early upwelling is a consequence of remote forcing by winds in the Bay of Bengal and southwest coast of India via the poleward propagation of Kelvin waves along the west coast of India, which propagates rossby waves (Mc Mcreary et al., 1993; Shanker and Shetye, 1997). With the onset of the SW monsoon, the enhanced local winds intensify the upwelling effect.

MATERIALS AND METHODS

A 4.2 m long gravity core was collected from the southeastern part of the Arabian Sea (10°30′ N and 75°22′ E; Fig. 2.1) at the water depth of 460 m during the 215th Cruise of *O.R.V. Sagar Kanya* which has been used for this study. The core was sub-sampled onboard at 2 cm intervals for the top 1 m and 5 cm interval for the rest of the core. All the sub-samples were oven dried at 55°C. Textural analysis of the sediments was carried out on 60 representative sub-samples as per the standard procedure (Folk, 1968). All the sub-samples were finely powdered using an agate pestle and mortar for organic carbon and carbonate determinations. Organic matter was determined as readily oxidizable organic carbon by acid dichromate digestion and subsequent titration with ferrous ammonium sulphate (Gaudette et al., 1974). Calcium carbonate ($CaCO_3$) was determined as Ca by EDTA titration using P&R as internal indicator (Shapero and Brannock, 1962). Specimens of planktonic foraminifera were picked from the >250 µm sediment fraction at five selected depth intervals in core SK215/5 (Table 2.1) for ^{14}C dating.

These specimens were dated with Accelerator Mass Spectrometry (AMS) at the Institute of Physics, Bhubaneswar, India. Age model was then obtained by applying a reservoir age correction of ΔR138 ± 64 years to the ^{14}C dates assumed for the core location (SE Arabian Sea off Malabar coast) (Southon et al., 2002). The conventional AMS ^{14}C dates were calibrated into calendar ages using the latest database of CALIB rev 5.0.2 program (modified from the version CALIB 5.0) (Stuiver and Braziunas., 1993) and linearly interpolated to provide a continuous age scale.

Table 2.1: Details of AMS ^{14}C ages and calibrated calendar ages of selected depth intervals of the core SK-215/5

Lab ID	*Sample ID*	*Depth Interval (cm bsf)*	*^{14}C age (BP)*	*Cal^{14}C age (BP)*	*Cal age (kyr BP)*
693	SK-215/5	44	3392 ± 112	3068 ± 302	2.90
694	SK-215/5	98	6029 ± 112	6299 ± 299	6.36
695	SK-215/5	145	7530 ± 210	7885 ± 419	7.89
696	SK-215/5	215	8924 ± 131	9468 ± 392	9.35
697	SK-215/5	360	10,929 ± 122	12,244 ± 509	12.27

RESULTS

Texture Profile

Sand content of the core SK-215/5 fluctuates between 1% and 13% for the last ~13.5 kyr. Depth profile of sand shows low contents; maximum ~2% was recorded in sediments deposited between ~13.5 and 8 kyr BP (Fig. 2.2), indicating less terrigenous input into the study area. An abrupt increasing trend of sand was evident around 8 kyr BP and reaches its maximum (13%) at ~6.4 kyr BP, suggesting increased terrigenous input between these time intervals. The profile reveals that terrigenous input was more or less constant during the middle and latter part of the Holocene. Similar to sand, very low clay contents between 4% and 10% suggest an unchanged chemical weathering of continental rocks in the western part of India during the last 13.5 kyr. In the entire core, the dominant textural fraction of the sediment is silt, which varies between 80% and 96%. In general, minimum clay and maximum silt characterise the sediments of Late Glacial Maximum and early Holocene, whereas the maximum sand characterises the mid and late Holocene, indicating enhanced detrital input.

Carbonate Profile

Carbonate content varies between 34% and 7% (Fig. 2.2). Sediments deposited between ~13.5 and 8 kyr BP show low $CaCO_3$ content of around 7%.

Sediments of mid-Holocene show as high as 34% of $CaCO_3$. Late Holocene sediments show an average carbonate content of 29% with significant variations that is two highest percentage (34%) peaks at mid-Holocene at ~6.3 kyr BP (98 cm of the core) and again at ~3 kyr BP (44 cm of the core). The reduced percentage (29%) at ~4.2 kyr BP (68 cm of the core) and again the reduced values we could see after ~2 kyr BP. Clear increasing trend of $CaCO_3$ from 7% to 30% very consistent to sand increase and silt decrease between ~8 and 6 kyr BP indicating an enhanced supply of terrigenous input into the Seas.

Organic Carbon Profile

Down-core C_{org} variation of the core SK-215/5 fluctuates between 4% and 2% (Fig. 2.2) with a Holocene average C_{org} content of 3.6%. The profile shows in general a decreasing trend since ~10 kyr BP with minimum values of C_{org} prior to the Holocene. This trend as well as a steady increase from early to mid-Holocene periods that reaches the highest percentage of C_{org} 4.6 at ~3.8 kyr BP around 58 cm of the core and reduces to 3.6% at ~3 kyr BP (46 cm of the core) and again shows an increased value of 4% occuring at 1.8 kyr BP.

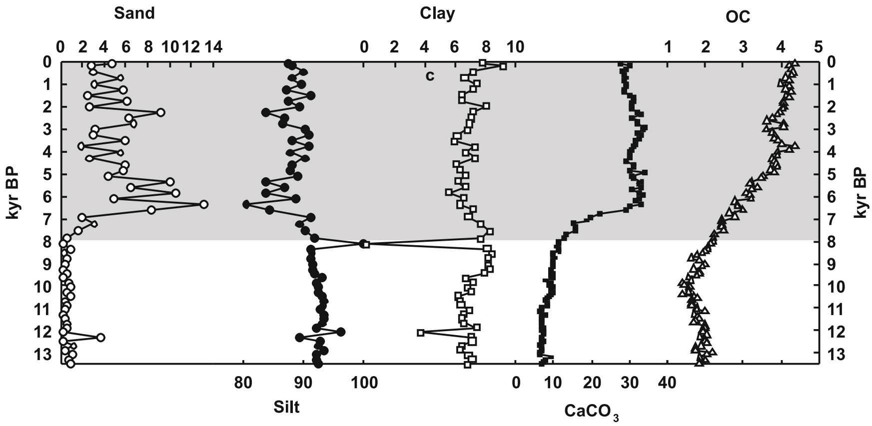

Fig. 2.2: Down-core profiles of sand, silt, clay, $CaCO_3$ and organic carbon in sediment core SK-215/5. All values are given in percentages. Gray bar highlights mid to late Holocene increased productivity.

DISCUSSION

The core SK-215/5 extends up to the late Glacial period (13.5 kyr BP) and this core has five age control points which reveal different sedimentation rates: late Holocene 15.4 cm/kyr, early Holocene 24.8 cm/kyr and late Glacial period records 31.16 cm/kyr. This record is comparable with sedimentation rate of shallow depth sediment core GC-5 (water depth: 280 m) studied by Thamban et al. (2001). The major difference between these two records is SK-215/5 shows an abrupt increase of sedimentation rate from the late Glacial to the early Holocene period which is not evident in GC-5 records. This increased sedimentation rate of SK-215/5 during late Glacial and early Holocene period may be due to high intensity monsoon/arid conditions in the hinterlands that might have increased the sediment depositional rate of SK-215/5 when compared to the shallow depth core GC-5.

Down-core profiles (Fig. 2.2) show reduced % of $CaCO_3$, C_{org} and reduced sand content and subsequent increased % of silt and clay between ~13.5 and ~8 kyr BP. This observation indicates reduced productivity during late Glacial to early Holocene period. This reduced productivity may be due to dilution of water column by fresh water input when the monsoon was intense, that might have altered the physico-chemical properties of the water column that favours the growth of the marine organisms. This interpretation is comparable with modern conditions along the southeastern Arabian Sea which gives supporting evidence to this argument. During intense monsoon low saline water column was observed in southeastern Arabian Sea (Naqvi, 1991; Stramma et al., 1996). Previous paleomonsoonal studies from the eastern Arabian Sea suggesting that intense precipitation had occurred during late Glacial to early Holocene period on the Indian subcontinent, which is coinciding with the Northern Hemisphere summer insolation maxima (Prell, 1984; Van Campo, 1986; Sirocko et al., 1993). Several workers have reported the major climatic, hydrographic and circulation change in the Indian monsoon regime immediately after ~16 kyr BP (Van Campo, 1986; Naqvi and Fairbanks, 1996; Overpeck et al., 1996; Thamban et al., 2001). The $\delta^{13}C$ record of peat from the Nilgiri Hills of the Western Ghats (South India) revealed that following dry LGM, moist conditions started at ~16 kyr BP (Sukumar et al., 1993). The recent multi proxy studies from Arabian Sea has proved that the summer monsoon, in general, was strongest in the early Holocene marked by high amplitude shifts between dry and wet phases (Guptha et al., 2005; Thamban et al., 2007; Tiwari and Ramesh, 2007; Yoganandan et al., 2009). The increased content of silt and clay and relatively high sedimentation rate are characteristic of late Glacial to early Holocene sediments from this region which was same as recorded in the earlier study (Thamban et al., 1997).

After this reduced productivity period all these proxies of the present studied core show distinct shift from low to high values between ~8.1 and 6.3 kyr BP. This shift indicates a major change in monsoonal rains from strong to weak Indian summer monsoon. The recent study from Arabian Sea also suggests gradual weakening of summer monsoon starting from ~8.2 kyr BP and this climate shift event is recorded in even other parts of the world (Guptha et al., 2005). Our data further shows that a significant shift (abrupt increasing trend) in carbonate % occurs between ~7 and 6.3 kyr BP, correlating with strong to weak summer monsoon transition during the mid-Holocene in India. A combination of archaeological and other land records in the Indian subcontinent also supports a substantial weakening of the summer monsoon at ~7 kyr BP (Gupta et al., 2006). After this major shift the increased % of $CaCO_{3,}$ C_{org} during the entire late Holocene period shows an increased productivity. This increased productivity may be due to weakening of summer monsoon which might have reduced fresh water input to the core site which might have favoured the marine organism to get suitable water column. This made the water column to become highly productive. This similar productivity trend was recorded by Thamban et al. (2001) and Pratima et al. (2010). The observed textural variation i.e. increased percentages of sand and silt after ~8.1 kyr BP may be due to rapid sea level rise which might have delivered the coarser grains to the core site due to coastal terrain erosion to maintain a dynamic equilibrium with static sea level.

The interesting observation from late Holocene section is the reduction of $CaCO_3$ and increase of C_{org} at ~4.2 kyr BP and ~2 kyr BP. This reduced productivity during these periods is due to the high intensity fresh water input resulting in dilution effect. This interpretation is supported by Indus river increased discharge events at ~4 kyr BP, revealed from the varve sediments record (Von Red et al., 1999). High intensity monsoon event at ~2 kyr BP is also recorded in an earlier study from the present study area (Thamban et al., 2001; Yoganandan et al., 2009). This reduced productivity events recorded from the present studied sediment core revealed that productivity of the southeastern Arabian Sea is highly influenced by paleomonsoon intensity of this region.

CONCLUSION

Texture, $CaCO_3$ and OC data of the present studied core recorded late Glacial to early Holocene reduced productivity and gradual increasing trend after ~8 kyr BP and reaches maximum ~6 kyr BP. Thereafter the increased productivity is continued till present except two major reduced productivity events. The interesting observation from this study shows that the water column productivity of the southeastern Arabian Sea, particularly southwest continental margin of India, is influenced by the paleoclimatic/paleomonsoon condition of the region, which is proved by the reduced productivity record of late Glacial to early Holocene; and ~4.2 kyr BP and ~2 kyr BP were the periods which injected large amount of fresh water to the southeastern Arabian sea due to high intensity of the monsoon. These high intensity monsoon periods were recorded very well in paleoclimatic studies from Indian continent.

REFERENCES

Anderson, D.M. and Prell, W.L. (1993). A 300 ky record of upwelling off Oman during the Late Quaternary: Evidence of the Asian southwest monsoon. *Paleoceanography.*, **8:** 193-208.

Bhushan, R., Dutta, K. and Somayajulu, B.L.K. (2001). Concentration and burial fluxes of organic carbon on the eastern margins of the Arabian Sea. *Marine Geology*, **178:** 95-177.

Chauhan, O.S. and Chaubey, A.K. (1991). Submarine physiography off Lakshadweep islands, north Indian Ocean. Paper presented at the International Symposium on the Oceanography of the Indian Ocean, 52 p.

Clemens, S., Prell, W.L., Murray, D., Shimmield, G.B. and Weedon, G. (1991). Forcing mechanisms of the Indian Ocean monsoon. *Nature*, **353:** 720-725.

Duplessy, J.C. (1982). Glacial to interglacial contrasts in the northern Indian Ocean. *Nature*, **295:** 494-498.

Folk, R.L. (1968). Petrology of sedimentary rocks. Hemphills, Austin, Texas.

Gaudette, H.E., Flight, W.R., Toner, L. and Folger, D.W. (1974). An inexpensive titration method for the determination of organic carbon in recent sediments. *Journal of Sedimentary Petrology*, **44:** 249-253.

Gupta, A.K., Anderson, D.M., Pandey, D.N. and Singhvi, A.K. (2006). Adaptation and human migration, and evidence of agriculture coincident with changes in the Indian summer monsoon during the Holocene. *Current Science*, **90:** 1082-1090.

Guptha, A.K., Das, M. and Anderson, D.M. (2005). Solar influence on the Indian summer monsoon during the Holocene. *Geophysical Research Letters*, **32:** L17703, doi: 10.1029/2005GL022685.

Mc Mcreary, J.P., Kundu, P.K. and Molinari, R.L. (1993). A numerical investigation of dynamics, thermodynamics and mixed-layer processes in the Indian Ocean. *Progress in Oceanography*, **31:** 181-224.

Naidu, P.D. and Malmgren, B.A. (1995). Monsoon upwelling effects on test size of some planktonic foraminiferal species from the Oman margin, Arabian Sea. *Paleoceanography*, **10:** 117-122.

Naidu, P.D. (1991). Glacial to interglacial contrasts in the calcium carbonate content and influence of Indus discharge in two eastern Arabian Sea cores. *Palaeogeography, Palaeoclimatology, Palaeoecology*, **86:** 255-263.

Nair, R.R. (1974). Holocene sea levels in the western continental shelf of India. *Proceedings Indian Academy of Sciences*, **79:** 197-203.

Naqvi, S.W.A. (1991). Georaphical extent of denitrification in the Arabian Sea in relation to some physical processes. *Oceanologica Acta.*, **14:** 281-290.

Naqvi, W.A. and Fairbanks, R.G. (1996). A 27,000-year record of Red Sea Outflow: Implications for timing of post-glacial monsoon intensification. *Geophysical Research Letters*, **23(12):** 1501-1504.

Overpeck, J., Anderson, D., Trumbore, S. and Prell, W. (1996). The southwest Indian Monsoon over the last 18,000 years. *Climate Dynamics*, **12:** 213-225.

Paropkari, A.L., Iyer, S.D, Chauhan, O.S. and Babu, C.P. (1991). Depositional environments inferred from variations of calcium carbonate, organic carbon and sulfur: A core from southwestern Arabian Sea. *Geo-Marine Letters*, **11:** 96-102.

Pattan, J.N., Masuzawa, T., Naidu, P.D., Parthiban, G. and Yamamoto, M. (2003). Productivity fluctuations in the southeastern Arabian Sea during the last 140 ka. *Palaeogeography, Palaeoclimatology, Palaeoecology*, **193:** 575-590.

Pratima, M. Kessarkar, Purnachandra Rao, V., Naqvi, S.W.A., Allan, R. Chivas and Saino, T. (2010). Fluctuations in productivity and denitrification in the southeastern Arabian Sea during the late Quaternary. *Current Science*, **99:** 485-491.

Prell, W.L. (1984). Variation of monsoonal upwelling: A response to changing solar radiation. *In:* Climate Processes and Climate Sensitivity. Hansen, J.E. and Takahashi, T. (eds). *Geophysical Monograph Series*, AGU, Washington D.C., **29:** 48-57.

Quasim, S.Z. (1977). Biological productivity of the Indian Ocean. *Indian Journal of Marine Science*, **6:** 122-137.

Reichart, G.J., Lourens, L.J. and Zachariasse, W.J. (1998). Temporal variability in the northern Arabian Sea Oxygen Minimum Zone (OMZ) during the last 225,000 years. *Paleoceanography*, **13:** 607-621.

Sarkar, A., Ramesh, R., Somayajulu, B.L.K., Agnihotri, R., Jull, A.J.T. and Burr, G.S. (2000). High resolution Holocene monsoon record from the eastern Arabian Sea. *Earth and Planetary Science Letters*, **177:** 209-218.

Shanker, D. and Shetye, S.R. (1997). On the dynamics of the Lakshdweep high and low in the southeastern Arabian Sea. *Journal of Geophysical Research*, **102(C6):** 12551-12562.

Shapero, L. and Brannock, W.W. (1962). Rapid analysis of silicate, carbonate and phosphate rocks. *United States Geological Survey Bulletin*, **1144:** A21-A22.

Shimmield, G.B., Mowbray, S.R. and Weedon, G.P. (1990). A 350 ka history of the Indian southwest monsoon—evidence from deep sea cores, northwest Arabian Sea. *Transactions of the Royal Society of Edinburgh Earth Sciences*, **81:** 289-299.

Sirocko, F., Sarnthein, M., Erlenkeuser, H., Lange, H., Arnold, M. and Duplessy, J.C. (1993). Century scale events in monsoon climate over the past 24,000 years. *Nature*, **363:** 322-324.

Southon, J., Kashgarian, M., Fontugne, M., Metievier, B. and Yim, W.W-S. (2002). Marine reservoir corrections for the Indian Ocean and SE Asia. *Radiocarbon*, **44:** 167-180.

Stramma, L., Fischer, J. and Schott, F. (1996). The flow field off southwest India at 8ºN during the southwest monsoon of August 1993. *Journal of Marine Research*, **54:** 55-72.

Stuiver, M. and Braziunas, T.F. (1993). Sun, ocean, climate and atmospheric $^{14}CO_2$: An evaluation of causal and spectral relationship. *Holocene*, **3:** 289-305.

Sukumar, R., Ramesh, R., Pant, R.K. and Rajagopalan, G. (1993). A $\delta^{13}C$ record of late Quaternary climate change from tropical peats in southern India. *Nature*, **364:** 703-706.

Thamban, M., Kawahata, H. and Rao, V.P. (2007). Indian Summer Monsoon Variability during the Holocene as Recorded in Sediment of the Arabian Sea: Timing and Implications. *Journal of Ocenaography*, **63:** 1009-1020.

Thamban, M., Purnachandra Rao, V. and Raju, S.V. (1997). Controls on organic carbon distribution in sediments from the eastern Arabian Sea margin. *Geo-Marine Letters*, **17:** 220-227.

Thamban, M., Rao, V.P., Schneider, R.R. and Grootes, P.M. (2001). Glacial to Holocene fluctuations in hydrography and productivity along the southwestern continental margin of India. *Palaeogeography, Palaeoclimatology, Palaeoecology*, **165:** 113-127.

Tiwari, M. and Ramesh, R. (2007). Solar variability in the past and palaeoclimate data pertaining to the southwest monsoon. *Current Science*, **134:** 149-169.

Van Campo, E. (1986). Monsoon fluctuation in two 20,000 yr B.P. oxygen-isotope/pollen records off southwest India. *Quaternary Research*, **26:** 376-388.

Von Red, U., Schaaf, M., Michels, K.H., Schulz, H., Berger, W.H. and Sirocko, F. (1999). A 5000-yr record of climate change in varved sediments from the oxygen minimum zone off Pakistan, northeastern Arabian Sea. *Quaternary Research*, **51:** 39-53.

Wyrtki, K. (1973). Physical oceanography of the Indian Ocean. *In:* The biology of the Indian Ocean. B. Zeitzschel (ed.). Springer, Berlin.

Yoganandan, V., Krishnaiah, C., Selvaraj, K., Ravi Prasad, G.V., Gangadhara, H., Bhat, H., Chen, C.T.A. and Koushik Dutta (2009). Late Glacial-Holocene Indian Monsoon changes: A sediment core record from the southeastern Arabian Sea. Paper presented at PAGES 1st Young Scientist Meeting on Retrospective view on our planet future held at Oregon State University, Corvallis, USA, during 6-7 July 2009.

CHAPTER

3

Prediction of Rain on the Basis of Cloud Liquid Water, Precipitation Water and Latent Heat in the Perspective of Climate Change over Two Coastal Stations

Rajasri Sen Jaiswal, Neela V.S., Sonia R. Fredrick, Rasheed M. and Leena Zaveri

Centre for Study on Rainfall and Radiowave Propagation (CRRP)
Sona College of Technology, Salem - 5
Tamil Nadu, India
crrp.official@yahoo.com

INTRODUCTION

Prediction of rainfall and its dependence on meteorological elements like temperature, pressure, dew point temperature, precipitable water, cloud liquid water, latent heat etc. need to be explored in depth. It is necessary to know the interaction between these parameters leading to rain. Precipitable water is defined as the depth of water that would result if all the water vapour in a unit column of air was condensed to precipitation (Max, 2001). Precipitation water (PW) is the actual amount of water vapour in the atmosphere that has condensed to rain. Total precipitable water is known to be closely related to precipitation (Battan and Kassander, 1960). Cloud liquid water affects radiative properties of clouds as increased water content leads to higher cloud albedo and emissivity (Taylor and Ghan, 1992). This, in turn, affects the radiation budget of the atmosphere. Latent heat budget, on the other hand, affects global circulation which, in turn, governs the weather system. At the same

J. Sundaresan et al. (eds.), *Climate Change and Island and Coastal Vulnerability*,
DOI 10.1007/978-94-007-6016-5_3, © 2013 Capital Publishing Company

time, latent heat released, or absorbed, in the atmosphere also seems to affect cloud liquid water as solar radiation absorbed by water bodies, and latent heat of condensation released at higher altitudes, trigger the entire mechanism of cloud formation. Thus, the study of cloud liquid water, precipitable water and latent heat is of immense importance in cloud physics.

In this article, an attempt has been made to discover imprints of rain on the basis of cloud liquid water, precipitation water and latent heat available at various levels in the atmosphere over Chennai (13.03 N 80.71 E) and Trivandrum (8.29 N 76.59 E). Moreover, as the two selected stations are vulnerable to climate change, an attempt has been made in particular to investigate the changes in these parameters over the period of study. Due to the proximity to the ocean, the socio-economic condition of these two stations is largely dependent on climate. Fishery and tourism are the two major sources of income in rural coastal areas of Trivandrum and Chennai, as well. While climate is the chief asset of tourism, climate change can pose a serious threat to it, affecting the rural industry here.

Impact of climate change is manifested in sea level rise and rise in sea surface temperature (SST), to name a few (World Bank, 2010; Cochin University of Science and Technology and Oak Ridge National Lab., 2003). Rise in SST leads to coral bleaching and destruction of ornamental organisms (Jeffrey et al., 2008). A rise in sea level will cause soil erosion, thereby weakening solid structures of hotels in the coastal areas. Rise in sea level can induce intrusion of salty water into agricultural land, affecting crop production and protection. A study shows that cashew production has been adversely affected in Kerala because of change in rainfall pattern in this state (Rao et al., 2009).

Increase in SST will lead to increased level of moisture into the atmosphere (Sem, 2007), thereby increasing humidity. Increased SST will lead to increased rainfall. Change in rainfall pattern and increase in SST will increase the frequency and intensity of cyclones and hurricanes (Michaels et al., 2006; Wolff et al., 2005), threatening the mangroves and the life and properties of mankind. Hence, it is necessary to closely monitor any changes in rainfall pattern and other meteorological elements over the coastal areas as an advanced safety measure. In this paper an attempt has been made to investigate the changes in rainfall pattern over Chennai and Trivandrum. In addition to this, changes in surface temperature and upper air meteorological elements, viz., CLW and PW from surface upto a height of 18 km have also been investigated.

These parameters are recorded by the Microwave Imager (TMI) onboard Tropical Rainfall Measuring Mission (TRMM) satellite. Validation of accumulated rainfall and rainfall intensities estimated by TRMM against those recorded by rain gauges and radar shows good agreement (Wolff et al., 2005). Study of Balaji et al. (2010) shows that TRMM estimated rainfall intensities match well with the Bayesian retrievals. Comparison of TRMM estimated rainfall intensities with RADAR-AMeDAS shows that the yearly rainfall amounts are almost the same (Oki and Kozu, 2000). Comparison of accumulated rainfall data product 3B42 V6 (disc.sci.gsfc.nasa, 2011) shows good agreement with that recorded by disdrometer over Calcutta (Maitra et al., 2009). However, TRMM algorithm estimates CLW, PW and LH only in rainy condition (personal communication with the TRMM group). Moreover, for precipitating systems smaller than PR footprints, the level 2 products 2A23 and 2A25 (disc.sci.gsfc.nasa, 2011) may give rise to error in estimating the vertical structure, rainfall classification and intensity (Heymsfield et al., 2000). For precipitating systems larger than the PR footprint, the reflectivity profiles of the PR match very well with the high-altitude Doppler radar (Heymsfield et al., 2000).

Present study consists of surface temperature, cloud liquid water, precipitation water and latent heat over two Indian coastal stations, namely, Chennai and Trivandrum. Particular attention has been given to find out the dominance of convective and stratiform rain over surface rainfall, i.e. the conditions under which convective/stratiform rainfall contributes more to surface rainfall. The primary aim of this study is to find out whether CLW, PW and LH can predict rainfall. Attempts are also made to find out whether any correlations exist between convective rainfall and precipitated water. Attempt has been made in particular, to investigate the changes in these parameters, if any, over the period of study.

MATERIALS AND METHODS

In the present study, cloud liquid water (CLW), precipitation water (PW) and latent heat (LH) values recorded by the TRMM Microwave Imager (TMI) onboard Tropical Rainfall Measuring satellite (TRMM) over Chennai and Trivandrum for the year 1999-2008 have been used. For validation of TRMM estimated rainfall with ground truth over Trivandrum, the rainfall recorded by TRMM and IMD during the period 1999-2008 has been used. It is noteworthy that over Chennai, rainfall data recorded by IMD were not available beyond 2005. Hence over Chennai, the validation has been performed for the period 1998-2005. The TMI profiling algorithm 2A12 generates vertical profiles of CLW, PW and LH from TMI brightness temperatures by combining the radiometric data with cloud models. These data are obtained at 14 vertical levels (Table 3.1) on a pixel by pixel basis, i.e. for each pixel, these values are given at 14 vertical levels.

The values of CLW and PW are in the range 0.00-10.00 gm^{-3}, and are multiplied by 1000, and stored as 2-byte integers (2008). The values of LH are in the range –256 °C/hr to 256 °C/hr. These values are multiplied by 10, and stored as 2-byte integers (ftp://disc2., 2008). The study also includes convective rainfall and surface rainfall data of 2A12 (2011). These data, the level 2 products 2A12 (disc.sci.gsfc.nasa, 2011) of the TMI are available in

Table 3.1: Vertical profile

14 Vertical profiling layers		*14 Vertical heating level*	
Layer index	*Layer height (km)*	*Level index*	*Level height (km)*
1	surface - 0.5	1	0
2	0.5-1.0	2	1.0
3	1.0-1.5	3	2.0
4	1.5-2.0	4	3.0
5	2.0-2.5	5	4.0
6	2.5-3.0	6	5.0
7	3.0-3.5	7	6.0
8	3.5-4.0	8	7.0
9	4.0-5.0	9	8.0
10	5.0-6.0	10	9.0
11	6.0-8.0	11	10.0
12	8.0-10.0	12	12.0
13	10.0-14.0	13	14.0
14	14.0-18.0	14	16.0

Hierarchical Data Format (HDF), and have been converted to ASCII before further analysis, taking care of the surface flag (2008). A surface flag “0” corresponds to the data recorded over ocean, and a surface flag “1” denotes the data recorded over land, while the data recorded over coastal region are represented by a surface flag “2”. It is noteworthy that TMI data product 2A12 gives correct estimation of parameters over ocean, but not over land, or coastal area (ftp://disc2., 2008). Hence, in this study, geo locations over ocean have been chosen. For example, stations “Chennai” and “Trivandrum” represent geo locations over ocean closest to Chennai and Trivandrum, respectively. It is further to note that in this study, only those rainfall events that had been recorded by TRMM were chosen. Several rainfall events had not been recorded by TRMM as there were no TRMM passes at those times.

In order to find out whether any correlations exist between the height of the levels and these parameters, and to seek for a functional relationship between them, if any, the values of PW, LH, CLW and level height recorded for the year 2007 have been fitted to different models, i.e. cubic, linear, quadratic, power, exponential, *s*, logarithmic, growth, inverse, logistic and compound. The validity of the relationship is judged by F test at a 5% level of significance. Particular attention has been given to find out the dependence of surface rainfall and convective rainfall on PW. For this purpose, the values of convective/surface rainfall and PW have been fitted to the above models. The validity of the relationship is judged by F test at a 5% level of significance.

The surface temperature data obtained from NOAA (2012) over the period of study have been used to find the changing trend in temperature over the two stations.

RESULTS AND DISCUSSION

Validation of TRMM Estimated Rainfall with Ground Truth

In order to validate TRMM estimated rainfall with ground truth, the daily rainfall data product 3B42 V6, which is a combined product of SSMI, AMSI and AMSU, has been compared with that obtained from the India Meteorological Department over Chennai and Trivandrum. The yearly accumulated rainfall shows good agreement between the two over Chennai (Fig. 3.1a). However, over Trivandrum, there exists some difference between the two (Fig. 3.1b).

Figure 3.1 further shows an increasing trend of rainfall over years over Chennai and Trivandrum. It is noteworthy that the rainfall trend is period sensitive, i.e. over a period of few years, the trend may be increasing, but

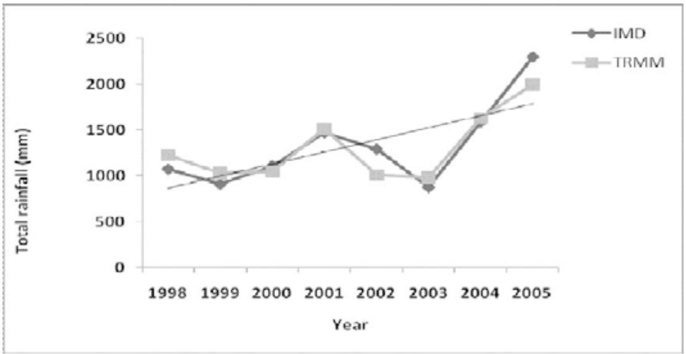

Fig. 3.1a: Yearly comparison of TRMM and IMD rainfall over Chennai.

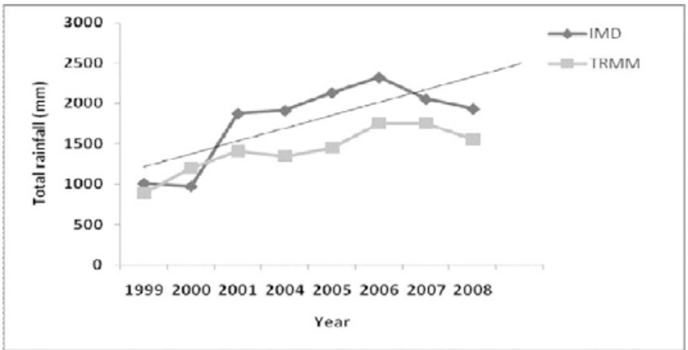

Fig. 3.1b: Yearly comparison of TRMM and IMD rainfall over Trivandrum.

over different period, the trend may or may not be the same. This is illustrated in Fig. 3.1c. It is seen from Fig. 3.1a and c that over Chennai, yearly rainfall shows an increasing trend till the year 2005, but during the period 2005-2008, it shows a decreasing trend.

The monthly accumulated rainfall also shows fairly good agreement (Figs 3.1d and 3.1e). However, the yearly accumulated rainfall shows better agreement than the monthly one in some cases, while in some cases the reverse is true.

A change in trend is observed in monthly rainfall as well, over these two stations. Over Trivandrum, the monthly rainfall shows an increasing trend in the months of March and April and during July-December, while the months of January, February, May and June show a decreasing trend (Figs 3.2a-l).

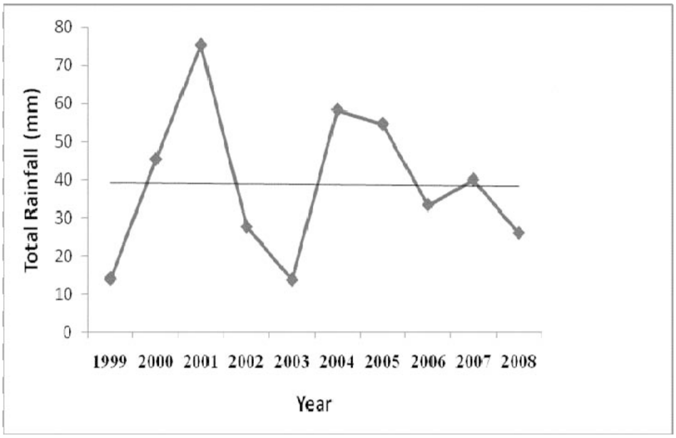

Fig. 3.1c: Yearly rainfall over Chennai for the years 1999 to 2008.

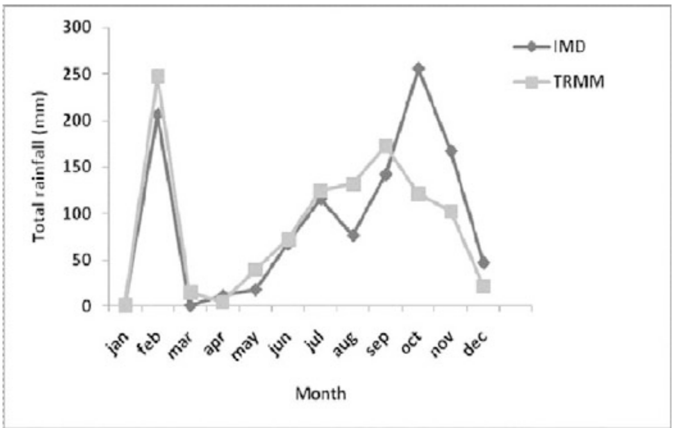

Fig. 3.1d: Monthly comparison of TRMM and IMD rainfall over Chennai for the year 2000.

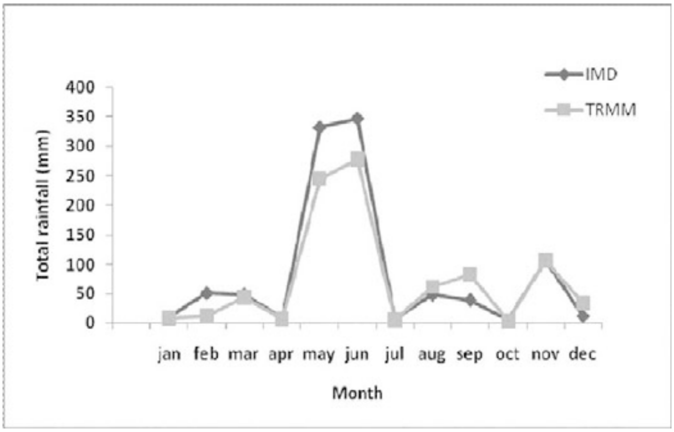

Fig. 3.1e: Monthly comparison of TRMM and IMD rainfall over Trivandrum for the year 1999.

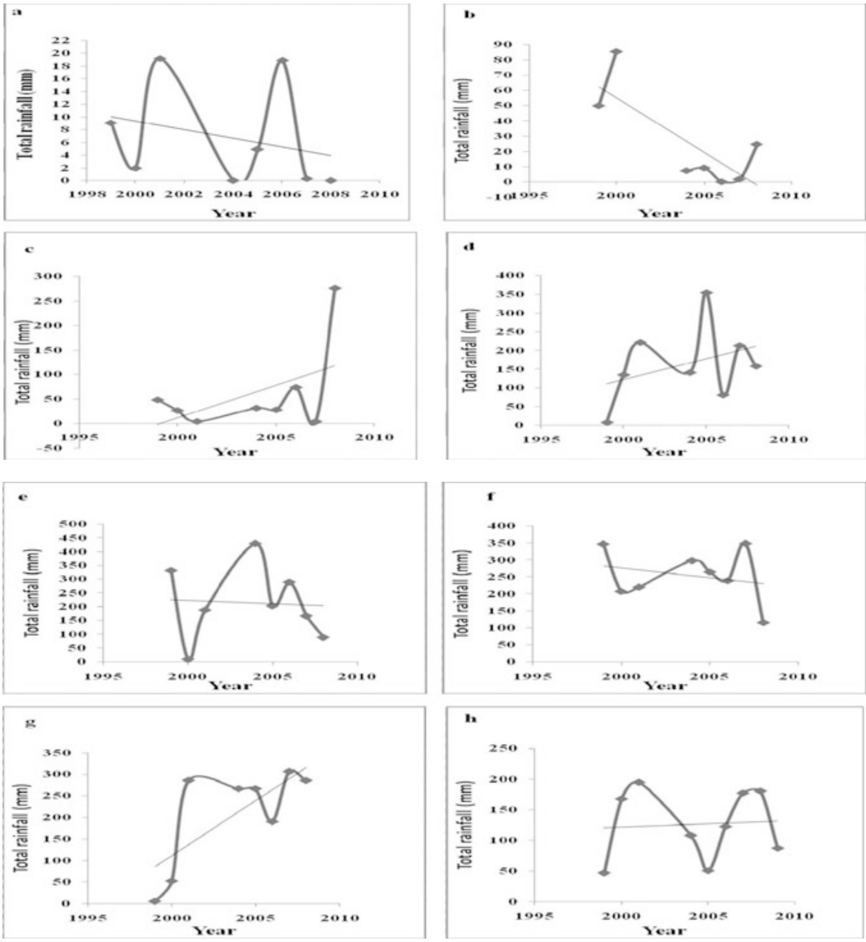

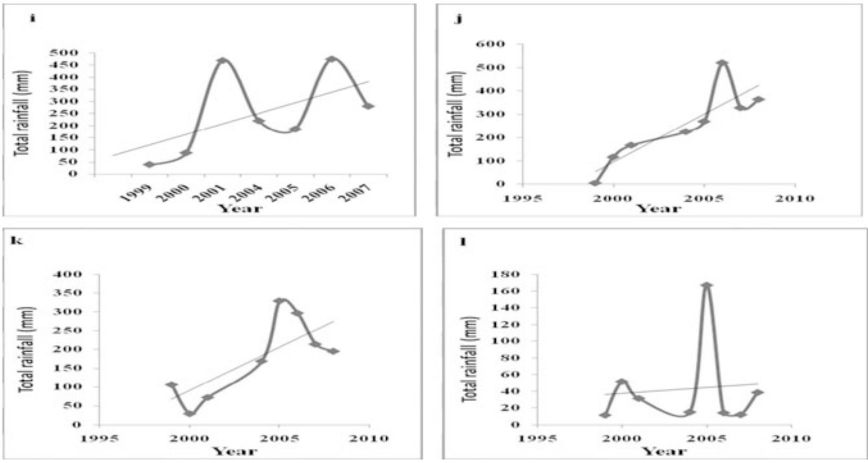

Fig. 3.2: Monthly rainfall trend over Trivandrum. (a) January, (b) February, (c) March, (d) April, (e) May, (f) June, (g) July, (h) August, (i) September, (j) October, (k) November and (l) December.

Over Chennai, monthly rainfall shows an increasing trend in the months of January, March-May, July and during September-December, while the months of February, June and August record a decreasing trend (Figs 3.3a-l).

This is noteworthy that due to lack of rainfall data from IMD, the monthly trend has not been investigated beyond 2005 over Chennai. The increasing trend in rainfall over Chennai and Trivandrum may be attributed to climate change owing to the fact that both these places lie in the coastal region, and that the coastal climates are largely affected by the atmosphere-ocean interactions. Severe weather phenomena, such as cyclones, hurricanes etc. influence coastal weather to a large extent (Hsu, 1988). In addition to

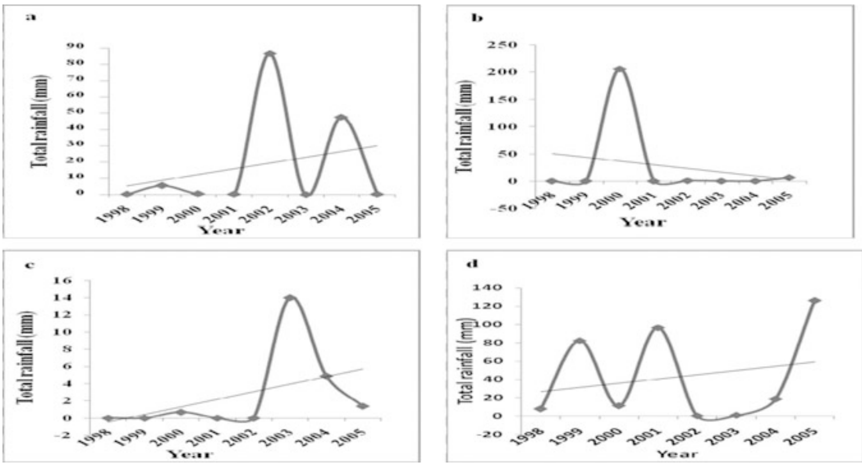

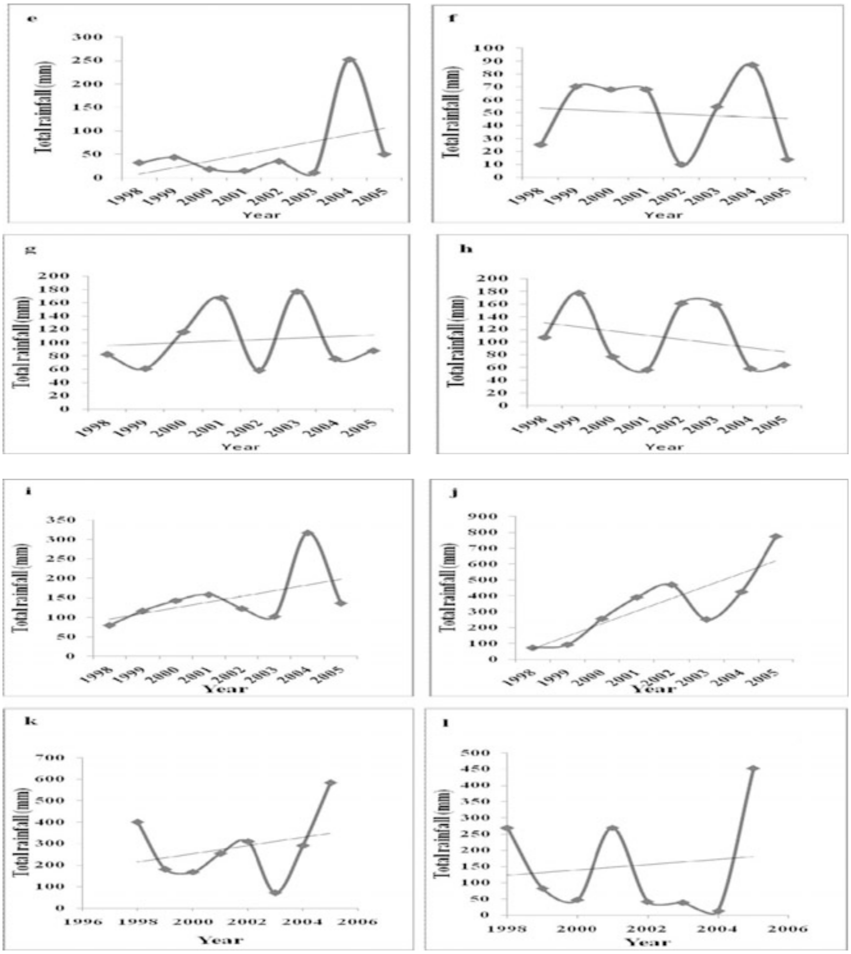

Fig. 3.3: Monthly rainfall trend over Chennai. (a) January, (b) February, (c) March, (d) April, (e) May, (f) June, (g) July, (h) August, (i) September, (j) October, (k) November and (l) December.

this, atmospheric tele-connections, viz., El Nino and La Nina also influence coastal climate (Ummenhofer et al., 2011) in terms of change in rainfall pattern and SST etc. Thus, the coasts and the islands are the worst affected by climate change.

Kumar et al. (2008) show the impact of climate change on local weather. It is found that rainfall is decreasing over most parts of central India during the pre-monsoon season, indicating reduction in convective activity during this time (Krishnakumar et al., 2009). Contribution of June rainfall has increased at several places of India, while it has decreased at several other places (Guhatakurta and Rajeevan, 2006).

Contribution of July rainfall has decreased in central and west peninsular India (Guhatakurta and Rajeevan, 2006). In order to find out the changes in rainfall pattern at these two coastal stations, authors have divided the rainfall into six categories (Jaiswal et al., 2011), viz., extreme rainfall (>50.0 mm/hr), very heavy rainfall (16.0-50.0 mm/hr), heavy rainfall (4.0-16.0 mm/hr), intermediate rainfall (1.0-4.0 mm/hr), low rainfall (0.25-1.0 mm/hr) and very low rainfall (<0.25 mm/hr), and have investigated the changes in the occurrence and contribution of these categories to total rainfall at the stations, over the period of study. It is found that over Chennai, most of the rainfall comes from extreme rainfall (37.4-58.6%), and 43.3-48.4% of the total rainfall comes from very heavy category. It is found over the period of study that there is a changing trend in these two categories of rainfall. This is illustrated in Fig. 3.4a and b. It is seen from Fig. 3.4 that both the extreme and very heavy rainfall categories show an increasing trend, justifying the increasing trend of total rainfall at this station (Fig. 3.1c).

Over Trivandrum, most of the rainfall comes from heavy rainfall (39.9-49.9%), and 19.8-38.9 % of the rainfall comes from very heavy category. Over Trivandrum, due to non-availability of continuous rainfall data for several years from IMD, the yearly trend for these two categories of rainfall could not be investigated.

In order to investigate the impacts of climate change in relation to other meteorological elements, surface temperature, total CLW and PW values from the surface up to 18 km in the atmosphere during the period 1999-2008 have been analyzed over these two stations for the period of study. It is found that over Chennai, CLW and PW show an increasing trend (Figs 3.5a and 3.5b), while surface temperature shows a decreasing trend (Fig. 3.5c).

However, over Trivandrum, CLW, PW and surface temperature show an increasing trend (Figs 3.6a-c).

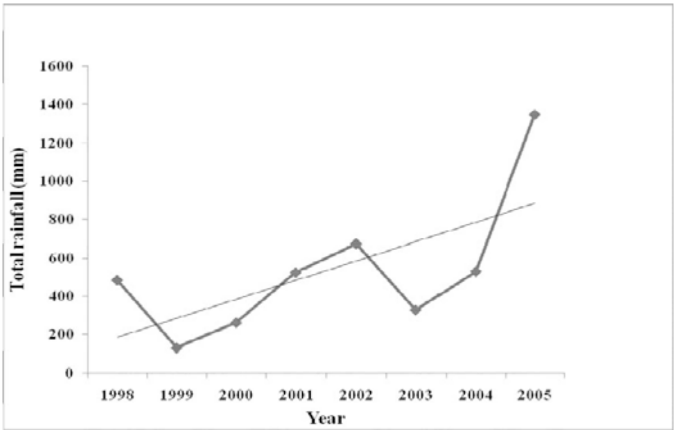

Fig. 3.4a: Extreme rainfall trend over Chennai during 1998-2005.

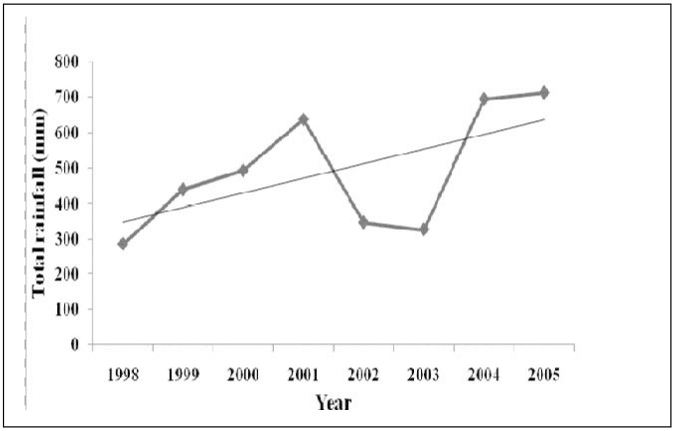

Fig. 3.4b: Very heavy rainfall trend over Chennai during 1998-2005.

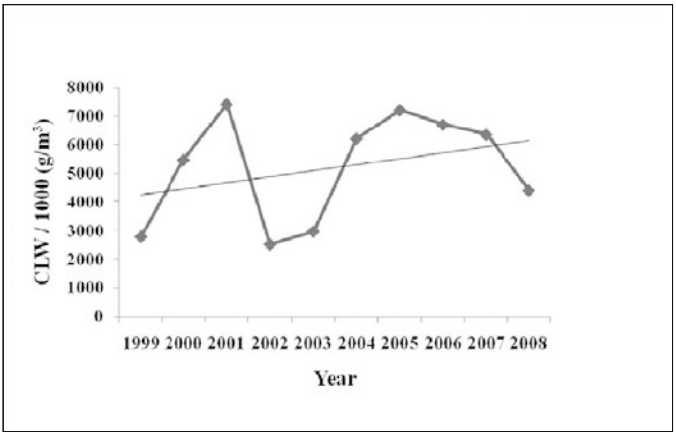

Fig. 3.5a: Yearly trend of CLW over Chennai during 1999-2008.

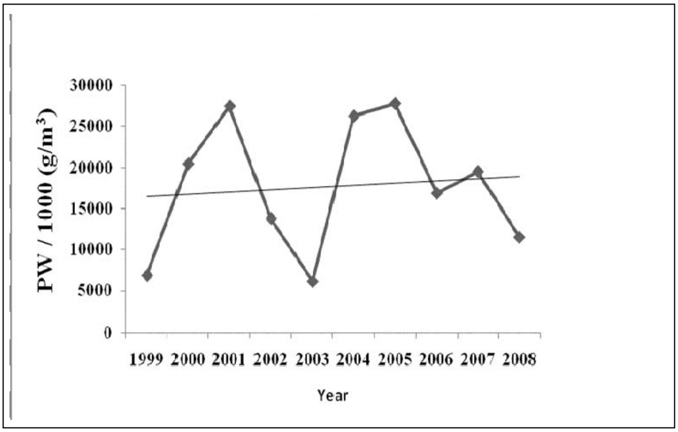

Fig. 3.5b: Yearly trend of PW over Chennai during 1999-2008.

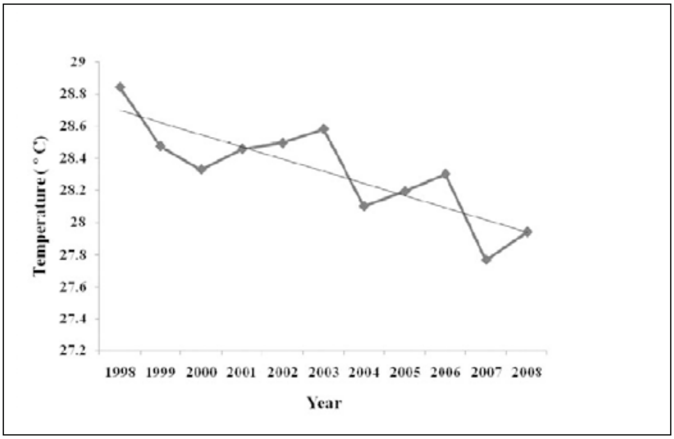

Fig. 3.5c: Yearly trend of temperature over Chennai during 1998-2008.

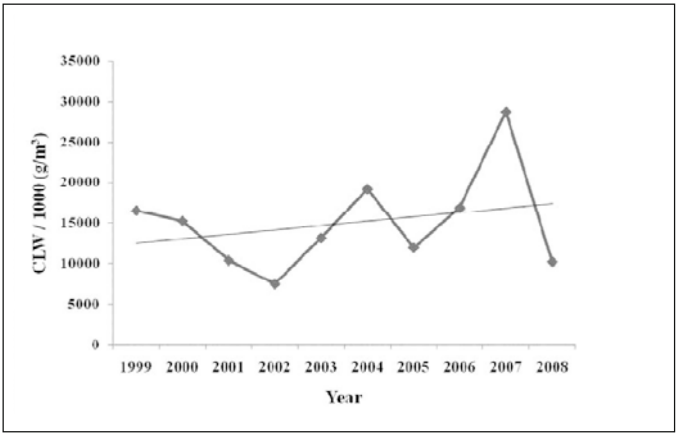

Fig. 3.6a: Yearly trend of CLW over Trivandrum during 1999-2008.

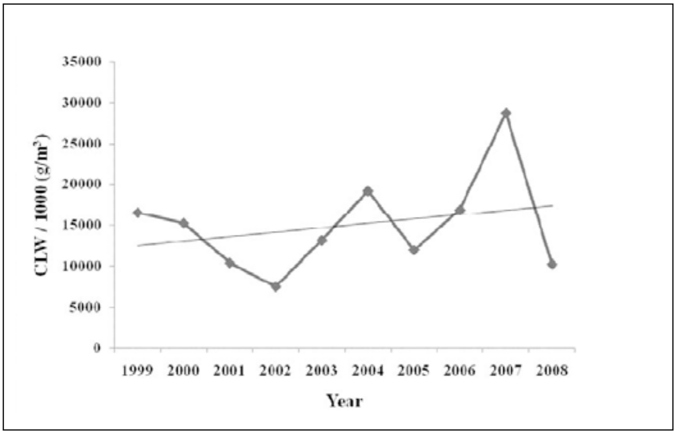

Fig. 3.6b: Yearly trend of PW over Trivandrum during 1999-2008.

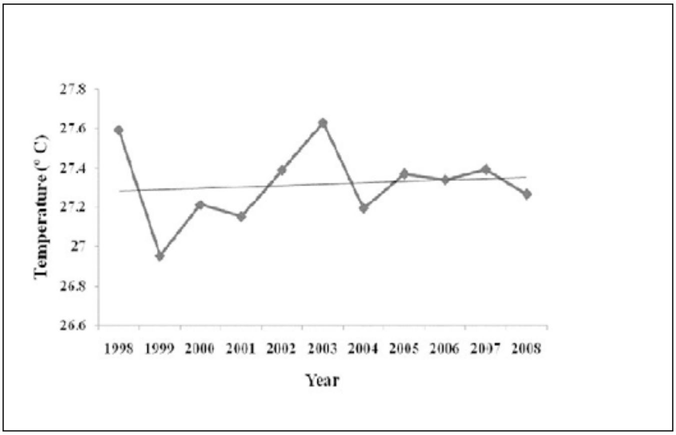

Fig. 3.6c: Yearly trend of temperature over Trivandrum during 1998-2008.

Vertical Profile of CLW, PW and LH

Values of CLW, PW and LH have been plotted against height (Fig. 3.7). The heights so chosen are TRMM vertical profiling heights, and are given in Table 3.1. It is seen from Figs 3.7a and 3.7b that as height increases from the surface, CLW also increases; reaches a maximum and then gradually decreases with increase in height. Profile of liquid water content over Kolkata shows the same result (Chakraborty and Maitra, 2012). Work of Taylor and Ghan (1992) shows that with increase in altitude cloud liquid water, averaged over time and entire global area decreases. For the entire study period, CLW is found to bear a cubic relation with height over Trivandrum and Chennai. CLW shows its peak always at 2.5-3.5 km, both over Trivandrum and Chennai.

Variation of PW with height shows that as height increases, PW also increases, the tail starting from a non-zero value; reaches its peak, and thereafter gradually decreases with increase in height (Fig. 3.7b). Over Trivandrum, PW shows its peak sometimes at 2.5-3.5 km, and on some days the peak lies at 1.0-1.5 km. Over Chennai, PW peak lies at 3.0-4.0 km on most of the days, and at 1.0-1.5 km on some days. PW bears a cubic relation with height irrespective of day and month studied.

LH varies in oscillatory manner with height (Figs 3.7c and 3.7d), and it shows a moving average relation with height on all days and in all months. Over Trivandrum, maximum LH evolved mostly occurs at 9.0 km. Several times it occurs at 3.0 km. Sometimes the peak is found at 2.0 km or 8.0 km. Rarely it occurs between 4.0 and 7.0 km. It is noteworthy that whenever the LH evolution peak occurs at 8.0-9.0 km, stratiform dominance is observed over surface rainfall. Moreover, it is found that in winter months during December-February, the LH evolution peak mostly occurs at 8.0-9.0 km, indicating lack of convective activity in the atmosphere during this season. It is further found that whenever the peak occurs at 2.0-6.0 km, the surface

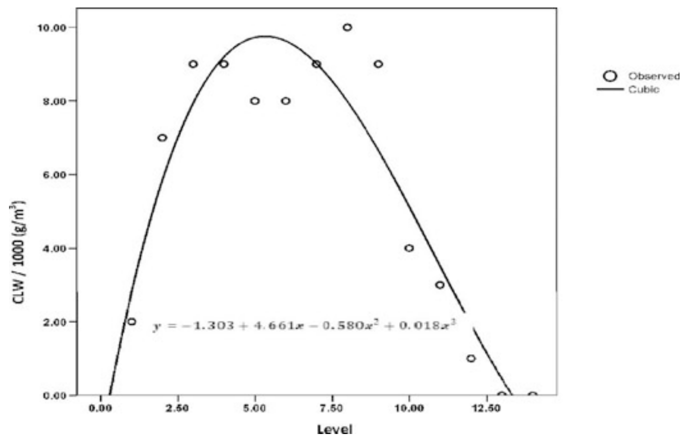

Fig. 3.7a: Variation of CLW with height over Chennai on 13 Sep 2007.

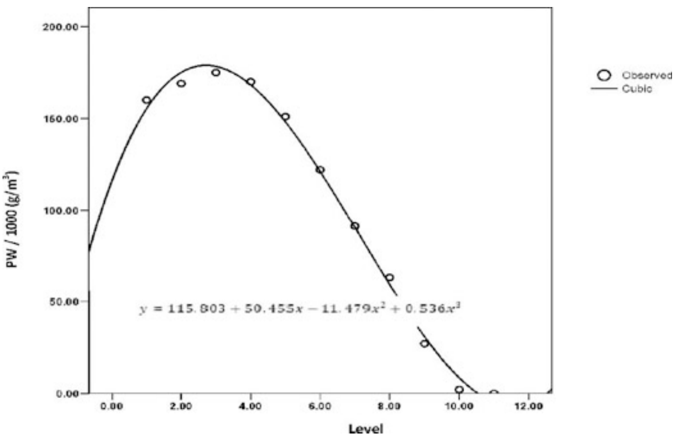

Fig. 3.7b: Variation of PW with height over Chennai on 1 Oct 2007.

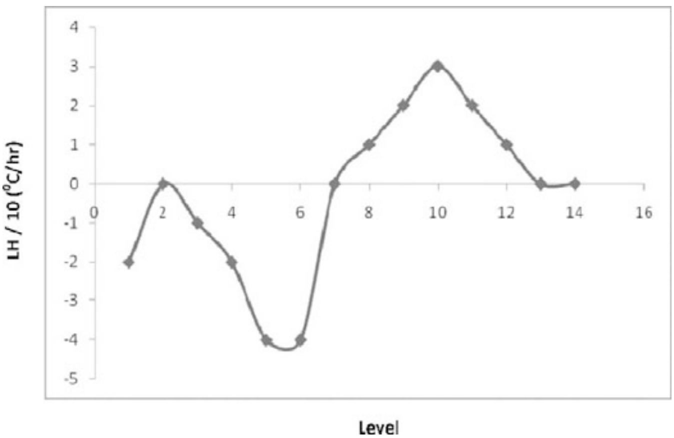

Fig. 3.7c: Variation of LH with height over Chennai on 2 Dec 2007.

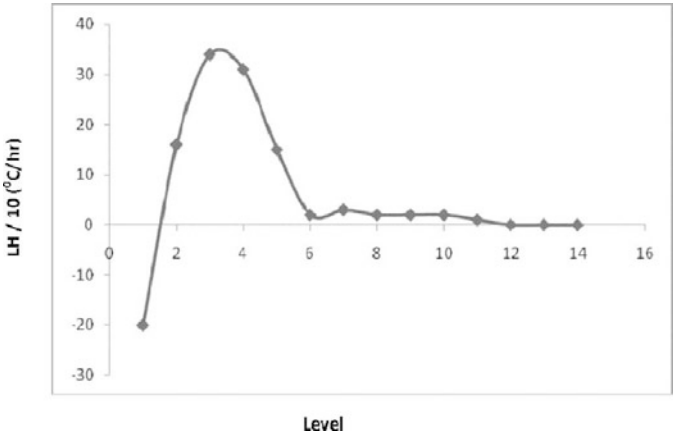

Fig. 3.7d: Variation of LH with height over Trivandrum on 29 Nov 2007.

rainfall is dominated by convective rain. Over Chennai, maximum heat evolved lies mostly at 9.0 km. However, on some days it lies at 8.0 km. Rarely the peak is found at 2.0 km, 3.0 km, 4.0 km and 7.0 km. Whenever the LH evolution peak occurs at 8.0-9.0 km, a stratiform dominance is observed on surface rainfall, while a convective dominance is noticed when the peak occurs at 2.0-7.0 km. During December-February and in July, mostly a stratiform dominance is observed, indicating lack of convective activity during this time. It is also found that maximum LH is absorbed at the surface level on some days, and sometimes the peak is found between 4.0-5.0 km, both over Chennai and Trivandrum.

Identification of Convective/Stratiform Contribution to Total Rainfall on the Basis of Vertical Profile of CLW, PW and LH on Daily Basis

It is found from Tables 3.2a and 3.2b that if the total PW in a day is very high along the entire vertical column, contribution of convective rain to surface rainfall is more than stratiform rain. Moreover, under such circumstances, i.e. if the total PW on a particular day is very high, the convective rainfall and surface rainfall also are very high on that day.

Observing the vertical profiles of LH (Tables 3.2a and 3.2b), it is found that if the net heat evolved is positive (i.e. the case of evolution) on a day, then the contribution of convective rain to surface rainfall is more on that day. It is further found from Tables 2a and 2b that if the latent heat absorption peak is over the surface, the contribution of convective rain to surface rainfall is more. However, the dominance of stratiform rain over surface rainfall is characterized by a net absorption of heat along the vertical column, or a net zero evolution of heat (Tables 3.2a and 3.2b). It is further found out that in case of stratiform dominance, the LH absorption peak lies at higher level, i.e. at 4.0-5.0 km. This result is observed in 100% cases.

Table 3.2a: Identification of convective/stratiform dominance over surface rainfall in view of daily vertical profile over Trivandrum in 2007

Date	*Convective rainfall (mm/hr)*	*Stratiform rainfall (mm/hr)*	*Surface rainfall (mm/hr)*	*Levels at which CLW peak occurs*	*PW/ 10^3 at CLW peak (g/m^3)*	*Maximum PW/10^3 on that day (g/m^3)*	*Total PW/10^3 (g/m^3)*	*Level at which LH absorbed is maximum*	*Total LH/10 (°C/hr)*	*Dominance over surface rainfall*
01 Mar	3.984	0.486	4.470	7	161	249	1722	Surface	204	Convective
17 Mar	3.213	2.020	5.233	4	280	289	2136	Surface	121	Convective
7 Apr	10.362	5.196	15.558	9	438	853	3486	Surface	613	Convective
9 Apr	1.177	1.398	2.576	5	125	198	1113	Surface	63	Stratiform
29 Apr	1.286	0.580	1.866	7	68	131	854	Surface	39	Convective
8 May	0.023	0.026	0.050	6,7	5,5	6	44	-	0	Stratiform
29 May	2.209	0.393	2.602	6	107	156	1004	Surface	76	Convective
30 May	0.250	1.253	1.502	8	113	117	946	5	-21	Stratiform
4 Jun	1.285	0.715	2.000	7	68	130	849	Surface	39	Convective
7 Jun	0.046	0.075	0.120	6,7	13,15	15	113	6	-6	Stratiform
16 Jun	6.913	1.708	8.620	8	275	466	3388	Surface	278	Convective
17 Jun	0.018	0.022	0.040	6,7	5,6	7	44	-	0	Stratiform
20 Jun	6.990	1.057	8.046	7	283	414	3015	Surface	272	Convective
03 Jul	0.012	0.013	0.024	6,7	3,3	4	26	-	0	Stratiform
09 Jul	1.287	0.615	1.903	7	68	133	865	Surface	39	Convective
21 Jul	4.453	0.848	5.301	7	177	294	2005	Surface	136	Convective
24 Jul	4.581	0.880	5.461	7	184	305	2079	Surface	140	Convective

(*Contd*)

Table 3.2a: *(Contd)*

2 Aug	7.456	2.500	9.957	8	349	535	4023	Surface	327	Convective
26 Aug	2.097	0.346	2.443	6	101	147	942	Surface	64	Convective
28 Aug	5.908	0.767	6.675	7	228	356	2505	Surface	209	Convective
30 Aug	0.115	0.244	0.359	7	35	35	279	6	-11	Stratiform
31 Aug	3.939	0.644	4.583	7	149	260	1738	Surface	118	Convective
4 Sep	0.072	0.117	0.190	6,7	18,19	20	153	6	-6	Stratiform
8 Sep	5.052	0.757	5.809	7	195	318	2187	Surface	165	Convective
13 Sep	0.126	0.310	0.436	7	41	41	328	6	-10	Stratiform
21 Sep	2.663	0.463	3.126	7	97	185	1198	Surface	79	Convective
7 Oct	0.045	0.060	0.105	6,7	11,13	13	92	5,6	-4	Stratiform
13 Oct	0.290	1.578	1.868	8	140	157	1180	5	-8	Stratiform
19 Oct	0.085	0.163	0.248	7	28	28	212	5,6	-10	Stratiform
29 Oct	1.341	0.530	1.870	7	70	131	858	Surface	36	Convective
3 Nov	0.110	0.359	0.469	7	48	48	381	6	-13	Stratiform
29 Nov	2.751	0.439	3.190	7	99	186	1210	Surface	88	Convective

LH values are 0 at all levels.

Table 3.2b: Identification of convective/stratiform dominance over surface rainfall in view of daily vertical profile over Chennai in 2007

Date	*Convective rainfall (mm/hr)*	*Stratiform rainfall (mm/hr)*	*Surface rainfall (mm/hr)*	*Levels at which CLW peak occurs*	*PW/ 10^3 at CLW peak (g/m^3)*	*Maximum PW/10^3 on that day (g/m^3)*	*Total PW/10^3 (g/m^3)*	*Level at which LH absorbed is maximum*	*Total LH/10 (°C/hr)*	*Dominance over surface rainfall*
16 Jun	0.079	0.124	0.203	6,7	20,21	21	162	5,6	-7	Stratiform
18 Jun	5.342	1.302	6.643	3	387	392	2898	Surface	334	Convective
29 Jul	0.263	1.469	1.732	3	119	135	1097	5	-24	Stratiform
1 Aug	0.019	0.020	0.039	6,7	4,4	5	34	-	0	Stratiform
13 Sep	0.196	1.063	1.259	8	101	105	827	5	-20	Stratiform
1 Oct	2.522	0.414	2.935	7	91	175	1130	Surface	72	Convective
28 Oct	0.733	4.065	4.798	9	216	369	3035	3	73	Stratiform
18 Nov	0.047	0.0657	0.113	6,7	13,14	15	103	5,6	-7	Stratiform
27 Nov	0.279	0.953	1.232	8	86	89	749	1,6	-15	Stratiform
18 Dec	0.161	0.404	0.565	6	48	50	406	6	-11	Stratiform
19 Dec	5.990	2.662	8.652	8	298	473	3496	Surface	242	Convective

LH values are 0 at all levels.

Occurrence of High Rainfall in the Light of PW Values at the Peak Cloud Water Level (PCL)

Observing the values of PW at the peak cloud water level (PCL), it is possible to say whether contribution of convective/stratiform rain to surface rainfall is more. It is found out from Tables 3.2a and 3.2b that dominance of stratiform rain over surface rainfall is characterized by very high PW at the PCL, and this value is found out to be the maximum, or close to the maximum among all levels in a day. On the other hand, a convective dominance is characterized by almost an intermediate PW value at the PCL on a particular day.

Tables 3.2a and 3.2b also show that it is possible to predict surface rainfall quantitatively from the knowledge of PW values at the PCL. Highest rainfall rate, may it be convective or stratiform, is found to correspond to the maximum PW value at the PCL. The same result is found out if the data of the whole year is considered.

It is found out that as the PW at the PCL decreases, rainfall also decreases in that month (Tables 3.2a and 3.2b). It is also found that in case of stratiform/convective dominance, the maximum PW value at the PCL of a particular month/year corresponds to the maximum stratiform/convective rainfall of that month/year. In order to find out if there exists any correlations between PW and convective rainfall, daily convective rainfall values have been plotted against total PW of a day for January-December (Fig. 3.8). It is found out that they bear a power relation. The surface rainfall and PW also show a power relation between them In a nutshell, it is revealed that watching the vertical profiles of PW, LH and CLW it is possible to say whether surface rainfall is dominated by convective rain, or stratiform rain. It is also possible to predict whether the surface rainfall is high, may it be convective or stratiform, from the PW values at the PCL.

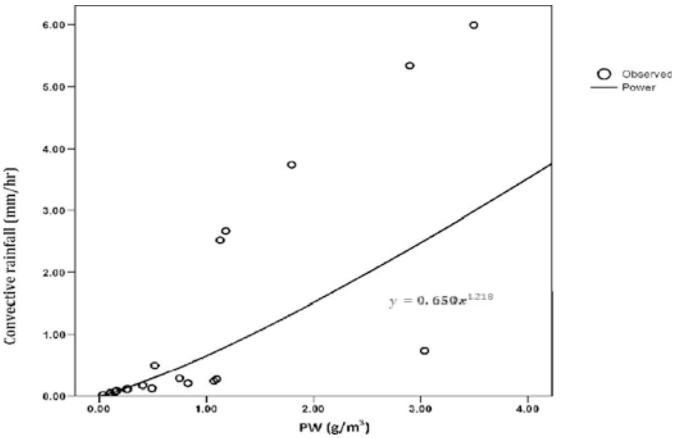

Fig. 3.8a: Variation of convective rainfall with total PW (level 1-14) over Chennai in 2007.

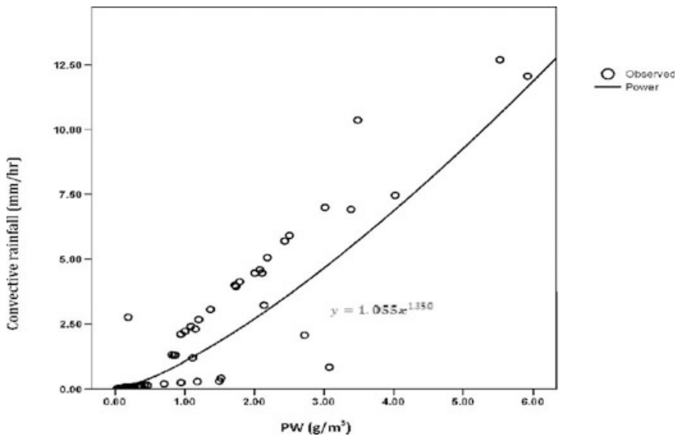

Fig. 3.8b: Variation of convective rainfall with total PW (level 1-14) over Trivandrum in 2007.

CONCLUSION

CLW and PW bear a cubic relation with height, whereas LH varies in an oscillatory manner. A convective dominance is marked by higher total PW along the vertical column than a stratiform one, a net LH evolution with the absorption peak certainly at the surface; and an intermediate PW value at the PCL, while a stratiform dominance is characterized by a net LH absorption, or zero evolution along the vertical column with the LH absorption peak (if any) far away from the surface and a very high PW at the PCL. PW values at the PCL can infer if surface rainfall is high.

An increasing trend in rainfall has been observed both over Chennai and Trivandrum. Moreover, monthly rainfall also shows an increasing trend in the N-E monsoon months and some of the S-W monsoon months. The pre-monsoon months show a decreasing trend in terms of rainfall over both the stations. It is further found out that extreme and very heavy rainfall contributes more to surface rainfall over Chennai, while over Trivandrum, the maximum contribution comes from heavy and very heavy rainfall. Also, these categories of rainfall are found to show increasing trends over the period studied.

ACKNOWLEDGEMENT

Authors are grateful to the management of Sona College of Technology, Salem for providing the necessary infrastructure. The authors convey sincerest thanks to the Indian Space Research Organization (ISRO) for funding the project of which the present paper is a part. The authors thank the India Meteorological Department for providing the necessary data. The data used in this study were acquired as part of the NASA's Earth-Sun System Division

and archived and distributed by the Goddard Earth Sciences (GES) Data and Information Services Center (DISC).

REFERENCES

Balaji, C., Deiveegan, M., Venkateshan, S.P., Gairola, R.M., Sarkar, A. and Agarwal, V.K. (2010). Retrieval of hydrometeors from microwave radiances with a polarized radiative transfer model. *J. Earth Syst. Sci.*, **119:** 97-115.

Battan, A.H. and Kassander, A.R. (1960). Design of a program of randomized seeding of orographic cumuli. *J. Meteorol.*, **17:** 583-590.

Chakraborty, S. and Maitra, A. (2012). A comparative study of cloud liquid water content from radiosonde data at a tropical location. *Int. J. Geo. Sci.*, **3:** 44-49.

Climate risks and adaptation in Asian coastal megacities: A synthesis report to the World Bank, 2010.

disc.sci.gsfc.nasa.gov/precipitation/documentation/TRMM_README/TRMM_3B42_readme.shtml. Last updated in 2011.

ftp://disc2.nascom.nasa.gov/ftp/data/s4pa/TRMM_L2/TRMM_2A12/doc/README.TRMM_2A12.pdf. Last updated in 2008.

Guhatakurta, P. and Rajeevan, M. (2006). Trends in the rainfall pattern over India. NCC Research Report.

Heymsfield, G.M., Geerts, B. and Tian, L. (2000). TRMM precipitation radar reflectivity profiles as compared with high resolution airborne and ground based radar measurements. *J Appl. Meteorol.*, **39:** 2080-2101.

Hsu, S.A. (1988). Coastal Meteorology. Academic Press Inc., San Deigo.

http://mirador.gsfc.nasa.gov/cgi-bin/mirador/presentNavigation.pl?tree=project&project=TRMM. Last updated in 2011.

http://www.ncdc.noaa.gov/oa/mpp/freedata.html. Last updated in May 2012.

Jaiswal, R.S., Neela, V.S., Rasheed, M., Fredrick, S.R. and Zaveri, L. (2011). Characteristics of S-W and N-E rainfall over Salem. *Ind. J. Radio and Space Phys.*, **40:** 257-266.

Jeffrey, A.M., Peter, J.T., Anthony, K.R.N., Baird, A.H., Berkelmans, R., Eakin, C.M., Johnson, J., Marshall, P.A., Packer, G.R., Rea, A. and Willis, B.L. (2008). Reef temp: An interactive monitoring system for coral bleaching using high resolution SST and improved stress. *Geophys. Res. Lett.*, **35:** 1-5.

Krishnakumar, K.N., Rao, P.G.S.L.H.V. and Gopakumar, C.S. (2009). Rainfall trends in twentieth century over Kerala, India. *Atmos. Environ.*, **43:** 1940-1944.

Kumar, R., Jawale, P. and Tandon, S. (2008). Economic impact of climate change on Mumbai, India. *Reg. Health Forum*, **12:** 38-42.

Maitra A, Sen Jaiswal, R, Sonia, R.F, Neela, V.S, Chakraborty, K., Adhikari, A., Bhattacharya, A., Rasheed, M. and Zaveri, L. (2009). Comparison of TRMM estimated rainfall with ground truth over Calcutta, paper presented at the 4th International Conference on Computers and Devices for Communication, Calcutta, 2009.

Max, J.R. (2001). Optical Design Fundamentals for Infrared Systems, 2nd edition. SPIE Press, Bellingham.

Michaels, P.J., Knappenberger, P.C. and Davis, R.E. (2006). Sea-surface temperatures and tropical cyclones in the Atlantic basin. *Geophys. Res. Lett.*, **33:** 1-4.

Oki, R. and Kozu, T. (2000). Comparison of TRMM/PR rain rate with ground-based observation. Paper presented at the Microwave Remote Sensing of the Atmosphere and Environment II, Sendai, Japan.

Possible vulnerabilities of Cochin, India to climate change impacts and response strategies to increase resilience. Report by Cochin University of Science and Technology and Oak Ridge National Lab., 2003.

Rao, P.G.S.L.H.V., Rao, K.A.V.R., Krishnakumar, K.N. and Gopakumar, C.S. (2009). Impact of climate change on food and plantation crops in the humid tropics of India. Paper presented at the ISPRS Archives XXXVIII- 8/ W3 Workshop Proceedings: Impact of climate change on agriculture, Ahmedabad, India.

Sem, G. (2007). Vulnerability and adaptation to climate change in small islands developing states. Paper presented at the UNFCC expert meeting on adaptation for small island developing states: Part II, Cook Islands.

Taylor, K.E. and Ghan, S.J. (1992). An analysis of cloud liquid water feedback and global climate sensitivity in a general circulation model. *J. Climate*., **5:** 907-919.

Ummenhofer, C.C., Gupta, A.S., Li, Y., Taschetto, A.S. and England, M.H. (2011). Multi decadal modulation of the El Nino-Indian monsoon relationship by Indian Ocean Variability. *Eviron. Res. Lett.*, **6:** 1-8.

Wolff, D.B., Marks, D.A., Amitai, E., Silberstein, D.S., Fisher, B.L., Tokay, A., Wang, J. and Pippitt, J.L. (2005). Ground validation for the Tropical Rainfall Measuring Mission (TRMM). *J. Atmos. Oceanic Technol.*, **22:** 365-380.

CHAPTER

4

Inter-annual Variability of Sea Surface Temperature in the Arabian Sea

C. Shaji, M.P. Sudev and M.V. Martin

Centre for Oceans, Rivers, Atmosphere and Land Sciences (CORAL)
Indian Institute of Technology (IIT), Kharagpur – 721302
West Bengal, India
cshaji@coral.iitkgp.ernet.in

INTRODUCTION

Sea surface temperature (SST) evolves in the upper ocean (~10 m) due to ocean dynamics such as mixing and advection and due to air-sea fluxes of heat, moisture and momentum (Bjerknes et al., 1969; Rasmusson et al., 1983; Webster et al., 1999; Legeckis et al., 1986). In the Arabian Sea (hereafter referred as AS), many previous studies (Shukla et al., 1975; Washington et al., 1977; Druyan et al., 1983) on the annual cycle of SST has shown that SST anomalies found in this ocean can influence the rainfall pattern of southwest monsoon over the Indian peninsula. Besides, many researchers (Rao and Goswami, 1988; Clark et al., 2000; Kothawale et al., 2008; Boschat et al., 2011) also explored the connection between inter-annual SST variations and rainfall distribution over India.

The goal of our study is to document the annual cycle and inter-annual variations of SST at various local regions in the AS by primarily analyzing the ship-observed and satellite-sensed SST and air-sea fluxes datasets. The ensuing sections in this paper are organized as follows. After a brief discussion of the data used (second section i.e. Materials and Methods), we deal with the annual cycle as well as the inter-annual variations of SST (in third

J. Sundaresan et al. (eds.), *Climate Change and Island and Coastal Vulnerability*,
DOI 10.1007/978-94-007-6016-5_4, © 2013 Capital Publishing Company

section i.e. Results and Discussions). We finalize with summary and conclusions of the present work.

MATERIALS AND METHODS

The Data and Analysis

Herein, we used a variety of SST as well as air-sea fluxes datasets to elucidate the signatures of seasonal and inter-annual variations of SST in the AS. Those datasets are briefly discussed below.

Sea Surface Temperature (SST)

To understand the seasonal variations of SST, we used climatology of monthly mean SST from five different datasets, which in effect gave us an opportunity for inter-comparing these datasets. First, we took the SST monthly climatology obtained from the Southampton Oceanography Centre (SOC) **(**Josey et al., 1998; Josey et al., 1999).

The SOC monthly SST climatology (hereafter referred as SOC-SST) is preferred to a similar climatology based on Comprehensive Ocean-Atmosphere Dataset (COADS) (Oberhuber et al.,1988) because it is more recent, uses better methods for preparing the climatology, and has been compared extensively with available observations (Josey et al., 1999; Weller et al., 1999). Second, we considered the monthly climatology of National Oceanic and Atmospheric Administration (NOAA) Optimum Interpolation (OI) Version 2.0 SST data (Reynolds et al., 2002). This dataset (hereafter referred as NOAAOI-SST) is based on both in situ observations from ships and buoys (both moored and drifting) and satellite observations from Advanced Very High Resolution Radiometer (AVHRR). Third, the National Centers for Environmental Prediction (NCEP) reanalysis (Kalnay et al., 1996) skin temperature covering the period January 1948 to December 2010 is used to prepare the monthly SST climatology (hereafter referred as NCEP-SST). Fourth, we used the high resolution (0.25° × 0.25°) Levitus temperature climatology (Boyer et al., 2005) to get the SST field (hereafter referred as LEVITUS-SST). Finally, we considered the National Oceanic and Atmospheric Administration - National Aeronautics and Space Administration (so called NOAA-NASA) very high horizontal resolution (4 km × 4 km) satellite-sensed Pathfinder Version 5 (PF5) AVHRR SST fields (Casey et al., 2010) from January 1985 to December 2009 (25 years) to prepare monthly SST climatology (hereafter referred as PF-SST).

To explore the inter-annual SST variations, we used two different NOAA datasets with each having different observational periods. First, the Extended Reconstructed SST dataset (Smith et al., 2004) (hereafter referred as ERSST), which was constructed based on the most recently available International Comprehensive Ocean-Atmosphere Dataset (ICOADS) SST data (Worley et al., 2005). Second dataset contains the monthly SST based on in situ and satellite SST plus SST simulated by sea ice coverage (Reynolds et al., 2002) (hereafter referred as Reynolds SST).

Air-sea Fluxes

We considered monthly mean air-sea fluxes from three datasets – SOC climatology (Josey et al., 1998, Josey et al., 1999), Japanese Ocean Flux Datasets with Use of Remote Sensing Observations (J-OFURO) (Kubota et al., 2002) and NCEP reanalysis (Kalnay et al., 1996). By considering air-sea fluxes from different sources, we were able to make inter-comparisons of the fluxes based on different datasets.

RESULTS AND DISCUSSIONS

Annual Cycle of Sea Surface Temperature

Semi-annually varying monsoon winds affect the circulation and hydrography of the Indian Ocean north of 10°S, whereas the southern Indian Ocean is a non-monsoonal region and is dominated by the almost steady southeast trade winds all year round (Shaji et al., 2003; Shankar et al., 2002). The AS wind stress fields [Figs 4.1(a-l)] show that during the first five months from November to March the winds are predominantly northeasterly and during the second five months from May to September the winds are dominated by strong southwesterly, with the appearance of weak, calm winds (maximum wind stress ~0.05 NM^{-2}) discerning the transition from northeast (southwest) to southwest (northeast) monsoon in April (October). The wind stress fields in April and October also reveal the appearance of weak anticyclonic atmospheric circulations.

Figures 4.1(m-o) illustrates the annual cycles of AS domain-averaged wind stress magnitude, SST based on five different datasets and net surface heat fluxes from SOC, NCEP and JOFURO. All three fields exhibit bimodal distributions. Figures 4.1(p-s) shows the annual cycles of AS domain-averaged net shortwave and longwave radiations (both from SOC and NCEP) and latent heat and sensible heat fluxes (both from SOC, NCEP and JOFORO). Positive (negative) values in any of the air-sea fluxes reveal heat gain by the ocean (heat loss from the ocean).

Annual cycles of SST from all the datasets (Fig. 4.1n) reveal that the amplitude of PF-SST is slightly high while that of NCEP-SST is slightly less almost year round. Throughout the year, domain-averaged SST in the AS lies above 26°C and particularly in May it is even above 29°C in all the datasets. Comparison of SST from five datasets during January and July [Figs 4.2 (a-j)] reveals that the spatial SST patterns are similar in all the datasets, but with the appearance of fine meso-scale features in the LEVITUS-SST and PF-SST because of its high spatial resolution. In January, SOC-SST does not show the presence of warm waters in the southeastern AS as observed in other datasets. The differences noted here in various monthly SST

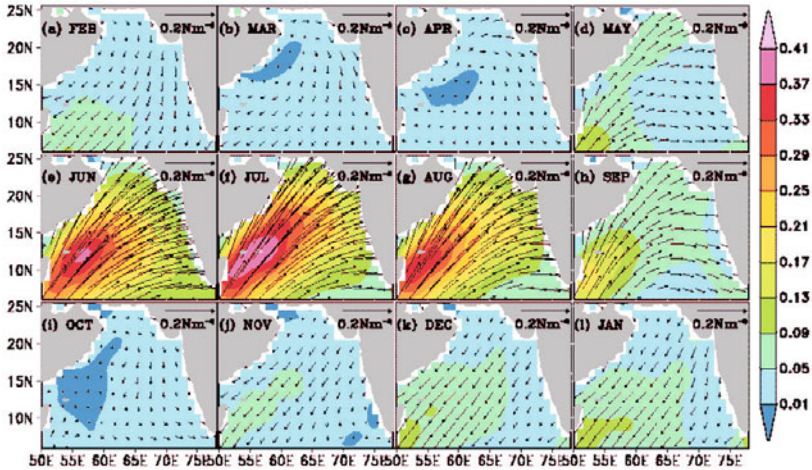

Top panel (a-l)

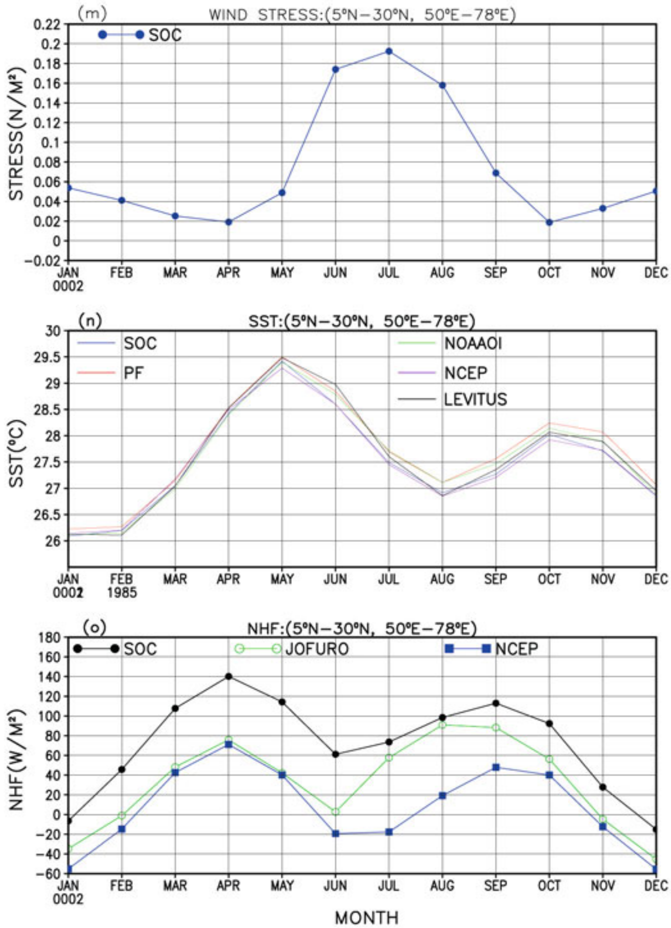

Middle panel (m-o)

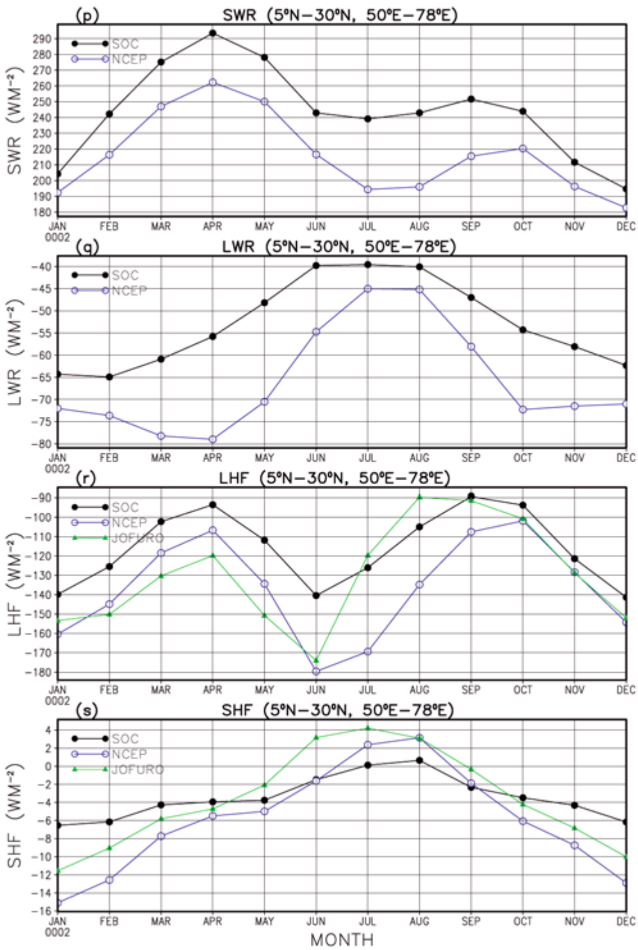

Bottom panel (p-s)

Fig. 4.1: *Top panel (a-l)* – Monthly mean wind stress (NM^{-2}) based on Southampton Oceanography Centre (SOC) climatology in the Arabian Sea during the months of (a) February, (b) March, (c) April, (d) May, (e) June, (f) July, (g) August, (h) September, (i) October, (j) November, (k) December and (l) January. The shading denotes the wind stress magnitude. *Middle panel (m-o)* – Monthly evolution of Arabian Sea (5°N-30°N, 50°E-78°E) domain averaged (m) wind stress magnitude (NM^{-2}) based on SOC dataset, (n) SST (°C) based on SOC, PF, NOAAOI, NCEP and LEVITUS datasets and (o) net surface heat flux (NHF) (WM^{-2}) based on SOC, JOFURO and NCEP datasets. *Bottom panel (p-s)* – Monthly evolution of Arabian Sea (5°N-30°N, 50°E-78°E) domain averaged (p) net shortwave radiation (WM^{-2}) based on SOC and NCEP datasets, (q) net longwave radiation (WM^{-2}) based on SOC and NCEP datasets, (r) latent heat flux (WM^{-2}) based on SOC, NCEP and JOFURO datasets and (s) sensible heat flux (WM^{-2}) based on SOC, NCEP and JOFURO datasets.

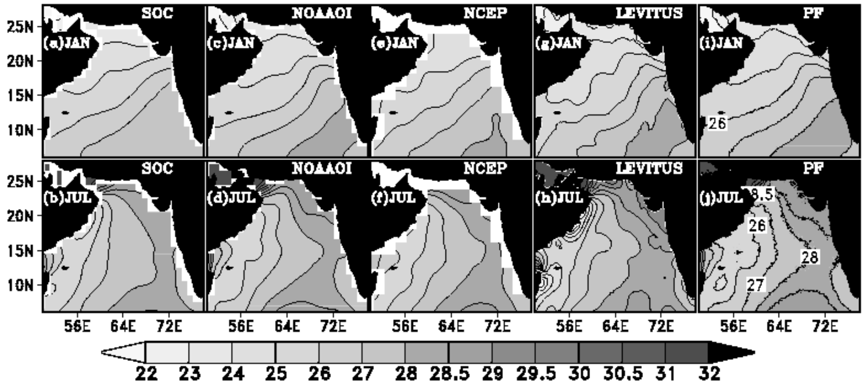

Fig. 4.2: Monthly mean SST (°C) in the Arabian Sea based on SOC, NOAAOI, NCEP, LEVITUS and PF datasets during the months of January (a, c, e, g and i) and July (b, d, f, h and j). The light shading denotes SST <28°C and dark with SST >28°C.

climatologies are quite inevitable as in each dataset the observational data used, analysis procedure adapted and averaging time interval considered for preparing the climatology are quite different.

The time series of net surface heat fluxes (Fig. 4.1o) based on SOC, JOFURO and NCEP shows differences in amplitudes, though annual cycles are clear in all datasets. While comparing to SOC and NCEP datasets, JOFURO displays a phase difference of one month with regard to the second peak in the annual cycle of net surface heat flux. Overall, SOC (NCEP) exhibits high (low) amplitudes throughout the year in all air-sea fluxes, except in sensible heat flux. It should be noted that NCEP air-sea fluxes is a reanalysis product, while fluxes computations in JOFURO uses satellite observations and that in SOC follows in situ ship observations. Besides the basic differences in the observations, the formula meant for fluxes computations and analysis procedure followed to get the final field are also quite different in each dataset. Thus, though there is a correspondence in the annual cycle of each field (SST or air-sea fluxes) from various datasets, the magnitudes are not always similar and sometimes the differences are even quite significant. This in fact makes the option of selecting better observational dataset a difficult endeavour. By considering this fact, in our following discussions, we preferred monthly climatology of (1) air-sea fluxes based on SOC dataset because as we mentioned earlier this dataset is good in many respects and (2) SST based on NOAAOI because the basic observations in this dataset follows both in situ ship observations and satellite-sensed AVHRR observations.

The AS annual SST cycle (Figs 4.3.1(a-l) and 4.1n) exhibits the following signatures.

Pre-monsoon Warming

Warming phase of AS starts in February and continues till May, by which time SST everywhere in the AS exceeds 28°C [Figs 4.3.1(a-d)]. In May, most of AS area is covered by a warm pool of water with SST > 30°C (Joseph, 1990). North of 22°N, warm water is observed till June (Fig. 4.3.1e) because the southwest monsoon induced cooling is yet to reach there. During pre-monsoon warming phase, SST distribution pattern in the AS [Figs 4.3.1 (a-d)] shows a good agreement with those of the net shortwave radiation [Figs 4.3.2(a-d)] and net surface heat flux [Fig. 4.4.3(a-d)], but with SST delaying about one month as to the net heat flux. Mechanisms causing pre-monsoon warming are different in the regions north of 12°N and south of 12°N. During February-May, the distributions of SST [Figs 4.3.1(a-d)], net shortwave radiation [Figs 4.3.2(a-d)] and net surface heat flux [Figs 4.4.3(a-d)] show increasing trend in the AS north of about 12°N. On the other hand, in the same region during February-May, sensible heat flux [Figs 4.4.2(a-d)] and net longwave radiation [Figs 4.3.3(a-d)] exhibit decreasing trend of heat loss. But latent heat flux shows decreasing trend of heat loss from February (Fig. 4.4.1a) to April (Fig. 4.4.1c), followed by increase in heat loss in May (Fig. 4.4.1d). The heat loss in May can be attributed to evaporation caused by the influence of southwest monsoon winds, with peak heat loss associated with it occurring in June (Fig. 4.4.1e). From the above it is apparent that the air-sea fluxes contribute greatly for the observed northern AS warming during pre-monsoon. South of 12°N, all the air-sea fluxes operate favourably for the observed SST increase from February till April. SST reaches its peak during May in the southern AS. But except net longwave radiation, all other fluxes are unfavourable for the observed SST peak in May. In the southern AS, ocean dynamics plays a cardinal role in warming the ocean during May. The presence of the Indian Ocean warm pool water (Joseph, 1990), with its geographical expansion to west and north during February to May in the Indian Ocean (Vinayachandran and Shetye, 1991) can contribute mainly for the observed SST rise in May.

Summer or Southwest Monsoon Cooling

Summer monsoon cooling begins in June in the western AS (Fig. 4.3.1e), reaches its peak in August (Fig. 4.3.1g) and by which time SST almost everywhere in the AS reach around <27°C, except in the southeastern region where the Indian Ocean warm pool effect keeps the ocean still warm. The SST distribution in the AS during southwest monsoon (June-September) shows a zonal gradient [Figs 4.3.1(e-h)], with SST in the west being less than that in the east. The net shortwave radiation and net surface heat flux during June-September [Figs 4.3.2(e-h) and 4.4.3(e-h) respectively] also show zonal gradients, with high (low) in the west (east). Hence the distribution of these fields is not conducive for the observed SST evolution during southwest monsoon. Besides, southwest monsoon cloudiness also show zonal gradient with high in the east and low in the west (not shown). Sensible heat flux shows heat gain (loss) in the west (east) during southwest monsoon [Fig. 4.4.2(e-h)], which in fact sets unfavourable condition for the observed zonal SST gradient. Since most of the air-sea flux fields are not conducive for the observed SST evolution pattern during southwest monsoon (June-September), it is clear that the oceanic processes might play a major role. During southwest monsoon, energetic monsoon winds induce coastal upwelling which then spreads cold water offshore (Shaji et al., 2003; Shankar et al., 2002) and (Duing and Leetmaa 1980; McCreary et al., 1993). Moreover, strong southwest monsoon winds are also responsible for transferring heat to deeper layers through overturning and turbulent mixing (Shenoi et al., 2002).

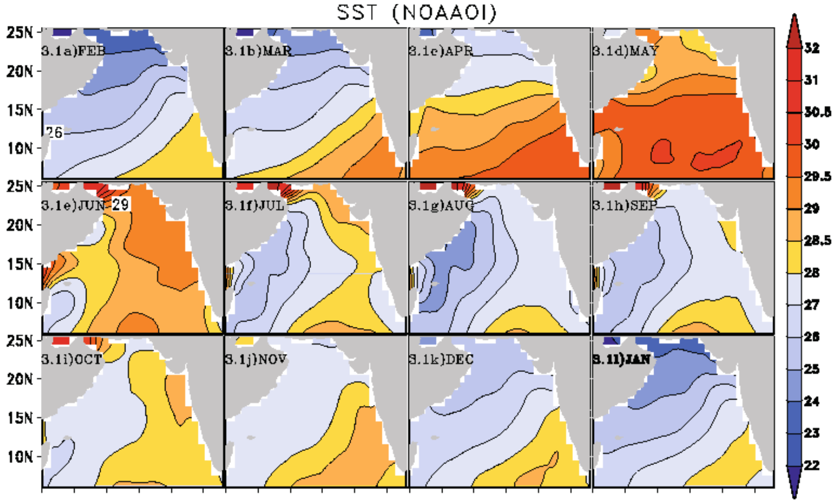

Top panel

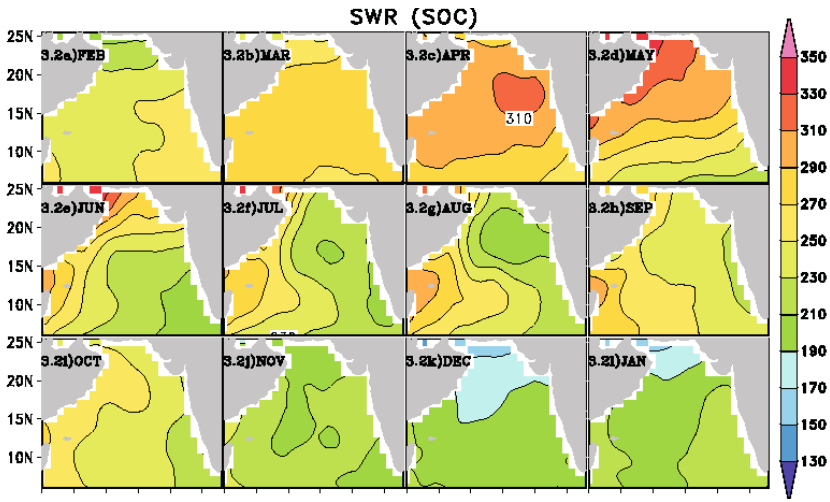

Middle panel

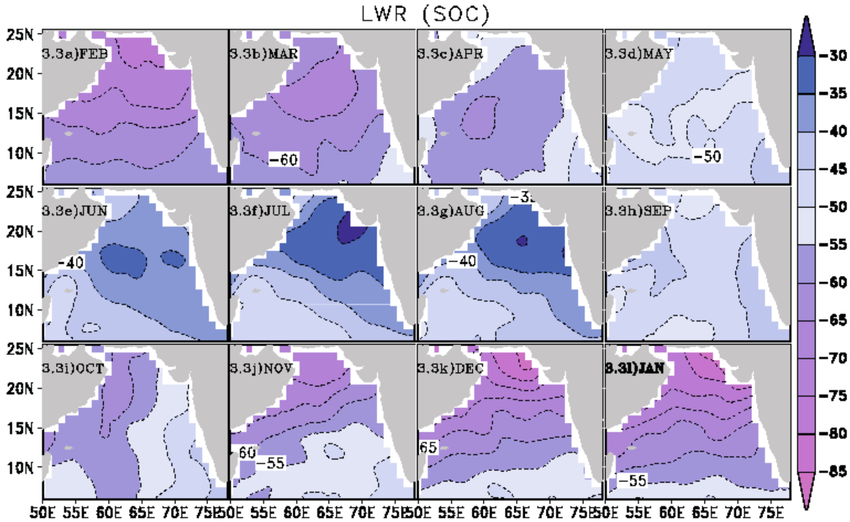

Bottom panel

Fig. 4.3: *Top panel 4.3.1(a-l)* – Monthly mean SST (°C) in the Arabian Sea based on NOAAOI dataset during the months of (a) February, (b) March, (c) April, (d) May, (e) June, (f) July, (g) August, (h) September, (i) October, (j) November, (k) December and (l) January. The blue shading denotes SST <28°C and yellow to red with SST >28°C. *Middle panel 4.3.2(a-l)* – Monthly mean net shortwave radiation (SWR) (WM^{-2}) in the Arabian Sea based on SOC dataset during the months of (a) February, (b) March, (c) April, (d) May, (e) June, (f) July, (g) August, (h) September, (i) October, (j) November, (k) December and (l) January. Positive values show heat gain by the ocean. *Bottom panel 4.3.3(a-l)* – Same as Figure 4.3.2(a-l) except the field is net longwave radiation (LWR) (WM^{-2}) based on SOC dataset. Negative values show heat loss from the ocean.

Post-monsoon Warming

The AS basin experiences a short period of secondary warming during September-October [Figs 4.3.1(h-i)]. During September-October, net surface heat flux shows decreasing (increasing) trend in the west (east) [Figs 4.3.3 (h-i)]. Net shortwave radiation increases (decreases) in the northern (southern) AS from September to October [Figs 4.3.2(h-i)]. Heat loss owing to net longwave radiation increases from September to October in the entire AS [Figs 4.3.3(h-i)]. Heat loss both due to latent heat flux and sensible heat flux increases (decreases) from September to October in the west (east) [Figs 4.4.1(h-i) and 4.4.2(h-i) respectively). Thus, air-sea fluxes operate differently at different local regions in the AS during post-monsoon. Besides air-sea fluxes, internal ocean dynamics can also contribute significantly in various local regions. In a previous study (Shaji et al., 2003), it has been shown that the vertical heat convergence in the AS contributes favourably for the post-monsoon warming.

Winter or Northeast Monsoon Cooling

Winter cooling first starts in November in the northern basin (Fig. 4.3.1j), reaches its peak in January (Fig. 4.3.1l) and by which time most of the northern AS is occupied by cold patches of SST with amplitude less than around 25°C. Net shortwave radiation in the AS is minimum during December-January [Figs 4.3.2(k-l)] due to cloudiness. Net surface heat flux exhibits maximum heat loss during December-January [Figs 4.4.3(k-l)], except the southeastern AS where there is heat gain at this time. Heat loss due to latent heat flux is high during December-January [Figs 4.4.1(k-l)] owing to strong northeasterly winds and low atmospheric humidity. Heat loss due to sensible heat flux and net longwave radiation shows increasing trend from November to January [Figs 4.4.2(j-l) and 4.3.3(j-l) respectively]. Overall, all the air-sea fluxes contribute greatly for the observed winter cooling.

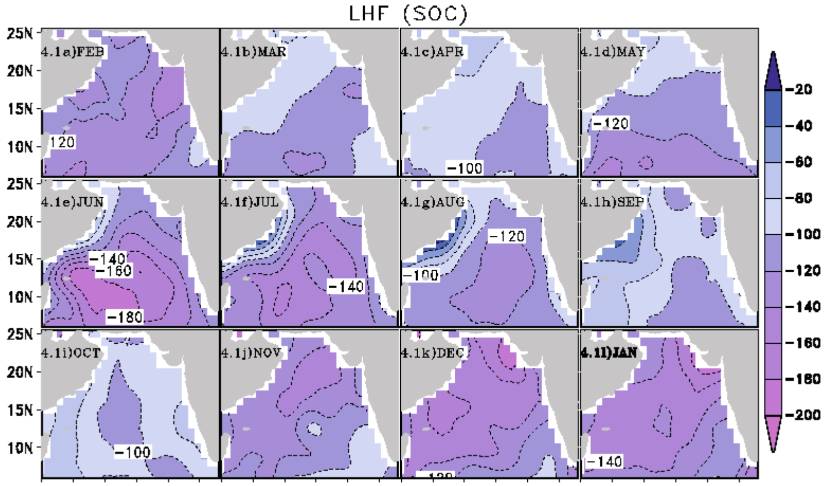

Top panel

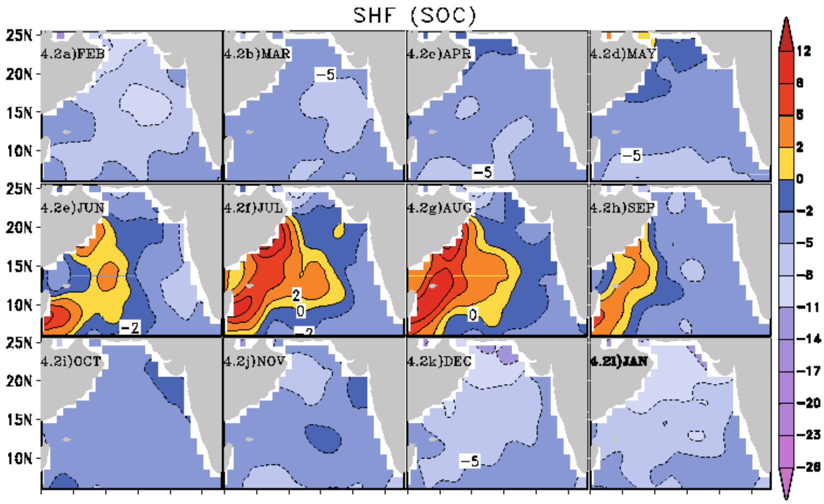

Middle panel

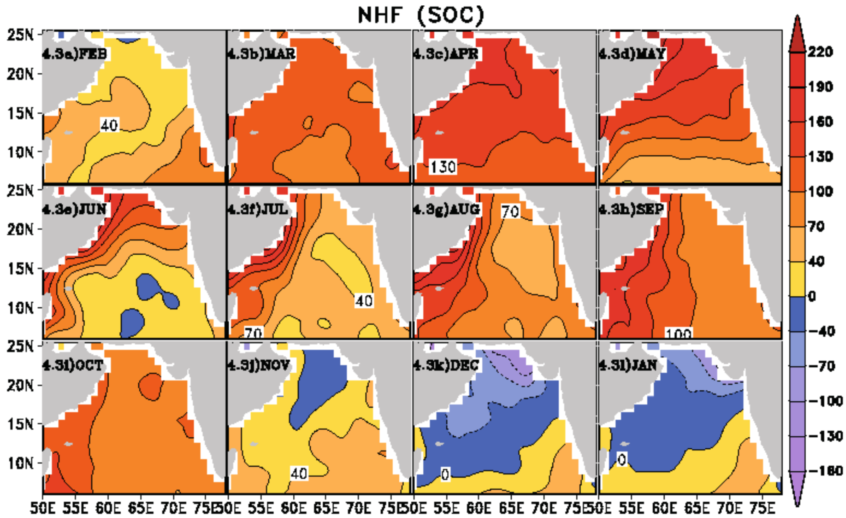

Bottom panel

Fig. 4.4: *Top panel 4.4.1(a-l)* – Same as Fig. 4.3.2(a-l) except the field is surface latent heat flux (LHF) (WM^{-2}) based on SOC dataset. Negative values show heat loss from the ocean. *Middle panel 4.4.2(a-l)* – Same as Fig. 4.3.2(a-l) except the field is surface sensible heat flux (SHF) (WM^{-2}) based on SOC dataset. The blue shading denotes heat loss from the ocean and yellow to red heat gain by the ocean. *Bottom panel 4.4.3(a-l)* – Same as Fig. 4.3.2(a-l) except the field is net surface heat flux (NHF) (WM^{-2}) based on SOC dataset. The blue shading denotes heat loss from the ocean and yellow to red heat gain by the ocean.

Inter-annual Variability of Sea Surface Temperature – Predominant SST Oscillations

To explore the predominant oscillations contained in a long-time series of SST data, we preferred the ERSST (Smith and Reynolds, 2004) dataset as it covers 152 years SST (January 1854 to December 2002) based on the ICOADS in situ observations. Figures 4.5(a-b), 4.6(a-b), 4.6(c-d), 4.6(e-f) and 4.6(g-h) respectively show the time series (during 1854-2005) of three-month running mean of monthly mean SST (blue curve) and annual mean SST (red curve) based on ERSST data for the whole AS (5°N-30°N, 50°E-78°E), northern AS (22°N-26°N, 58°E-70°E), central Arabian Sea (10°N-20°N, 55°E-65°E), western Arabian Sea (5°N-18°N, 50°E-55°E) and eastern Arabian Sea (5°N-18°N, 65°E-75°E) regions. It is apparent that in all regions the amplitudes of SST in the annual cycles are not always the same from one year to the other. To effectively capture the dominant SST oscillations existing in different local regions of the AS, we performed a Fast Fourier Transform (FFT) analysis to the time series of demeaned and detrended annual mean SST dataset. The demeaning will give annual SST anomalies or residuals during 1854-2005, which are obtained by subtracting the climatology of annual mean SST from the annual mean SST of each individual year. Positive (negative) anomalies indicate warming (cooling). The 152 years monthly SST data from January 1854 to December 2005 is used to prepare the climatology of annual mean SST value. The resultant time series of annual SST anomalies in each local region in fact shows non-linear trends. Non-removal of such trends can lead to the distortion of low frequency components existing in the time series of SST anomaly spectrum. Hence, we have effectively detrended the time series SST anomaly data before carrying out FFT analysis. Figure 4.7(a-e) shows the spectral peaks after performing the FFT analysis in the whole as well as at the above mentioned selected local regions of the AS.

It can be noted that in the whole AS, SST oscillations show peaks with periods in order of preference of 5.1, 3.5, 5.8, 9.5 and 8.9 years (Fig. 4.7a). Thus it can be confirmed that in the AS pentadal SST oscillations are the most dominant ones, followed by decadal oscillations. In Figs 4.5(a-b), pentadal oscillations with apparent signatures are noticeable during the periods 1855-1865, 1875-1905, 1925-1950, 1955-1990 and 1995-2005. In the AS, lowest annual mean SST value of about 26.2°C in 1893 and highest value of about 28.1°C in 2003 were observed. The annual mean SST also showed a clear warming trend from 1950 onwards with annual mean SST of around 27°C in 1950 and further increased to reach a maximum of around 28.1°C in 2003. The annual mean SST trend in the AS further indicates that during 1854-1879 SST stayed slightly above 27°C, during 1880-1925 SST was more or less 27°C or a little below that and since 1925 onwards SST was always above 27°C with appreciable warming from 1990 onwards (SST 28°C and above). A recent study (Levitus et al., 2000) also indicated the world ocean warming from mid-1990 onwards.

In the northern AS region, SST oscillations with dominant peaks have periods in order of preference of 5.8, 5.1, 8.9, 4 and 6.6 years (Fig. 4.7b). Here also pentadal oscillations play the leading role and then oscillations with period of nearly decadal. After that SST peaks occur with periods of

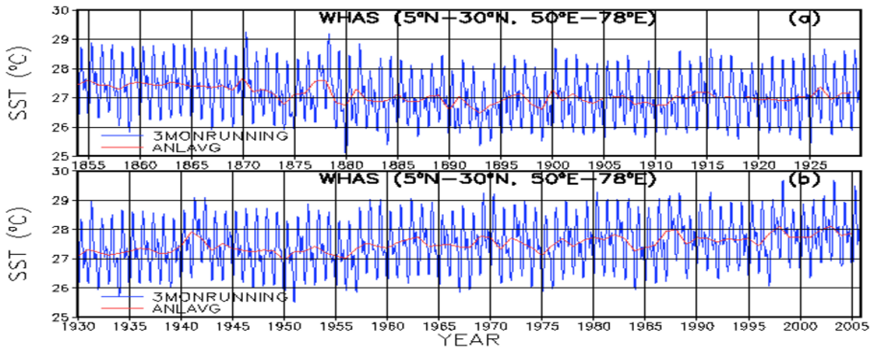

Top panel

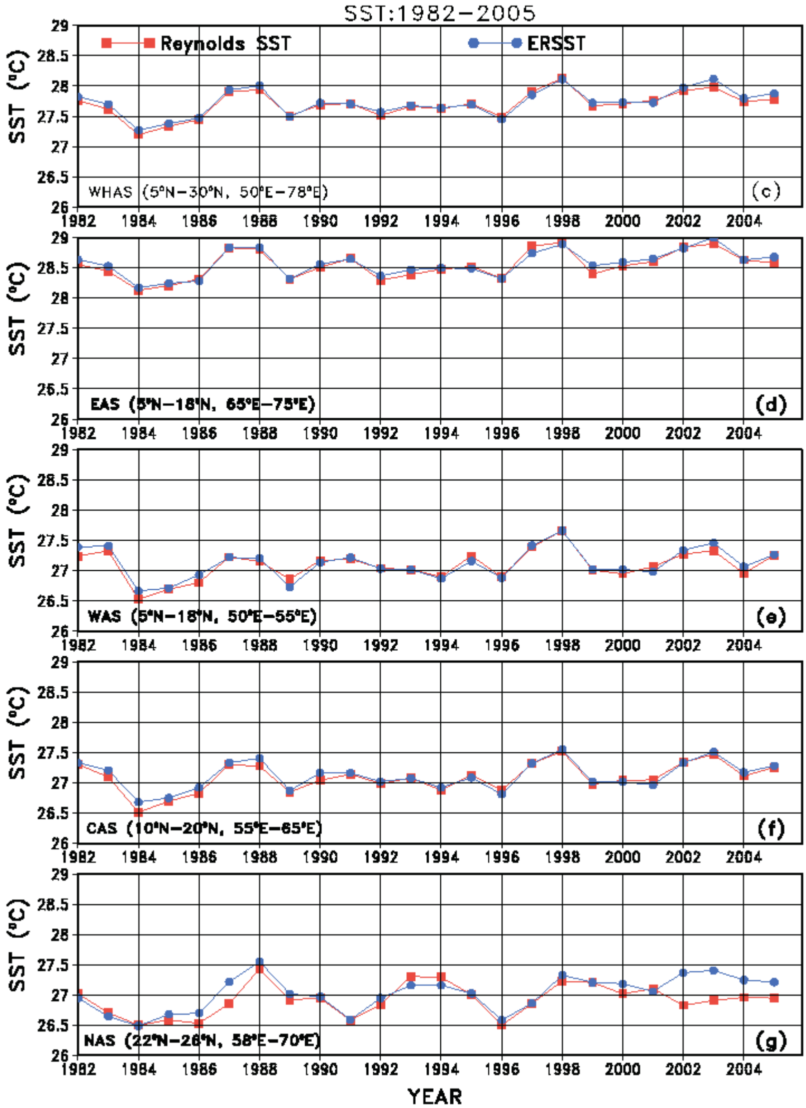

Bottom panel

Fig. 4.5: *Top panel 4.5.1(a-b)* – Time series of three-month running mean of monthly mean SST (blue curve) and annual mean SST (red curve) based on ERSST data for the whole Arabian Sea region (5°N-30°N, 50°E-78°E) during the period 1854-2005. The blue curve in fact represents the seasonal cycles of SST during the 152 years from 1854 to 2005. *Bottom panel 4.5.2(c-g)* – Time series of annual mean SST during the period 1982-2005 using ERSST data (blue curve) and Reynolds SST data (red curve) in the (c) whole Arabian Sea (5°N-30°N, 50°E-78°E), (d) eastern Arabian Sea (5°N-18°N, 65°E-75°E), (e) western Arabian Sea (5°N-18°N, 50°E-55°E), (f) central Arabian Sea (10°N-20°N, 55°E-65°E) and (g) northern Arabian Sea (22°N-26°N, 58°E-70°E) regions.

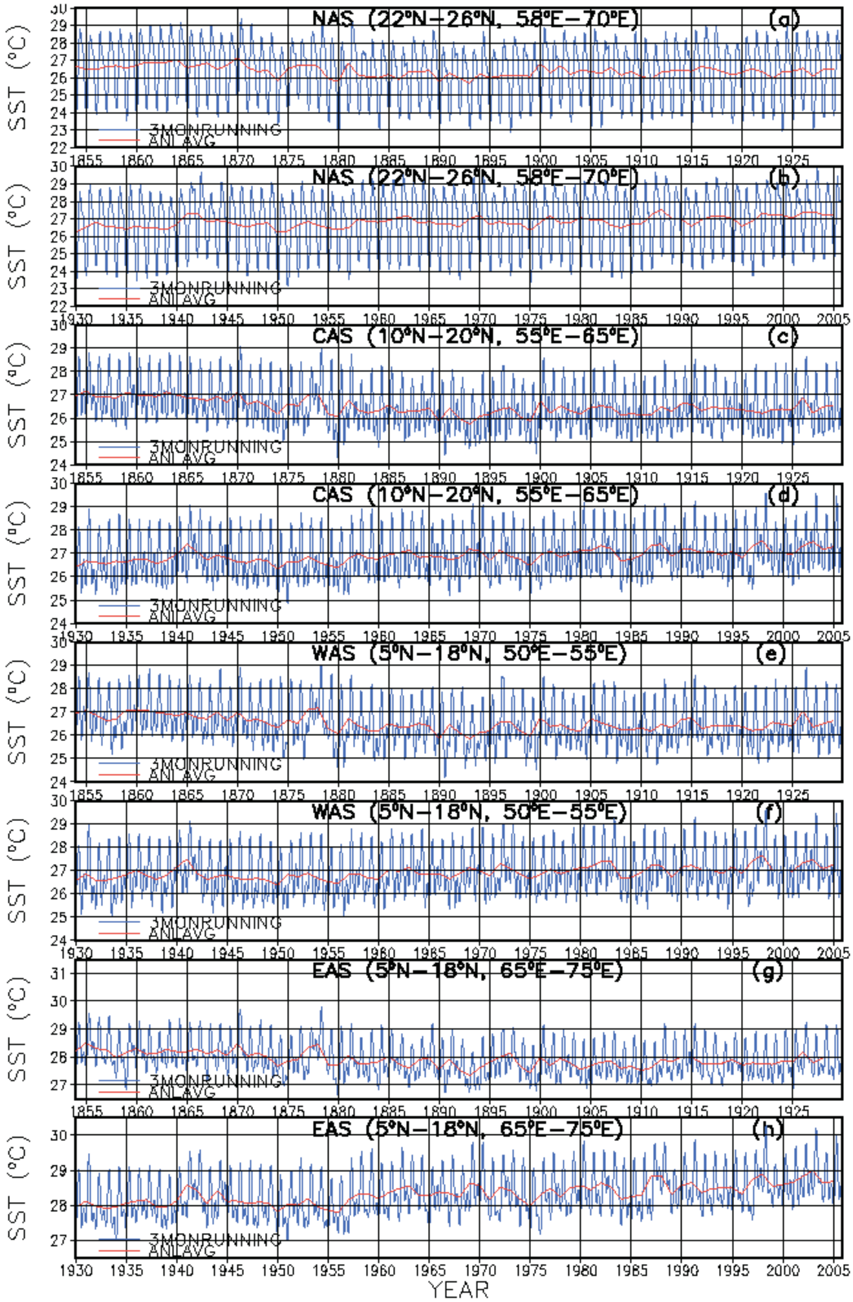

Fig. 4.6: Same as Fig. 4.5.1(a-b) except the selected regions representing the a-b) northern Arabian Sea (22°N-26°N, 58°E-70°E), (c-d) central Arabian Sea (10°N-20°N, 55°E-65°E), (e-f) western Arabian Sea (5°N-18°N, 50°E-55°E) and (g-h) eastern Arabian Sea (5°N-18°N, 65°E-75°E) respectively.

about 4-7 years. The year 1893 was marked with the lowest annual mean SST of 25.7°C and the year 1988 was marked with that of the highest value (27.5°C). Also the minimum and maximum annual mean SSTs observed in the northern AS [Figs 4.6(a-b)] during the analyzed 152 years were about 0.5°C lower than that of the whole AS region [Figs 4.5(a-b)]. In almost all years, annual mean SST in the northern AS stayed between 26 and 27 °C except a significant warming trend since 1997 onwards, in which SST exceeded 27°C.

In the central AS region, SST oscillations with dominant peaks have periods in order of preference of 5.1, 9.5, 2.7, 5.8 and 3.5 years (Fig. 4.7c). Thus, in this region also pentadal SST oscillations are the predominant ones, followed by decadal oscillations and then oscillations with periods of ~3-6 years. That the time series of annual mean SST in the central AS is primarily governed by the existence of pentadal oscillations in major periods such as during the decade 1855-1865, 1875-1950, 1955-1990 and 1995-2005 is very clear from Fig. 4.6(c-d). In the central AS annual mean SST reached a maximum of 27.6°C in 1998 and a minimum of 25.7°C in 1893 [Figs 4.6 (c-d)], the northern AS also showed the same minimum in the same year [Figs 4.6(a-b)]. It can also be noted that the whole AS, northern AS and central AS regions illustrated cool state during 1854-1888 and warm state during 1920-1940. The whole AS and central AS also showed a secondary warm state from 1960 onwards, whereas in the northern AS this warm state was apparent from mid-1990s onwards.

In the western AS region, SST oscillations with dominant peaks have periods in preferential order of 5.1, 9.5, 4.8, 2.7 and 4.5 (Fig. 4.7d). Similar to central AS, in this region also pentadal oscillations dominate, followed by decadal oscillations and then oscillations with periods of ~ 3-5 years. In this region, minimum annual mean SST of 25.8°C in 1893 and maximum of 27.6°C in 1998 were noted. A cool state was observed in the western AS during 1854-1880, followed by two warm states during 1920-1940 and since 1960 onwards.

In the eastern AS, SST oscillations with dominant peaks have periods in preferential order of 5.1, 3.5, 9.5, 5.8 and 5.6 years (Fig. 4.7e). Here also pentadal oscillations dominate, followed by decadal oscillations. Annual mean SST was minimum in 1893 (27.3°C) and maximum in 2003 (29°C). Like western AS, eastern AS also displayed a cool state during 1854-1880 and two warm states during 1920-1940 and since 1960 onwards.

SST Inter-comparisons and Cooling and Warming Periods

Here, we focus on to inter-compare two different monthly SST time series datasets and also to discuss about certain cooling and warming periods encountered in the analysis.

Figure 4.5(c-g) illustrate the time series of annual mean SST during 1982-2005 obtained from two datasets – the red curve showing Reynolds

SST (Reynolds et al., 2002) and the blue curve showing ERSST (Smith and Reynolds, 2004) – for the whole, eastern, western, central and northern AS regions. Both the datasets show that during 2000-2003, eastern AS experienced

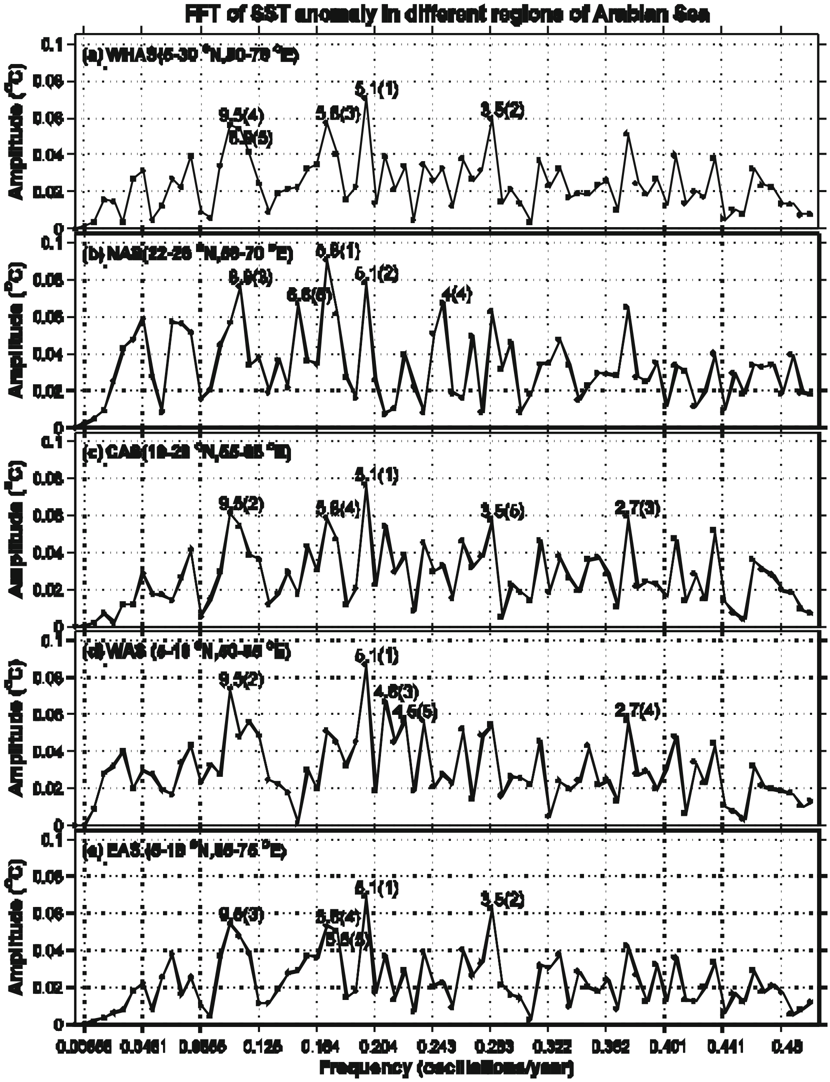

Fig. 4.7: Fast Fourier Transform (FFT) Analysis of the demeaned annual mean SST based on ERSST dataset. Before performing the FFT analysis, climatological annual mean is removed from the time series of annual mean SST. The abscissa is the frequency and the ordinate is the amplitude. The periods corresponding to the first five prominent peaks is shown by the numbers (in years) and the numbers written within the brackets of those periods show how much predominant ([1]: first, [2]: second, [3]: third, [4]: fourth and [5]: fifth) the specified periods are.

a gradual warming with an annual mean SST rise of 0.2°C per year (Fig. 4.5d). After 2003, though annual mean SST dropped in the eastern AS, it still showed a warming tendency (Fig. 4.5d) and the same is true in the western and central AS regions too [Figs 4.5(e-f)]. In the western and central AS, the warming tendency can be noted during 2001-2003 in both the datasets. However, the northern AS behaved quite differently (Fig. 4.5g). Here, ERSST data exhibited a warming tendency during 2001-2003 and after that a cooling tendency. But Reynolds SST illustrated cooling during 2001-2002, followed by warming tendency in the remaining period. The SST amplitudes of both the datasets also display significant differences during 1982-2005. Thus, while comparing both the datasets, it has been identified that besides the discrepancy in the magnitudes of SST, the warming and cooling tendency also differs in both the datasets (e.g. as noted in the northern AS). The northern AS (Fig. 4.5g), besides being a relatively cool region, also displayed large differences as the SST magnitudes of both the datasets are concerned.

The annual SST anomaly based on ERSST data during 1854-2005 is displayed as Figs 4.8(a-b) in the whole AS region. From Figs 4.8(a-b) it is apparent that the whole AS region underwent a warm state during 1854-1870 before a long duration of 69 years of cool state from 1871 to 1939, though short warm states such as those during 1877-1878, 1926, 1936-1937 also existed within the cool period of 1871-1939. Since 1957 onwards AS is experiencing a warming tendency, which still continues, except a cool state observed in the year 1975. Besides small oscillations, the warming trend in the AS which started in 1957 is found to be accelerated since 1990 onwards, with 1998 and 2003 as the two intense warming years. The annual mean SST anomaly in 1998 was 0.8°C, while that in 2003 exceeded 0.8°C. Previous study (Levitus et al., 2000) showed that both the Atlantic and Indian Oceans were in a relatively cool state before mid-1970s and after that in a warm state. A very recent study (Vargas-Yáñez et al., 2008) indicated the warming of western Mediterranean Sea during the 20th century. Thus, the observed AS warming in the recent decades is in conjunction with the warming noticed elsewhere in other oceanic regions.

It should be noted that the SST of each month during the 152 years (1854-2005) can obviously deviate from its climatological value. Hence, next we examined how far monthly SST departs from climatology and also the trend of departure as far as two particular months January and July representing northern hemisphere winter and summer seasons respectively in the whole AS are concerned. Figures 4.8(c-d) and 4.8(e-f) illustrate the SST anomaly for January and July months respectively. In each year of the 152 years period, monthly SST anomalies either for January or July are prepared by subtracting the climatology of monthly SST of the representative month (January or July) from each year's representative month's (January or July) monthly SST. It is interesting to note that in the AS during the long period of cooling in 1871-1939, both winters and summers [Figs 4.8(c-d) and

4.8(e-f) respectively] also showed SSTs below the climatological SSTs. Also during the present warming trend, which started from 1957 onwards [Figs 4.8(a-b)], the winters and summers [Figs 4.8(c-d) and 4.8(e-f) respectively] are also in a warm state and the trend still continues.

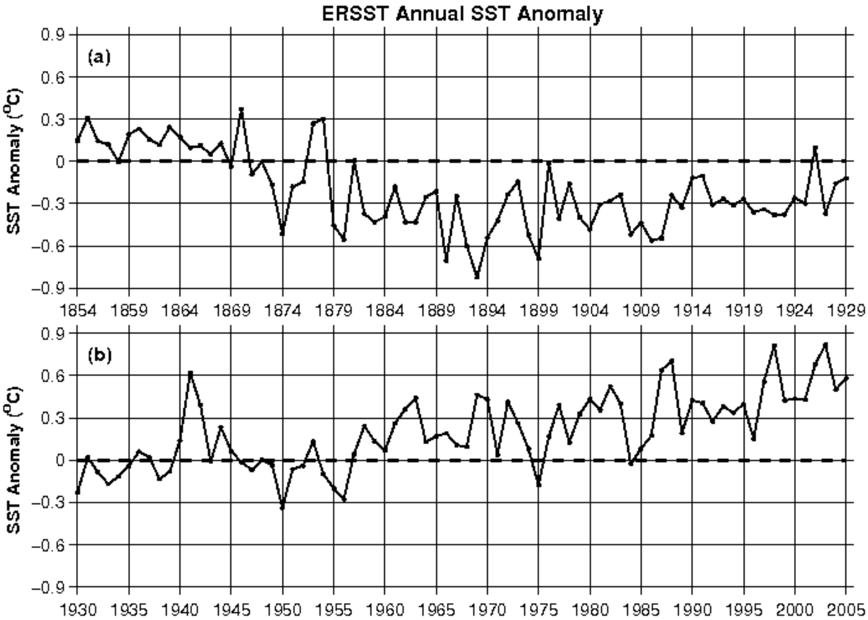

Top panel

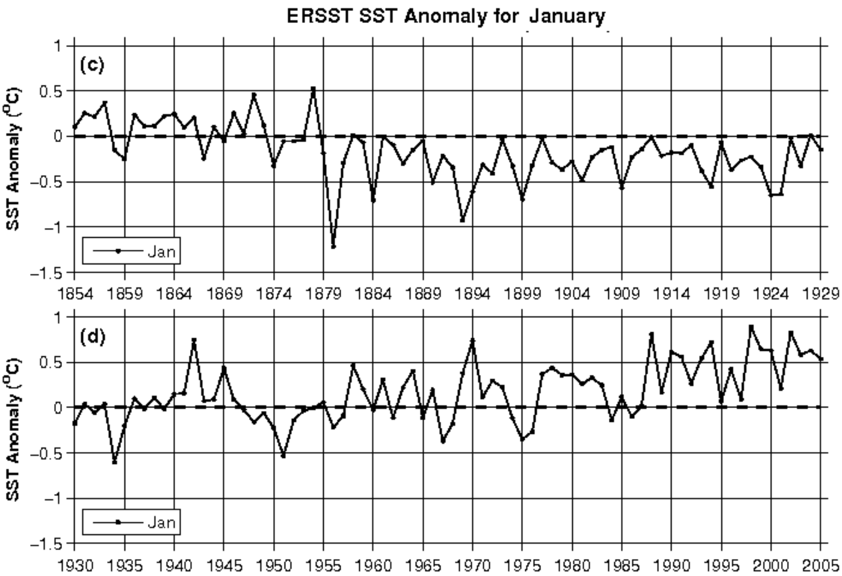

Middle panel

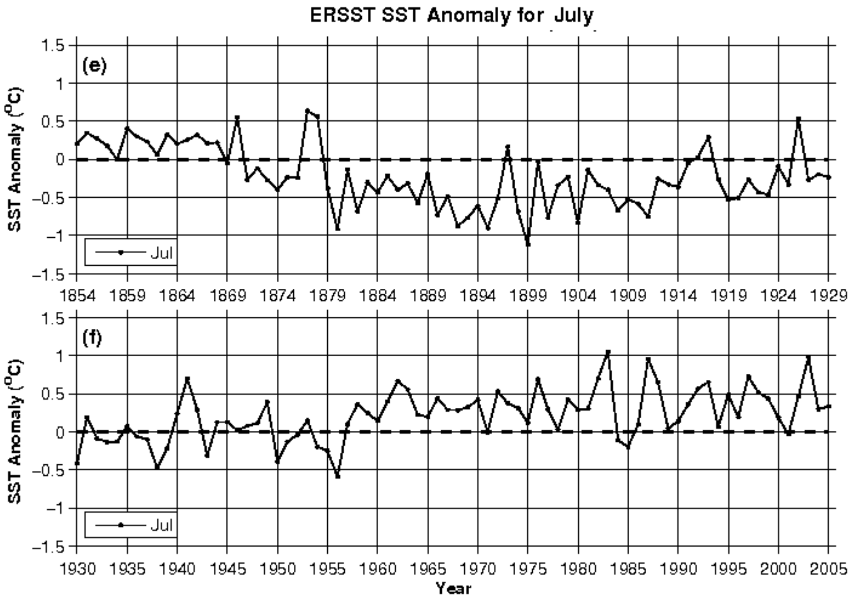

Bottom panel

Fig. 4.8: *Top panel (a-b)* – Time series of annual SST anomalies (residuals) during the period 1854-2005 using ERSST data in the whole Arabian Sea (5°N-30°N, 50°E-78°E) region. Annual SST anomalies during 1854-2005 are obtained by subtracting the climatology of annual mean SST from the annual mean SST of each individual year. *Middle panel (c-d)* – Time series of SST anomalies for January during the period 1854-2005 using ERSST data in the whole Arabian Sea (5°N-30°N, 50°E-78°E) region. The anomalies during 1854-2005 are obtained by subtracting the climatology of January mean SST from the January mean SST of each individual year. *Bottom panel (e-f)* – Same as Fig. 4.9 except that the anomalies are computed for July. Positive (negative) anomalies indicate warming (cooling). The 152 years monthly SST data from January 1854 to December 2005 is used to prepare the climatology of annual mean SST, January and July mean SSTs.

In the last three decades, year 1975 was a relatively cool SST year and year 2003 was a relatively warm SST year. Figure 4.9.1(a-l) shows the monthly SST difference between the warm year 2003 and the cool year 1975. Overall, during all the months in the year 2003, SST was high in the entire AS. The SST difference was found to be less in the Somali region during summer upwelling time. Significant SST differences could be seen in the northern and eastern AS regions during almost all months. Next, we compared the SST differences between two warm years 2003 and 2005 [Figs 4.9.2(a-l) and 4.9.3(a-l)]. The year 2005 was relatively less warm as to the year 2003. But SST differences between these two years show that year

2005 was warm in certain months – January in the northern AS, May in the entire AS and October-November – in the northeastern AS as revealed through ERSST dataset [Figs 4.9.2(a-l)]. This SST differences can be noted in the Reynolds SST dataset also [Figs 4.9.3(a-l)], but with certain discrepancies while comparing to ERSST. For example, during June, August and September months Reynolds SST showed localized warm regions in the AS, which is in fact found to be so meagre in the ERSST.

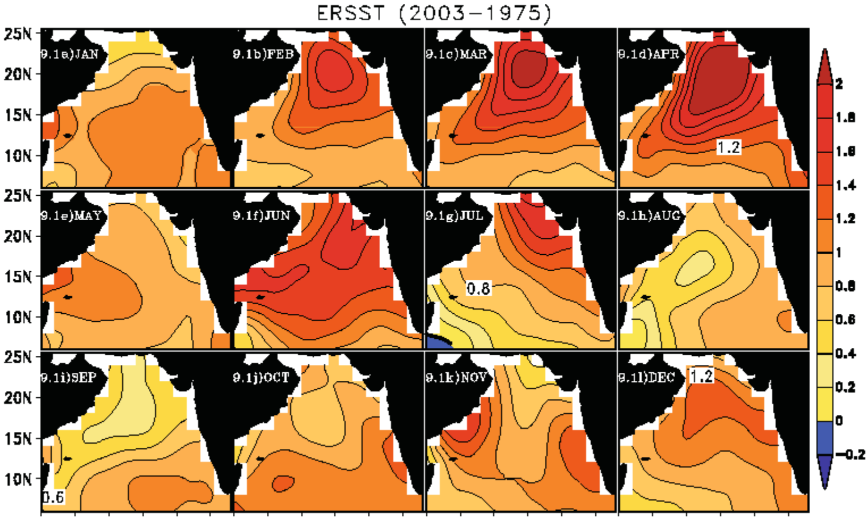

Top panel 4.9.1(a-l)

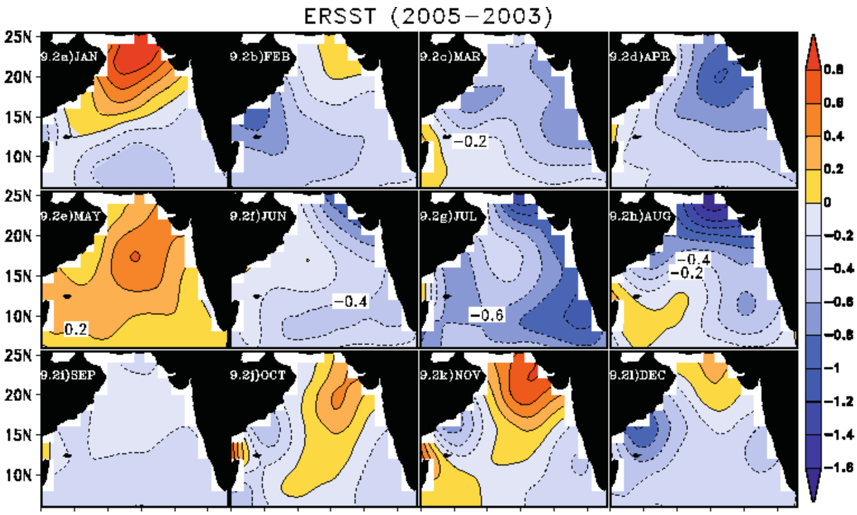

Middle panel 4.9.2(a-l)

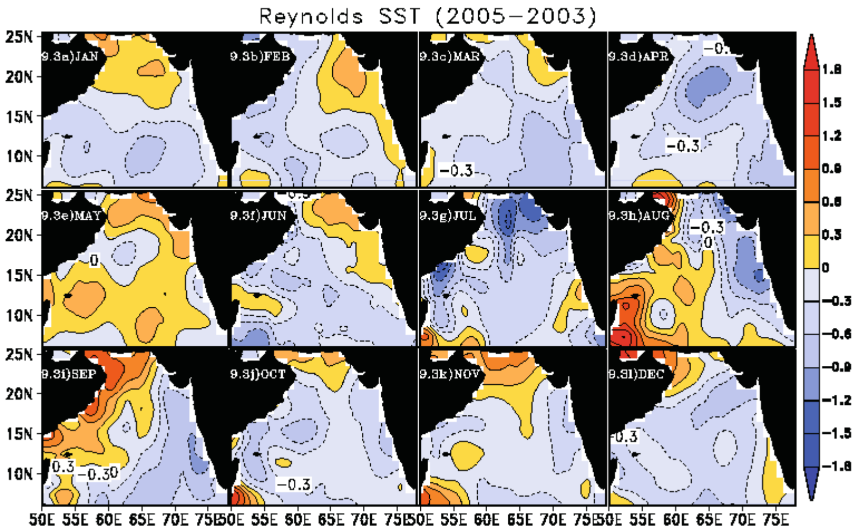

Fig. 4.9: *Top panel 4.9.1(a-l)* – Monthly mean SST (°C) difference between the warm year 2003 and the cold year 1975 (year 2003 minus year 1975) in the Arabian Sea based on ERSST data during the months of (a) January, (b) February, (c) March, (d) April, (e) May, (f) June, (g) July, (h) August, (i) September, (j) October, (k) November and (l) December. *Middle panel 4.9.2(a-l)* – Monthly mean SST (°C) difference between the years 2005 and 2003 (year 2005 minus year 2003) in the Arabian Sea based on ERSST data during the months of (a) January, (b) February, (c) March, (d) April, (e) May, (f) June, (g) July, (h) August, (i) September, (j) October, (k) November and (l) December. *Bottom panel 4.9.3(a-l)* – Same as Fig. 4.9.2(a-l) except the data being Reynolds SST data. The blue shading denotes negative values (cooling) and yellow to red indicates positive values (warming).

SUMMARY AND CONCLUSIONS

The annual cycle of SST shows that surface heat and momentum fluxes are important during the pre-monsoon and post-monsoon warming phases and winter cooling phase, whereas ocean dynamics and thermodynamics are important during the summer cooling phase. The intensity of pre-monsoon and post-monsoon warming as well as summer and winter cooling in the AS reveals local variations. Overall, the pre-monsoon warming in the AS is very prolonged (February-May) and stronger compared to the short-lived (September-October) post-monsoon warming. The southwest monsoon cooling is primarily triggered by upwelling, entrainment and heat loss at the ocean surface (Shaji et al., 2003; Shankar et al., 2002) and (Duing et al., 1980; McCreary et al., 1993; Shenoi et al., 2002). The winter monsoonal cooling is long-lasting (December-March) in the AS north of 16°N, with low SST observed during January-February. Most of the air-sea fluxes are found to be favourable for the observed winter AS cooling.

The FFT analysis reveals that at most of the analyzed local regions in the AS, pentadal SST oscillations predominate, followed by oscillations with decadal period. SST oscillations with peaks having period of ~2-4 years is found to be important in the central, western and eastern AS regions. It should be noted that the inter-annual SST variations in the Indian Ocean is affected by the El Niño-Southern Oscillation (ENSO) and Indian Ocean Dipole (IOD) events. The ENSO usually occurs with a period ranging from 2 to 7 years with an average of about four years (MacMynowski and Tziperman, 2008; Ashok et al., 2003). On the other hand, the IOD occurs with a periodicity of about quasi-biennial, quasi-pentadal or quasi-decadal (Ashok et al., 2003; Saji et al., 1999). From the 152 years SST analysis it is evident that the whole AS underwent certain warming and cooling episodes. It was in a small warm state during 1854-1870 before the arrival of a long duration of cool state during 1871-1956, with certain small warm years noticed within the cool period. Currently AS is experiencing a warming tendency, which began in 1957 and accelerated since 1990 onwards, with 1998 and 2003 as the largest warm years (with annual mean SST anomaly of 0.8°C in 1998 and >0.8°C in 2003). The AS warming noticed during the recent decades is in conjunction with the warming observed in other oceanic regions. From the 152 years' SST time series dataset, it is clear that in most of the years the annual SST cycles occurred in the (i) northern AS with SST ranging between 23°C and 29°C [Figs 4.7(a-b)], (ii) central and western AS with SST ranging between 25°C and a little less than 29°C [Figs 4.6(c-d) and (e-f)] and (iii) eastern AS with SST ranging between 27°C and equal or above 29°C [Figs 4.6(g-h)]. In most of the years, SST in the northern AS is at least 1°C lower than that of whole AS and other local regions. The year 1893 can be marked as the minimum SST observed year in all the regions such as whole (26.2°C), northern (25.7°C), central (25.7°C), western (25.8°C) and eastern (27.3°C) AS. But the maximum SST observed year is different in different regions – 1998 in the central and western (same 27.6°C), 1988 in the northern (27.5°C) and 2003 in the whole and eastern (28.1°C and 29°C respectively) AS regions. A comparison of ERSST and Reynolds SST in all the local regions shows that northern AS is a relatively cool region, while eastern AS is a relatively warm region. The amplitudes of SST in both ERSST and Reynolds SST datasets are also quite different. For example, in the whole and eastern AS regions, ERSST is higher than Reynolds SST in most of the years except during 1994-1998. The SST of each month during the 152 years is also observed to be deviated from the climatological value. During the cool (warm) state of AS, both winters and summers were also observed to be cooled (warmed). The SST differences between a warm year 2003 and a cool year 1975 reveals that significant SST differences are noticeable in the northern and eastern AS in all the months, except Somali region where SST differences are less significant during southwest monsoon.

ACKNOWLEDGEMENTS

Authors are thankful to the anonymous reviewers for their comments that helped us to improve this paper. We also express our gratitude to K.S. Sreejith, CORAL, IIT, Kharagpur for the assistance to prepare the final figures.

REFERENCES

Ashok, K., Guan, Z. and Yamagata, T. (2003). A look at the relationship between the ENSO and the Indian Ocean Dipole. *J. Meteor. Soc. Japan*, **81:** 41–56.

Bjerknes, J. (1969). Atmospheric teleconnections from the equatorial Pacific. *Mon. Weather Rev.*, **97:** 163-172.

Boschat, G., Terray, P. and Masson, S. (2011). Interannual relationships between Indian summer monsoon and Indo-Pacific coupled modes of variability during recent decades. *Clim. Dyn.*, **37:** 1019-1043, doi: 10.1007/s00382-010-0887-y.

Boyer, T., Levitus, S., Garcia, H., Locarnini, R.A., Stephens, C. and Antonov, J. (2005). Objective analyses of annual, seasonal, and monthly temperature and salinity for the World Ocean on a 0.25° grid. *Int. J. Clim.*, **25:** 931-945, doi:10.1002/joc.1173.

Casey, K.S., Brandon, T.B., Cornillon, P. and Evans, R. (2010). The Past, Present and Future of the AVHRR Pathfinder SST Program. *In:* Oceanography from Space: Revisited. Barale, V., Gower, J.F.R. and Alberotanza, L. (eds), Springer, doi: 10.1007/978-90-481- 8681-5_16.

Clark, C.O., Cole, J.E. and Webster, P.J. (2000). Indian Ocean SST and Indian summer rainfall: predictive relationships and their decadal variability. *J. Clim.*, **13:** 2503-2519.

Druyan, L.M., Miller, J. and Russel, G. (1983). Atmospheric general circulation model simulations with an interactive ocean: Effect of SST anomalies in the Arabian Sea. *Atmos.-Ocean.*, **21:** 94-106.

Duing, W. and Leetmaa, A. (1980). Arabian Sea cooling: A preliminary heat budget. *J. Phys. Oceanogr.*, **10:** 307-312.

Josey, S.A. Kent, E.C. and Taylor, P.K. (1998). The Southampton Oceanography Centre (SOC) Ocean-Atmosphere Heat. *Momentum and Freshwater Flux Atlas*. Southampton Oceanography Centre, Southampton, UK, 6.

Josey, S.A., Kent, E.C. and Taylor, P.K. (1999). New insights into the ocean heat budget closure problem from analysis of the SOC air-sea flux climatology. *J. Clim.*, **12:** 2856-2880.

Joseph, P.V. (1990). Warm pool in the Indian Ocean and monsoon onset. *Trop. Ocean-atmos. Newsl.*, **53:** 1-5.

Kothawale, D.R., Munot, A.A. and Borgaonkar, H.P. (2008). Temperature variability over Indian Ocean and its relationship with Indian summer monsoon rainfall. *Theor. Appl. Climatol.*, **92:** 31-45, doi: 10.1007/s00704-006-0291-z.

Kalnay, E., Kanamitsu, M., Kistler, R., Collins, W., Deaven, D., Gandin, L., Iredell, M., Saha, S., White, G., Woollen, J., Zhu, Y., Chelliah, M., Ebisuzaki, W., Higgins, W., Janowiak, J., Mo, K.C., Ropelewski, C., Wang, J., Leetmaa, A., Reynolds, R., Jenne, R. and Joseph, D. (1996). The NCEP/NCAR 40-year reanalysis project. *Bull. Am. Meteorol. Soc.*, **77:** 437-471.

Kubota, M., Iwasaka, N., Kizu, S., Konda, M. and Kutsuwada, K. (2002). Japanese ocean flux datasets with use of remote sensing observations (192×94). *J. Oceanogr.*, **58:** 213-225.

Legeckis, R. (1988). Upwelling off the gulfs of Panama and Papagayo in the Tropical Pacific during March 1986. *J. Geophys. Res.*, 93(C12) **15:** 15485-15489.

Levitus, S., Antonov, J., Boyer, T.P. and Stephens, C. (2000). Warming of the world ocean. *Science*, **287:** 2225-2229.

McCreary, J.P., Kundu, P.K. and Molinari, R.L. (1993). A numerical investigation on dynamics, thermodynamics and mixed-layer processes in the Indian Ocean. *Prog. Oceanogr.*, **31:** 181-244.

MacMynowski, D.G. and Tziperman, E. (2008). Factors affecting ENSO's period. *J. Atmos. Sci.*, **65:** 1570-1586.

Oberhuber, J.M. (1988). An atlas based on the COADS data set: The budgets of heat, buoyancy and turbulent kinetic energy at the surface of the global ocean. Tech. Rep. MPI Rep. Max-Plank-Inst. für Meteorol., Bundestrasse, Germany, 15.

Rasmusson, E.M. and Wallace, J.M. (1983). Meteorological aspects of the El Niño/ Southern Oscillation. *Science*, **222:** 1195-1202.

Rao, K.G. and Goswami, B.N. (1988). Interannual variations of the sea-surface temperature over the Arabian Sea and the Indian Monsoon: A new perspective. *Mon. Weather Rev.*, **116:** 558-568.

Reynolds, R.W., Rayner, N.A., Smith, T.M., Stokes, D.C. and Wang, W. (2002). An improved in situ and satellite SST analysis for climate. *J. Clim.*, **15:** 1609-1625.

Shukla, J. (1975). Effect of Arabian sea surface temperature anomaly on Indian summer monsoon: A numerical experiment with GFDL model. *J. Atmos. Sci.*, **32:** 503-511.

Smith, T.M. and Reynolds, R.W. (2004). Improved Extended Reconstruction of SST (1854-1997). *J. Clim.*, **17:** 2466-2477.

Shaji, C., Iizuka, S. and Matsuura, T. (2003). Seasonal variability of near-surface heat budget of selected oceanic areas in the north tropical Indian Ocean. *J. Oceanogr.*, **59:** 87-103.

Shankar, D., Vinayachandran, P.N. and Unnikrishnan, A.S. (2002). The monsoon currents in the north Indian Ocean. *Prog. Oceanogr.*, **52:** 63-120.

Shenoi, S.S.C., Shankar, D. and Shetye, S.R. (2002). Differences in heat budgets of the near-surface Arabian Sea and Bay of Bengal: Implications for the summer monsoon. *J. Geophys. Res.*, **107** (doi: 10.1029/2000JC000679).

Saji, N.H., Goswami, B.N., Vinayachandran, P.N. and Yamagata, T. (1999). A dipole mode in the tropical Indian Ocean. *Nature*, 401: 360-363.

Vinayachandran, P.N. and Shetye, S.R. (1991). The warm pool in the Indian Ocean. *Proc. Indian Acad. Sci. (Earth Planet Sci.)*, **100(2):** 165-175.

Vargas-Yáñez, M., García, M.J., Salat, J., García-Martínez, M.C., Pascual, J. and Moya, F. (2008). Warming trends and decadal variability in the Western Mediterranean shelf. *Global and Planetary Change*, **63:** 177-184.

Webster, P.J., Moore, A., Loschnigg, J. and Leben, R. (1999). Coupled ocean-atmosphere dynamics in the Indian Ocean during 1997-1998. *Nature*, **401:** 356-360.

Washington, W., Chervin, R. and Rao, G. (1977). Effect of a variety Indian Ocean surface temperature patterns on the summer monsoon circulation: experiment with NCAR GCM. *Pure and Appl. Geophys*., **115:** 1335-1356.

Weller, R.A., Baumgartner, M.F., Josey, S.A., Fischer, A.S. and Kindle, J.C. (1999). Atmospheric forcing in the Arabian Sea during 1994-1995: Observations and comparisons with climatology and models. *Deep-Sea Res.,* Part II, **45:** 1961-1999.

Worley, S.J., Woodruff, S.D., Reynolds, R.W., Lubker, S.J. and Lott, N. (2005). ICOADS Release 2.1 data and products. *Int. J. Clim*., **25:** 823-842, doi:10.1002/joc.1166.

CHAPTER

5

Paleoclimate of Peninsular India

R. Ramesh, S.R. Managave[1] and M.G. Yadava

Physical Research Laboratory, Navrangpura, Ahmedabad – 380009, India
[1]Department of Earth Sciences, Pondicherry University
Puducherry – 500055, India
rramesh@prl.res.in

INTRODUCTION

The limited spatial and temporal coverage of instrumental weather records precludes the knowledge of long-term climatic changes. To infer such changes, recourse is taken to natural archives that serve as climate proxies. The prominent proxies that offer annual to seasonal temporal resolution include annual rings of trees (Ramesh et al., 1985; Ramesh et al., 1986a; Ramesh et al., 1986b; Ramesh et al., 1988; Ramesh et al., 1989; Managave et al., 2010a; Managave et al., 2010b; Sano M. et al., 2010; Managave et al., 2010c; Managave et al., 2010d; Managave et al, 2010e), corals (Chakraborty et al., 1992; Chakraborty et al., 1993a; Chakraborty et al., 1993b; Chakraborty et al., 1993c; Chakraborty et al., 1994; Chakraborty et al., 1997), ice cores (Nijampurkar et al., 1986), speleothems (Yadava et al., 2004) in some cases and varved sediments (Von Rad et al., 1999). Among these, tree-rings have specific advantages: they have a wide geographic distribution, are annually resolved, show a continuous record, and are easily dated by ring-counting. Seasonality in the growth rate of trees driven by seasonality in the climatic factors can result in well-defined annual growth rings in trees. Individual tree-rings faithfully record contemporary climatic signatures and hence provide an opportunity to decipher the variation in climatic parameters for a duration equivalent to the life-span of the tree. Using a technique called cross-dating, a procedure of matching ring patterns among trees and wood fragments in a given area (Fritts et al., 1976), it has been possible to stretch back tree-ring

J. Sundaresan et al. (eds.), *Climate Change and Island and Coastal Vulnerability*,
DOI 10.1007/978-94-007-6016-5_5, © 2013 Capital Publishing Company

record for thousands of years (Leuschner et al., 2002; Spurk et al., 2002). In the early years, only the width of the rings was used for climate reconstruction; wider (narrower) ring denoting higher (lower) temperature/precipitation. However, this simple relationship between width and climate is complicated by a variety of non-climatic factors (Fritts et al., 1976). For example, the site specific factors such as topography, soil type, forest thinning and ecological parameters like pest/insect infestations on trees can modify the climate-ring-width relationship. Isotopic composition (e.g., $\delta^{18}O$) of tree cellulose is believed to be less influenced by biological and ecological parameters in relation to ring-widths and can be used effectively in climate reconstruction. It has been shown by previous studies (Ramesh et al., 1986b; Schiegl et al., 1974; Gray et al., 1976; Epstein et al., 1977; Burk et al., 1981; Edwards et al., 1985; Lipp et al., 1991; Feng et al., 1994), that isotopic record of oxygen and hydrogen from individual tree-rings can be successfully used as proxies to decipher climatic parameters such as rainfall, humidity and temperature.

Tropics and Teak (*Tectona grandis*)

Tropical area appears to play a crucial role in global climate through El Niño-Southern Oscillation (ENSO), a coupled atmospheric-ocean phenomenon affecting climate of tropical, subtropical and mid-latitude areas (Diaz et al., 2000). In India, the relationship between ENSO and monsoonal rainfall has been established (Pant et al., 1981; Krishna Kumar et al., 1995). Limited time span covered by instrumental rainfall record demands finding proxies to understand past variations in ENSO. Corals have been used to reconstruct past variation in ENSO (Cole et al., 2000; Cole et al., 1993; Tudhope et al., 2001). Tree rings provide excellent terrestrial archives for the past variation in ENSO related rainfall (Stahle et al., 1998; D'Arrigo et al., 2005; Christie et al., 2008). As there is no pronounced seasonality in temperature, a factor responsible for growth rings in temperate regions (Fritts et al., 1976), tropical trees rarely exhibit well developed annual growth rings. Nevertheless, seasonality in precipitation and relative humidity in some tropical areas does result in the development of annual growth rings in a few species. Teak is one such species with reliable growth rings and is distributed throughout tropical Asia, parts of Africa and Latin America. Several regional chronologies have been developed using teak trees (Berlage et al., 1931; Pumijumnong et al., 1995; Borgaonkar et al., 2007; Buckley et al., 2007).

Oxygen Isotopes in Tree Cellulose

Stable isotope ratios of carbon (^{13}C), hydrogen (H) and oxygen (^{18}O) in tree rings have been used to get information about past climate. Although ^{13}C of the tree rings have been used to understand past variations in ^{13}C of atmospheric CO_2 and climatic parameters such as temperature and relative humidity, its interpretation is complicated by variety of environmental effects.

These effects include juvenile effect (rings corresponding to the early years of growth are depleted in ^{13}C as they ingest ^{13}C depleted CO_2 released by respiration of other plants and soil, and the degradation of organic matter) and pollution/anthropogenic effect (tree rings since the industrial era, i.e. from around AD 1850 are progressively depleted in ^{13}C due to introduction of ^{13}C depleted CO_2 in the atmosphere produced by fossil fuel burning, and a plant's response to increasing CO_2 concentration in atmosphere; also known as the 'Suess Effect'. In addition, different levels of solar radiance and nutrients available to plants, and water stress cause variations in ^{13}C around the circumference of a ring (intra-ring variation) (Francey et al., 1982) ^{18}O of tree cellulose, on the contrary, is directly related to the oxygen isotopic ratio of the plant's source water (and hence that of precipitation) and relative humidity (Roden et al., 2000). Since oxygen isotope ratio of precipitation is directly related to temperature (Dansgaard et al., 1964), and/or amount of precipitation (Dansgaard et al., 1964; Rozanski et al., 1993; Yadava et al., 2007) it is conceivable that ^{18}O signature of tree cellulose is a more powerful tool in reconstructing past climate.

Oxygen isotope composition (^{18}O) of plant material depends upon ^{18}O of the source water, the level of evaporative enrichment of the source water in the leaf during transpiration, biochemical fractionation associated with the synthesis of sucrose in the leaf and the extent of exchange between sucrose and xylem water during cellulose synthesis. A detailed description of processes that govern the above mentioned factors is given elsewhere (Managave et al., 2010d). Teak (*Tectona grandis* L.F.) is an important tropical tree species that has good potential in the reconstruction of past rainfall. Dendroclimatologists have built several teak chronologies using variations in the annual growth rings of teak that date back to several centuries. Compared to ring-width variations in teak, the isotopic variations in teak have not been fully exploited for past climate reconstruction even though their potential was realized as early as 1989. In this context, the present study aims at understanding the relationship between oxygen isotopic composition (^{18}O) of teak and climate on sub-annual and inter- annual time scales. Towards this, teak trees growing in different climatic settings of India were analyzed for cellulose ^{18}O variations.

Climatology of Sample Locations

To understand how teak growing in different climatic settings responds to ambient climate, trees from different parts of the peninsular India were selected. While selecting the locations care was taken with respect to duration, pattern and amount of rainfall these locations receive. Figure 5.1 shows locations of the trees used in the present study (locations indicated by circles and bold letters). The samples are from locations near Thane, Jagdalpur, Hanamkonda and Perambikulam. Figure 5.1 also shows IMD weather stations (Mumbai, Jagdalpur, Hanamkonda and Palakkad, also known as Palghat)

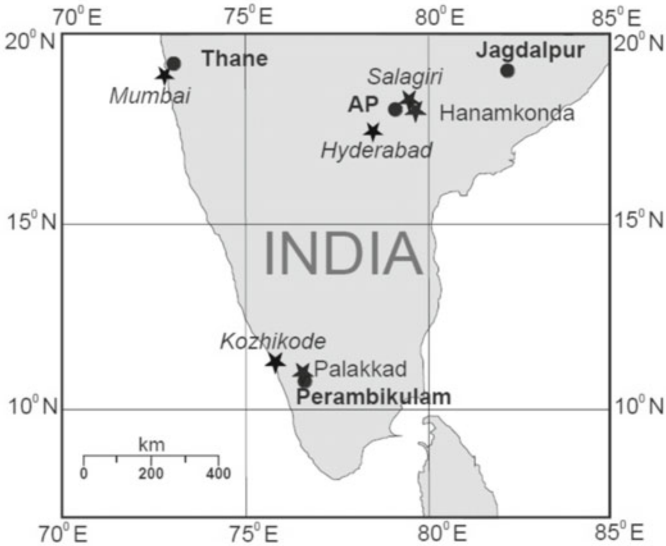

Fig. 5.1: Locations of the teak tree samples (circles and bold letters) and IMD/GNIP stations (starts and letters in italics).

near the sample locations. Figures 5.2a and 5.2b show the climatologies of Mumbai and Palakkad, respectively. Similar figures for the other two locations are presented elsewhere (Managave et al., 2010b). The data used in these figures is monthly mean data of climatological parameters based on observations from year 1951 to 1980 CE. Among these locations, Palakkad receives the highest amount of rainfall (2163 mm) and has the highest number of rainy days (~103 days). Mumbai (earlier called Bombay), although receives rainfall comparable to Palakkad, yet has only ~76 rainy days. Hanamkonda receives the lowest amount of rain and has the least number of rainy days.

Summer monsoon is the prominent source of rainfall at Mumbai, Jagdalpur and Hanamkonda. The summer rainfall is associated with formation of monsoon depressions which form in the Bay of Bengal north of 18°N latitude and their west-northwest movement along the monsoon trough (Pant et al., 1997). It is also known that the north-south movement of the monsoon trough can affect rainfall over this region: north-ward shift of monsoon trough towards the foot-hills of the Himalaya results in decrease and increase in the rainfall over the peninsular India and the foot-hills of the Himalaya, respectively. Rainfall over Palakkad, on the contrary, is also dominated by winter monsoon, mainly due to the passage of cyclonic systems passing over the southern part of India during October to December. The ratios of NE to SW monsoon rainfall at these stations are ~0.04 (Mumbai), ~0.11 (Jagdalpur), ~0.17 (Hanamkonda) and ~0.27 (Palakkad).

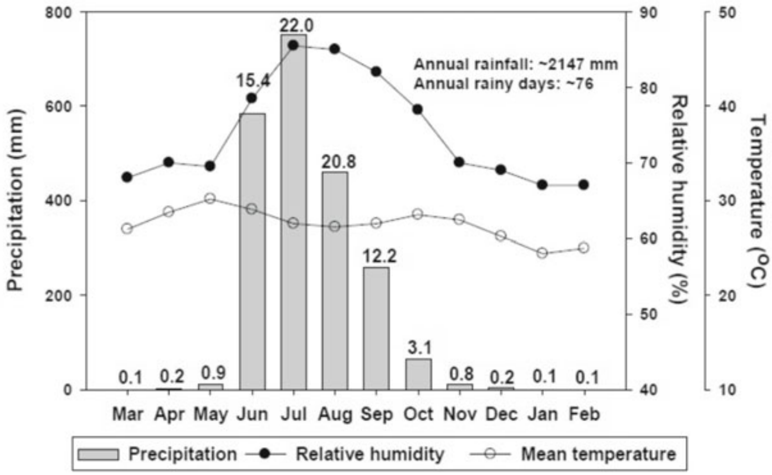

Fig. 5.2a: Climatology of Mumbai, Maharashtra. Numbers above the histogram bars indicate number of rainy days in the respective month.

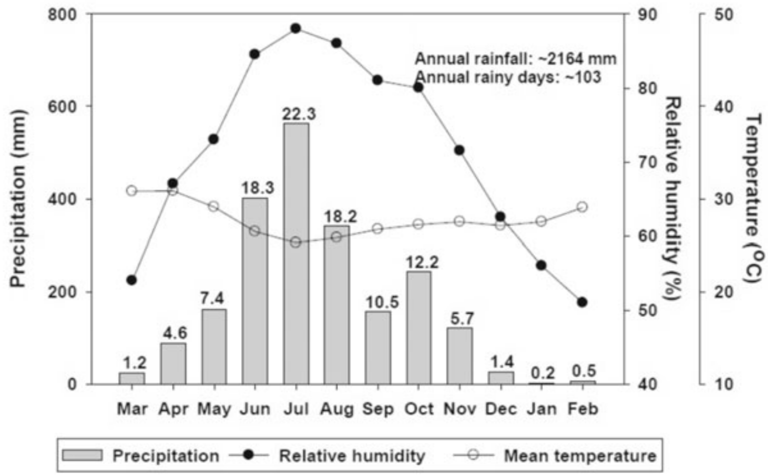

Fig. 5.2b: Climatology of Palakkad, Kerala. Numbers above the histogram bars indicate number of rainy days in the respective month.

Rainfall ^{18}O Record

Isotope data of rainwater is available for GNIP (Global Network of Isotopes in Precipitation) stations located near the sample locations (Fig. 5.1, location indicated by 'star' marks and letters in italics). These stations are Mumbai (18.9°N, 72.82°E), Kozhikode (11.25°N, 75.78°E), Hyderabad (17.45°N, 78.47°E) and Salagiri (18.19°N, 79.44°E). Mumbai covers data from year 1961 to 1966 CE and from 1972 to 1976 CE; Hyderabad, from 1997 to 2000 CE; Kozhikode, from 1997 to 2004 CE; and Salagiri, for 1977 CE only.

Mean weighted (by 161 amount of precipitation) monthly oxygen isotopic composition (^{18}O) of rainfall and monthly precipitation for the corresponding period for Mumbai, Kozhikode and Salagiri is shown in Table 5.1. Along with Salagiri, GNIP has also recorded monthly ^{18}O of nearby stations viz. Bhopalpalli (18.27°N and 79.52°E), Chinpak (18.28°N and 79.44°E), Kamalpur (18.29°N 165 and 79.54°E), Nasarampur (18.26°N and 79.47°E) and Tundla Buzurg (18.32°N and 166 79.47°E). All these stations show (Fig. 5.3) a similar pattern of monthly ^{18}O values indicating similarity in the monthly ^{18}O of rainfall.

Table 5.1: Monthly ^{18}O of rainfall for the locations near the sample locations

Month	*Mumbai*		*Salagiri*		*Kozikhode*	
	Amount, mm	*Weighted mean $\delta^{18}O$, ‰*	*Amount, mm*	*Weighted mean $\delta^{18}O$, ‰*	*Amount, mm*	*Weighted mean $\delta^{18}O$, ‰*
April					73	-4.3
May					335	-3.0
June	544	-1.1			687	-2.1
July	698	-1.7	286	-2.2	608	-1.8
August	395	-1.1	145	-3.6	396	-1.5
September	248	-1.8	140	-10.7	181	-3.4
October	90	-4.8	18	-7.8	311	-4.5
November	15	-5.4	51	-9.1	125	-7.3
December	19	-0.2			58	-6.2

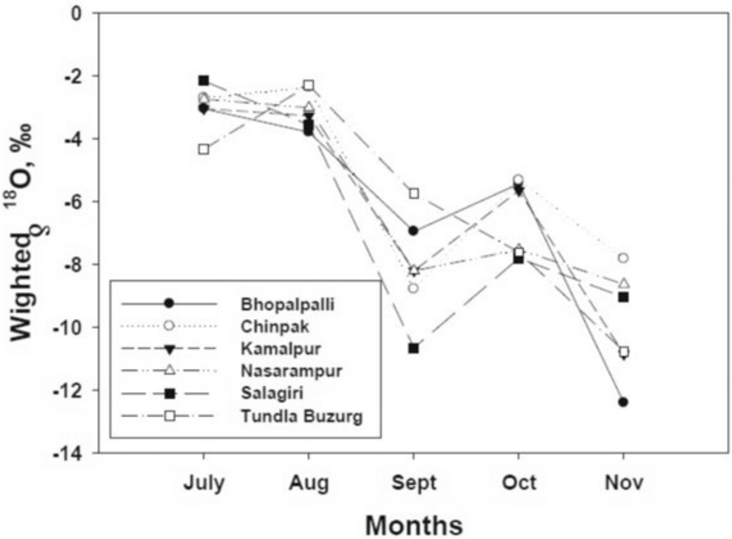

Fig. 5.3: Monthly rainfall ^{18}O values for various stations in central India for year 1977 CE.

Yearly fluctuations in the amount weighted mean yearly ^{18}O of rainfall for Kozhikode are shown elsewhere (Managave et al., 2010a). For Mumbai, such yearly fluctuations in ^{18}O can be as high as 2‰. Relation between weighted (by amounts of precipitation) monthly rainfall ^{18}O and monthly amount of rainfall for station Kozhikode is also shown elsewhere. ^{18}O record at Kozhikode shows a large variation in the mean monthly rainfall ^{18}O values which are not necessarily correlated with the amount of rainfall in the respective months. Figure 5.4 shows the spread in monthly rainfall ^{18}O values based on observations from year 1997 to 2004 CE. In addition to GNIP stations, rainfall isotopic composition (Yadava et al., 2005) at Jharsuguda (22°N and 84°E) for the year 1999 and Mangalore (Yadava et al., 2007) for June to October 2000 to 2002 CE. An inverse relation between amount of rainfall and its ^{18}O i.e. amount effect was found (Yadava et al., 2005). They observed a depletion rate of –9.2 ± 1.1‰ and –2.2 ± 0.8‰ for 100 mm rain for each rain event and total monthly rain, respectively for Jharsuguda. The ^{18}O depleted nature of rainfall during NE monsoon and a positive amount effect for Mangalore was also reported (Yadava et al., 2007).

Based on GNIP precipitation and its ^{18}O record and other such data, the following points can be deduced:

1. NE monsoon rainfall is depleted in ^{18}O than the SW monsoon rainfall.
2. Amount effect is observed in individual rain events and monthly rainfall of particular season i.e. the SW or NE monsoon season.
3. During the SW monsoon season, rain at central India (Salagiri) is more depleted in ^{18}O than at southern India (Kozhikode).

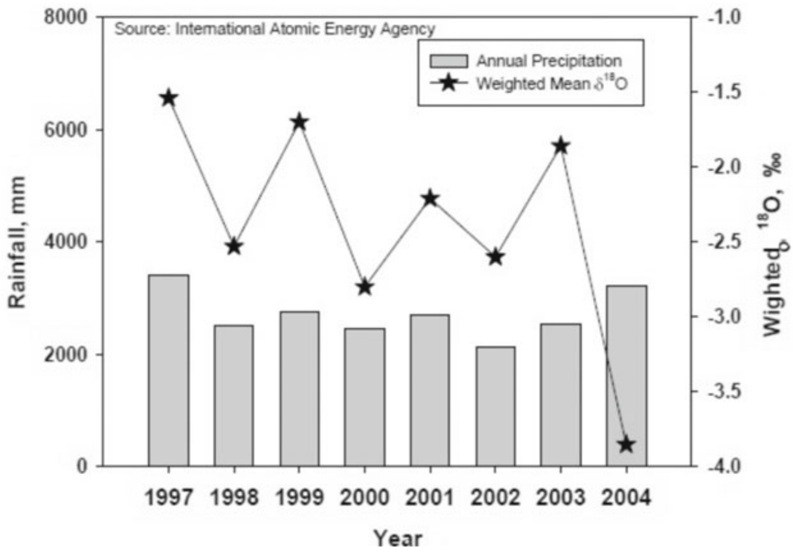

Fig. 5.4: Yearly rainfall (bars) and weighted annual rainfall ^{18}O (stars) observed at 198 Kozhikode, Kerala.

EXPERIMENTAL METHOD

Sample Collection

All the samples used in the present study are tree discs collected either by the Indian Institute of Tropical Meteorology (IITM), Pune, India or the Birbal Sahani Institute of Palaeobotany (BSIP), Lucknow, India. IITM and BSIP are routinely involved in tree-ring width based dendrochronological and dendroclimatological investigations. The locations and time spans covered by the samples used in the present study are given in Table 5.2.

The samples from the western (Thane) and central (Jagdalpur and Hanamkonda) India were obtained from the IITM collection. The details regarding the collection of several tree discs from the Murbad forest, Maharashtra, India (19°14′ N, 73°24′ E), and their dating is given elsewhere (Pant et al., 1983). Standard procedures were employed for dating these discs and the discs showed a good cross-match with no double or missing rings. Borgaonkar collected (years 2000 and 2004 CE) several tree cores and discs from central India and found a good cross matching between the cores from the same tree and from different trees at the same site for some sites (Borgaonkar et al., 2007). These discs and cores are currently being studied for the development of tree ring index chronologies. In the present study, two tree discs (Jag03 and Jag04) were selected out of this collection and used for climate reconstruction. These discs were taken from wind-felled tree from Chhattisgarh and the distance between them is about 25 km. Based on their year of fall, years 2003 and 2004 CE were assigned to the outermost rings of Jag03 and Jag04, respectively. Two more cross dated tree discs (AP1 and AP2) were selected from the IITM collection. These trees belong to area near Hanamkonda, Andhra Pradesh and are located about 100 km south of trees selected from Chattisgarh. Tentative cross dating yielded years 1960 and 1952 CE to the outermost rings of AP1 and AP2, respectively. The sample from southern India was collected and dated by Amalava Bhattacharyya of BSIP. The sample was collected from area near

Table 5.2: Names and locations of the samples collected in the present study and time spans covered by them

Sample name	*Nearest town*	*Latitude*	*Longitude*	*Years covered CE*
THN	Thane	19°12′N	73°02′E	1920-1962
Jag03	Jagdalpur	19°03′N	82°03′E	1824-2003
Jag04	Jagdalpur	19°05′N	82°20′E	1866-2004
AP1	Hanamkonda	18°03′N	79°02′E	1875-1960
AP2	Hanamkonda	18°03′N	79°02′E	1929-1952
PKLM	Perambikulam	10°-20′-10°-26′N	76°-35′-76°-50′E	1943-1988

Parambikulam (10°20′–10°26′N; 76°35?–76°50′E) during March 2000 CE. It is a disc cut out of a wind-felled tree. The dating of the sample was done through cross dating with the master tree ring plot for the area. The sample dates from 1743 to 1986 CE and the dates were checked using the computer program COFECHA (Holmes et al., 1983). The details regarding sample collection and the master tree ring plot is described elsewhere (Bhattacharyya et al., 2007). For the purpose of the present work, it is assumed that the dates are correct to ± 1 year.

Ring Separation and Powdering

The experimental procedure adopted in the present study is shown in Fig.5.5. Radial strips along the selected directions were cut from the discs mentioned above. The radial strips were manually polished thoroughly using different grades of sandpaper. Upon polishing all the samples showed clear ring-porous structure (Fig. 5.6). The vesicle size and frequency decreased from the pith-side to the bark-side. Rings were counted under microscope and calendar years were assigned to them by counting the rings, knowing the year of felling/fall.

Subsequent to the dating of samples, individual rings were separated using scalpel, chisel and hammer. The resolution with which the rings were separated depended upon width of the rings; rings with widths less than 0.6mm were combined together. Use of recently developed cellulose extraction methods, which are described later, enabled to extract cellulose from small amounts of wood material and hence facilitated a higher resolution sampling. While separating the rings, maximum care was taken to avoid contamination

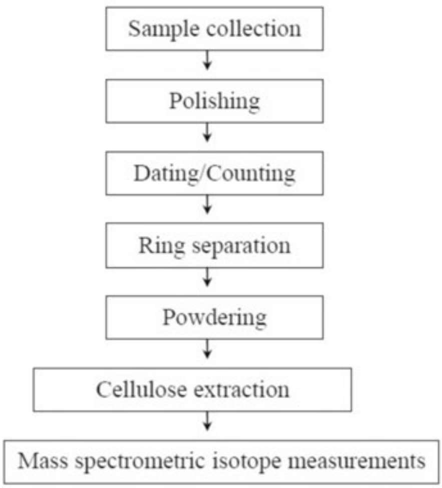

Fig. 5.5: Flow chart showing the experimental procedure followed in the present study.

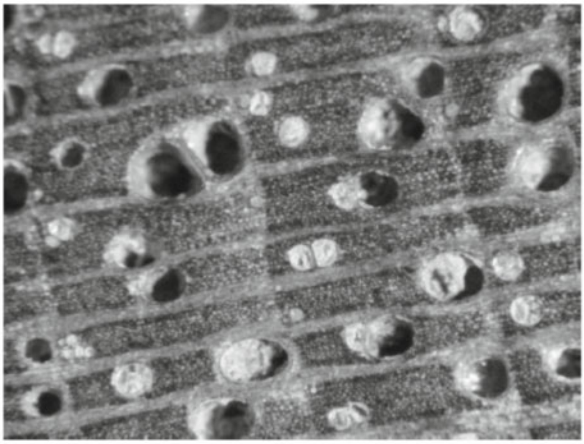

Fig. 5.6: Ring porous vesicle structure observed in the teak samples.

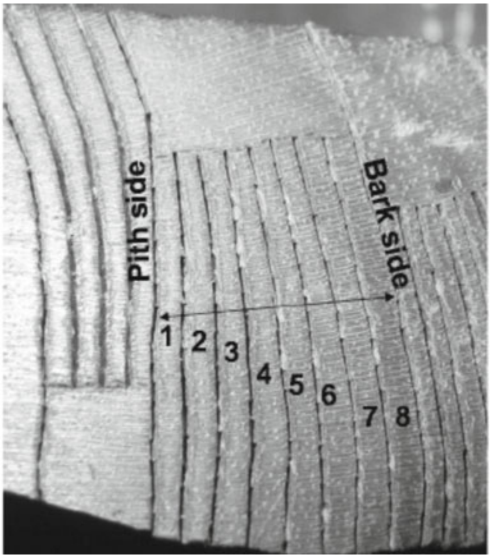

Fig. 5.7: Photograph of a ring subdivided into eight parts for studying sub-annual $\delta^{18}O$ variations.

from the adjacent rings. Intra-ring sampling was done to understand how the isotopic composition of photosynthates varied along the radial direction within a ring. For this, about 10 rings from each sample (except the sample from Thane) were selected randomly and further separated into four equal parts. Some of these rings which were comparatively wider were sampled with higher as well as lower resolutions. In the higher resolution sampling, the rings were subdivided into 6 or 8 or 12 or 16 parts. The widest ring from central Indian sample (Jag03) was sampled with the highest resolution: the ring was subdivided into 16 parts. Figure 5.7 depicts a representative photograph of a ring which was subdivided into eight parts. The separated rings/parts of the rings were powdered in a Wiley mill. The mill was cleaned thoroughly after powdering of each ring sample. The powdered material was transferred to a plastic vial with screw cap and stored for further treatment.

Extraction of Cellulose

Cellulose was extracted from the powdered wood material using a method (Gaudinski et al., 2005) with some modifications. Gaudinski's method called 'MBrendel' method, is a modification of another method. The steps followed in the present study are as follows.

Step 1

- Take about 50 mg of wood powder in a dry round bottom glass tube with stoppers
- Add 2 ml of 80% acetic acid
- Add 0.2 ml of 69% nitric acid
- Seal the tube with stoppers using Teflon tape
- Boil at 120°C for 30 minutes

Step 2

- Allow the tubes to cool (~5-10 min)
- Transfer the solution to glass centrifuge tubes having screw caps with Teflon inliners
- Add 2.5 ml 99% ethanol

Step 3

- Vortex
- Centrifuge for five minutes at 3500 rpm or higher
- Decant supernatant

Step 4

- Add 2 × 2.5 ml 99% ethanol in two steps; the first 2.5 ml is added and mixed, the second addition is to make wash down the sides of the glass tube to force samples back to solution
- Repeat Step 3

Step 5

- Add 2 × 2.5 ml of distilled deionised water (DDI)
- Repeat Step 3

Step 6

- Add 2 × 2.5 ml 17% (w/v) NaOH using glass pipettes
- Stir the sample pellets with thin glass rod
- Ultrasonicate the mixture for ~5 min
- Let the mixture sit for one hour
- Repeat Step 3

Step 7

- Add 2 × 2.5 ml DDI water
- Repeat Step 3

Step 8

- Add 2.2 ml DDI water + 0.6 ml acetic acid
- Vortex
- Add 2.2 ml DDI water to wash the sides of the glass tubes and mix gently
- Repeat Step 3

Step 9

- Repeat Step 3 three times

Step 10

- Add 2 × 2.5 ml 99% ethanol
- Repeat Step 3

Step 11

- Add 2 × 2.5 m acetone
- Repeat Step 3

Step 12

- Allow the sample to dry overnight in an oven at 50°C
- Transfer the sample to 1.5 ml polypropylene centrifuge tube and keep the tube in desiccator

In the present study, some modifications were introduced in the Step 6 of Gaudinski's method. These modifications are ultrasonicating the mixture (sample and NaOH) for ~5 min and keeping the solution for one hour instead of ~10 min as suggested in the original method. In a day, cellulose was extracted from two batches of samples each containing 16 samples, a number determined by the capacity of the centrifuge.

Mass Spectrometric Isotope Measurements and Analytical Precision

The isotopic measurements were done using Thermo Quest's Finnigan Delta plus continuous flow Isotope Ratio Mass Spectrometer (IRMS) available at the National Facility, University of Agricultural Sciences, Bangalore, India. The peripherals attached with the mass spectrometer were High Temperature Conversion Elemental Analyzer (TC/EA) and ConFlo III. TC/EA was operated at 1350°C to ensure complete pyrolysis of the samples. To avoid isotopic interference of CO and N_2 the pyrolyzed gases were then passed through Gas Chromatograph (GC) column (0.6 m × 1/4″ × 4 mm, stainless steel). The molecular sieve used in GC was 5Å, 80-100 mesh size. ConFloIII is a device coupling TC/EA and IRMS. It works with an open-split arrangement whereby a gas flow of ~80-100 ml/min coming from TC/EA is reduced to ~0.3 ml/min, a rate at which gas is introduced into the IRMS. ConFloIII contains two open split cells: one 'sample section' and the other 'reference section'. 'Sample section' and 'reference section' split the gas coming from TC/EA and reference gas cylinder, respectively.

For isotopic measurement, about 0.85 mg of cellulose was packed in silver foil and the sample capsules were put in oven kept at 60°C for at least 10 hours before measurements. Typically, 50 samples were analyzed in a single run. These contained 44 cellulose samples and six standards at 1st, 10th, 20th, 30th, 40th and 50th positions. The standards used were in-house calibrated starch ($\delta^{18}O$ = 26.8‰) and Australian National University (ANU) sucrose ($\delta^{18}O$ = 36.4‰). All the measurements were done with ConFloIII on 'He dilution ON' mode. During measurement of a sample, three reference gas pulses were injected in IRMS first followed by a sample gas injection and again reference gas injection. Time required for the measurement of one sample was 10 min. The reference gas injections gave internal precision less than 0.1‰. The external precision of the measurements were consistently less than 0.3‰. Table 5.3 gives precisions of the ANU sucrose $\delta^{18}O$ values measured during individual runs and the date of respective runs. Plot of $\delta^{18}O$ measurements of all the ANU sucrose standards used during cellulose sample measurements is shown in Fig. 5.8. Oxygen isotopic composition of all the samples reported in the present study are in relation to VSMOW.

Typically the reactor was changed every 250 samples. The system was degassed overnight with TC/EA at 1350°C and GC at 300°C after changing the reactor. After checking for leak in the connections, background levels were measured. The typical background on CUP1 for peaks 28, 29 and 30 were 7 mV, 4 mV, and 29 mV, respectively with He dilution in ConFloIII ON (48 mV, 32 mV and 29 mV when He dilution in ConFloIII was OFF). The backgrounds for masses 18, 28, 32 and 44 on CUP2 were 7000 mV,

Table 5.3: Standard deviations (1 sigma) of $\delta^{18}O$ measurements of ANU Sucrose samples (367) measured during various runs in July 2008. Mean of the measurements is 36.4‰.

Date	*External precision*	*Date*	*External precision*	*Date*	*External precision*	*Date*	*External precision*
July 7	± 0.3	July 12	± 0.2	July 16	± 0.2	July 25	± 0.3
July 8	± 0.3	July 13	± 0.2	July 17	± 0.1	July 26	± 0.3
July 8	± 0.2	July 14	± 0.3	July 17	± 0.2	July 26	± 0.2
July 9	± 0.1	July 14	± 0.2	July 21	± 0.3	July 28	± 0.2
July 10	± 0.3	July 15	± 0.3	July 22	± 0.4	July 29	± 0.2
July 10	± 0.3	July 15	± 0.2	July 23	± 0.3	July 30	± 0.2
July 11	± 0.3	July 16	± 0.3	July 24	± 0.4		

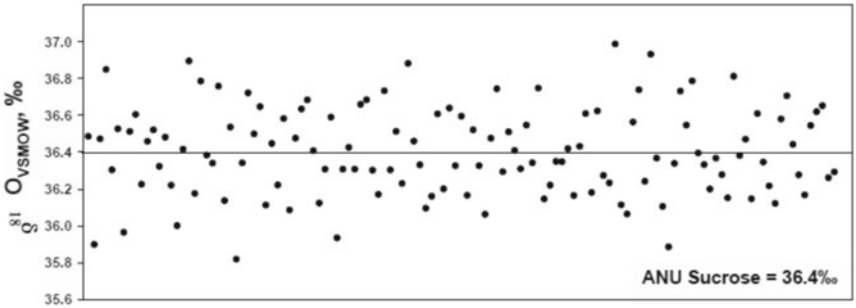

Fig. 5.8: Scatter plot showing $\delta^{18}O$ values of all the ANU sucrose standards measured along with cellulose samples in the present work over a period of ~20 days.

500 mV, 900 mV and 105 mV, respectively. After this, internal precision of the mass spectrometer was checked by 'Zero Enrichment or Standard ON/OFF' method in which a reference CO gas was injected repeatedly and its $\delta^{18}O$ was measured. This is followed by $\delta^{18}O$ measurements of external standards (in-house calibrated starch and ANU sucrose) for checking external precision.

RESULTS AND DISCUSSION

Sub-annual ^{18}O analysis of several annual growth rings of three teak trees from central India revealed a seasonal cycle with higher values in the early and late growing seasons and lower values in the mid growing season, with amplitudes of 1.9 to 5.0‰ and up to 6.8‰ in coarse and fine resolution samplings, respectively. Relative humidity rather than the amount of rainfall appears to control the sub-annual ^{18}O variations. Further, a comparison of the ^{18}O profile of a ring (year 1971 CE), analyzed with the highest resolution, and a model profile based on concurrent local meteorological data reveals the possibility of achieving a resolution of ~20 days, (Managave et al., 2010b) in monsoon reconstruction by sub-annual ^{18}O measurements.

Coarse and fine resolution sub-annual ^{18}O analyses of three teak trees from central India show a trend with ^{18}O enriched in extremities of the rings and depleted in the intermediate parts. The amplitude of such variations is from 2‰ to 7‰. This shows the need to obtain truly representative samples of the ring when a relationship is established between climate and tree cellulose ^{18}O values on an inter-annual scale. The results indicate the possibility of using currently available plant physiological models for interpreting sub-annual ^{18}O variations. A seasonal cycle in ^{18}O enables to divide the rings into parts containing photosynthates formed during the pre-, main and post-monsoon seasons hence identify the growth that occurred during these seasons. The width/^{18}O signature of these portions can be used to reconstruct past climate of respective sub-seasons. Relative humidity, rather than rainfall amount, governs the sub-annual ^{18}O variations in the present study area. It is observed that about 50% of ring cellulose is synthesized from the photosynthates formed during relatively lower humidity conditions suggesting a period of lower relative humidity i.e. the pre- and post-monsoon seasons are equally important in deciding whole ring cellulose ^{18}O.

High and coarse resolution sub-annual analyses of ^{18}O of teak cellulose from southern India, receiving both rains, the south-west (SW) (summer) and the north-east (NE) (winter, more depleted in ^{18}O) monsoons, show a seasonal cycle, with some degree of incoherence. The amplitudes vary between 1 to 3‰, with lower ^{18}O values at the early and late growing seasons and higher values at the middle. The observed pattern is opposite to that reported for teak trees from central India, where the annual rainfall is unimodal, with much less NE monsoon rains. Comparison of the observed and modelled profiles reveals that the observed pattern of sub-annual $\delta^{18}O$ variation can be explained only if the tree sampled rainfall from both the monsoons (Managave et al., 2010c). Thus it appears possible to detect excess NE monsoon years in the past by analyzing the ^{18}O of cellulose from latewood of teak trees. Sub-annual ^{18}O analysis of 17 arbitrarily selected teak rings from southern India shows a pattern opposite to the one reported for teak trees from central India (Managave et al., 2010c). These and the model-calculated values from local meteorological data appear to suggest that ^{18}O values associated with the middle and end of the growing season are respectively relatable to the ^{18}O of SW and NE monsoon rains. Thus the relative strengths of both the monsoons could be reconstructed by high-resolution sub-annual isotope analysis of teak from this bimonsoon climatic regime. Further, care should be taken while interpreting inter-annual ^{18}O variations of trees from bimonsoonal regimes: the varying amounts of isotopically different rains are likely to affect the bulk ring cellulose ^{18}O.

The sub-annual isotope pattern in teak observed in the present study corroborates the approach (Evans et al., 2004) ‘tropical isotope dendrochronology’ wherein wood corresponding to one seasonal cycle of ^{18}O is considered as a ‘ring’ and regular dating/counting methods are used to assign calendar years to tropical trees lacking visible growth rings. The ^{18}O record between teak trees from the same region appears to be more coherent than the ring-width record. The observed yearly (5-yearly moving averages) correlations and common signals in ^{18}O record of Jag03 and Jag04 are 0.66 (0.77) and 66% (73%), respectively. The correlations observed are significant at $P < 0.0005$. These values are higher than those observed for ring-width and ring-width index records – yearly (5-yearly) common signal for the ring-width and ring-width index are respectively 36% (44%) and 13% (6%).

Further, the correlation and common signal obtained for ^{18}O record are higher than that reported in literature for various ring-indices based teak chronologies from central and southern India. This, in conjunction with the common signal reported earlier for the D record of two teak trees (60%), appears to suggest that the isotope record in teak is able to capture more common variance than the ring-width/ring-width index record.

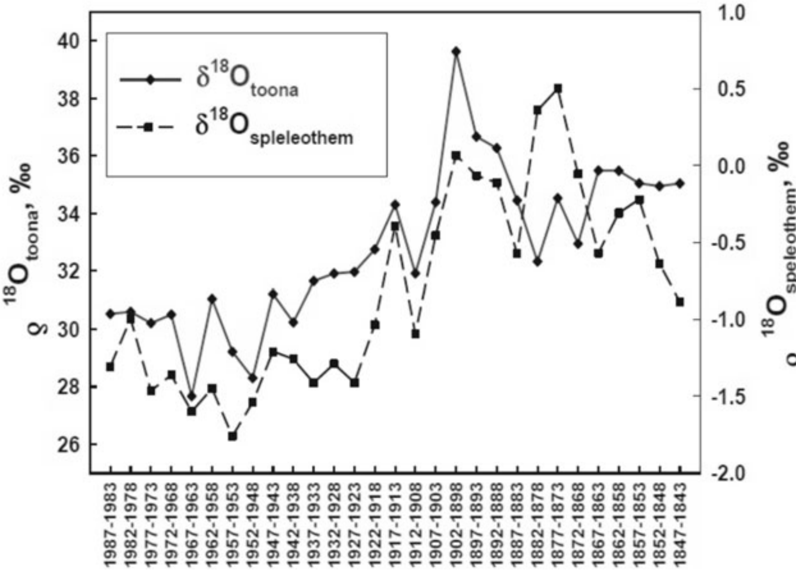

Fig. 5.9: Comparison of oxygen isotope trends in a speleothem from Akalagavi, Dandeli, Uttar Kannada District, Karnataka and in a tuna tree (*Cedrela toona*) from Chikamagalur, Karnataka (1847-1987 CE).

Teak from western India (THN) and central India (Jag03) shows a weak positive correlation ($r \sim 0.4$) between cellulose ^{18}O and rainfall record whereas teak from southern India (PKLM) exhibits a negative relationship ($r \sim -0.5$). The former could be explained by invoking lengthening of the growing season as a consequence of higher rainfall. During years of higher rainfall teak grows until a period of lower relative humidity leading to more evaporative enrichment of the leaf water and hence higher ^{18}O values of cellulose. The plausible reasons for the negative correlation in the case of the latter could be the presence of relatively strong rainfall event in the region, i.e. higher rainfall during the north-east (NE) monsoon. Depleted ^{18}O in one sample is due to relatively lesser effect of lower relative humidity conditions in deciding tree ^{18}O.

Based on the relationship observed between PKLM ^{18}O record and rainfall record, past rainfall record for Palakkad, Kerala was reconstructed back to 1743 CE. It was further realized that the reconstructed record is also valid for most of southern India. The cellulose ^{18}O based rainfall record extends the existing record back in time by 70 and 128 years for southern India and Palakkad, respectively. The reconstructed rainfall period partly covers the Little Ice Age (~1350-1900 CE). Most of the high and low rainfall events in the reconstructed and instrumental record match. One of the conspicuous features of the extended record is higher precipitation during 1743-1830 CE as compared to the later period. This is also verified by similar trends in the

^{18}O values (Fig. 5.9) of a tune tree (*Cedrela toona*) from Chikamagalur, Karnataka; it matches well with ^{18}O record of a contemporaneous stalagmite from the Akalagavi cave, Dandeli, Uttara Kannada district, Karnataka. Both these records show that during the period of Little Ice Age, the rainfall was higher.

CONCLUSIONS AND RECOMMENDATIONS

By analyzing the cellulose extracted from teak trees that grew in different parts of peninsular India for stable oxygen isotope ratios ($\delta^{18}O$) with both inter- and intra-annual resolutions, we have shown that: (i) Trees receiving only south west monsoon rainfall exhibit a different sub-annual cycle (roughly 'u' shaped) compared to trees that received both the south-west and the north-east monsoon rainfall (e.g. teak from Kerala; roughly inverted 'u' shaped). (ii) This allows the north-east and south-west monsoons to be independently reconstructed. (iii) The extended series of monsoon rainfall over Kerala back in the past beyond the period of instrumental observations shows that the north-east monsoon was stronger during the Little Ice Age, when the south west monsoon was perhaps somewhat weaker. (iv) Because the amount effect in rainfall seems to be positive in the Western Ghats, the tree-ring $\delta^{18}O$ is also positively correlated with the amount of rainfall. This is explained as due to increased growing season during years of higher rainfall and growth during the later months of lower ambient relative humidity, which increases the evaporative isotopic enrichment of leaf water and hence that of cellulose. (v) Checking the rainfall reconstruction using the $\delta^{18}O$ of a tuna tree that grew in Karnataka against the annually layered speleothem lends confidence to the reconstructed rainfall series, as reconstructions from the two independent proxies are concordant.

These new results significantly boost the prospect of reconstructing monsoon rainfall over the peninsular India, with seasonal resolution. For future work we recommend that: (1) To fully exploit the isotope dendroclimatological potential of teak and other suitable trees from tropical areas an extensive characterization of the amount effect in rainfall is necessary. Existing temporal and spatial coverage of isotopes in rainfall is too inadequate to realize their effect on isotopic composition of plants. (2) To use various plant physiological models for interpreting sub-annual as well as inter-annual ^{18}O variations in teak, better understanding of stomatal behaviour of teak is necessary. In the present study, the stomatal conductance was calculated based only on relative humidity. Soil moisture content and light availability are also known to affect the stomatal conductance. In addition to this, the Peclet effect, an advective mixing of the enriched leaf water and un-enriched source water, was reported to affect plant ^{18}O values. Clearly, more field investigations are needed in this direction. (3) In the present study, time assigned to the different sub-annual parts of the rings was based on the general growth pattern of teak. Assigning more precise time to the sub-annual parts would give higher credibility to the correspondence established between the sub-annual ^{18}O variations and ambient climate. For this, cambial pinning should be carried out on trees and rings from such trees should be studied for sub-annual isotopic analysis. (4) The present study shows that sub-annual ^{18}O variations are affected by climatic conditions during the growing season. One of the important aspects of Indian monsoon is ‘active’ and ‘break’ spells of rainfall within the summer monsoon season (June-Sept). Such monsoon ‘breaks’ influence the mean summer monsoon rainfall received. In this context, it would be worth probing whether the ‘breaks’ in monsoon leave any distinct signature on intra-annual ^{18}O variability. (5) The depleted ^{18}O values of the early wood observed in a teak tree from Kerala suggests likely transfer of photosynthates formed during the end of previous year. To verify this, an experiment could be conducted by irrigating teak trees with water having distinct ^{18}O in the late growing season (Oct-Nov). ^{18}O analysis of the subsequent year’s ring will help to resolve the issue of transfer of photosynthates from one year to the next year. (6) It has been observed that there is a substantial spatial variation in rainfall over Indian region with different regions showing differing long-term trends in rainfall (Guhatakurta and Rajeevan, 2008). Hence reconstructed temporal trend in rainfall based on tree ring studies is likely to be regional and may not follow trend in all-Indian monsoon rainfall. To get a more representative trend for the all-India summer monsoon rainfall (ISMR), trees from the core monsoon zone5 (Sikka et al., 1980) should be used.

ACKNOWLEDGEMENTS

Authors thank R.A. Jani (PRL, Ahmedabad), M.S. Sheshshayee (UAS, Bangalore), H.B. Borgaonkar and G.B. Pant (IITM, Pune), and Amalava Bhattacharyya (BSIP, Lucknow) for samples and assistance on various aspects of this research. Financial support from ISRO-GBP is gratefully acknowledged.

REFERENCES

Berlage, H.P. (1931). On the relationship between thickness of tree rings of Djati trees and Rainfall on Java. *Tctona*, **24:** 939-953.

Bhattacharyya, A., Eckstein, D., Shah, S.K. and Chaudhary, V. (2007). Analysis of climatic changes around Perambikulum, South India, based on early wood mean vessel area of teak. *Current Science*, **93(8):** 1159-1164.

Borgaonkar, H.P., Sikder, A.B., Somaru Ram, Rupa Kumar, K. and Pant, G.B. (2007). Dendroclimatological investigations of high altitude Himalayan conifers and tropical teak in India. *The Korean Journal of Quaternary Research*, **21(1):** 15-25.

Brendel, O., Iannetta, P.P.M. and Stewart, D. (2000). A rapid and simple method to isolate pure alpha-cellulose. *Phytochemical Analysis*, **11:** 7-10.

Buckley, B.M., Palakit, K., Duangsathaporn, K., Sanguantham, P. and Prasomsin, P. (2007). Decadal scale droughts over northwestern Thailand over the past 448 years: Links to the tropical Pacific and Indian Ocean sectors. *Climate Dynamics*, **29:** 63-71.

Burk, R.L. and Stuiver, M. (1981). Oxygen isotope ratios in trees reflect mean annual temperature and humidity. *Science*, **211:** 1417-1419.

Chakraborty, S. and Ramesh, R. (1992). Climatic significance of ^{18}O and ^{13}C variations in a banded coral (*Porites*) from Kavaratti Lakshadweep islands. *In:* Proc. Int Symp. on the Oceanography of the Indian Ocean. B.N. Desai (ed.), Oxford IBH.

Chakraborty, S. and Ramesh, R. (1993). Monsoon record in Indian corals. *In:* Proc. Int. Symp. Global Change. IGBP, Tokyo, Japan.

Chakraborty, S. and Ramesh, R. (1993a). Stable isotope variations in a coral from the Gulf of Kutch: Environmental implications. Global Change Studies: Scientific results from ISRO GBP-SR 42, **94:** 245-255.

Chakraborty, S. and Ramesh, R. (1993b). Monsoon induced sea surface temperature changes recorded in Indian corals. *Terra Nova*, **5:** 545-551.

Chakraborty, S. and Ramesh, R. (1997). Environmental significance of carbon and oxygen isotope ratios of banded corals from Lakshadweep, India. *Quaternary International*, **37(1):** 55-65.

Chakraborty, S., Ramesh, S. and Krishnaswami, S. (1994). Air sea exchange of CO_2 in the Gulf of Kutch, northern Arabian Sea based on bomb carbon in corals and tree rings. *Proc. Ind. Acad. Sci. (Earth & Planet. Sci.)*, **103:** 329-340.

Christie, D.A., Lara, A., Barichivich, J., Villalba, R., Morales, M. and Cuq, E. (2008). El Niño-Southern Oscillation signal in the world's highest-elevation tree-ring chronologies from the Altiplano, Central Andes. *Palaeogeogr. Palaeoclimatol. Palaeoecol*. In press.

Cole, J.E., Dunbar, R.B., McClanahan, T.R. and Muthiga, N. (2000). Tropical Pacific forcing of decadal variability in the western Indian Ocean over the past two centuries. *Science*, **287:** 617-619.

Cole, J.E., Fairbanks, R.G. and Shen, G.T. (1993). The spectrum of recent variability in the Southern Oscillation: Results from a Tarawa Atoll coral. *Science*, **262:** 1790-1793.

D'Arrigo, R.D., Cook, E.R., Wilson, R.J., Allan, R. and Mann, M.E. (2005). On the variability of ENSO over the past six centuries. *Geophys. Res. Lett.*, **32**. doi:10.1029/2004GL022055.

Dansgaard, W. (1964). Stable isotopes in precipitation. *Tellus*, **16:** 436-468.

Diaz, F.H. and Markgraf, V. (2000). El Nino and the Southern Oscillation: Multiscale Variability and Global and regional Impacts. Cambridge Uni Press.

Edwards, T.W.D., Aravena, R.O., Fritz, P. and Morgan, A.V. (1985). Interpreting paleoclimate from ^{18}O and ^{2}H in plant cellulose: Comparison with evidence from fossil insects and relict permafrost in southwestern Ontario. *Can. J. Earth Sci.*, **22:** 1720-1726.

Epstein, S. and Yapp, C.J. (1977). Isotope tree thermometers. *Nature*, **266:** 477-478.

Evans, M.N. and Schrag, D.P. (2004). A stable isotope-based approach to tropical dendroclimatology. *Geochimica et Cosmochimica Acta*, **68(16):** 3295-3305.

Feng, X. and Epstein, S. (1994). Climatic implications of an 8000-year hydrogen isotope time series from bristlecone pine trees. *Science*, **265:** 1079-1081.

Francey, R.J. and Farquhar, G.D. (1982). An explanation of $^{13}C/^{12}C$ variations in trees. *Nature*, **297:** 28-31.

Fritts, H.C. (1976). Tree Rings and Climate. Academic Press.

Gaudinski, J.B., Dawson, T.E., Quideau, S., Schuur, E.A.G., Roden, J.S., Trumbore, S.E., Sandquist, D.R., Oh, S. and Wasylishen, R.E. (2005). Comparative Analysis of Cellulose Preparation Techniques for Use with ^{13}C, ^{14}C, and ^{18}O Isotopic Measurements. *Anal. Chem.*, **77:** 7212-7224.

Gray, J. and Thompson, P. (1976). Climatic information from $^{18}O/^{16}O$ ratios of cellulose in tree rings. *Nature*, **262:** 481-482.

Guhatakurta, P. and Rajeevan, M. (2008). Trends in the rainfall pattern over India. *Int. J. Climatol.*, **28:** 1453-1469.

Holmes, R.L. (1983). Computer assisted quality control in tree ring dating and measuring. *Tree-Ring Bull.*, **43:** 69-78.

Krishna Kumar, K., Soman, M.K. and Rupa Kumar, K. (1995). Seasonal forecasting of Indian summer monsoon rainfall. *Weather*, **50:** 449-467.

Leuschner, H.H., Saas-Klassen, U., Jansma, E., Baillie, M.G.L., Spurk, M. (2002). Subfossil European bog oaks: Population dynamics and long-term growth depressions as indicators of changes in the Holocene hydro-regime and climate. *The Holocene*, **12:** 695-706.

Lipp, J., Trimborn, P., Fritz, P., Moser, H., Becker, B. and Franzel, B. (1991). Stable isotopes in tree ring cellulose and climatic change. *Tellus*, **43B:** 322-330.

Managave, S.R. and Ramesh, R. (2012). Isotope dendroclimatology: A review with a special emphasis on tropics. *In:* Hanbook of Environmental Isotope Geochemistry. M. Baskaran (ed.), Springer, **1:** 811-834.

Managave, S.R., Sheshshayee, M.S., Bhattacharyya, A. and Ramesh, R. (2010c). Intra-annual variations of cellulose ^{18}O of teak from Kerala, India: Implications to reconstruction of past summer and winter monsoon rains. *Climate Dynamics*, in the press (doi:. DOI: 10.1007/s00382-010-0917-9). Editorial manuscript number: CLIDY-D-09-00384.2.

Managave, S.R., Sheshshayee, M.S., Borgaonkar, H.P. and Ramesh, R. (2010a). Past break-monsoon conditions detectable by high resolution intra-annual ^{18}O analysis of teak rings. *Geophysical Research Letters*, **37:** L05702, doi:10.1029/2009GL041172.

Managave, S.R., Sheshshayee, M.S., Borgaonkar, H.P. and Ramesh, R. (2010b). Intra-annual oxygen isotope variations in central Indian teak cellulose: Possibility of improved resolution for past monsoon reconstruction. *Current Science*, **98:** 930-937.

Managave, S.R., Sheshshayee, M.S., Ramesh, R., Borgaonkar, H.P., Shah, S.K. and Bhattacharyya, A. (2011). Response of cellulose ^{18}O of teak trees in differing monsoon environments to monsoon rainfall. *Dendrochronologia*, **29(2):** 89-97 Manuscript number: DENDRO-D-09-00030R1.

Nijampurkar, V.N., Bhandari, N., Bhattacharya, S.K. and Ramesh, R. (1986). Climatic significance of D/H ratios in a temperate glacier in Sikkim. *Curr. Sci.*, **55(18):** 910-912.

Pant, G.B. and Borgaonkar, H.P. (1983). Growth rings of teak trees and regional climatology: An ecology study of Thane region. *In:* Environmental management. L.R. Singh, R.C. Tiwari and R.P. Srivastava (eds). Allahabad Geophysical Society, University of Allahabad.

Pant, G.B. and Parthasarathy, B. (1981). Some aspects of an association between the southern oscillation and Indian summer monsoon. *Arc Met Geophy Biok*, **lB, 29:** 245-252.

Pant, G.B. and Rupa Kumar, K. (1997). Climate of South Asia. Wiley, New York.

Pumijumnong. N., Eckstein, D. and Sass, U. (1995). Tree-ring research on Tectona grandis in Northern Thailand. *IAWA Journal*, **16(4):** 385-392.

Ramesh, R., Bhattacharya, S.K. and Gopalan, K. (1985). Dendroclimatological 558 implications of isotope coherence in trees from Kashmir Valley, India. *Nature*, **317:** 802-804.

Ramesh, R., Bhattacharya, S.K. and Gopalan, K. (1986a). Climatic correlations of the stable isotope records of silver fir (*Abies pindrow*) trees from Kashmir, India. *Earth. Planet. Sci. Lett.*, **79:** 66-74.

Ramesh, R., Bhattacharya, S.K. and Gopalan, K. (1986b). Stable isotope systematics in tree cellulose as paleoenvironmental indicators – A review. *J. Geol. Soc. Ind.*, **27:** 154-167.

Ramesh, R., Bhattacharya, S.K. and Gopalan, K. (1988). Climatic significance of variations in width and stable isotope ratios of tree rings. *British Archeological Records*, **196:** 591-609.

Ramesh, R., Bhattacharya, S.K. and Pant, G.B. (1989). Climatic significance of D variations in a tropical tree species from India. *Nature*, **337:** 149-150.

Roden, J.S., Lin, G. and Ehleringer, J.R. (2000). A mechanistic model for interpretation of hydrogen and oxygen isotope ratios in tree-ring cellulose. *Geochimica et Cosmochimica Acta*, **64(1):** 21-35.

Rozanski, K., Araguas-Araguas, L. and Giofiantini, R. (1993). Isotopic patterns in modern global precipitation. *Geophysical Monograph*, **78:** 1-36.

Sano, M., Sheshshayee, M.S., Managave, S.R., Ramesh, R., Sukumar, R. and Sweda, T. (2010). Climatic potential of ^{18}O of *Abies spectabilis* from the Nepal Himalaya. *Dendrochronologia*, **28(2):** 93-98.

Schiegl, W.E. (1974). Climatic significance of deuterium abundance in growth rings of *Picea*. *Nature*, **251:** 582-584.

Sikka, D.R. and Gadgil, S. (1980). On the maximum cloud zone and the ITCZ over India longitude during the Southwest monsoon. *Mon. Weather Rev.*, **108:** 1840-1853.

Spurk, M., Leuschner, H.H., Baillie, M.G.L., Briffa, K.R. and Friedrich, M. (2002). Depositional frequency of German subfossil oaks: Climatically and non-climatically induced fluctuations in the Holocene. *The Holocene*, **12:** 707-715.

Stahle D.W., D'Arrigo, R.D., Krusic, P.J., Cleveland, M.K., Cook, E.R., Allan, R.J., Cole, J.E., Dunbar, R.B., Therrel, M.D., Gay, D.A., Moore, M.D., Stokes, M.A., Burns, B.T., Villanueva-Diaz, J. and Thompson, L.G. (1998). Experimental dendroclimatic reconstruction of the Southern Oscillation. *Bull. Am. Meteorol. Soc.*, **79:** 2137-2152.

Tudhope, A.W. et al. (2001). Variability in the El Niño-Southern Oscillation through a Glacial-Interglacial Cycle. *Science*, **291:** 1511-1517.

von Rad, U., Schaaf, M., Michels, K.H., Schulz, H., Berger, W.H. and Sirocko, F. (1999). A 5000-yr record of climate change in varved sediments from the oxygen minimum zone off Pakistan, Northeastern Arabian Sea. *Quat. Res.*, **51:** 39-53.

Yadava, M.G. and Ramesh, R.R. (2005). Monsoon reconstruction from radiocarbon dated tropical speleothems. *The Holocene*, **15:** 48-59.

Yadava, M.G., Ramesh, R. and Pandarinath, K. (2007). A positive amount effect in the Sahayadri (Western Ghats) rainfall. *Current Science*, **93(2):** 560-564.

Yadava, M.G., Ramesh, R. and Pant, G.B. (2004). Past monsoon rainfall variations in peninsular India recored in a 331-year-old speleothems. *The Holocene*, **14(4):** 517-524.

PART II

Biotic Changes and Responses (Stresses and Vulnerability)

CHAPTER

6

Marine Biodiversity: Climate Impact and Conservation Planning

Leonard Sonnenschein

World Aquarium and Conservation for the Oceans Foundation
St. Louis, Missouri 63103, USA
info@worldaquarium.org

INTRODUCTION

The effects of climate change on terrestrial ecosystems are well-known. Though over 70% of the Earth's surface is covered by water, still little is known about the effects of global warming on aquatic ecosystems. Changes and challenges caused by these temperature abnormalities can range from climate change patterns that cause tsunamis, hurricanes, excessive or deficient rainfall, floods, and droughts, to changes in fisheries productivity. Advance planning is necessary for effectively dealing with the conservation and economic effects of climate change.

THE PROBLEM

According to the Millennium Ecosystem Assessment (MEA, 2005), the world's oceans and coasts are highly threatened and subject to rapid environmental change. Major threats to marine and coastal ecosystems include: (i) land-based pollution and eutrophication; (ii) overfishing, destructive fishing, and illegal, unreported and unregulated (IUU) fishing; (iii) alterations of physical habitats; (iv) invasion of exotic species; and (v) global climate change (Kumar et al., 2010). The changing climatic regime also demands making the coastal fishing communities adapt to the situation. We need to develop a better understanding of the impact of climate changes on fish stocks in our coastal waters at the national level, with proper modelling

J. Sundaresan et al. (eds.), *Climate Change and Island and Coastal Vulnerability*,
DOI 10.1007/978-94-007-6016-5_6, © 2013 Capital Publishing Company

studies as the first step towards planning and framing better management strategies. Any kind of programmes to address climate change should also consider other pertinent anthropogenic interventions in marine ecosystems, such as overfishing, as they are closely interrelated (Vivekanandan and Rao, 2009).

EFFECTS OF GLOBAL WARMING ON OCEAN WATER

Climate change, rising atmospheric carbon dioxide, excess nutrient inputs, and pollution create heightened toxicity through increases in temperature changes, chemical solubility differences, and concomitant microfaunal alterations. It is fundamentally altering the chemistry of the ocean, often on a global scale and, in some cases, at rates greatly exceeding those in the historical and recent geological record. Major observed trends include a shift in the acid-base chemistry of seawater, reduced subsurface oxygen both in near-shore coastal water and in the open ocean, rising coastal nitrogen levels, widespread increase in mercury and persistent organic pollutants. Most of these perturbations, are linked either directly or indirectly to fossil fuel combustion, fertilizer use, and industrial activity. It is projected to grow in coming decades, resulting in increasing negative impacts on ocean biota and marine resources.

EFFECTS OF GLOBAL WARMING ON THE FISHERIES INDUSTRY

Billions of people throughout the world rely on fish as a primary source of protein, particularly in developing countries with rapidly expanding populations. Worldwide, fish provide over 2.6 billion people with more than 20% of their animal protein. The world's fisheries generate over US$130 billion annually, and contribute significantly to the economies of many countries. Even where fisheries are not important on a national level, they can be critical for regional employment. In these regimes entire communities of small-scale fishermen rely on fishing as their primary source of income. In Tamil Nadu region of southeastern India, one third of the population depends on the sea for their livelihood. Their average incomes had declined by 50% when false trevally (the most valuable local fish) suffered a sharp decline—blamed partly on climate change. Worldwide, over 38 million people earn an income by fishing or raising fish. If activities associated with fisheries production are included, fisheries support over 200 million people. It feeds billions of people who rely on fish as their primary source of protein, particularly in some of the most populous and poorest countries on the planet.

EFFECTS OF GLOBAL WARMING ON FISH

Whether rise in temperature is a real problem to fish and fisheries sector? Fish can be impacted in the following ways: cells, organ systems, the whole organism, reproduction and behaviour. It may alter pollutant interactions, ecology and population dynamics, physiological function, protein metabolism, stress, muscle function, cardiovascular performance, embryonic and larval development, pollutant stress, growth rate, wild fish stocks, growth rage, physiology, and biogeography.

Metabolic Changes

Fish are more sensitive to temperature than many animals because they cannot maintain a constant body temperature. In most cases, their body is exactly the same temperature as the water they are swimming in. Different species can live in very cold or very hot water, but each species has a range of temperatures that it prefers. Fish can't survive in temperatures too far out of this range. These necessitate lesser variability and smaller range of successful breeding temperature conditions. If there is not enough food, all of a fish's available energy goes to fueling its high metabolism, and less energy is available for growth and reproduction. Rainbow trout grow significantly more slowly when their water temperature is raised only 2°C and food is also limited due to fluctuation in plankton levels. To make matters worse, fish may not have enough oxygen to breathe as the water grows warmer. Fish filter oxygen from the water they are swimming in, but the saturation amount of oxygen dissolved in water decreases as temperatures rise. So many fish need more oxygen to support their elevated metabolisms. The above may not be able to get it from the warmer, oxygen-poor water around them. Also, the warmer temperatures affect the metabolism of the planktonic level to increase numbers and increase in respiration further lowers oxygen levels. This also varies significantly at different times of the day. Stress conditions for fish produced physiologically significant changes. The same have been prone to cause viral susceptibility which has been known to cause systemic fish kills.

Reproductive Changes

Warmer water fish tend to mature more quickly, but the cost of this speedy lifestyle is often a smaller body size. Fish raised in warm water end up smaller than their peers raised at cooler temperatures. Many fish will also have less offspring as temperatures rise, and some may not be able to reproduce at all.

Geographical Changes

Naturally, when fish find themselves in hot water, they head out in search of cooler locales, but this can leave other animals with few options. When fish in the Gulf of Mexico moved deep in 1993, 120,000 seabirds starved to death, most likely because they could not dive deep enough to catch their relocated prey (World Wide Fund for Nature, 2005).

Invasive Species

As cool and cold water species decline or move poleward, fish that don't mind the heat will become much more common. Many areas have been colonized by new species as water has warmed in the last few decades, and invasions are likely to increase such as with tilapia, goldfish, carp and other species. Newly arrived species can wreak havoc in a number of ways, such as out-competing native fish for food and spawning habitat, devouring the eggs and juveniles of native fish, while larger predators prey on native adults or even by bringing in new disease into an area with an otherwise healthy population.

Phytoplankton Productivity

Evidence has shown that the surface layers of the ocean hold nitrogen-fixing cyanobacteria, which supply 50% of the nitrogen required for phytoplankton to live. The enormous food web in the oceans that depend on phytoplankton makes phytoplankton the most important primary producer. For phytoplankton to thrive, there must be an appropriate supply of nutrients. Also, the water must not be too warm, or too acid. All these conditions are deteriorating on account of global warming, bringing the prospect of a collapse in the marine biota and ecosystems.

Dead Zone Expansion

Higher water temperatures increase solubility of nitrate which is a well-known accomplice for creation of coastal eutrophic zones, also known as "Dead Zones." Fertilizers are a major contributor to this non-point pollution. Sulphur and iron as micronutrients can be added to coastal ecosystems to improve natural productivity by providing nutrients to reduce the farm fertilizer effects on alga and phytoplankton. Phytoplankton is a free-floating alga upon which numerous ocean fauna feed. Phytoplankton utilize the micronutrient iron within the photosynthetic complex. It has been proposed by scientists to advocate iron fertilization as a means to counteract the effects of carbon dioxide created by climate change in the ocean and to aide phytoplankton in their growth and increase photosynthetic productivity. Iron promotes phytoplankton growth and removes excess carbon dioxide in the ocean (Pollard, 2009). Also, by sinking steel-hulled ships to the ocean floor to create artificial reefs allows for the slow, continuous release of iron into the coastal aquatic ecosystem, thereby feeding phytoplankton.

Disease and Toxins

As water warms up, many parasites, viruses and microbes that cause fish diseases grow faster and become more virulent. Parasites in cooler climates are more likely to survive the winter and produce multiple generations of offspring each year, so more fish may become infected. And as harmful viruses, microbes and parasites become stronger and more numerous, fish whose immune systems are already stressed by warm water, low oxygen, and crowding, become even more susceptible to diseases and parasites. As warmer water increases the toxicity of pollutants, and as fish pump more water through their gills to meet increased metabolic needs, they also collect more pollutants.

EFFECTS OF GLOBAL WARMING ON BIODIVERSITY

Many individual studies have examined the evidence for recent biological changes in relation to climatic changes. These have mostly concentrated on a limited set of taxa, or been restricted to particular countries or regions. However, two recent meta-analyses combine a broad spectrum of results to test whether a coherent pattern exists across regions and for a diverse array of species. One analysis (Root et al., 2003) examined the results of 143 studies on a wide spectrum of species, totaling 1473 organisms from all regions of the world. Of the 587 species showing significant temperature-related changes (in distribution, abundance, phenology, morphology or genetic frequencies), 82% had shifted in the direction expected from climate change (e.g. distributions moving towards higher latitudes or altitudes). The timing of spring events, such as egg-laying by birds, spawning by amphibians and flowering by plants, was shown (by 61 studies) to have shifted earlier by 5.1 days per decade on average over the last half-century, with changes being most pronounced at higher latitudes. The second analysis (Parmesan and Yohe, 2003) reviewed studies of over 1700 species, and found similar results: 87% of phenology shifts and 81% of range shifts were in the direction expected from climate change. These studies give us a very high confidence that global climate change is already impacting biodiversity.

Biodiversity Maps

A study released in July 2010 showed the effects of temperature rise upon biodiversity and distribution of taxa. In a study of general marine biodiversity, scientists have made the first global map of the biodiversity of the oceans for more than 11,000 marine species, from tiny shrimp-like creatures to whales, building on 6.5 million records from the Census for Marine Life and other databases. Of all the factors they looked at to explain why some regions had more or fewer types of creatures, the only factor that consistently explained the patterns for the 13 groups of marine life they studied was temperature.

ECONOMIC IMPACTS OF GLOBAL WARMING

Food Security

Future climate change is expected to put close to 50 million extra people at risk of hunger by 2020 rising to an additional 132 million and 266 million by 2050 and 2080 respectively, says the report of the Intergovernmental Panel on Climate Change working group (Jerath et al., 2010).

Coastal Development

Coastal land and water resources, essential to development and livelihoods, are particularly vulnerable to impacts of climate change. Actions to adapt to climate change through an integrated approach to land and water management are urgently needed. As the popularity of living on coastal lands increases, the propensity for development oversights increases. Coastal development along with farming processes bring more silt, clogging our waterways which in turn choke corals, cover vital algae and kills microorganisms which are at the base of the food chain which supplies the nutrients to support biodiversity and indeed our fisheries which we depend on to feed the world.

In addition, the rise of global sea levels is expected to increase by 2.3 feet by the year 2050. Planning is our best strategy. In spite of living in the 21st century and having advanced technology, we cannot solve these problems; we can't hold back the seas. Even the EPA's best recommendations are to "retreat and relocate," leaving sufficient buffer zones between the water's edge and all future permanent structures.

CASE STUDIES

The state of Kerala in India is the home to one of the most diverse populations of freshwater, estuarine and marine species of fish and invertebrates (Benziger et al., 2010). Because of this abundance, the people of Kerala have benefited from the economics that the fisheries offer and the sustainability of foods brought to their tables. Due to the adverse effects of climate change and the increase of fishing pressure provided primarily by outside agencies, the above aspects of fisheries have changed (Benziger et al., 2010). With the economics of Kerala taking a turn for the worse, the need for subsistence for food and income of this regime has placed the fisheries at an even further decline. The role of fisheries in societal issues in Kerala is ubiquitous. Marine biodiversity affects the economic, environmental, and social sectors of society and is challenged by climate change.

Due to the lack of infrastructure for mangroves, the coral reefs were decimated. Consequently, without mangroves, it takes much longer for coral reefs to recover from hurricanes, tsunamis and other weather incidents. This fact has been demonstrated from the Indian Ocean Tsunami in 2004 in the

Maldives, which is an island nation a few hundred miles away wherein protections exist for both mangroves and coral reefs due to their economy's reliance upon tourism to their coral reefs. In comparison, the devastation from the tsunami on each of these areas from hurricanes was vastly different due to their protection of mangroves and attitudes regarding coastal development. In the Maldives, even though the government has established a green+blue policy, the lack of infrastructure within its school system and the general community creates a barrier to understanding the fragility of these ecosystems as well as the importance of governmental support for conservation. Recent changes within the Maldivian government indicate that these governmental attitudes without general populous support may change and therefore good conservation practices lose out.

WHAT CAN WE DO ABOUT GLOBAL WARMING?

Establishment of Coral Farms

Coral farming is a large conservation effort that will acquire a wealth of knowledge, based upon (1) identifying species at risk or imperiled; (2) identifying biology for those species and methods necessary for maintenance, propagation and reintroduction; and (3) Coral Park programme which will also need to identify partner organizations to maintain living species banks for appropriate reintroduction. Information from this programme can be shared globally in order to build the bank resource as well as target specific regional goals.

Form Local Fish Farming Associations or Other Support Systems for Fish Suppliers

In order to support regional development amongst individual farmers, a central holding system needs to be developed in order to (1) identify species that are at risk or needing conservation activities and those that have commercial and ornamental values; (2) maintain quality control for best practices of aquaculture and fisheries activity to ensure decrease in pollution activities, appropriate feeding, filtration, and processing; (3) by combining individual fishermen into a co-op for best products and prices for those products can be ensured; (4) ongoing education regarding aquaculture production and fisheries best practices, to those who participate in the ornamental and marine fisheries industries; and (5) utilizing this system, databases about fisheries may be established.

Hold Regular Multistakeholder Meetings with Surveys to Measure Results

The effects of global warming can be extremely regionalized by convening regional stakeholders at every level of the fisheries industry in order to establish agreements on best practices, sustainability, conservation, etc. These meetings give a voice to participants at all levels and are structured to give every interest in civil society a fair and equal hearing. It also allows for an evaluation of regional global warming effects, establishment of solutions and the ability to monitor those solutions for their efficiency in resolving conservation, economic and social dilemmas.

In light of the already measured effects of global warming on the ornamental fish trade and fisheries productivity, it is recommended that a further set of actions be taken for protection and preservation of aquatic biodiversity, food security and the environment:

1. Prediction of localized effects of global warming for rapid recovery.
2. Appropriate coastal protection such as mangroves, fishing quotas, and MPAs, etc.
3. Measurements of productivity with rubrics for changes.
4. Evaluation of coral species with the intent to create living ARKS in aquaculture conditions for later re-implantation or implantation in new areas based upon temperature, water quality and other conditions.
5. Surveillance for invasive species.
6. Measurement of water quality: chemical and biological indicators.
7. Appropriate protection for preservation of production relative to local, regional and national food security issues.
8. Cut carbon dioxide emissions.
9. Invest in clean energy – most of the carbon dioxide comes from electricity generation (37% worldwide).
10. Change fertilizer mixes to include sulphur.
11. Create artificial reefs with iron-hulled ships.
12. Improve mangrove protection and restoration.

National Actions

Foster and bolster development of resources to support economic drivers to ensure

- Improved training for best practices and educational support system
- Planting trees and mangroves with appropriate legal protection thereof
- Protection of coral reefs with the idea towards reserving species in the aquaculture programmes for future implantation
- Education programmes at each level of the society to inform, instruct and evaluate the processing of each initiative

CONCLUSION

Present study infers the effects of climate and conservation planning upon marine biodiversity. It looked at three different communities: a fisheries community and two island systems. It is clear that conservation practices supported by good government initiatives with wide-scale community planning and educational infrastructure can lead to better protection of marine biodiversity as well as improvement of sustainability. Suggestions were made for local and national actions to further sustainability regarding climate change challenges.

REFERENCES

Bird Life International (2004). There is strong evidence that climate change is impacting a wide range of organisms. Presented as part of the BirdLife State of the world's birds website. Available from: http://www.birdlife.org/datazone/sowb/casestudy/169. Checked: 27/10/2011

Combes, Stacey (2005). Are we putting our fish in hot water? World Wildlife Fund, 2005.

Kumar, Biju et al. (2010). Conservation of Aquatic Biodiversity of Kerala: Need for Protected Areas and Community Initiatives. *In:* Leonard Sonnenschein and Allen Benziger (eds). Conservation of Fishes in Kerala, India. World Aquarium/CFTO, pp. 194-205.

Jerath et al. (2010). Climate Change, Biodiversity and Food Security in the South Asian Region. United Nations Educational, Scientific & Cultural Organization.

Millennium Ecosystem Assessment (2005). Ecosystems and Human Well-being: Biodiversity Synthesis. World Resources Institute, Washington, DC.

Parmesan, C. and Yohe, G. (2003). A globally coherent fingerprint of climate change impacts across natural systems. *Nature*, **421:** 37-42. < http://www.seaturtle.org/PDF/Parmesan_2003_Nature.pdf>

Pollard et al. (2009). *Nature*, **457:** 577 (doi:10.1038/nature07716).

Root et al. (2003). Fingerprints of global warming on wild animals and plants. *Nature*, **421:** 57-60.

Sonnenschein, L. and Benziger, A. (2010). Conservation of Fishes in Kerala, India. World Aquarium/CFTO.

Vivekanandan, E. and Rao, G. (2009). Options for adaptation, though limited do exist. *The Hindu* Survey of Indian Agriculture.

APPENDIX

Projected Impact of Climate Change

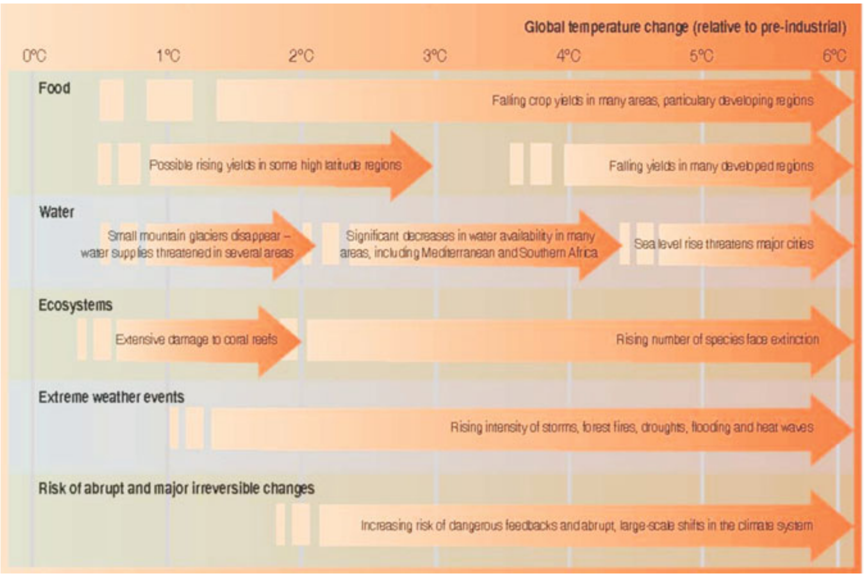

Diagram Source: Stern Review/UNEP Source: http://maps.grida.no/go/graphic/projected-impact-of-climate-change

Average Sea Surface Temperature (ºC)

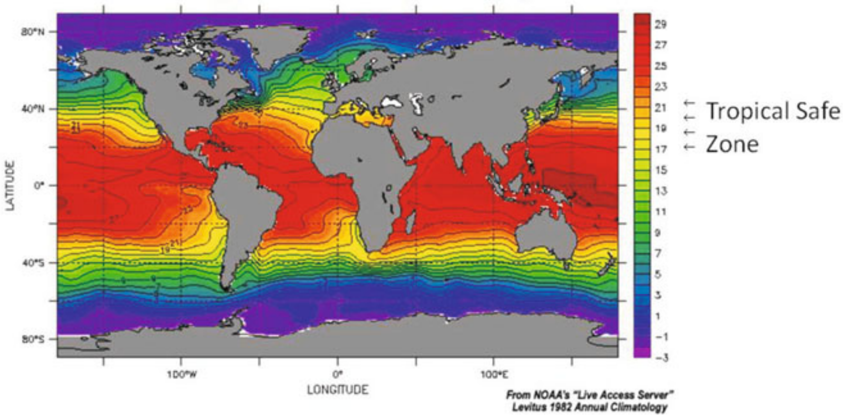

Diagram Source: http://aquarius.nasa.gov/prop_fresh_sea.html

Map of Coral Reefs of the World

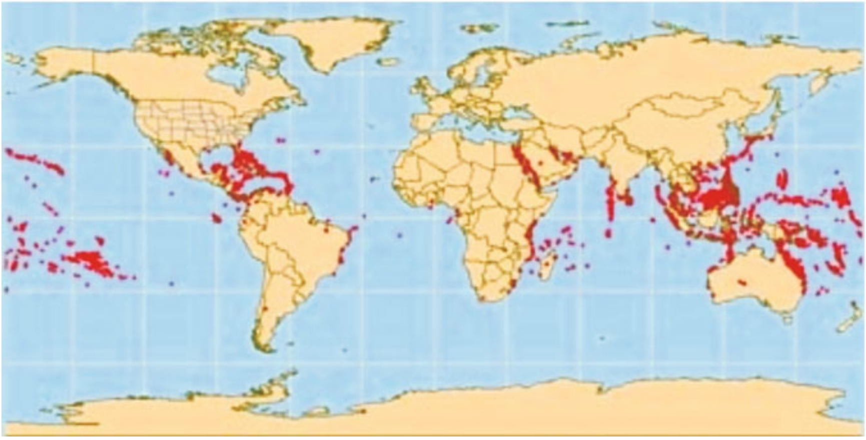

Diagram Source: NOAA

Major coral reef sites are seen as red dots on this world map. Most of the reefs, with a few exceptions are found in tropical and semitropical waters, between 30° north and 30° south latitudes.

Distribution of Coral Bleaching Events, 1988

Natural Catastrophes Worldwide, 1980-2010

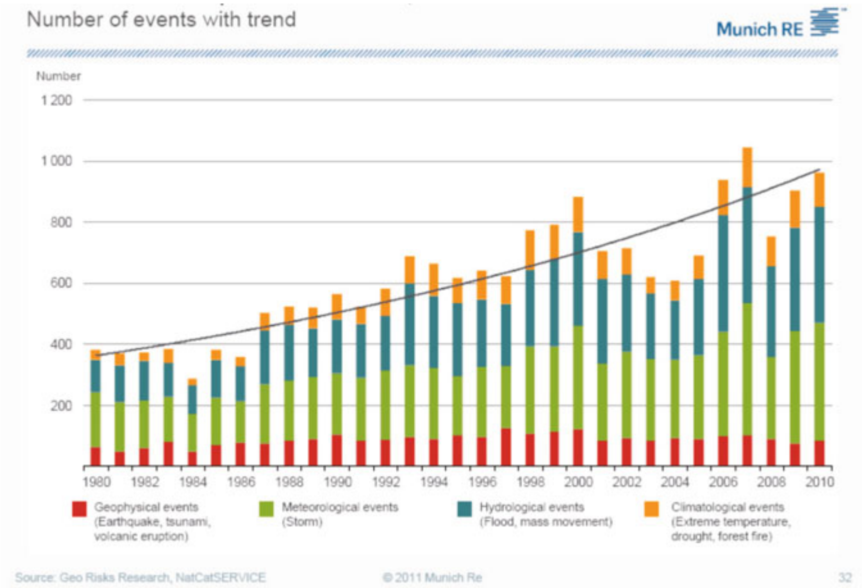

Diagram Source: Geo Risks Research, NatCatSERVICE, 2011

Direction of Changes in Phenology and Distribution of Species Compared to Those Predicted from Climate Change

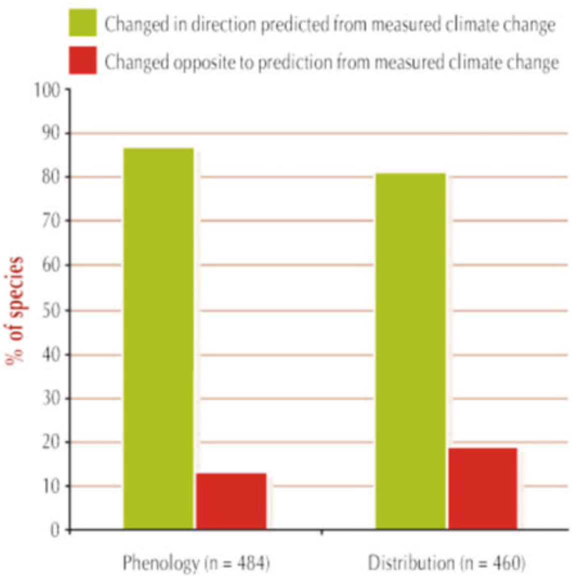

Diagram Source: Parmesan and Yohe, 2003

Biodiversity Map of Coastal and Oceanic Marine Creatures (Red boxes mark hotspots)

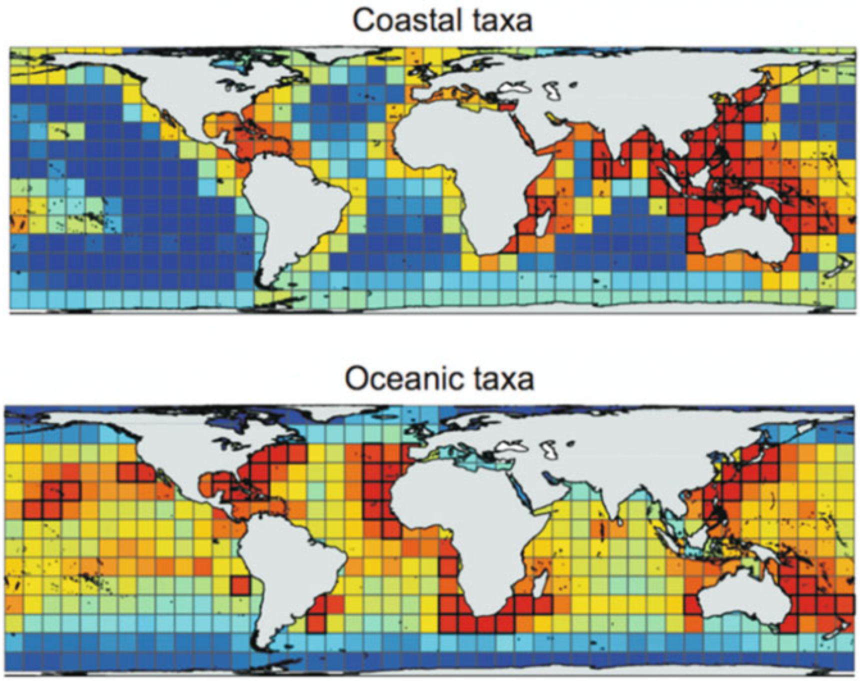

Diagram Source: Tittensor 2010

CHAPTER

7

Inventory and Monitoring of Coral Reefs of United Arab Emirates (UAE), Arabian Gulf, Using Remote Sensing Techniques

Dimpal Sanghvi, Richa Tiwari, Nandini Ray Chaudhury[1], Alpana Shukla and Ajai[1]

Department of Botany, M.G. Science Institute
Ahmedabad – 380009, India
[1]Marine & Earth Sciences Group, Space Applications Centre (ISRO)
Ahmedabad – 380015, India
dimpalsanghvi@gmail.com

INTRODUCTION

Coral reefs have often been described as fragile ecosystem in delicate balance with nature (Dubinsky, 1990; Loya and Rinkevich, 1980; Endean, 1976; Loya, 1976; Johannes, 1975). Coral reefs are indicators of environmental and climate changes that cause flashing damage to reefs. As an integral part of reefs, corals are especially vulnerable to anthropogenic pressures and climate change related threats. Arabian Gulf is a vast, shallow, marine basin which is formed on the north-eastern edge of the Arabian tectonic plate. Arabian Gulf has an average depth of thirty five metres and, at its deepest point in the southeast, it reaches about hundred metres. Most of the Gulf is sub-tropical and is surrounded by arid land masses which drive extremes of temperatures, with air temperatures frequently reaching 50°C in the summer and falling to 0°C in the winter (Spalding et al., 2001). Arabian Gulf comprises coastlines of six countries: Kuwait, Saudi Arabia, Bahrain, Qatar, United Arab

J. Sundaresan et al. (eds.), *Climate Change and Island and Coastal Vulnerability*,
DOI 10.1007/978-94-007-6016-5_7, © 2013 Capital Publishing Company

Emirates (UAE) in south and Iran to its north. Fringing and patch reefs along the mainland and island coastlines have developed in a number of places in Arabian Gulf. In many areas the division between true reefs and carbonate structures with little active coral growth is obscure (Spalding et al., 2001).

The near-shore waters of the western part of UAE are shallow with relatively low water circulation and share some of the highest salinities in the Gulf. UAE corals thus survive high annual temperature variability and represent a classic case of reefs under environmental stress compared to their purely tropical Indian Ocean counterparts. Low winter water temperature of UAE is considered to be a favourable factor for coral macro-algal competition in the UAE reefs (Coles, 2003). In UAE coast there are fringing reefs and patch reefs around many of the islands. Coral diversity is overall low in all areas and many coral communities are dominated by large monospecific stands (Spalding et al., 2001). Up to 18 species of hard corals have been found on healthy coral reef near Dalma Island (Pilcher et al., 2000; http://www.reefbase.org). The offshore islands and banks of Abu Dhabi support some of the most important coral resources in the Arabian Gulf. In few, limited areas, coral communities have formed a rudimentary reef framework several metres thick (Maghsoudlou et al., 2008; http://www.reefbase.org), while the majority of corals occur in the form of either high cover coral carpets or in sparse communities of widely spaced colonies (Maghsoudlou et al., 2008; http://www.reefbase.org).

A coral reef monitoring programme has been maintained in Jebel Ali Marine Sanctuary and Marawah Marine Protected Area. The highest cover and diversity of corals along the mainland coast of UAE is in Dubai, to the southwest of Jebel Ali Port in the Jebel Ali Marine Sanctuary established in 1997 (Pilcher and Abdullah, 2002; http://www.reefbase.org). Those areas of corals have been surveyed extensively and it was found that there are 34 hard coral species and 77 species of reef fishes. The sanctuary has a wide diversity of habitats (Wilson et al., 2002; http://www.reefbase.org). However coastal and urban developmental activities like dredging, jetty construction, related with urban centres like Abu Dhabi, Dubai and Jebel Ali airport have been associated with release of sediments in the coastal waters. Construction of Palm Island and World Map along with many such human activities on the UAE coast is quite well known and also noticed on satellite imageries. Coral reefs thus stand the threat of anthropogenic activities in UAE.

Present study is an attempt to inventorize and monitor the UAE coral reefs with multi-spectral and multi-temporal data of Indian Remote Sensing Satellite: Resourcesat-1 (IRS-P6). The change detection approach undertaken for the present study combines standard protocols for satellite (digital) data processing and subsequent “vector-based analysis” in GIS domain. The approach is unique as it incorporated ‘object-shape’ criteria to detect the footprints of human activities in the reef habitat area. This customized approach has been attempted for monitoring reef habitats at a country level (for UAE) for the first time.

MATERIALS AND METHOD

Study Area

The present study area is located within the geo-coordinates of 24°14’19”N to 25°38′36″N and 51°35′00″E to 55°43′21″E within the UAE coast (Fig. 7.1). The Arabian Gulf coastline of UAE is characterized with fringing and patch types of coral reefs occupying the shallow, near-shore waters with relatively low water circulation, seasonally high temperatures and high salinity. Arabian Gulf is one of the areas in the world which is most severely affected by loss and degradation of coral reefs (http://www.earthdive.com). According to a recent estimate, 30% of the Gulf’s coral reefs are threatened at a critical stage and upto 65% may have already been lost due to anthropogenic stressors (oil pollution, unmanaged coastal development, unregulated commercial and recreational fishing, etc.) and natural causes (temperature fluctuation, macro-algal growth, diseases, etc.) (http://www.earthdive.com). Much of the reef sites of UAE have been affected by continuous urban and industrial development, especially in the central and eastern parts of its Arabian Gulf coastline. Considerable amount of dredging activities has also modified the coastal area of UAE. Arabian Sea, including Arabian Gulf, is classified by the World Wide Fund for Nature (WWF) as a “critically endangered” eco-region of the world and, therefore, is in the focus of a priority conservation action (http://www.earthdive.com).

Data Used

Resourcesat-1 satellite data have been used for mapping coral reefs of India as well as of Central Indian Ocean (Navalgund et al., 2010). It has three on-board sensors: Advanced Wide Field Sensors (AWiFS) and two Linear Imaging and Self Scanning Sensors (LISS-III and LISS-IV). Standard digital data products in Landsat Ground Station Operators Working Group (LGSOWG) format obtained from AWiFS and LISS III sensors (specifications given in Table 7.1) have been used for this study. Resourcesat-1, AWiFS data

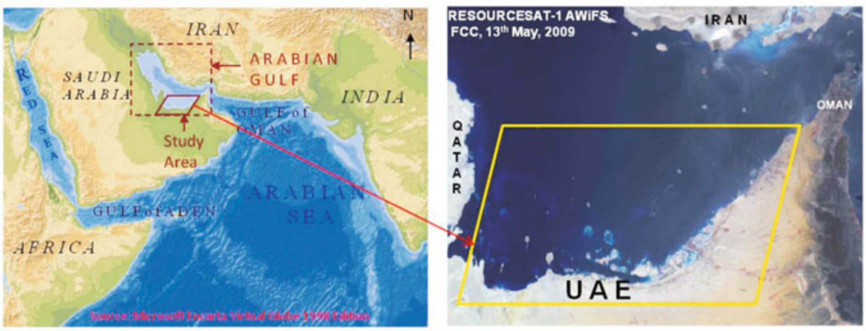

Fig. 7.1: Study area: UAE Coast, Arabian Gulf.

of 16th April, 2006 and 13th May, 2009 were visually compared to initially detect the changes in coastal landuse with the changes observed in coral reef habitats of UAE (Fig. 7.2). ERDAS IMAGINE (version 9.1) and Arc GIS (version 9.2) softwares have been used for satellite data analysis and automated area computation.

Table 7.1: Resourcesat-1 AWiFS and LISS III sensor specifications

Sensors	*Swath (km) and spatial resolution (m)*	*Spectral channels (in µm)*	*Radiometric resolution*	*Temporal resolution*
AWiFS	740 km, 56 × 56 m	0.52-0.59 0.62-0.68 0.77-0.86 1.55-1.70	10 bits	5 days
LISS-III	141 km, 23.5 × 23.5 m	0.52-0.59 0.62-0.68 0.77-0.86 1.55-1.70	7 bits	24 days

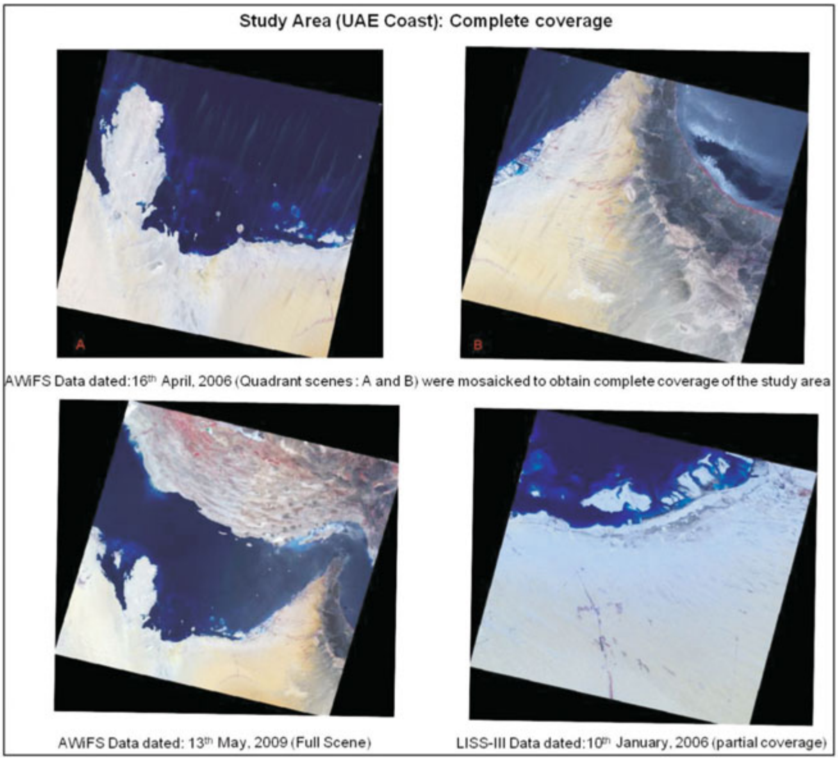

Fig. 7.2: Data used for this case study of UAE coral reefs.

Data Preparation

The methodology is depicted in Fig. 7.3. Resourcesat-1 (IRS-P6) AWiFS (2006 and 2009) and LISS III data (2006) were used for preparation of the spatial inventory of UAE coral reefs. The data analysis has been done with the help of ERDAS Imagine 9.1 software. Original digital data was downloaded and False Colour Composites (FCC) was prepared by projecting the NIR band as red, Red band as green and Green band as blue. Geo-referencing of each satellite scene was done. The images were projected to Geographic (lat/long) and Modified Everest as spheroid and datum. Area of interest (i.e. the coral reef area) was extracted from the original image using the "Subset" function of the software. For better visual appreciation of the reef features, the subset images were enhanced by the available Linear, Standard Deviation and % LUT enhancement algorithms of the software in case by case basis.

Pixel values in the satellite imagery represent the radiance of the earth's surface in the form of Digital Numbers (DN) which was calibrated to fit a certain range of values for comparative analysis of images taken by different sensors on different dates. Since each sensor has its own calibration parameters, conversion of DN values to absolute radiance values is essential to understand the appearance of different types of reef features and their overlying substrates. In order to obtain radiometrically comparable spectral radiance data, the integer DN values for each band of all images were

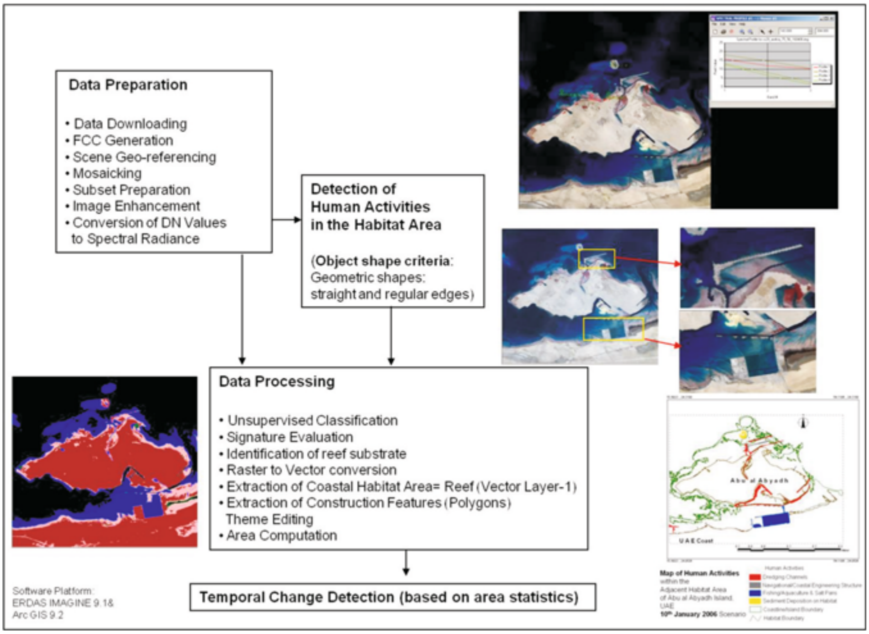

Fig. 7.3: Flow chart showing methodology.

transformed into continuous data using the spectral calibration parameters with the help of 'Modeler' module available in the software.

Data Processing

Reef/island-wise subsets were extracted from the radiometrically corrected images. Coral reefs and reef features were identified by spectral signatures. Footprints of human constructions on coral reef areas were detected based on visual detection of structures with regular geometric shapes. Iterative Self-Organizing Data Analysis (ISODATA) clustering algorithm available in the ERDAS Imagine 9.1 software was used for Unsupervised Classification. The classification was based on spectral properties of each pixel pertaining to different reef and other coastal features/categories. The number of classes was neither similar for all areas nor known; hence classification operation was performed for approximately 50 to 65 classes for a maximum of ten iterations. Fifty to 65 classes were later merged into restricted number of classes conforming to reef categories based on FCC signatures and familiarity. While working on reef mapping and studying the ecological conditions of Indian reefs, extensive ground truthing has been done for all types of reefs in India. UAE reefs mainly comprise fringing and patch type of reefs. The spectral signatures generated for these reef features (found extensively in India) based on extensive ground truthing and satellite images have been extended for classification and monitoring of UAE reefs. Raster data were finally converted into vector using the "Raster to Vector" function of the software. The vector layer was reprojected to UTM projection with WGS 84 spheroid and datum. The attributes for class/category names and codes were updated for vectorized polygons pertaining to different reef and coastal landuse categories. The resultant vector data were then used for the computation of change in the area of coral reef habitats. Arc-GIS-9.2 software was used for the area computation. Areas under four thematic classes of reef, construction, sediments and algae on reef have been automatically generated from the digital database summing the area of the polygons falling into these four discrete categories.

RESULTS AND DISCUSSION

The use of satellite data has proved its importance in mapping and monitoring the extent, geomorphological zones, ecological categories of reefs and conditions of coral reefs of the world (Navalgund et al., 2010). On the basis of a two-time, Resourcesat-1 data, anthropogenic activities and natural stresses were identified on coral reefs within the study region in UAE (summarized in Table 7.2). The study region occupies 6228.00 sq km reef area. The initial comparisons between AWiFS data dated 16th April, 2006 (Timeframe 1:T1) and 13th May, 2009 (Timeframe 2:T2) revealed an increase in anthropogenic construction activities such as jetties, dredging lines, salt pans, etc. from

Table 7.2: Temporal status of coral reef habitats of UAE

Sr. No.	*Data*	*Total area of reef (sq km)*	*Total area of construction (sq km)*	*Total area of sediments (sq km)*	*Total area of algae (sq km)*	*Construction/ Total reef area (%)*	*Sediments/ Total reef area (%)*	*Algae/ Total reef area (%)*
1.	16th April, 2006 AWiFS(T1)	6228.00	172.80	366.78	788.932	2.77	5.89	12.67
2.	13th May, 2009 AWiFS(T2)	6228.00	322.38	846.43	629.602	5.18	13.59	10.11

172.80 sq km in 2006 to 322.38 sq km in 2009 area on the reef over a short period of three years (Figs 7.4-7.6 and Table 7.2). The impact of these human activities were discernible on the satellite data as indicated by the changes in the water quality (increasingly becoming turbid) in areas adjacent to the above anthropogenic activities. Anthropogenic activities affecting the reef ecology in the area have also been reported by Pilcher et al. (2000) and Coles (2003).

The overall change detected in the study area was supported by similar observations in certain smaller hotspots identified within the study region. Abu-al-Abyadh Island in central part of UAE coast occupies 296.52 sq km reef area. In this region, construction activities in 2006 were spread over 26.84 sq km which were continued in 2009 and expanded to 36.26 sq km. Construction activities on this reef have increased from 9.05% in year 2006 to 12.23% of the reef area by the year 2009, thus showing an increase of 3.18% area in three-year timeframe (Fig. 7.5). Eastern part of the UAE coast near Abu Dhabi occupies 643.73 sq km reef areas. In this particular region, construction activities in 2006 were spread over 10.42 sq km. These construction activities continued in 2009 and extended to 14.45 sq km showing an increase from 1.02% in year 2006 to 2.24% of its reef area by 2009. Therefore, construction activities in this region have increased by 1.22% of reef area in three-year time period (Fig. 7.6).

Comparisons of anthropogenic activities in 2006 and 2009 AWiFS data indicated that construction activities in 2006 were spread over 172.80 sq km areas. These activities were continued in 2009 and were spread over

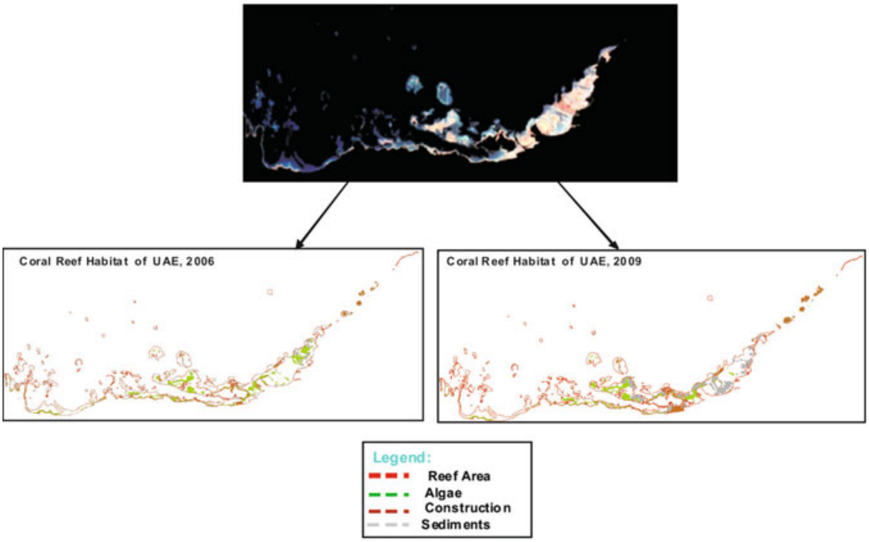

Fig. 7.4: Status of coral reef habitats of UAE coast.

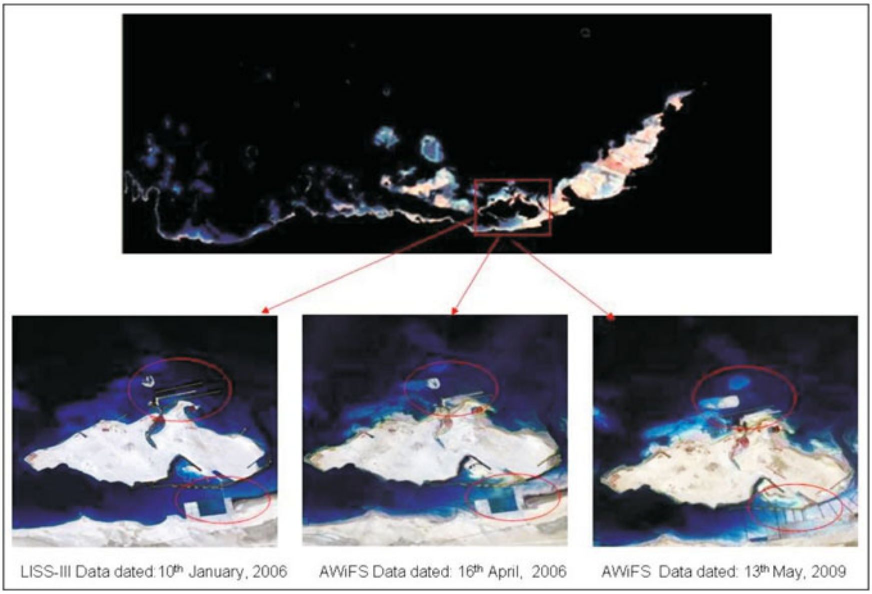

Fig. 7.5: Construction activities more prominent on Abu-al-Abyadh Island, in central part of UAE coast.

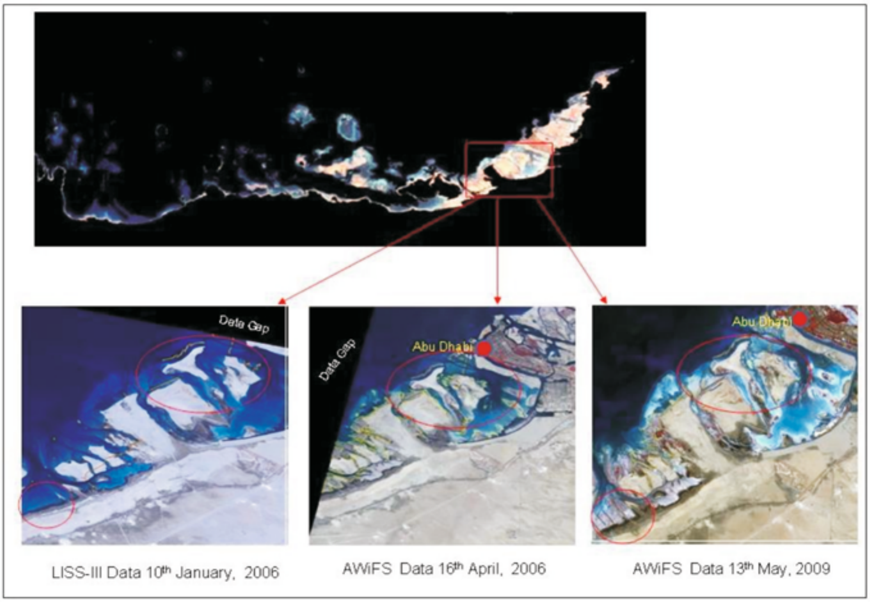

Fig. 7.6: Construction activities and macro-algal growth more prominent near Abu Dhabi, eastern part of UAE coast.

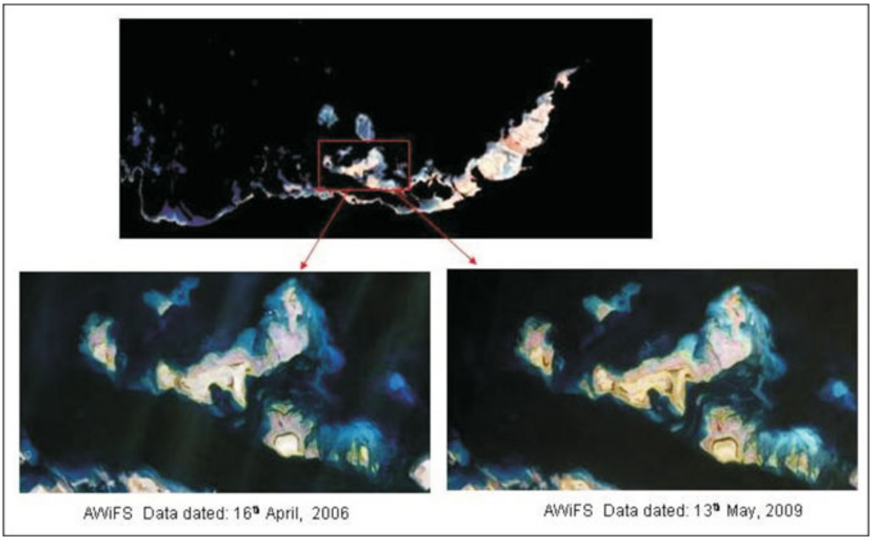

Fig. 7.7: Macro-algal growth on the off shore coral reef islands of UAE.

322.38 sq km. Thus, construction activities on reefs have increased from 2.77% to 5.18% of total reef area from 2006 to 2009. This indicates that construction activities have been expanded over 2.41% of total reef area in three years' time (Fig. 7.4).

Spectral signature of macro algae was detected in the southern Arabian Gulf coral reefs on Resourcesat-1, AWiFS data of 16th April, 2006. This data was compared with Resourcesat-1, LISS-III data of earlier date: 10th January, 2006 which showed sparse or no colonization of macro algae on the reef habitats. AWiFS data of 16th April, 2006 showed very high colonization of macro algae on the reef habitats equivalent to 788.93 sq km. Further, this data was compared with AWiFS data of 13th May, 2009 which showed withdrawal signs of macro algae from the reef habitat and exposure of the underlying, bare litho-substrates. In April, 2006 macro algae had covered 12.67% of coral reef area while in May, 2009, algae had covered only 10.11% of coral reef area. The 10thJanuary, 2006 data however showed no colonization of macro algae on the reef habitats (Fig.7.7). It appears that macro algal occupancy on reef habitats of UAE is a seasonal phenomenon (with peak growth period coinciding in April). To establish algal occupancy as a case of phase shift in the reefs under study, a rigorous analysis of frequent temporal data sets over a long period is needed.

The comparison between the multi temporal AWiFS data indicates that the anthropogenic activities on UAE coast have definitely increased within three-year period. Along with construction activities, increase in sediment deposition is also noticed on the coral reefs. It has been observed on AWiFS data of 16th April, 2006 (T1) and 13th May, 2009 (T2) that the footprints of construction activities are more prominent on the central and eastern parts of the study region (Fig. 7.4). The western part is relatively free of such anthropogenic activities, so are some of the small off-shore islands. However, in the central part near Abu al Abyadh Island, a network of construction lines is traced, indicative of island and coastal developmental activities. In the eastern part, such construction lines are found in the vicinity of urban centres like Abu Dhabi, Jebel Ali air port and Dubai.

It was observed that as construction features expanded over three years' period, there was also a consequent increase in the turbidity in the coastal waters adjacent to those features. However, macro-algal occupancy showed a decrease over the three years' period. Hence, in order to understand the temporal dynamics of algal overgrowth on reefs the AWiFS data were compared with a LISS-III data of earlier month (i.e. January 2006). The LISS-III data rather showed no colonization of macro algae on reefs which were later colonized in April 2006 in considerable extent. In May, 2009 the same showed much less macro-algal cover on the same reef locations. This gives an indication of seasonal nature of the macro-algal overgrowth on UAE reefs and not a case of pure phase shift.

CONCLUSION

The present study on UAE coast demonstrated the potential of Resourcesat-1 (IRS-P6) AWiFS data in preparing a spatial inventory of coral reef habitats at a country level. AWiFS sensor has a moderate spatial resolution of 56 m, which is effective to map and monitor the moderate to large scale habitat dynamics. Moreover, this sensor has a revisit period of five days that can well be used to monitor habitat level changes over such a short period. This can also be complemented with LISS-III kind of sensor which has a finer spatial resolution of 23.5 m. Moreover, their multi-spectral nature helps in identifying different reef substrates. Hence, for country-scale temporal monitoring and assessment where sizeable reef habitat exists like UAE, AWiFS data can be used as a reliable remote sensing data.

ACKNOWLEDGEMENT

The authors are thankful to Dr. B.K. Jain, Principal, M.G. Science Institute, Dr. R.R. Navalgund, Director, Space Applications Centre (SAC), Indian Space Research Organization (ISRO), Ahmedabad and Dr. J.S. Parihar, Deputy Director, EPSA, SAC, ISRO, Ahmedabad for their constant encouragement and support. Support of Ms. Vanya Bajpai, Junior Research Fellow, SAC in troubleshooting on ArcGIS software is duly acknowledged.

REFERENCES

Coles, S.L. (2003). Coral species diversity and environmental factors in the Arabian Gulf and the Gulf of Oman: A Comparisons to the Indo-Pacific region. *Atoll Research Bulletin* **507**. National Museum of Natural History, Smithsonian Institute, Washington, D.C., U.S.A.

Dubinsky, Z. (1990). Ecosystem of the World, 25: Coral Reefs. Elsevier Science Publishers.

Endean, R. (1976). Destruction and recovery of coral reef communities. *In:* Jones, O.A. and Endean, R. (eds), Biology and Geology of Coral Reefs, 3. Biology 2. Academic Press, New York.

http:// www.earthdive.com/site/news/newsdetails.asp

http://www.reefbase.org/global_database/default.aspx?section

Johannes, R.E. (1975). Pollution and degradation of coral reef communities. *In:* Ferguson Wood, E.J. and Johannes, R.E. (eds), Tropical Marine Pollution. Elsevier Scientific Publishing. Amsterdam.

Loya, Y. and Rinkevich, B. (1980). Effects of oil pollution on coral reef communities. *Mar. Ecol. Prog. Ser.*, **3:** 167-180.

Loya, Y. (1976). Recolonization of Red Sea corals affected by natural catastrophes and man-made perturbations. *Ecology*, **57:** 278-289.

Maghsoudlou, A., Araghi, P.E., Wilson, S., Taylor, O. and Medio, D. (2008). Status of the coral reefs in the ROPME Sea Area (The Persian Gulf, Gulf of Oman and Arabian Sea). *In:* Status of Coral Reefs of the World: 2008. Wilkinson, C. (ed.). Global Coral Reef Monitoring Network and Reef and Rainforest Research Center, Townsville, Australia.

Navalgund, R.R., Ajai, Bahuguna, A., Ray Chaudhury, N., Bhattji, N.S., Madhupriya, N., Sharma, S., Parihar, J.S., Panigrahi, S., Chakraborty, M., Dwivedi, R.M., Ramdass, S. and Swaroop, P. (2010). Coral Reef Atlas of the World, Vol. 1. Central Indian Ocean. Space Applications Centre, Ahmedabad.

Pilcher, N.J., Wilson, S., Alhazeem, S.H. and Shokri, M.R. (2000). Regional status of coral reefs in the Arabian/Persian Gulf and Arabian Sea Region (Middle East). *In:* Status of Coral Reefs of the World, 2000. Wilkinson C. (ed.). GCRMN Report, Australian Institute of Marine Science, Townsville.

Spalding, M.D., Ravilious, C. and Green, E.P. (2001). World Atlas of Coral Reefs. University of California Press.

Wilson, S., Fatemi, S.M.R., Shokri, M.R. and Claereboudt, M. (2002). Status of Coral Reefs of the Persian/Arabian Gulf and Arabian Sea Region. *In:* Status of Coral Reefs of the World, 2002. Wilkinson, C. (ed.). GCRMN Report, Australian Institute of Marine Science, Townsville.

CHAPTER

8

Impact of Climate Change in the Sundarban Aquatic Ecosystems: Phytoplankton as Proxies

Dola Bhattacharjee, Brajagopal Samanta, Anurag Danda[1] and Punyasloke Bhadury

Integrative Taxonomy and Microbial Ecology Group, Department of Biological Sciences, Indian Institute of Science Education and Research Kolkata (IISER-K), Mohanpur Campus
Mohanpur – 741252, Nadia, India
[1]Sundarbans Programme and Climate Adaptation (Coastal Ecosystems)
WWF-India, Hindustan Park, Kolkata – 700029, India
pbhadury@iiserkol.ac.in

INTRODUCTION

Phytoplankton has played a central role in mitigating and amplifying climate change in the past and may have contributed to stabilizing the climate by influencing the partitioning of climate-relevant gases between the ocean and atmosphere (Schlesinger, 2005). In modern day, phytoplankton can be used as excellent proxies for detecting changes in the water column as a result of anthropogenic activities (Moncheva et al., 2001). At present, the pCO_2 has reached about 380 μatm and is expected to rise to 750 μatm by the end of this century (Houghton et al., 2001) or even values >1000 μatm (Raven et al., 2005). Such changes can alter the biota and associated physicochemical conditions in different environments including in mangrove ecosystem. Visible changes within phytoplankton communities have been reported in the North-east Atlantic and North Sea as a result of spreading of unusually cold water from the Arctic (Reid et al., 1998; Beaugrand et al., 2003). Reduction in

J. Sundaresan et al. (eds.), *Climate Change and Island and Coastal Vulnerability*,
DOI 10.1007/978-94-007-6016-5_8, © 2013 Capital Publishing Company

phytoplankton diversity and unusual dominance of diatoms and cyanobacteria in relation to global climate changes were also identified in the Oder estuary, Germany (Godhantaraman, 2009). Increase in biomass and abundance of diatoms were documented from the middle Adriatic Kastela Bay, Croatia, over an extended period of 51 years (Jan Ben, 2007). In the Indian subcontinent a long-term study spanning over a period of 20 years showed changes in species distribution, abundance and community shifts in coastal marine plankton from Southern India (Godhantaraman, 2009). A recent report illustrated the impacts of climate change being stronger on small phytoplankton groups than on diatoms (Marinov et al., 2010). Presently, abundance and diversity of phytoplankton assemblages in marine ecosystems are used as proxies to follow climate induced changes over an eco-region (Marinov et al., 2010; Richardson and Schoeman, 2004).

Mangrove ecosystems are highly productive and are vulnerable to even slight changes in physicochemical and biological properties of the water column (Kannan and Vasantha, 1992). Several investigations addressing the phytoplankton abundance and diversity as an index of the prevailing water quality from the Indian mangroves have been carried out in the past (e.g. Ajithkumar et al., 2006; Anilakumari et al., 2007; Prabu et al., 2008), but comparatively few studies have focussed on the impacts of climate change on biota and physicochemical parameters in mangrove environments including the Indian Sundarbans. The Sundarbans mangrove eco-region is the world's largest mangrove ecosystem, lying in the vast delta formed by the confluence of the Brahmaputra, Ganges and Meghna rivers across India and Bangladesh. A recent study has predicted significant loss of Sundarbans by the end of the 21st century because of rising sea level and related climatic changes (UNESCO, 2007; Danda 2010). Already, locations like the Lohachara Island and New Moore Island in the Indian Sundarbans have disappeared under the sea, and Ghoramara Island is half submerged (George, 2010).

The Indian Sundarbans is characterized by marked shifts in natural phytoplankton assemblages at a seasonal time scale (De et al., 1991; Biswas et al., 2010; Manna et al., 2010; Duarte et al., 2006). There are recent reports of significant changes in physicochemical parameters including surface water temperature, salinity and pH in the coastal waters of Indian Sundarbans based on the analysis of datasets collected over a period of more than two decades (Mitra et al., 2009). However not much literature resources are available detailing small scale temporal variations of biota and associated physicochemical parameters in the mangrove waters of Indian Sundarbans, the nursery ground for fisheries of the Bay of Bengal. This lack of primary information in lieu of the current climate change patterns in the ecoregion prompted us to undertake the present study. The objective of this study was to investigate the dynamics of natural eukaryotic phytoplankton assemblages along a short temporal gradient in relation to physicochemical parameters of the water column in Sundarbans which can lead towards long-term understanding of the impacts of climate change on the ecoregion.

MATERIALS AND METHODS

Study Area

The study was carried out in spring till the early summer of 2010 across four sites in the Chemaguri creek and Mooriganga estuary in Sagar Island of the Indian Sundarbans (Fig. 8.1). The study sites are tidally influenced by the coastal waters of Bay of Bengal on a daily basis. Sagar Island, the largest tide-dominated island (tidal range 5-6 m) in the Indian Sundarbans is only 6.5 m above the sea level (Mukherjee, 1983). The island has unique mangrove vegetation and surrounded by the river Hoogly in the north and its west, Mooriganga in the eastern side, while the southern part faces the Bay of Bengal. Chemaguri creek is the most prominent tidal creek system in Sagar with planted mangroves along its length and supports an endangered population of the King crab *Carcinoscorpius rotundicauda* that adds to the importance of this site (Mitra et al., 2000). The effects of climate change are well documented in and around Sagar Island (Mitra et al., 2009).

Surface water samples were collected from 23rd March to 27th May 2010 from each station, once per week, at an equilibrium phase of daytime tidal action. No samples were collected on 6th, 7th, 9th and 10th week as the sites were on cyclone alert (Laila).

Phytoplankton Collection and Taxonomic Enumeration

Water samples were collected in 1 L sample bottles and preserved in neutral formalin (4%) solution immediately. In the laboratory, preserved water samples were concentrated for phytoplankton by gravity sedimentation (24 h) and counted based on drop-count method under a bright-field microscope (Magnus, MLX-Bi). Taxonomic identifications were done following standard identification keys (Subrahmanyan, 1946; Desikachary, 1959, 1987).

Physicochemical Analyses

Physicochemical parameters including salinity, water temperature, pH, turbidity and specific gravity were recorded using refractometer (Erma, Japan), digital thermometer (Eurolab ST9269B), pH meter (Eco tester) and a Secchi disc respectively, at time of sampling in each station. For nutrient analysis, pre-cleaned amber bottles (125 mL) were used for collecting water samples from the stations, fixed in 1% neutral formalin immediately and transported into the laboratory and analyzed in a spectrophotometer (Beckman Coulter, DU730) for determination of nitrate, (ortho)-phosphate and silicate concentrations (Strickland and Parsons, 1972; Parsons et al., 1984; Turner et al., 1998; Finch et al., 1998; Nussler et al., 2006).

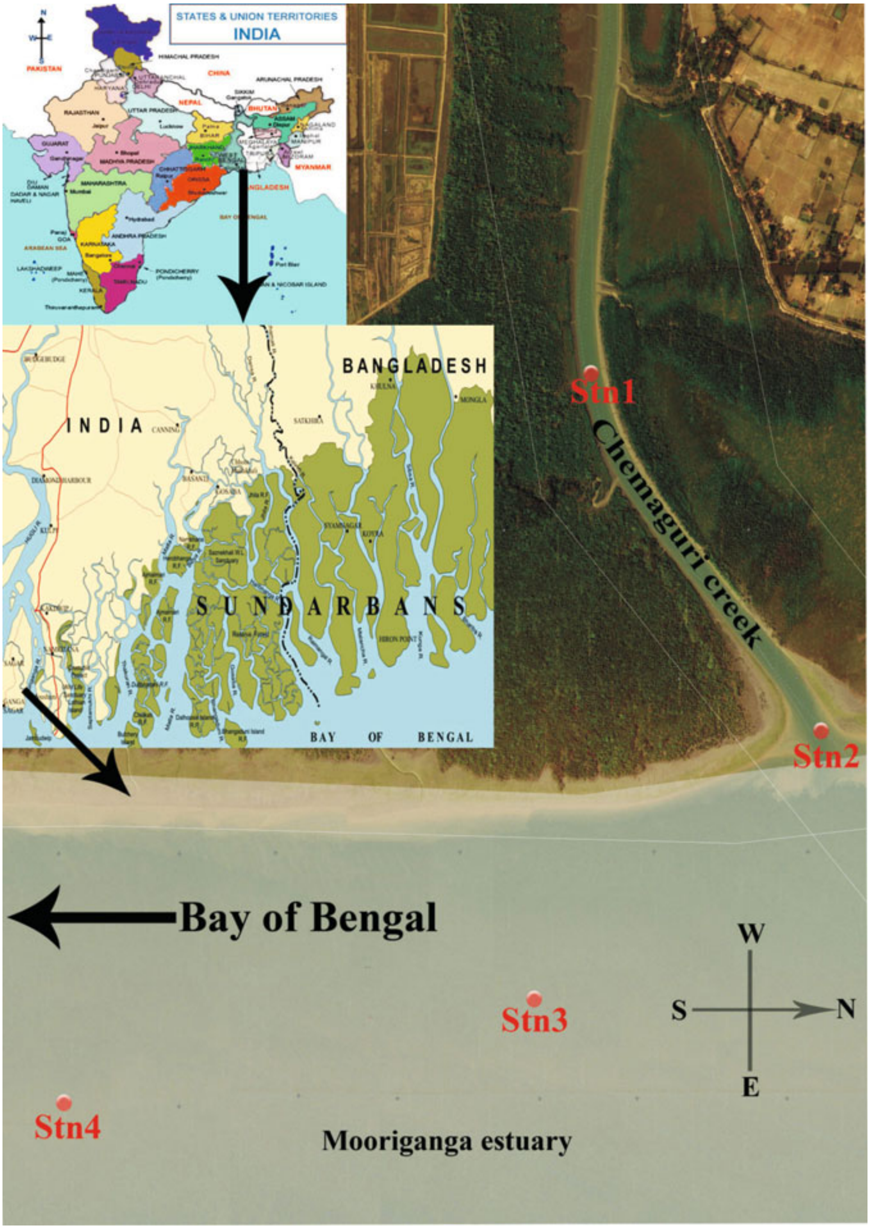

Fig. 8.1: Map of the study area. Stn1, Stn2, Stn3 and Stn4 are the sampling stations whose geographical locations are as follows: Stn1 (N21º40′44.4″ E88º08′49.5″) and Stn2 (N21º40′59.3″ E88º09′13.1″) in Chemaguri creek; Stn3 (N21º40′40.6″ E88º09′19.2″) and Stn4 (N21º40′09.8″ E88º09′21.2″) in Mooriganga estuary.

Photosynthetic Pigment Analysis

Surface water sample of one litre was collected separately in dark bottles for photosynthetic pigment analysis. It was filtered onto 0.45 µm GF/F filters (Millipore) and extracted overnight in 90% acetone under 4°C in the dark. Pigment extracts for chlorophyll-*a*, -*b*, fucoxanthin and peridinin were centrifuged and subsequently quantified in a spectrophotometer (Shimadzu, UV1800).

RESULTS

A total of 22 genera of net eukaryotic phytoplankton were documented in the present study. Generic presence or absence of phytoplankton from each station is highlighted in Table 8.1. Among the net phytoplankton, diatoms consisting of centric and pennate forms represented bulk of the assemblages. Centric diatoms were represented by 12 genera while the pennate forms were represented by eight genera including the araphid diatom *Thalassionema*. Centric diatoms like *Coscinodiscus* and *Thalassiosira,* and pennate diatoms like *Thalassionema* and *Navicula* dominated in almost every sample across all the four sites. Many of the diatom genera such as *Cyclotella, Bellerochea, Guinardia, Melosira, Odontella* and *Lauderia* were identified in the water samples at a later part (4-5th week) of the study. Besides diatoms, dinophytes represented by two genera, viz., *Ceratium* and *Peridinium* were documented in our study. The abundance of phytoplankton was highest at the site Stn4 for the season (mean 6.31×10^3/L), while lowest at the site Stn2 (mean 7.63×10^3/L). A considerable increase in phytoplankton abundance was observed across all the stations in the 4th week of sampling (in early April, 2010) (Fig. 8.2), with no fall in net generic diversity (Fig. 8.3).

The physicochemical parameters recorded from all the stations are depicted in Table 8.2. Surface water temperature ranged between 29.2 and 32.3°C in this period. The salinity ranged between 10.5 and 21 psu across the study sites for the sampled period. Salinity was highest in Stn2 and Stn3 (21 psu) and lowest in Stn2 and Stn4 (10.5 psu) as part of this study. The pH values were rather consistent for all the stations in the study period (7.15 on an average). Turbidity values ranged between 1.5 and 9 inches based on secchi measurements during the study and water was least turbid in Stn1 during 3rd week.

A temporal shift in dissolved nutrient concentrations was noted from all the stations with a drop in nitrate concentration in the 4th week (Fig. 8.4a). Dissolved (ortho)-phosphate concentration dropped in the 3rd-5th week of sampling (Fig. 8.4b) while in case of dissolved silicate it was in the 5th week of sampling (Fig. 8.4c).

The photosynthetic pigment data illustrated hikes in the concentration of Chlorophyll-*a* in the 4th and 5th weeks with a maximum concentration recorded from the station Stn4 (mean 8.3 mg/cu.m). Other pigments indicative of

Table 8.1: Generic shifts ('presence-absence') in phytoplankton assemblages from the study area during the study period

Genera	*W1*				*W2*				*W3*				*W4*				*W5*				*W8*				*W11*	
	Stn1	*Stn2*	*Stn3*	*Stn4*	*Stn1*	*Stn2*	*Stn3*	*Stn4*	*Stn1*	*Stn2*	*Stn3*	*Stn4*	*Stn1*	*Stn2*	*Stn3*	*Stn4*	*Stn1*	*Stn2*	*Stn3*	*Stn4*	*Stn1*	*Stn2*	*Stn3*	*Stn4*	*Stn1*	*Stn2*
Amphora	-	✓	-	-	-	-	-	-	-	-	-	-	-	-	-	-	-	-	✓	-	-	✓	✓	-	-	
Coscinodiscus	✓	✓	✓	✓	✓	✓	✓	✓	✓	✓	✓	✓	✓	✓	✓	✓	✓	✓	✓	✓	✓	✓	-	✓	✓	✓
Navicula	✓	-	-	-	✓	✓	✓	✓	✓	✓	✓	✓	✓	✓	✓	-	✓	✓	✓	-	✓	-	-	✓	✓	✓
Nitzschia	✓	-	-	✓	-	✓	-	✓	-	✓	-	-	-	-	-	✓	-	✓	✓	✓	-	-	-	✓	-	✓
Cyclotella	-	-	-	-	-	-	-	-	-	-	-	-	-	-	-	-	-	-	✓	-	-	✓	✓	✓	✓	-
Bellerochea	-	-	-	-	-	-	-	-	-	-	-	-	-	-	-	-	-	-	✓	✓	-	-	-	-	-	-
Chaetoceros	-	-	-	-	✓	✓	-	✓	-	-	-	-	✓	✓	✓	-	✓	✓	-	-	✓	✓	-	-	-	✓
Guinardia	-	-	-	-	-	-	-	-	-	-	-	-	-	-	-	-	-	-	-	✓	-	-	-	-	-	-
Pleurosigma	✓	✓	✓	-	-	-	✓	-	-	-	✓	-	-	-	✓	✓	-	-	-	✓	-	✓	-	-	✓	-
Melosira	-	-	-	-	-	-	-	-	-	-	-	-	-	-	✓	-	-	-	✓	-	-	-	-	-	-	-
Odontella	-	-	-	-	-	-	-	-	-	-	-	-	-	-	-	-	-	-	-	✓	-	✓	✓	-	-	-
Rhizosolenia	-	-	-	✓	-	-	✓	✓	-	-	-	✓	-	-	-	✓	-	✓	-	-	-	✓	-	-	✓	-
Skeletonema	-	-	-	✓	-	-	-	-	-	-	-	-	-	-	-	-	-	-	-	✓	✓	-	-	✓	-	-
Thalassiosira	✓	✓	✓	✓	✓	✓	✓	-	-	✓	✓	✓	✓	✓	✓	-	✓	✓	-	-	✓	-	-	-	-	✓
Thalassionema	✓	✓	-	-	-	✓	✓	✓	✓	-	✓	✓	✓	✓	-	-	-	-	-	-	-	-	✓	-	-	-
Ceratium	✓	-	✓	✓	-	-	-	✓	-	-	✓	✓	-	✓	✓	✓	-	✓	✓	-	-	-	-	-	-	✓
Lauderia	-	-	-	-	-	-	-	-	-	-	-	-	-	-	-	-	-	-	-	-	-	-	-	✓	-	-
Amphipleura	✓	-	-	-	-	-	-	-	-	-	-	-	-	-	-	-	-	-	-	-	-	-	-	-	-	-
Cymbella	-	-	-	-	✓	-	-	-	✓	-	-	-	✓	-	-	-	✓	-	-	-	-	-	-	-	✓	✓
Fragilaria	-	-	-	-	✓	-	-	-	-	✓	-	-	-	-	-	-	✓	-	-	✓	-	-	-	-	-	-
Triceratium	-	-	-	-	-	✓	-	-	✓	-	✓	✓	-	✓	✓	✓	-	-	-	-	-	-	✓	-	-	-
Peridinium	✓	✓	✓	✓	✓	-	✓	-	✓	-	-	-	-	-	-	-	-	-	-	-	-	-	-	-	-	-

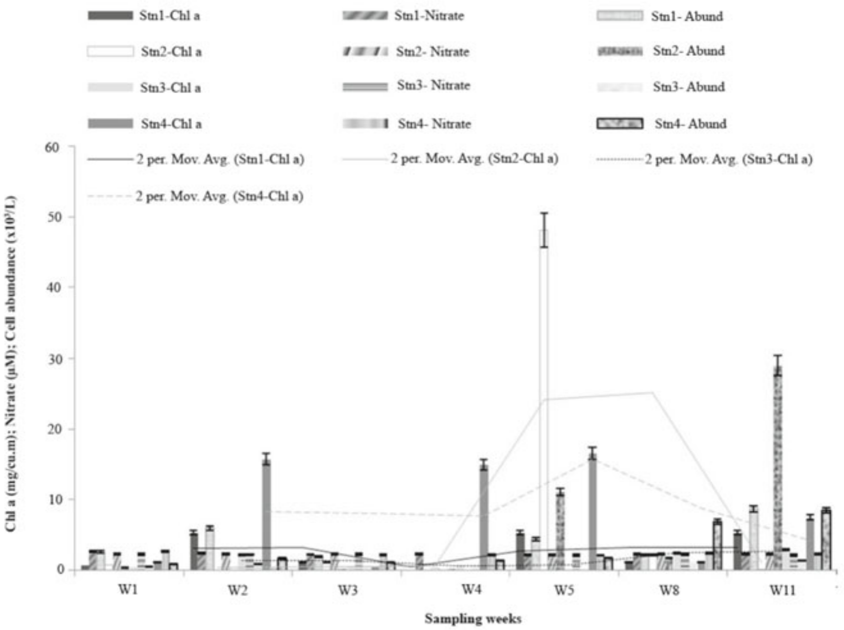

Fig. 8.2: Shifts in abundance of phytoplankton (cells/L) with respect to dissolved nitrate (µM) and Chlorophyll-*a* (mg/cu.m) concentrations from (a) Stn1, (b) Stn2, (c) Stn3 and (d) Stn4, along the sampling weeks.

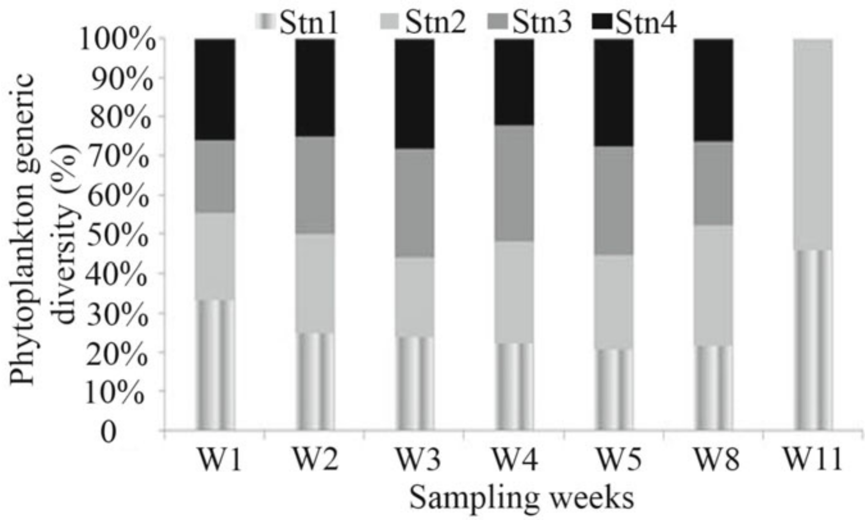

Fig. 8.3: Shifts in the diversity of phytoplankton genera (percent) along the sampling weeks.

major phytoplankton functional groups like chlorophyll-*b*, fucoxanthin and peridinin also exhibited temporal shifts (Figs 8.5a, b and c).

Table 8.2: Physicochemical parameters recorded from the stations during the study period

Weeks	*Stations*	*Surface water temperature (°C)*	*Salinity (psu)*	*pH*	*Secchi depth (inches)*	*Specific gravity*
1	Stn1	30.5	17	7	8	1.013
	Stn2	30	18	7	7	1.013
	Stn3	30.5	19	7	6	1.014
	Stn4	30	20	7.1	5	1.015
2	Stn1	30	18.5	7.2	5	1.013
	Stn2	29.5	21	7.2	4	1.016
	Stn3	29.2	21	7.2	5	1.016
	Stn4	30	20	7.1	5.5	1.014
3	Stn1	29.8	12	7.2	9	1.009
	Stn2	29.8	11.5	7.1	7.5	1.009
	Stn3	29.8	11	7.2	6.5	1.009
	Stn4	29.2	12.5	7.2	6	1.01
4	Stn1	30.1	11.5	7	5	1.009
	Stn2	30.1	15	7	8	1.01
	Stn3	30.1	16	7	5.2	1.012
	Stn4	30.2	18	7.1	6.5	1.013
5	Stn1	29.9	13	7.2	2	1.01
	Stn2	30	10.5	7.2	3	1.008
	Stn3	30	11	7.2	4	1.009
	Stn4	30	10.5	7.2	4	1.009
8	Stn1	29.4	16.5	7.3	4	1.012
	Stn2	29.5	16.5	7.3	3	1.012
	Stn3	30	17	7.3	5	1.013
	Stn4	30	17	7.4	2.5	1.013
11	Stn1	32.3	16	N.A.	1.5	1.012
	Stn2	32.2	16	N.A.	1.5	1.012

DISCUSSION

Present study indicates a shift in net phytoplankton abundance and diversity along a short temporal gradient with dominance of diatoms (Bacillariophyceae) across all the sites. Like any other mangrove ecosystem, diatoms represent a major part of the phytoplankton functional groups in the Indian Sundarbans (Biswas et al., 2010). Centric diatoms were generally found to dominate bulk of eukaryotic phytoplankton assemblages and there was a shift in the assemblage patterns which corresponded with changing surface water temperature and other environmental variables across the progressing weeks of sampling. In the late 1980s surface water temperature ranged from 21 to 31°C for the months of January-June in Chemaguri while surface water

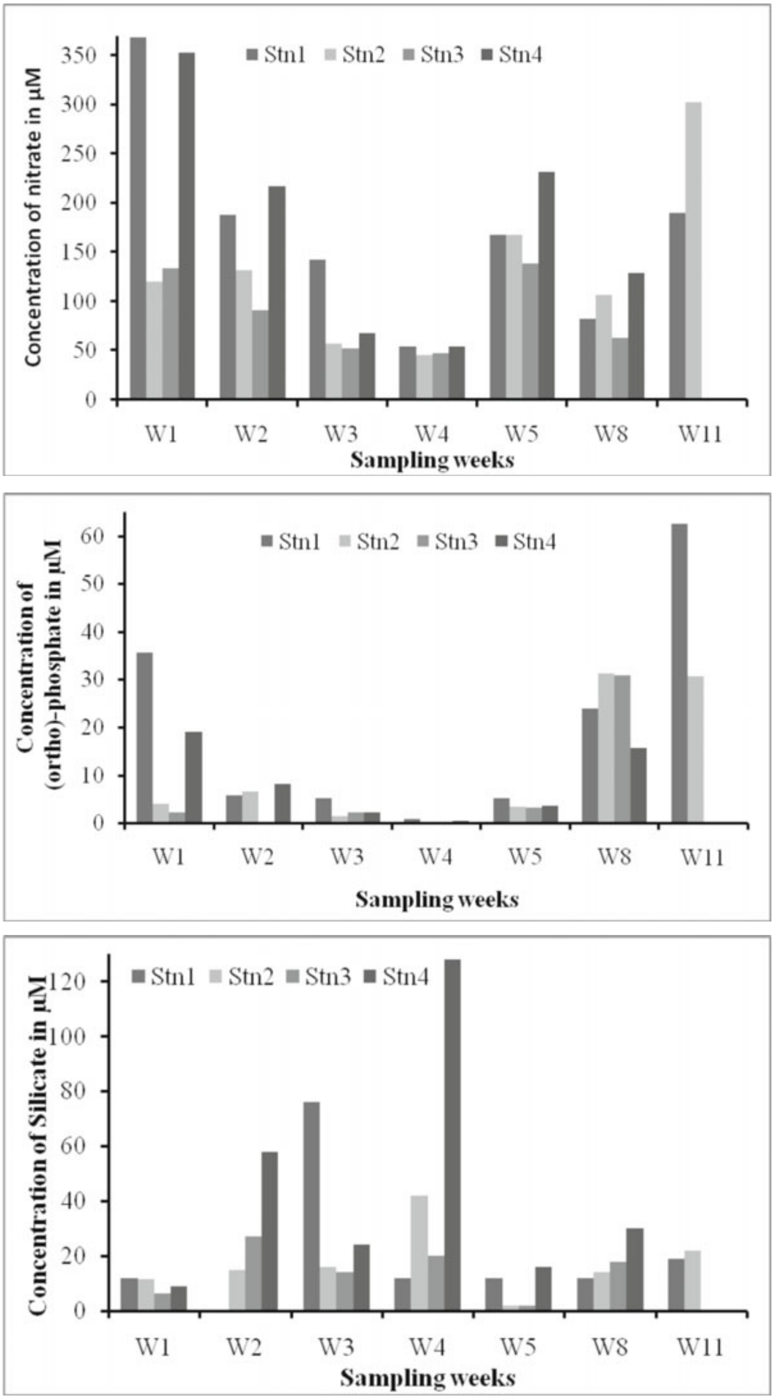

Fig. 8.4: Shift in dissolved nutrient concentrations (µM) from the stations along the sampling weeks: (a – above) nitrate, (b – middle) (ortho)-phosphate and (c – bottom) silicate.

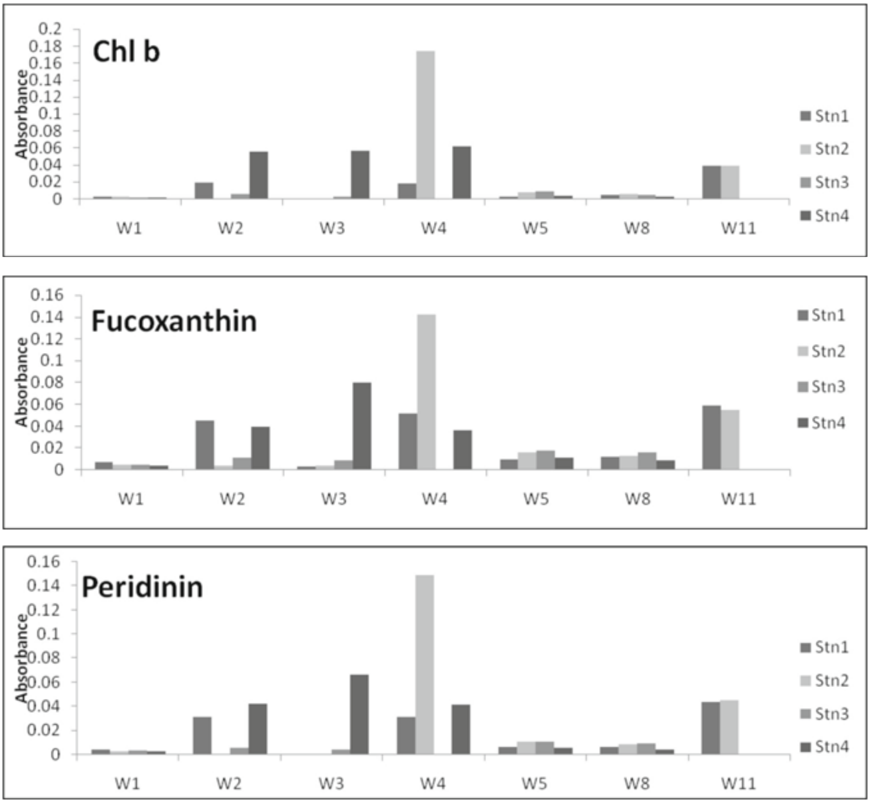

Fig. 8.5: Accessory photosynthetic pigment profiles for the sampling season: (a – above) Chlorophyll-*b*, (b – middle) fucoxanthin and (c – bottom) peridinin (in relative absorbance).

temperature ranged from 29.2 to 32.3°C in 2010 indicating a shift for the same period. We have also observed changes in the surface water temperature in Chemaguri and adjoining Mooriganga estuary in an extended sampling encompassing additional 30 weeks (June 2010 to May 2011) (data not shown). Since 1990, an increasing trend in net phytoplankton genera has been reported by several authors from the Indian Sundarbans (Biswas et al., 2010; Manna et al., 2010). In this study we report a total of 22 eukaryotic phytoplankton genera for the entire study period which is usually lesser than previously reported from Sagar Island (Chaudhuri and Chaudhuri, 1994).

Earlier investigations reported blooms of *Ditylum brightwelli* in 1990 and *Coscinidiscus* sp. and *Bacillaria* sp. in 2007 for this season (March-April) from Sundarbans (Biswas et al., 2010). We also documented high abundance of the centric diatom *Coscinodiscus radiatus* in the 3rd and 4th week (early and mid-April) from our study sites. To the best of our knowledge the presence of polyhaline centric diatom *Triceratium* sp. from this part of the Sundarbans was reported only once before (Biswas et al., 2004) and here we have documented the same across all the stations encompassing Chemaguri creek and Mooriganga river estuary in the months of March and April. Interestingly, we also recorded the presence of dinoflagellate genus like *Peridinium* only in the beginning but the other dinoflagellate genus *Ceratium* was recorded more or less throughout the study period. A separate study undertaken by Samanta and Bhadury (2012) has detected signatures of *rbcL* phylotypes of potentially harmful genera including *Phaeocystis* for the first time from Indian Sundarbans based on molecular approaches from samples collected in April, December of 2010 and March 2011 in Chemaguri creek and adjoining Mooriganga estuary.

Long-term (decadal) observations revealed a progressive shift in pH (from 8.325 to 8.28 over three decades) in water column from the northern part of Sagar Islands at a rate of –0.015 units/decade (Mitra et al., 2009). We report an average pH of 7.15 from the study area for the season, which is different, although in 2006 average pH for one of the sites in Chemaguri Creek was 8.1. Additional sampling efforts from June 2010 to May 2011 undertaken in some of the study sites in Chemaguri creek and Mooriganga river estuary indicated that the average pH was 8.09 (data not shown). It seems that the observed variation in pH across the studied sites could be controlled by dynamic environmental parameters. However more studies are needed to link the observed pH variation with climate-induced factors and work is presently underway in this regard involving state-of-the-art measurements. All other physicochemical parameters are generally comparable with that of previous datasets (Biswas et al., 2010). It has been reported that the dissolved oxygen concentration (D.O.) in the eastern sector of Sundarbans has decreased significantly from 1995 at a rate of about 0.5 ppm per decade and the opposite in the western sector but based on unpublished data the D.O. level in one of our study sites in Chemaguri has remained more or less same (average 3.47 ml/L).

Nutrient concentrations from our study showed significant variability when compared with previous studies from the region. For example, dissolved nitrate concentration across our study sites ranged from 45 to 368 μM (mean 133.65 μM) while a recent study from the Sundarbans reported sum of nitrate and nitrite concentration as 12.25±7.29 μM (Biswas et al., 2010) but not from the Chemaguri and adjoining areas. Silicate (mean 24.08 μM) and phosphate values (mean 8.81 μM) measured during our study was different than previously reported values (silicate=46.3±18.32 μM, phosphate = 0.68±0.46 μM) (Biswas et al., 2010). On the contrary nutrient value (ammonia, nitrite, silicate and phosphate) in 2008-2009 from a creek in Jharkhali located north-east off the Sagar Island was found to be much lower (Manna et al., 2010) when compared with our study. Variation in nutrient concentration is usually controlled by environmental and other associated factors at the temporal and spatial scales. In Indian Sundarbans such variability gets amplified in creeks and estuaries which are strongly influenced by the availability of tidal waters from coastal Bay of Bengal as well as anthropogenic inputs. Therefore fluctuating nutrient concentrations in the water column play an important role in controlling the dynamics of the biota including that of natural phytoplankton assemblages.

A drop in dissolved nutrients concentration in the 4th sampling week indicated its rapid removal from the system over a short time; however, it was weakly reflected in the net phytoplankton cell densities. A separate study reported seasonal increase in chlorophyll-*a* concentration in relation to decreasing phytoplankton counts in Jagannath Canal (Sundarbans) from March through September of 1995 (Saha et al., 2001). It has been shown that in mangrove environments photosynthetic picoplanktonic groups are responsible for upto 29% of the net primary production (Teixeira and Gaeta, 1991) and perhaps these groups are also playing an important role in uptake of nutrients from the water column across our study sites and thereby contributing in net primary production. This is well reflected with the corresponding increase in chlorophyll-*a* concentration in our study. It seems more plausible that picophytoplankton communities may have contributed to net increase in chlorophyll pigment concentration in our study sites. While enumerating phytoplankton genera we found equal dominance of pico-phytoplankton (unidentified) and benthic cyanobacteria (e.g. *Phormidium* sp., *Oscillatoria* sp.) in the natural assemblages. The role of cyanobacteria as a significant contributor in primary production is well documented in Sundarbans (Debnath et al., 2007). As of now there is no report of the presence of picophytoplankton, in particular picoeukaryotes, a taxonomically intractable functional group in Sundarbans and here we report for the first time the presence of picophytoplankton in Sagar Island and their possible role in primary production.

It has been documented that 80% of the bacterial cells in mangroves are free cells ($1\text{-}2\times10^6$ cells/mL) that contribute in the removal of dissolved nutrients from water (Alongi, 1994). In a very recent study from the Sundarbans it has been shown that the bacterial count ranges from 1×10^9 to 4.52×10^{10} cells/L during summer (Manna et al., 2010). Thus heterotrophic bacterial community in the water column may be also responsible for rapid removal of nitrate across our study sites.

At the study area, the increasing concentrations (in relative absorbance) of fucoxanthin corresponded with an increased diatom abundance in the 4th sampling week. Lower peridinin concentrations observed during this study were indicative of and corresponding with low number of dinoflagellates. Despite the inherent environmental variability of the sampling locations pigment profiles did provide division-level phylogenetic evaluation of short-term changes in the phytoplankton compositions, a finding which is in agreement with an earlier study (Tester et al., 1995). The findings from our study [Chl-*a* concentration of 0.08-48.11 mg/cu.m (= 0.08-48.11 μg/L)] can be compared with another study from the north-eastern part of the Sundarbans eco-region (Jharkhali creek) where chlorophyll-a concentration ranged between 5.9 and 43.80 μg/L (Manna et al., 2010).

In this study we have documented succession of natural phytoplankton assemblages in relation with shifts in environmental parameters from the Sundarban waters along a short temporal gradient. We also found that surface water temperature from 1980s to present has undergone changes in this site and we suspect that the succession of diatom communities is largely influenced by change in temperature. Presence of the centric diatom *Triceratium* sp. reported only once before also indicates that marine phytoplankton genera have started appearing in this fragile estuarine ecosystem. In case of dinoflagellates we also found pattern similar to diatoms. The molecular detection of new harmful algal *rbcL* phylotypes indicates increasing prevalence of these organisms in the Indian Sundarbans which can be linked to changing environmental variables in the mangrove environment based on long-term studies. The temperature shift is related to climate change as it is clearly evident from other studies that the eastern sector of Indian Sundarbans is reeling from the effect of sea-level rise and climate change driven factors (UNESCO, 2007; Mitra et al., 2009; George, 2010). Pico-eukaryotes detected as part of this study could be effectively used as sentinel organisms for biogeochemical fluxes under the situation of climate change in future studies focussed on this fragile mangrove ecosystem.

ACKNOWLEDGEMENTS

Authors would like to thank Ranasish Roy Choudhury and Kunal Das Mahapatra for sampling assistance. This work is supported by grants awarded to Punyasloke Bhadury from WWF-India.

REFERENCES

Ajithkumar, T.T., Thangaradjou, T. and Kannan, L. (2006). Physico-chemical and biological properties of the Muthupettai mangrove in Tamil Nadu. *J Mar. Biol. Ass. India*, **48:** 131-138.

Alongi, D.M. (1994). The role of bacteria in nutrient recycling in tropical mangrove and other coastal benthic ecosystems. *Hydrobiologia*, **285:** 19-32.

Anilakumari, K.S., Abdul Aziz, P.K. and Natrajan, P. (2007). Water quality of the Adimalathma estuary, southwest coast of India. *J Mar. Biol. Ass. India*, **49:** 1-6.

Beaugrand, G. and Reid, P.C. (2003). Long-term changes in phytoplankton, zooplankton and salmon related to climate. *Glob. Change Biol.*, **9:** 801-817.

Biswas, H., Dey, M., Ganguly, D., De, T.K., Ghosh, S. and Jana, T.K. (2010). Comparative analysis of phytoplankton composition and abundance over a two-decade period at the land–ocean boundary of a tropical mangrove ecosystem. *Estuar Coast*, **33:** 384-394.

Biswas, H., Mukhopadhyay, S.K., De, T.K., Sen, S. and Jana, T.K. (2004). Biogenic controls on the air-water carbon dioxide exchange in the Sundarban mangrove environment, northeast coast of Bay of Bengal, India. *Limnol. Oceanogr.*, **49:** 95-101.

Chaudhuri, A.B. and Choudhury, A. (1994). Mangroves of the Sunderbans, India. World Conservation Union, Gland.

Danda, A. (2010). Sundarbans: Future imperfect. Climate Adaptation Report, WWF-India.

De, T.K., Ghosh, S.K., Jana, T.K. and Chowdhury, A. (1991). Phytoplankton bloom in the Hooghly estuary. *Indian J. Mar. Sci.*, **20:** 134-137.

Debnath, M., Mandal, N.C. and Ray, S. (2007). Survey of cyanobacterial flora of Sagar Island, West Bengal. *J. Botan. Soc. Beng.*, **61:** 83-89.

Desikachary, T.V. (1987). Atlas of diatoms. Monographs fasicle II, III and IV. Madras Science Foundation, Madras.

Desikachary, T.V. (1959). Cyanophyta. Indian Council of Agricultural Research, New Delhi.

Duarte, P., Macedo, M.F. and Fonseca, L.C. (2006). The relationship between phytoplankton diversity and community function in a coastal lagoon. *Hydrobiologia*, **555:** 3-18.

Finch, M.S., Hydes, D.J., Clayson, C.H., Weigb, B., Dakin, J. and Gwilliam, P. (1998). A low power ultra-violet spectrophotometer for measurement of nitrate in seawater: introduction, calibration and initial seawater trials. *Analytica. Chimica. Acta.*, **377:** 167-177.

George, Nirmala (2010). Disputed isle in Bay of Bengal disappears into sea. Associated Press, via Yahoo News, accessed 24 March 2010.

Godhantaraman N. (2009). Impacts of climate variability and change on marine plankton communities in tropical coastal ecosystems, South India. Paper presented at the symposium on Climate change: Global risks, challenges and decisions. Copenhagen.

Houghton, J.T., Ding, Y., Griggs, D.J. and Nouger, M. (2001). Climate change 2001: The scientific basis. Contribution of working group I to the 3rd assessment report of the Intergovernmental Panel of Climate Change. Cambridge University Press, Cambridge.

JanBen, H. (2007). Climate change in the Oder/Odra estuary region. *In:* Coastal development: The Oder estuary and beyond. G. Schernewski, S. Sek?ci?ska and Thamm (eds). Coastline Reports 8.

Kannan, L. and Vasantha, K. (1992). Micro phytoplankton of the Pichavaram mangroves, southeast coast of India: Species composition and population density. *Hydrobiology*, **247:** 77-86.

Manna, S., Chaudhuri, K., Bhattacharyya, S. and Bhattacharyya, M. (2010). Dynamics of estuarine ecosystem: eutrophication induced threat to mangroves. *Saline Syst.*, **6:** 1-16.

Marinov, I., Doney, S.C. and Lima, I.D. (2010). Response of ocean phytoplankton community structure to climate change over the 21st century: Partitioning the effects of nutrients, temperature and light. *Biogeosciences Discuss*., **7:** 4565-4606.

Mitra, A., Gangopadhyay, A., Dube, A., Schmidt, A.C.K. and Banerjee, K. (2009). Observed changes in water mass properties in the Indian Sundarbans (northwestern Bay of Bengal) during 1980-2007. *Curr. Sci.*, **97:** 1145-1152.

Mitra, A., Srimal, Subita, Das, K.L., Choudhury, A. and Bhattacharyya, D.P. (2000). Copper concentration in water, sediment and haemolymph of horseshoe crab in deltaic Sundarbans, India. *Proc. Zool. Soc. (Calcutta)*, **53:** 84-87.

Moncheva, S., Gotsis-Skretas, O., Pagou, K. and Krastev, A. (2001). Phytoplankton blooms in Black Sea and Mediterranean coastal ecosystems subjected to anthropogenic eutrophication: Similarities and differences. *Est. Coast. Shelf. Sci.*, **53:** 281-295.

Mukherjee, K.N. (1983). Nature and problems of neoreclamation in the Sundarbans. *Indian Journal of Landscape system and Ecological studies*, **6:** 1-19.

Nussler, A.K., Glanemann, M., Schirmeier, A., Liegang, L. and Nussler, N.C. (2006). Fluorometric measurement of nitrite/nitrate by 2,3-diaminonaphthalene. *Nat. Protoc.*, **1:** 2223-2226.

Parsons, T.R., Maita, Y. and Lalli, C.M. (1984). A manual of chemical and biological methods for seawater analysis. Pergamon Press Ltd., Great Britain.

Prabu, V.A., Rajkumar, M. and Perumal, P. (2008). Seasonal variations in physico-chemical characteristics of Pichavaram mangroves, southeast coast of India. *J Environ. Biol.*, **29:** 945-950.

Raven, J., Caldeira, K., Elderfield, H. and Hoeg-Guldberg, O. (2005). Ocean acidification due to increasing atmospheric carbon dioxide. Policy Document 12/05, The Royal Society, London. ISBN 0854036172.

Reid, P., Edwards, M., Hunt, H. and Warner, A. (1998). Phytoplankton change in the North Atlantic. *Nature*, **391:** 546.

Richardson, A.J. and Schoeman, D.S. (2004). Climate impact on plankton ecosystems in the northeast Atlantic. *Science*, **305:** 1609-1612.

Saha, S.B., Bhattacharyya, S.B. and Choudhury, A. (2001). Photosynthetic activity in relation to hydrobiological characteristics of a brackishwater tidal ecosystem of Sundarbans in West Bengal, India. *Trop. Ecol.*, **42:** 111-115.

Samanta, B. and Bhadury, P. (2012). Molecular diversity of phytoplankton assemblages in a mangrove ecosystem (submitted).

Schlesinger, W.H. (2005). Biogeochemistry. Elsevier Science, Amsterdam.

Strickland, J.D.H. and Parsons, T.R. (1972). A practical handbook of seawater analysis. Fisheries Research Board of Canada, Ottawa.

Subrahmanyan, R. (1946). A Systematic account of the marine plankton diatoms of the Madras coast. *Proc. Ind. Acad. Sci.*, **24:** 85-197.

Teixeira, C. and Gaeta, S.A. (1991). Contribution of picoplankton to primary production in estuarine, coastal and equatorial waters of Brazil. *Hydrobiologia*, **209:** 117-122.

Tester, Patricia A., Geesey, Mark E., Guo, Chunzhi Paerl, Hans, Millie W. and David, F. (1995). Evaluating phytoplankton dynamics in the Newport River Estuary. North Carolina, USA by HPLC-derived pigment profiles. *Mar. Ecol. Prog. Ser.*, **124:** 237-245.

Turner, R. Eugene, Qureshi, N., Rabalais, N., Dortch, Q., Justic, D., Shaw, R. and Cope, J. (1998). Fluctuating silicate: Nitrate ratios and coastal plankton food webs. *Proc. Natl. Acad. Sci. U.S.A.*, **95:** 13048-13051.

UNESCO (2007). Case studies of climate change.

CHAPTER

9

Elevated CO_2 and Temperature Affect Leaf Anatomical Characteristics in Coconut (*Cocos nucifera* L.)

Muralikrishna K.S.[1], S. Naresh Kumar[1,2] and V.S. John Sunoj[1]

[1]Plant Physiology and Biochemistry Section
Central Plantation Crops Research Institute, Kasaragod – 675124, India
[2]Division of Environmental Sciences, Indian Agricultural Research Institute
New Delhi – 110012, India
nareshkumar.soora@gmail.com

INTRODUCTION

Climate change impacts on plants are mainly through elevated carbon dioxide [CO_2] and air temperature [T] apart from rainfall variability. Plant responses to external factors include anatomical changes, which are relatively less studied as compared to physiological responses. It is important to study the anatomical changes since they bring about stability to adaptation of plants to external stresses. Leaf structural aspects play major role in acclimatization to the external conditions. Studies showed that most plant species would increase their leaf thickness when exposed to enriched [CO_2]. Studies indicated that elevated CO_2 increased leaf thickness in 81% of the 16 species (Pritchard et al., 1999), increased palisade parenchyma in *Glycine max* and *Castanea sativa* (Roger et al., 1983; Gaudillere and Mousseau, 1989), increased cuticle thickness (North et al., 1995) and reduced stomatal aperture (Morison, 1990; Mansfield et al., 1990), but with a few exceptions (Deng and Donnelly, 1993; Ellsworth et al., 1995).

J. Sundaresan et al. (eds.), *Climate Change and Island and Coastal Vulnerability*,
DOI 10.1007/978-94-007-6016-5_9, © 2013 Capital Publishing Company

The increase in leaf thickness observed in wheat under enriched carbon dioxide was due to larger and additional layer of mesophyll cells, while epidermal characters may remain same (Masle, 2000) or change (Ferris et al., 1996). A 30% thicker cuticle in *Opuntia ficus-indica* cladodes under doubled CO_2 is reported to maintain higher water status (North et al., 1995). Generally, leaf thickness increased in C3 plant species but it decreased in C4 species under enriched [CO_2] conditions. On the other hand, leaf thickness decreased in C3 species and increased in C4 species in elevated air temperature conditions (Mei et al., 2007). Stomatal density and index are treated as indicators of atmospheric CO_2 concentration fluctuation and there exists an inverse relationship between CO_2 concentration and stomatal density (Pal et al., 2005; Chen et al., 2001; Royer, 2001; Woodward, 2002).

Among the plantation crops, coconut plays an important role in providing livelihood security to about a million farmers in India. Coconut palm is a C3 source limited tree and has to face the impact of climate change even during a single generation, since its economic life span is over 50 years (Naresh et al., 2002). Studies are under progress at Central Plantation Crops Research Institute, Kasaragod on quantifying the response of coconut to elevated [CO_2] and temperature using the open top chamber (OTC) facility. Results indicated that elevated CO_2 improved the growth of coconut seedlings in OTCs (Naresh, 2007). The simulation modelling studies using InfoCrop-Coconut (Naresh et al., 2008) projected increase in coconut yields in west coast of India, part of Karnataka and Tamil Nadu due to climate change (Naresh et al., 2008; Naresh et al., 2009). Earlier studies have shown that coconut cultivar WCT and hybrid WCT × COD possessed thick leaves, thicker cuticle, larger sub-stomatal cavity, etc. which contributed towards imparting tolerance to drought conditions (Naresh et al., 2000). Hence it becomes relevant to study the anatomical modifications under elevated [CO_2] and elevated [T] conditions.

Most of the previous studies (Ferris et al., 1996; Engloner et al., 2003), with a few exceptions (Tognetti et al., 2001), concentrated only on two levels of CO_2, i.e. ambient (360 ppm) and double the level of ambient; but it is better to have an intermediate level of CO_2 since increase in atmospheric CO_2 happens gradually. Apart from this, the available literature on influence of elevated CO_2 and temperature on leaf anatomical characters is mostly on annual crops and very limited on perennial species. Keeping these in view, this study was designed to identify the effect of three levels of CO_2 (ambient, 550 and 700 ppm) and elevated air temperature (2°C above the temperature in control chamber) on leaf anatomical characteristics of coconut seedlings.

MATERIALS AND METHODS

Experimental Site and Field Set Up

Seedlings of three coconut cultivars viz., WCT, LCT and COD and two hybrids viz., WCT × COD and COD × WCT were grown in six 4 m^3 OTCs at Central Plantation Crops Research Institute, Kasaragod (12°18' N, 75° E, ~7 m AMSL). Seedlings, raised in poly bags with adequate irrigation and uniform nutrition in the form of vermicompost, were transferred to OTCs after six months. In OTCs, they were exposed separately to (i) elevated [CO_2] at 550 ppm in one OTC, (ii) elevated [CO_2] at 700 ppm in another OTC and (iii) elevated temperature [T] at 2ºC above chamber control in two other OTCs. One set of seedlings was maintained in the fifth and sixth OTCs without any additional treatment to serve as the chamber control. This is done to discount the chamber effects on the growth of seedlings. In each OTC eight seedlings/cultivar were maintained. Apart from these, one more set of seedlings were also maintained under shade net (SN)-with 75% light transmittance to serve as the absolute control. The CO_2 levels were maintained at set level of 550 and 700 ppm with constant supply of commercial CO_2 using the automated CO_2 supply and monitoring SCADA system. Rise of temperature by 2°C above chamber control was realized by using the hot air blowers, which was dynamically controlled by the SCADA system. The temperature, relative humidity and CO_2 levels were monitored at 10 minutes interval. Seedlings were maintained for more than four years in these conditions. Several anatomical parameters were studied in the leaflet samples drawn from the third frond (leaf) from top.

Stomata Structural Analysis

For taking stomatal prints, clear transparent nail varnish was applied at about 10 AM on a clear sky day on the abaxial surface of the middle portion of middle leaflets of the third frond from top. Dried peel was removed using forceps and then mounted on glass slide. For each cultivar prints were taken from six seedlings. At least ten digital images from each slide were captured using Leitz Diaplan (Germany) microscope connected with camera, which in turn was connected to a computer. Images were captured at 25× resolution and were analyzed for area of stomatal aperture and guard cells using Leica Q win software (Leica, Germany). Images were also analyzed for density of epidermal cells (*ED*) and for stomatal density (*SD*). From *ED* and *SD* the area-independent stomatal index (Salisbury, 1927) (SI) was calculated using the formula: SI (%) = $((SD) / (SD+ED)) \times 100$.

Leaf Anatomy

The leaf segments (4 cm length) from middle portion of middle leaflets of the third frond from top were sampled at about 10 AM on a clear sky day. They were immediately fixed in Carnoys fixative (chloroform:alcohol:glacial acetic acid mixture in 30:60:10 ratio) for 48 hours. Specimen was dehydrated through series of alcohol grades and butanol mixtures by keeping 24 hrs in each grade. Samples were infiltrated with molten paraffin wax at 62°C for 48 hrs. The infiltrated samples were embedded in wax and 10 μ thick sections were taken on Leica RM 2145 rotary microtome using Leica disposable blades. Sections were adhered to glass microscopic slide using 3% gelatin solution and then were air dried. Slides were stained with 0.5% aqueous safranin for two minutes and then mounted with DPX mountent. Stained sections were observed under light microscope (Leitz Diaplan, Germany) connected with a Leica camera. At least ten digital images were captured for each section in 25× and observations were recorded on several anatomical features using Leica Q win (Leica, Germany) image processing software.

All data were analysed for testing statistical significance by following the ANOVA (RBD) in (SPSS v10) package. Critical difference (CD at 5% level) values were calculated for main and interactional effects (treatments and cultivars) for all parameters.

RESULTS AND DISCUSSION

Seedlings were grown for over four years in the open top chambers provided with elevated [CO_2] at 550 and 700 ppm and elevated [T] (+2 ^{o}C above chamber control). Hence they were fully acclimatized to the changed environment and also shown responses to the treatments. One leaf emerges out at almost monthly interval, the canopy of seedlings at the time of sampling has initiated, emerged and grown in the changed environment. Seedlings were also fully acclimatized to the environment in which they were growing. In order to discount the chamber effects, results were compared with seedlings growing in control chamber, where no additional CO_2 or temperature is provided. Hence the differences noted in anatomical features can be attributed mainly due to the individual effects of elevated [CO_2] and elevated [T].

Stomatal Characteristics under Elevated CO_2 and Temperature

Stomata, which play key role in leaf physiology, are found to be sensitive to increased CO_2 concentrations and temperature. Stomata aperture area declined under elevated [CO_2] 550 and 700 ppm and [T] conditions. This decrease was linear with increasing levels of CO_2 inspite of cultivar differences (Table 9.1, Fig. 9.1). Under both the elevated [CO_2] treatments maximum reduction in stomatal aperture area was found in the leaves of WCT cultivar, where the decrease was to the tune of about 70% as compared to that of seedlings grown in control OTC. Reduction in stomatal aperture area in elevated [CO_2] conditions was also observed in several crops such as wheat (Masle, 2000) and *Vicia* (Frechilla et al., 2003). Despite of reduction in stomata size, photosynthetic rate (Pn) under elevated [CO_2] increased (Naresh et al., 2007; Muralikrishna et al., 2009). Elevated [T] reduced the stomata aperture area by about 18% as compared to that in control seedlings (Fig. 9.1). Such stomatal response to elevated [CO_2] and temperature may be attributed to the plant efforts to maintain optimal leaf moisture potentials by regulating the gas exchange particularly that of water vapour.

Table 9.1: ANOVA for area of leaf stomata and the change in area of leaf stomata (Δ percent change from the chamber control) of coconut seedlings of three cultivars and two hybrids grown in elevated [CO_2] 550 and 700 ppm and temperature (+2°C over control OTC) conditions

Treatments/ cultivars	*Area of leaf stomata*					
	Elevated temperature [T] (+2°C)		*Elevated carbon dioxide [CO_2]*			
			550 ppm		*700 ppm*	
	Change	D%	*Change*	D%	*Change*	D%
WCT	*	-40.8	*	-71.7	*	-73.0
LCT	NS	8.51	NS	-6.71	*	-52.5
COD	*	-57.3	*	-27.0	*	-54.8
WCT × COD	*	-23.1	*	-16.0	*	-43.7
COD × WCT	*	20.9	*	-50.0	*	-39.7
Mean		-18.3		-34.2		-52.7

*Significant at $P < 0.05$, NS: Non significant

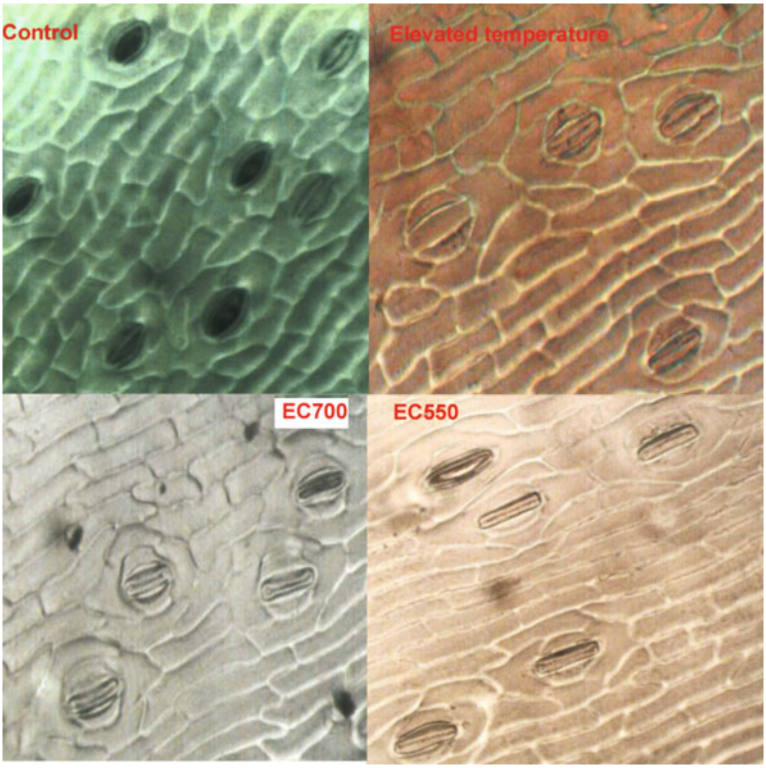

Fig. 9.1: Epidermal impression showing the stomatal response of coconut leaf to elevated [CO_2] 550 and 700 and temperature (+2°C over control OTC) conditions.

Elevated CO_2 and [T] caused significant reduction in guard cells area (Fig. 9.2). Decrease was more in WCT and WCT × COD in [CO_2] 550 and 700 ppm, respectively compared to other cultivars. Overall reduction to the tune of 15% in guard cell area was observed in seedlings grown under elevated [T] as compared to that in control seedlings. However, COD cultivar was more sensitive with 32% reduction. This type of response was also reported in *Lolium perenne* L. as a consequence of elevated [CO_2] (Ferris et al., 1996). Total area of stomatal complex including subsidiary cells has reduced in elevated [CO_2] and [T] treatments (Fig. 9.2). Similar response of stomata complex at elevated CO_2 and temperature were reported in oak trees (Miglietta and Raschi, 1993). Even though elevated [CO_2] had no significant effect on stomatal index (SI), indicating its stability under elevated [CO_2] conditions; however the SI decreased under elevated [T], particularly in LCT and WCT × COD where more than 20% reduction was observed (Fig. 9.3). Our results indicate that elevated temperature causes change in spacing of stomata and in turn influence the stomata index as also was reported in perennial rye grass (Ferris et al., 1996). However, in some cultivars such as WCT, COD and COD × WCT, the SI was relatively stable even under elevated [T] conditions.

Effect of Elevated CO_2 and Temperature on Leaf Anatomy

Coconut leaf thickness increased in elevated [CO_2] conditions (Table 9.2). Cultivars like WCT and COD, and their hybrid COD × WCT were more responsive to elevated [CO_2] as far as increase in leaflet thickness is concerned. Since leaf thickness is an indicator of higher assimilation of photosynthates,

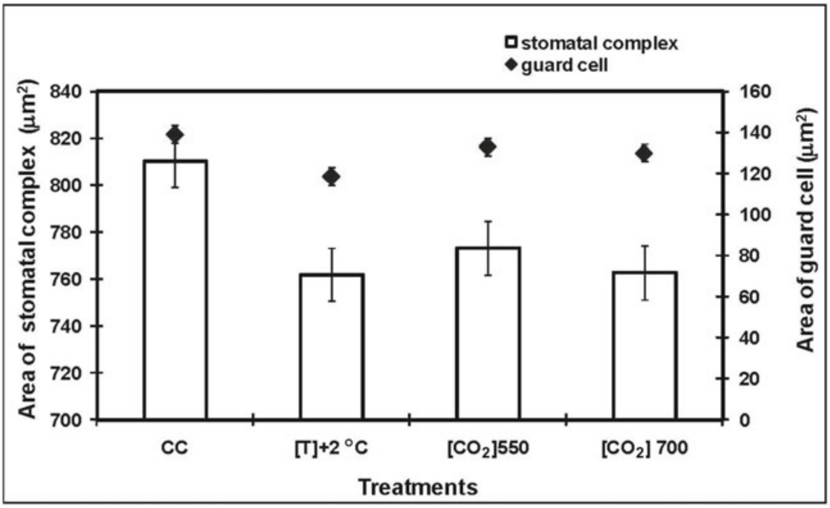

Fig. 9.2: Total area of stomatal complex and guard cell in leaf of coconut seedlings of three cultivars and two hybrids grown in elevated [CO_2] 550 and 700 ppm and temperature (+2°C over control OTC) conditions.

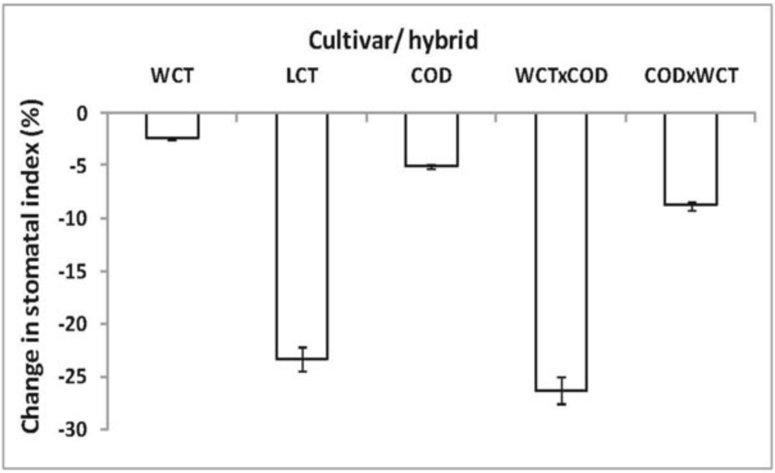

Fig. 9.3: Change (% change from chamber control) in stomatal index (SI) in leaf of coconut seedlings of three cultivars and two hybrids grown in elevated temperature (+2°C over control OTC) conditions.

Table 9.2: Change in the leaflet thickness of five cultivars of coconut seedlings of three cultivars and two hybrids grown in elevated [CO_2] 550 and 700 ppm and temperature (+2°C over control OTC) conditions

Cultivars/hybrids	*Thickness of leaflet (µm)*				
	Open top chamber treatments				
	Shade net (SN)	*Chamber control (CC)*	*Elevated temperature [T] (+2°C)*	*Elevated [CO_2] 550 ppm*	*Elevated [CO_2] 700 ppm*
WCT	170.8	141.8	137.1	172.1	152.9
LCT	172.7	180.9	139.6	177.5	209.6
COD	175.5	139.6	130.4	186.6	142.7
WCT × COD	169.5	180.2	155.5	179.8	160.2
COD × WCT	201.0	96.5	146.8	153.3	162.3
Mean	177.9	147.8	141.9	173.9	165.58
CD at 5%					
Cultivar (C)	1.10*				
Treatment (T)	1.10*				
C × T	5.48*				
S.E/Plot	0.96				
C.V. (%)	6.12				

*Significance at P <0.05, NS: Non significant

thicker leaflets under elevated [CO_2] indicated increased CO_2 fixation in all cultivars used in this study. On the other hand elevated [T] caused reduction in leaf thickness (Table 9.2) and maximum reduction (22%) was recorded in

LCT cultivar. These responses are typical to C3 plants as also reported earlier (Zhu et al., 1997; Mei et al., 2007). Overall, the seedlings grown under shade net had thicker leaves as compared to those grown in OTCs, indicating the influence of chamber on seedling growth. However, seedlings grown in elevated [CO_2] conditions had leaflet thickness similar to that of those grown under shade net.

Cuticle plays important role in maintaining the leaf water balance and thicker cuticle is reported to impart drought tolerance in coconut (Naresh et al., 2000). Elevated [CO_2] and [T] had significant impact on cuticle deposition on leaf surfaces (Table 9.3). Thickness of upper cuticle significantly increased in elevated [CO_2] and [T] conditions. Under elevated [CO_2] conditions, increase in thickness of upper cuticle was more in hybrids than in cultivars, whereas in elevated [T] conditions, increase was more in cultivars. As far as lower cuticle thickness is concerned, elevated [T] did not significantly influence it. But elevated [CO_2] increased the thickness of lower cuticle marginally in cultivars and significantly in hybrids. Cultivars/hybrids like WCT, WCT × COD were reported to possess several anatomical adaptations making them tolerant to drought situations. Thicker cuticle deposited over leaf surfaces reduce water loss and assist in retaining normal physiological activities in coconut (Naresh et al., 2000).

Leaf upper and lower epidermal cells were thicker under elevated [CO_2] conditions though the response was inconsistent across the cultivars. The influence was significant in COD and hybrids, indicating the positive impact of [CO_2] on epidermal cell expansion as also reported earlier in perennial grass species (Ferris et al., 1996). On the other hand elevated [T] did not have significant effect on upper epidermal cell thickness but 26% wider and 12% thicker lignin walled metaxylem vessels are formed in hybrids seedlings grown in elevated [T] conditions as compared to those grown in chamber control. Response of cultivars for this parameter was also not consistent. On the other hand, elevated [CO_2] caused increase in the metaxylem diameter in all cultivars and hybrids except in LCT. Increase in vessel diameter was found to be more in hybrids than in cultivars (Table 9.3). Such increasing tendency in vessel diameter was observed with stem metaxylem in some tree species (Gartner et al., 2003). Overall response of xylem vessels can contribute to the maintenance of optimal water potentials.

Elevated [CO_2] and [T] reduced the area of stomatal aperture, stomatal complex and guard cells. Elevated temperature significantly reduced stomatal index and leaflet thickness (Table 9.4). On the other hand, leaflets were thicker under elevated [CO_2] conditions. Leaf xylem vessels were wider and thicker in seedlings grown in elevated [T] compared to that in chamber control. The upper and lower cuticles were thickened under elevated [CO_2] treatments which may assist seedlings to reduce non-stomatal loss of water thereby improving leaf water status. There existed cultivar variations as well. Results indicate that coconut seedlings are able to adapt to climate change through anatomical adjustment as well.

Table 9.3: Change (Δ percent change from the chamber control) in thickness of cuticle (upper and lower) and upper epidermis, and diameter of metaxylem lumen of leaf of coconut seedlings of three cultivars and two hybrids grown in elevated [CO_2] 550 and 700 ppm and temperature (+2ºC over control OTC) conditions

Parameters/	*Upper cuticle thickness (D%)*			*Lower cuticle thickness (D %)*			*Upper epidermis thickness (D %)*			*Leaf metaxylem lumen diameter (D %)*		
	[T]+2ºC	*[CO_2]*		*[T]+2ºC*	*[CO_2]*		*[T]+2ºC*	*[CO_2]*		*[T]+2ºC*	*[CO_2]*	
Treatments/Cultivars		*550 ppm*	*700 ppm*		*550 ppm*	*700 ppm*		*550 ppm*	*700 ppm*		*550 ppm*	*700 ppm*
WCT	44.8*	27.0*	23.9*	NS	-10.0*	8.3*	NS	NS	NS	NS	12.5*	12.0*
LCT	18.7*	28.7*	23.2*	NS	NS	17.6*	-16.6*	-11.4*	-11.3*	NS	-25.8*	-10.3*
COD	35.9*	49.7*	18.3*	NS	-19.7*	-8.4*	NS	45.7*	29.8*	-18.4*	44.2*	-27.5*
WCT × COD	19.9*	52.5*	22.3*	NS	71.1*	26.0*	NS	17.1*	23.5*	77.7*	45.0*	42.7*
COD × WCT	NS	75.1*	45.1*	27.0*	42.6*	42.3*	10.7*	78.7*	39.4*	74.0*	38.6*	59.0*
CD at 5%												
Cultivar (C)		0.04*			0.04*			0.10*			0.46*	
Treatment (T)		0.04*			0.04*			0.10*			0.46*	
C × T		0.20*			0.21*			0.48*			2.32*	
S.E/Plot		0.10			0.10			0.24			1.15	
C.V. (%)		12.69			15.06			15.20			8.22	

*Significance at $P < 0.05$, NS: Non significant

Table 9.4: Influence of elevated temperature and CO_2 on leaflet anatomical parameters of coconut seedlings

Parameter	*Shade net*	*Chamber control*	*Elevated temperature (+2°C)*	*Elevated [CO_2] 550 ppm*	*Elevated [CO_2] 700 ppm*	*C.V (%)*	*CD at 5%*
Leaf stomata aperture area (μm^2)	41.6	37.7	31.5	23.5	17.8	18.5	0.63
Stomata index (%)	10.2	9.8	8.5	9.4	9.8	8.1	0.09
Leaflet thickness (μm)	178.0	147.9	141.9	173.9	165.6	6.1	1.10
Hypodermis cell length (μm)	17.9	15.0	16.1	17.3	17.0	18.7	1.73
Leaf lower cuticle thickness (μm)	2.9	2.2	2.3	2.6	2.6	15.1	0.04
Leaf upper cuticle thickness (μm)	3.4	2.2	2.8	3.3	2.8	12.7	0.04
Leaf lower epidermis cell thickness (μm)	5.8	5.0	5.1	5.4	5.1	13.3	0.08
Leaf upper epidermis cell thickness (μm)	6.2	5.2	5.3	6.3	5.9	15.2	0.10
Leaf metaxylem vessel lignification (μm)	1.9	1.6	1.7	1.7	1.6	15.1	0.03
Leaf metaxylem vessel diameter (μm)	32.1	26.5	31.0	30.2	28.8	8.2	0.46

Mean values of five cultivars. Each datum is a mean of 100 observations.

Present study infers that the coconut seedlings respond to elevated [CO_2] and temperature by adjusting stomatal aperture and modifying leaf anatomy as well. However, there exists differential response of cultivars and hybrids to these external factors. The anatomical modifications in seedlings indicate the ability of coconut for long-term adaption to climate change.

ACKNOWLEDGEMENTS

Authors are grateful to Director CPCRI for his constant support and providing the facilities. This work is funded by ICAR National Network Project on 'Impact, Adaptation and Vulnerability of Indian Agriculture to Climate Change'.

REFERENCES

Chen, L., Li, C., Chaloner, W.G., Beerling, D.J., Sun, Q., Collinson, M.E. and Mitchell, P.L. (2001). Assessing the potential for the stomatal characters of extant and fossil *ginkgo* leaves to signal atmospheric CO_2 change. *Am. J. Bot*., **88:** 1309-1315.

Deng, R. and Donnelly, J. (1993). In vitro hardening of red raspberry through CO_2 enrichment and relative humidity reduction on sugar-free medium. *Can. J. Plant Sci*., **73:** 1108-1115.

Ellsworth, D.S., Oren, R., Huang, C., Phillips, N. and Hendrey, G.R. (1995). Leaf and canopy responses to elevated CO_2 in a pine forest under free-air CO_2 enrichment. *Oecologia*, **104:** 139-146.

Engloner, A.I., Kovacs, D., Balogh, J. and Tuba, Z. (2003). Anatomical and ecophysiological changes in leaves of couch grass (*Elymus repens* L.), a temperate loess grassland species, after 7 years grown under elevated CO_2 concentration. *Photosynthetica*, **41:** 185-189.

Ferris, R., Nijs, I., Behaeghe, T. and Impens, I. (1996). Elevated CO_2 and temperature have different effects on leaf anatomy of perennial ryegrass in spring and summer. *Ann. Bot*., **78:** 489-497.

Frechilla, S., Talbott, L.D. and Zeiger, E. (2003). The CO_2 response of *Vicia* guard cells acclimate to growth environment. *J. Exp. Bot*., **53:** 545-550.

Gartner, B.L., Roy, J. and Huc, R. (2003). Effects of tension wood on specific conductivity and vulnerability to embolism of *Quercus ilex* seedlings grown at two atmospheric CO_2 concentrations. *Tree Physiol*., **23:** 387-395.

Gaudillere, J.P. and Mousseau, M. (1989). Short-term effect of CO_2 enrichment on leaf development and gas exchange of young poplars *(Populus euramericana* cv1 214). *Oecolog. Plantar*., **10:** 95-105.

Mansfield, T.A., Hetherington, A.M. and Atkinson, C.J. (1990). Some current aspects of stomatal physiology. *Annu. Rev. Plant Phys*., **41:** 55-75.

Masle, J. (2000). The Effects of Elevated CO_2 Concentrations on cell division rates, growth patterns, and blade anatomy in young wheat plants are modulated by factors related to leaf position, vernalization and genotype. *Plant Physiol*., **122:** 1399-1415.

Mei, H., Chengjun, J.I., Wenyun, Z. and Jinsheng, H.E. (2007). Interactive effects of elevated CO_2 and temperature on the anatomical characteristics of leaves in eleven species. *Front. Biol. China.*, **2(3):** 333-339.

Miglietta, F. and Raschi, A. (1993). Studying the effect of elevated CO_2 in the open in a naturally enriched environment in central Italy. *Plant Ecol.*, **104:** 391-400.

Morison, J.I.L. (1987). Intercellular CO_2 concentration and stomatal response to CO_2. *In:* Zeiger, E., Cowan, I.R., Farquhar, G.D. (eds), Stomatal function. Stanford University Press.

Muralikrishna, K.S., Naresh Kumar, S., John Sunoj, V.S. and Kasturi Bai, K.V. (2009). Elevated carbon dioxide and temperature reduce stomatal density in coconut (*Cocos nucifera* L.). *In:* Proceedings of National workshop on climate and development. Kerala Agricultural University.

Naresh Kumar, S. and Aggarwal, P.K. (2009). Impact of climate change on coconut plantations. *In:* Climate Change and Indian Agriculture. P.K. Aggarwal (ed.). ICAR Publication, New Delhi.

Naresh Kumar, S. (2007). Climate change effects on growth and productivity of plantation crops with special reference to coconut and black pepper: Impact, adaptation and vulnerability and mitigation strategies. Final Report on ICAR Network Project on Impact of Climate Change on Indian Agriculture.

Naresh Kumar, S. (2008b). Global warming to raise coconut yield on India's west coast: Study:http://www.livemint.com/2008/06/13003015/Global-warming-to-raise-coconut.html.

Naresh Kumar, S., Kasturi Bai, K.V., Rajagopal, V. and Aggarwal, P.K. (2008a). Simulating coconut growth, development and yield using InfoCrop-coconut model. *Tree Physiol.*, **28:** 1049-1058.

Naresh Kumar, S., Rajagopal, V. and Karun, A. (2000). Leaflet anatomical adaptations in coconut cultivars for draught tolerance. *In:* Recent advance in plantation crops research. N. Muralidharan and R. Raj Kumar (eds).

Naresh Kumar, S., Rajagopal, V., Laxman, R.H., Dhanapal, R. and Maheswarappa, H.P. (2002). Photosynthetic characters and water relation in coconut palm under drip irrigation levels. *In:* Plantation crops research and development in the new millenium. Proc. PLACROSYM XIV. P. Rathinam, H.H., Khan, V.M., Reddy, P.K. Mandal and K. Suresh (eds). Coconut Development Board, Kochi (Kerala), India.

North, G.B., Moore, T.L. and Nobel, P.S. (1995). Cladode development for *Opuntia-ficus-indica* (Cactaceae) under current and doubled CO_2 concentrations. *Am. J. Bot.*, **82(2):** 159-166.

Pal, M., Rao, L.S., Jain, V., Srivastava, A.C., Pandey, R., Raj, A. and Singh, K.P. (2005). Effects of elevated CO_2 and nitrogen on wheat growth and photosynthesis. *Biolo. Plantarum*, **49(3):** 467-470.

Pritchard, S.T., Rogers, H.H., Prior, S.A. and Peterson, C.M. (1999). Elevated CO_2 and plant structure: A review. *Global Change Biol.*, **5:** 807-837.

Roger, H.H., Thomas, J.F. and Bingham G.E. (1983). Response of agronomic and forest species to elevated atmospheric carbon dioxide, *Science*, **220:** 428-429.

Royer, D.L. (2001). Stomatal density and stomatal index as indicators of paleoatmospheric CO_2 concentration. *Rev. Palaeobot. Palyno.*, **114:** 1-28.

Salisbury, E.J. (1927). On the causes and ecological significance of stomatal frequency, with special reference to the woodland flora. *Philos. Trans. Roy. Soc.* (London), **B216:** 1-65.

Tognetti, R., Sebastiani, L., Vitagliano, C., Raschi, A. and Minnocci, A. (2001). Responses of two olive tree (*Olea europaea* L.) cultivars to elevated CO_2 concentration in the field. *Photosynthetica*, **39:** 403-410.

Woodward, F.I. (2002). Potential impacts of global elevated CO_2 concentration on plants. *Plant Biol.*, **5:** 207-211.

Zhu, J., Bartholomew, D.P. and Goldstein, G. (1997). Effect of elevated carbon dioxide on the growth and physiological responses of pineapple, a species with crassulacean acid metabolism. *J. Ame. Soc. Horti. Sci.*, **122(2):** 233-237.

CHAPTER

10

Biochemical Composition of Seaweeds after the Influence of Oil Spill from 'Tasman Spirit' at the Coast of Karachi

Qaisar Abbas, Rashida Qari and Fozia Khan

Institute of Marine Sciences, University of Karachi
Karachi – 75270, Pakistan
rqari2002@yahoo.com

INTRODUCTION

In Pakistan first ever major oil spill hit the Karachi coast on 27th July 2003 when a twenty-four years old Greek oil tanker "Tasman Spirit" ran aground near the Karachi harbour. It was carrying more than 67,532 tons of crude oil. The spill caused major disaster after the ship broke into two pieces on 14th August 2003. It has affected 14 km long Clifton beach including whole sea view area and Shireen Jinnah colony. Referring to the figures published in newspapers that have been given by the officials from time to time about 20,000-30,000 tons of oil, out of a total 67,532 tons, leaked from the grounded Greek tanker Tasman Spirit and spread all along the Clifton beach (*Daily Dawn*, 29th July- 2nd September 2003; *Daily Jang*, 29th July- 24th August 2003). Later oil has started to drift in some directions and as a result some traces of it reached other coastal areas of Karachi like Sandspit and Manora. From this mishap the situation became highly dangerous for marine life. The beach was covered with thick black crude oil for a few weeks littered with carcasses of a large variety of dead marine organisms. These included benthic, planktonic and nektonic individuals, which most probably died of suffocation as their entire bodies were covered with a thick coating of oil. A thin film of

J. Sundaresan et al. (eds.), *Climate Change and Island and Coastal Vulnerability*,
DOI 10.1007/978-94-007-6016-5_10,

oil also covered the surface of the seawater adjacent to the affected area (Saifullah and Chaghtai, 2005).

Marine algae constitute the basic link in marine food chain. Bryan and Hummerstone (1973) and Melhus et al. (1978) reported that marine algal or seaweeds species have been suggested to be the indicators of pollution. Beside this, several marine algal species are being considered as raw material for various economically important products and this has resulted in their increasing demand. A number of studies have been made on the biochemical composition of seaweed from Karachi coast (Qasim, 1981; Shameel, 1987; Qari, 1988; Qari and Qasim, 1993; Qari and Siddiqui, 1993; Hayee-Memon and Shameel, 1999).

Biochemical constituents of seaweeds such as ash, protein, lipid, carbohydrates, crude fibre and amino acid, etc. have been extensively investigated in various parts of the world like Sunderban, India (Chakraborty and Santra, 2008), Vellar estuary, Parangipettai coast (Shanmugam and Palpandi, 2008), China (Dawczynski et al., 2007) and Japan sea of Toyama, Japan (Hossain et al., 2003). Sumitra-Vijaya Raghavan et al. (1980) studied some seaweed from Goa coast, India. Dhargalkur (1986) studied the biochemical composition in *Ulva reticulata* from Chapora Bay, Goa and Dhargalkur et al. (1980) worked on the forty-three species of red, brown and green seaweeds along the Maharashtra coast, India.

Large quantities of seaweed are washed ashore along the Karachi coast (Anand, 1940; Anand, 1943; Saleem, 1965; Saifullah, 1973; Qari and Qasim, 1988; Qari and Qasim, 1994; Shameel and Tanaka, 1992). Recently Qari (2002) has also reported seasonal variation in biomass and distribution of seventy-five algal species and their chemical composition from Karachi coast. Data on the biochemical composition of seaweeds in Karachi coast after the oil spill by Tasman Spirit is not available. The present study is based on post Tasman Spirit spill incidence and will provide the information regarding the impact of oil on the biochemical constituents (protein, lipid, carbohydrates, crude fibre, ash, moisture and water) of seaweeds along the Karachi coast. The present study deals with the detail survey of seaweeds along the beaches (Clifton, Korangi Creek, Buleji, Sandspit and Manora) of the Karachi because many adverse effects of oil spills were expected in these areas.

MATERIALS AND METHODS

Karachi is the largest city of Pakistan located between longitude 66°59′E and at latitude 24°48′N at the North Eastern border of the Arabian Sea. Clifton is most approachable picnic beach of Karachi near Keamari oil terminal. The largest number of animals and plants were present in the intertidal zone at Clifton during the winter season. Korangi Creek is situated in the south of Karachi. It is covered by muddy creeks. This creek receives effluents from domestic, industrial and oil refinery. Its domestic wastes come from adjoining fishing villages (Waguder, Ibrahim Haydri, and township of Korangi). Malir River is another source of domestic and industrial wastes to Creek area. This area receives discharges from Pakistan Refinery, soda ash factory and National Refinery as well as Karachi Electric Supply Corporation Power Plant etc. Manora is rocky-cum-sandy shore. This island is divided into three sections: the South-East and North-West sections are mostly rocky (rocks, boulders, stones etc.) with patches of sand, the middle section is a sandy beach and the south-east side of the Island is steep. Sandspit is 20 km away from centre of Karachi, which forms the westernmost part of the Indus Delta mangrove ecosystem. It offers a rare example where two entirely different habitats occur very close to each other separated by a very narrow sandy bar. The rocky Buleji coast is located near the fishermen's villages between Hawkes Bay and Paradise Point covering a distance of about 800 metre. This is a triangular rocky platform of a wave-beaten shore with slightly uneven profile and protruding out in the open Arabian Sea.

Both the attached and drifted seaweeds were sampled from 2004 to 2005 on different dates to cover all the seasons at five different affected sites of Karachi coast i.e., Clifton, Korangi Creek, Sandspit, Buleji and Manora at low tide (Fig. 10.1). The sampling method (Chapman, 1964) was used and quadrates of 1 m^{-2} sizes were randomly selected in the intertidal zone of each beach. All the seaweeds species were handpicked in each quadrate. In the laboratory, seaweeds were carefully cleaned from mud debris and other epiphytes with filtered seawater followed by fresh water. The specimen were identified with the help of authentic available literature viz. Anand (1940 and 1943), Smith (1955), Round (1973), Morris (1976) and Shameel (2001).

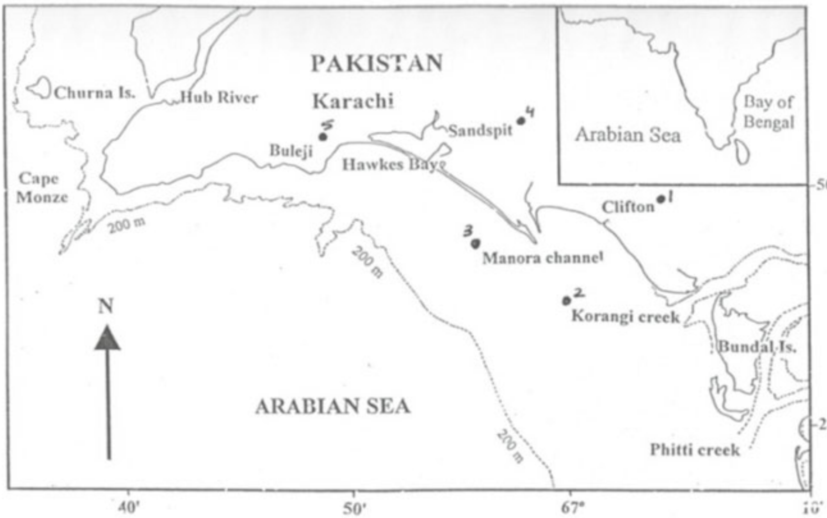

Fig. 10.1: Map showing sampling beaches: 1. Clifton, 2. Korangi Creek, 3. Manora, 4. Sandspit and 5. Buleji.

The herbarium specimens have been placed in herbarium of Institute of Marine Science, University of Karachi. Washed seaweeds were dried in an oven at 70 °C and then grinded and stored in plastic containers at room temperature for biochemical studies. The protein in seaweeds was determined by Micro-Kjeldahl method after acid hydrolysis (Hawk et al., 1954). The total lipid was extracted by soxhelt extraction method (Folch et al., 1957). The crude fibre, ash and moisture was determined by the standard method of Association Official Analytical Chemists (A.O.A.C.) (1990). Total carbohydrates were calculated by subtracting the protein, lipid, crude fibre, ash and moisture from 100 (Dare and Edwards, 1975). The results are expressed in percentage. The results obtained in the present study were compared with results reported in various literatures in the past for the study area.

RESULTS AND DISCUSSION

The total 20 species of seaweeds (six green, eight brown and six red) were collected from five affected beaches viz., Clifton, Korangi Creek, Manora, Sandspit and Buleji. Biochemical parameters estimated were protein, lipid, carbohydrates, crude fibre, ash, moisture and water content. The values of each parameter are the mean of three observations expressed as gram percentage dry weight. The data present in Tables 10.1-10.5 show the mean concentration with standard deviation of each parameter (protein, lipid, carbohydrates, crude fibre, ash, moisture and water) in all species of seaweed samples that were collected from all five beaches (Clifton, Korangi Creek, Manora, Sandspit and Buleji) of Karachi coast.

The range of biochemical constituents in green seaweeds were: protein 7.98-16.2%, lipid 4.47-14.77%, carbohydrates 29.05-50.30%, crude fibre 2.55-11.42% and ash 21.55-32.5%. In brown seaweeds the constituents were protein 6.96-12.49%, lipid 3.9-9.33%, carbohydrates 29.9-54.81%, crude fibre 3.05-15.9% and ash 23.75-36.5% whereas in red seaweeds protein 6.92-15.23%, lipid 3.4-14.13%, carbohydrates 27.13-46.3%, crude fibre 2.6-5.85% and ash 23.2-38.9%.

The mean values of protein, lipid, carbohydrates, crude fibre, ash and moisture content varied among different species of seaweed. The highest percentage for different parameters were observed for Clifton: carbohydrates (42.68%) in *Enteromorpha compressa*; ash (28.32%) in *Ulva fasciata*; lipid (10.17%) in *Enteromorpha compressa*; protein (9.65%) in *Ulva fasciata* and crude fibre (4.24%) in *Ulva fasciata*. In Korangi Creek highest percentage of carbohydrates (43.98%) in *Enteromorpha compressa*; ash (30.33%) in *Ulva fasciata*; protein (9.59%) in *Ulva fasciata*; lipid (7.98%) in *Ulva fasciata*; and crude fibre (5.05%) in *Ulva fasciata* were found. In Manora the highest percentage of carbohydrates (44.54%) in *Bryopsis harveyana*; ash (38%) in *Codium iyengarii*; protein (15.23%) in *Botryocladia leptopoda*; lipid (14.76%) in *Caulerpa racemosa*; and crude fibre (11.42%) in *Caulerpa taxifolia* were

Table 10.1: Mean with standard deviation of biochemical constituents (%) of seaweeds at Clifton beach

Species	*Protein*		*Lipid*		*Carbohydrates*		*Crude fibre*		*Ash*		*Moisture*		*Water*	
	Mean	*Sd*	*Mean*	*Sd*	*Mean*	*Sd*	*Mean*	*Sd*	*Mean*	*Sd*	*Mean*	*Sd*	*Mean*	*Sd*
Enteromorpha compressa	8.66	0.002	11.00	0.001	42.68	0.001	2.55	0.001	25.55	0.003	9.56	0.001	58.5	0.001
Ulva fasciata	9.65	0.51	10.18	2.69	34.94	5.30	4.24	0.99	28.33	5.34	12.67	0.89	62.22	2.06

Table 10.2: Mean with standard deviation of biochemical constituents (%) of seaweeds at Korangi Creek

Species	*Protein*		*Lipid*		*Carbohydrates*		*Crude fibre*		*Ash*		*Moisture*		*Water*	
	Mean	*Sd*	*Mean*	*Sd*	*Mean*	*Sd*	*Mean*	*Sd*	*Mean*	*Sd*	*Mean*	*Sd*	*Mean*	*Sd*
Enteromorpha compressa	8.67	0.001	6.55	0.001	43.98	0.001	5.00	0.003	26.5	0.003	9.30	0.001	68.44	0.002
Ulva fasciata	9.59	0.50	7.97	0.69	35.11	4.08	5.05	0.039	30.33	3.29	11.95	0.49	67.95	10.94

Table 10.3: Mean with standard deviation of biochemical constituents (%) of seaweeds at Manora beach

Species	*Protein*		*Lipid*		*Carbohydrates*		*Crude fibre*		*Ash*		*Moisture*		*Water*	
	Mean	*Sd*	*Mean*	*Sd*	*Mean*	*Sd*	*Mean*	*Sd*	*Mean*	*Sd*	*Mean*	*Sd*	*Mean*	*Sd*
Bryopsis harveyana	16.2	0.99	5.82	0.59	44.54	4.02	3.86	0.39	21.55	3.04	8.045	0.21	54.86	3.49
Caulerpa racemosa	11.7	0.99	14.78	1.49	33.54	2.39	4.87	0.39	24.45	2.05	9.66	0.22	66.97	5.0
Caulerpa taxifolia	12.33	0.59	6.88	0.89	37.38	3.12	11.42	1.99	26.62	2.62	5.37	0.79	73.99	19.29
Codium iyengarii	7.98	0.19	7.43	1.09	33.85	2.59	4.77	1.52	38.00	2.69	7.96	0.39	76.72	14.42
Enteromorpha compressa	11.44	0.001	10.67	0.001	41.52	0.002	4.00	0.001	23.87	0.002	8.50	0.002	66.50	0.003
Ulva fasciata	11.00	0.001	9.50	0.003	29.05	0.001	4.55	0.004	32.5	0.001	12.5	0.001	68.50	0.001
Cystoseira indica	12.24	0.91	9.33	3.32	30.47	0.94	7.08	1.39	33.47	1.40	7.40	0.29	71.64	7.24
Padina pavonica	7.07	0.49	7.22	0.31	43.01	6.10	4.88	3.0	33.65	1.62	4.18	0.69	84.38	4.41
P. tetrastromatica	9.30	0.33	7.13	0.80	34.78	0.49	5.54	0.44	31.72	0.89	11.53	0.61	58.49	8.39
Sargassum boveanum	8.86	0.30	5.95	1.13	32.45	2.29	7.65	0.79	35.13	1.99	9.95	0.91	59.94	4.63
Spatoglossum variabile	6.96	0.004	3.90	0.001	54.81	0.001	4.35	0.002	22.2	0.006	7.78	0.001	64.75	0.001
Stoechospermum marginatum	8.83	0.33	7.38	0.69	42.28	4.29	3.91	0.81	27.3	3.89	9.90	0.52	65.48	15.39
Botryocladia leptopoda	15.23	0.001	4.87	0.004	43.7	0.004	5.8	0.001	23.2	0.001	7.20	0.004	59.16	0.002

Table 10.4: Mean with standard deviation of biochemical constituents (%) of seaweeds at Sandspit beach

Species	*Protein*		*Lipid*		*Carbohydrates*		*Crude fibre*		*Ash*		*Moisture*		*Water*	
	Mean	*Sd*	*Mean*	*Sd*	*Mean*	*Sd*	*Mean*	*Sd*	*Mean*	*Sd*	*Mean*	*Sd*	*Mean*	*Sd*
Enteromorpha compressa	9.31	0.70	7.68	0.83	46.42	1.89	4.59	0.46	26.16	1.34	5.82	0.42	79.68	8.29
Ulva fasciata	8.07	2.29	4.87	1.99	50.30	4.79	3.65	0.41	26.5	1.5	6.6	0.19	67.57	3.71
Sargassum boveanum	8.00	0.006	8.45	0.001	29.90	0.001	7.65	0.004	36.50	0.001	9.50	0.005	56.45	0.003
Halymenia porphyraeformis	10.4	0.001	4.70	0.001	46.30	0.002	2.60	0.004	28.50	0.002	7.50	0.003	71.40	0.002

Table 10.5: Mean with standard deviation of biochemical constituents (%) of seaweeds at Buleji beach

Species	*Protein*		*Lipid*		*Carbohydrates*		*Crude fibre*		*Ash*		*Moisture*		*Water*	
	Mean	*Sd*	*Mean*	*Sd*	*Mean*	*Sd*	*Mean*	*Sd*	*Mean*	*Sd*	*Mean*	*Sd*	*Mean*	*Sd*
Codium iyengarii	8.02	0.26	4.47	0.52	40.20	1.97	3.055	0.99	37.05	3.606	8.60	0.14	59.36	9.70
Enteromorpha compressa	8.85	0.40	8.13	0.29	44.23	2.1	4.21	0.29	25.95	0.07	8.67	2.62	48.49	9.61
Ulva fasciata	11.00	0.004	5.55	0.002	42.39	0.002	3.56	0.003	29.00	0.008	8.50	0.002	66.50	0.003
Colpomenia synosa	8.87	0.51	4.32	0.005	38.86	1.49	15.90	0.14	23.75	1.06	8.31	0.29	87.75	0.39
Cystoseira indica	9.53	0.99	5.56	1.29	42.45	6.69	6.45	1.74	26.44	4.70	9.57	0.50	51.72	27.83
Iyengaria stellata	12.49	0.002	5.66	0.002	36.00	0.001	3.05	0.001	38.90	0.003	3.90	0.001	69.11	0.002
Sargassum boveanum	8.25	0.69	6.32	0.69	37.15	5.73	5.87	1.29	33.23	6.39	9.92	0.21	57.44	15.02
Stoechospermum marginatum	7.65	0.39	7.78	0.31	35.73	0.92	6.60	0.19	31.70	0.42	10.20	0.49	53.48	14.71
Agardhilla robusta	8.82	0.001	3.40	0.003	44.23	0.005	2.85	0.005	35.80	0.001	4.90	0.002	49.17	0.002
Botryocladia leptopoda	9.67	0.001	4.20	0.001	39.57	0.002	2.35	0.001	38.11	0.001	6.10	0.007	53.57	0.001
Coelarthrum muelleri	6.92	0.007	3.60	0.001	41.18	0.001	2.90	0.001	38.90	0.005	6.50	0.001	49.34	0.002
Gracilaria corticata	11.65	0.54	14.13	4.69	27.13	3.11	3.85	0.89	36.90	3.01	6.34	0.19	55.62	1.99
Halymenia porphyraeformis	9.89	0.002	5.32	0.003	45.69	0.002	4.50	0.001	27.20	0.002	7.40	0.001	66.71	0.001
Hypnea musciformis	7.69	0.001	3.50	0.001	44.91	0.001	3.70	0.002	32.00	0.007	8.20	0.003	66.25	0.001

Table 10.6: Analysis of variance (ANOVA) of major and minor elements in seaweed from five beaches (Clifton, Korangi Creek, Manora, Sandspit and Buleji) of Karachi coast

Source	*DF*	*Seq SS*	*Adj SS*	*Adj MS*	*F*	*P*
Lipid						
Beaches	4	66.347	67.635	16.909	2.11*	0.090
Years	1	15.459	15.459	15.459	1.93	0.170
Error	63	505.378	505.378	8.022		
Total	68	587.184				
Protein						
Beaches	4	20.271	19.876	4.969	1.23	0.308
Years	1	0.414	0.414	0.414	0.10	0.750
Error	63	255.021	255.021	4.048		
Total	68	275.705				
Carbohydrate						
Beaches	4	494.53	503.03	125.76	3.35*	0.015
Years	1	179.42	179.42	179.42	4.78*	0.032
Error	63	2364.22	2364.22	37.53		
Total	68	3038.18				
Crude Fibre						
Beaches	4	31.915	31.061	7.765	1.02	0.406
Years	1	1.398	1.398	1.398	0.18	0.670
Error	63	481.309	481.309	7.640		
Total	68	514.621				
Ash						
Beaches	4	159.34	157.17	39.29	1.33	0.268
Years	1	11.46	11.46	11.46	0.39	0.536
Error	63	1860.17	1860.17	29.53		
Total	68	2030.97				
Moisture						
Beaches	4	135.607	142.124	35.531	10.78**	0.000
Years	1	13.590	13.590	13.590	4.128*	0.047
Error	63	207.737	207.737	3.297		
Total	68	356.934				
Water						
Beaches	4	295	299	75	0.07	0.990
Years	1	85	85	85	0.08	0.776
Error	63	65763	65763	1044		
Total	68	66143				

(DF is degree of freedom, F is the F-statistics and P is the probability level)
* Significant at $P < 0.05$, **Significant at $P < 0.001$. All others significant at $P < 0.01$.

observed. In Sandspit the high content of carbohydrate (50.30%) was found in *Ulva fasciata*; protein (10.4%) in *Halymenia porphyraeformis*; lipid (7.68%) in *Enteromorpha compressa*; crude fibre (7.65%) in *Sargassum boveanum* whereas at Buleji the highest percentage of carbohydrates (45.69%) in *Halymenia porphyraeformis*; ash (38.9%) in *Iyengaria stellata* and *Coelarthrum muelleri*; crude fibre (15.9%) in *Colpomenia sinuosa*; lipid (14.1333%) in *Gracilaria corticata*; and protein (12.49%) in *Iyengaria stellata*.

The values of protein, lipid, carbohydrates, crude fibre, ash and moisture content of green, brown and red seaweed species obtained in the present work agreed well with the previous studies (Qari, 1985, 1988 and 1993) whereas the present result showed that the high lipid contents were observed in oil polluted seaweeds as compared to previous study with non-polluted seaweeds (Zahid and Jabeen, 2001). ANOVA analysis showed that significant variations in lipid ($F = 2.11$) and carbohydrates ($F = 3.35$) whereas highly significant variations were found in moisture ($F = 10.78$) (Table 10.6).

During the study period the total number of seaweed species were 35. Tables 10.1-10.5 also show that the Manora (13) and Buleji beaches (14) were richest in seaweed species than the other beaches (Clifton, two; Korangi Creek, two and Sandspit, four). From Clifton and Korangi Creek only two green seaweeds *Enteromorpha compressa* and *Ulva fasciata* were collected. It means the seaweeds production from these two beaches are affected by oil spill by Tasman Spirit. Although Saifullah and Chaghtai (2005) recently reported that Clifton beach is mainly sandy and, therefore, devoid of any attached seaweed growth. However, it receives seaweeds from other areas as drift forms, and all these seaweeds were dead due to polluted black oil during the period of the spill. They also reported that there were, however, some very small patches of rocks scattered along the beach which allowed growth of some seaweeds like green seaweeds *Ulva* and *Enteromorpha* spp. and a few others insignificant microscopic forms. These attached seaweeds survived the entire period of the spill. It seems that these algae are resistant to oil pollution. However the present results obtained from the five beaches of Karachi coast (Clifton, Korangi Creek, Manora, Sandspit and Buleji) show that oil spill have big effect on seaweeds growth and distribution of Clifton (only two species) and Korangi Creek (only two species) as compared to Manora (13), Buleji (14) and Sandspit (four).

High ash content was associated with high concentration of major and minor elements. High percentage of carbohydrates and lipid in the present study is due to oil pollution in beaches studied especially at Clifton beach. In few species of seaweed, protein were high, may be due to fact that plants collected for biochemical analysis might have reproductive or fertile stage (Qari, 1993). It is also concluded that the number of species were low as compared to previous studies which indicate that all beaches of Karachi coast (Clifton, Korangi Creek, Manora, Sandspit and Buleji) are highly affected by oil spill and have huge effect on the distribution of seaweeds.

Due to climate change, oil spill changed the temperature (increased) of these beach waters that may disturb the life cycle or reproduction time of the plants. The increase in temperature may also change the metabolic activity and afterall decrease the growth of marine plants.

REFERENCES

A.O.A.C. (1990). Official methods of analysis of association of official analytical chemists. Association Official Analytical Chemists. Arlington, VA.

Anand, P.L. (1940). Marine algae from Karachi. I: Chlorophyceae. Punjab University botanical publications.

Anand, P.L. (1943). Marine algae from Karachi. II: Rhodophyceae. Punjab University botanical publications.

Bryan, G.W. and Hummerstone, L.G. (1973). Brown seaweed as an indicator of heavy metal in estuaries in South-West England. *J. Mar. Biol. Ass. U.K.*, **53:** 705-720.

Chakraborty, S. and Santra, S.C. (2008). Biochemical composition of eight benthic algae collected from Sunderban. *Indian Journal of Marine Sciences*, **37:** 329-332.

Chapman, V.J. (1964). Coastal vegetation. Pergamon Press, Oxford.

Daily Dawn (2003). 29th July-2nd September. Herald Publication.

Daily Jang (2003). 29th July-24th August. Javed Press, Printing House, Karachi.

Dare, P.J. and Edwards, D.S. (1975). Seasonal changes in fresh weight and biochemical composition of mussels (*Mytilus edulis* L.) in the Conwy estuary, North Wales. *J. Exp. Mar. Biol. Ecol.*, **18:** 89-97.

Dawczynski, C., Schubert, R. and Jahreis, G. (2007). Amino acids, fatty acids and dietry fibre in edible seaweed products. *Food Chemistry*, **103:** 891-899.

Dhargalkar, V.K. (1986). Biochemical studies in *Ulva reticulate* Forsskal. *Mahasagar*, **19:** 45-51.

Dhargalkar, V.K., Jagtap, T.G. and Untawale, A.G. (1980). Biochemical constituents of seaweeds along the Maharashtra coast. *Indian J. Mar. Sci.*, **9:** 297-299.

Folch, J., Lees, M. and Sloane-Slanley, G.H. (1957). A simple method for the isolation and purification of total lipids from animal tissues. *Journal of Biological Chemistry*, **226:** 497-509.

Hawk, B.P., Oser, L.B. and Summerson, H.W. (1954). Practical Physiological Chemistry. McGraw Hill Book Co, London.

Hayee-Memon, A. and Shameel, M. (1999). Phycochemical studies on *Melanothamnus afaqhusainii* (Ceramiales, Rhodophyta). *Pakistan J. Mar. Biol.*, **5:** 185-194.

Hossain, Z., Kurihara, H. and Takahashi, K. (2003). Biochemical composition and lipid compositional properties of brown Alga *Sargassum horneri*. *Pakistan Journal of Biological Sciences*, **6:** 1497-1500.

Melhus, A., Seip, K.L., Seip, H.M. and Myklested, S. (1978). A preliminary study of the use of benthic algae as biological indicators of heavy metal pollution in Sorfjorden, Norway. *Environ. Pollut.*, **15:** 101-107.

Morris, I. (1976). An introduction to the algae. Hutchinson and Co, London, England.

Qari, R. and Qasim, R. (1993). Biochemical constituents of seaweed from Karachi coast. *Indian J. Mar. Sci.*, **22:** 229-231.

Qari, R. and Qasim, R. (1988). Seasonal change in the standing crop of intertidal seaweeds from the Karachi coast. *In:* Thompson, M.F., Tirmizi, N.M. (eds), Marine Science of the Arabian Sea. American Institute of Biological Science, Washington D.C.

Qari, R. and Siddiqui, S.A. (1993). Biochemical composition and yield of agar from the *Gracilaria corticata* of Karachi. *Pakistan J. Mar. Biology*, **2:** 77-81.

Qari, R. and Qasim, R. (1994). Seasonal change in the standing crop of intertidal seaweeds from Manora coast, Karachi. *In:* Majid, A., Khan, M.Y., Moazzam, M. and Ahmed, J. (eds.) Proc. Nat. Sem. Fish Policy and Plan. Marine Fisheries Department, Karachi.

Qari, R. (1988). Seasonal changes in Biochemical composition of seaweed from Karachi coast of Pakistan. *Pakistan J. Sci. Ind. Res.*, **31:** 94-96.

Qari, R (1985). Seasonal variation in biomass and biochemical composition of some edible seaweeds from Karachi coast. M. Phil thesis, University of Karachi, Pakistan.

Qari, R. (2002). Studies of biodeposited trace metals and minerals in marine algae from Karachi coast. PhD thesis, University of Karachi, Pakistan.

Qasim, R. (1981). Biochemical studies on some seaweed from Karachi coast. *Karachi Univ. J. Sci.*, **9:** 105-111.

Round, F.E. (1973). The biology of algae. St. Martin's Press, New York.

Saifullah, S.M. (1973). A preliminary survey of the standing crop of seaweeds from Karachi coast. *Bot. Mar.*, **16:** 139-144.

Saifullah, S.M. and Chagtai, F. (2005). Effect of "Tasman Spirit" on Marine plants in Coastal Area of Karachi. *Int. J. Biotech.*, **2:** 299-306.

Saleem, K.M. (1965). The distribution of marine algae along Karachi. *Bot. Mar.*, **8:** 183-195.

Shameel, M. and Tanaka, J. (1992). A preliminary checklist of marine algae from the coast and inshore waters of Pakistan. *In:* Nakaike, T. and Malik, S. (eds), Cryptogamic Flora of Pakistan. Nat. Sci. Mus., Tokyo.

Shameel, M. (1987). A preliminary survey of seaweed from the coast of Lasbella, Pakistan. *Bot. Mar.*, **30:** 511-515.

Shameel, M. (2001). An approach to the classification of algae in the new millennium. *Pak. J. Mar. Biol.*, **7:** 233-250.

Shanmugam, A. and Palpandi, C. (2008). Biochemical composition and fatty acid profile of the green alga *Ulva reticulate*. *Asian Journal of Biochemistry*, **3:** 26-31.

Smith, G.M. (1955). Cryptogamic Botany, vol. I. McGraw Hill, New York.

Sumitra-Vija-Yaraghavan, Rajagopal, M.D. and Wafer, M.V.M. (1980). Seasonal variation in biochemical composition of some seaweed from Goa Coast. *Ind. J. Mar. Sci.*, **9:** 61-63.

Zahid, P.B., Jabeen, M.Z. and Humera Usman (2001). Quantitative studies on agar-agar from different species of red seaweeds of Karachi coast, Pakistan. *Pak. J. Mar. Biol.*, **7:** 291-297.

CHAPTER

11

Distribution of Ostracoda in the Mullipallam Lagoon, near Muthupet, Tamil Nadu, Southeast Coast of India – Implications on Microenvironment

S.M. Hussain and A. Kalaiyarasi

Department of Geology, University of Madras, Guindy Campus
Chennai – 600025, India
smhussain7@hotmail.com

INTRODUCTION

Microfossils have been very well proved useful for ecologic/paleoecological and paleoclimatic applications. Puri (1966) stated that ostracods live in an environment in which the controlling factors are temperature, bottom topography, depth, salinity, pH, alkalinity, dissolved oxygen, food supply, substrate and sediment organic matter content. Among all the physical parameters, the major controlling factors governing the ostracod distribution in estuarine and continental shelf environments are salinity, water temperature and substrate (Zhao et al., 1985; Bentley, 1988; Yassini and Jones, 1995; Shyam Sunder et al., 2000). These fauna are showing their utility in delineating changes in the environment. In the recent past, large scale land use/land cover modifications have been identified in the Ashtamudi estuary, a largest wetland region of Kerala, due to human activities (Sanjeev and Subramanian, 2003) and also in the Vedaranyam wetland (Selvaraj et al., 2005). The present work dealing with the microfaunal analysis of the Mullipallam lagoon

J. Sundaresan et al. (eds.), *Climate Change and Island and Coastal Vulnerability*,
DOI 10.1007/978-94-007-6016-5_11, © 2013 Capital Publishing Company

ascertains and supports the environmental conditions that exist/changes and also generates a data base on Ostracoda for future reference.

Present study consists the sedimentological parameters such as organic matter, sand-silt-clay ratio, $CaCO_3$ and hydrographical characteristics such as temperature, salinity, dissolved oxygen along with their correlation of the standing crop of ostracod population size and discuss on the environmental settings of the lagoon.

MATERIALS AND METHODS

The study area under investigation is Mullipallam lagoon area (Lat. 10°18′13″ to 10°20′71″ N; and Long. 79°30′90″ to 79°34′87″ E) is located near Muthupet, along the coastal zone of Bay of Bengal and Palk Strait (Fig. 11.1). It is a part of large coastal wetland complex called the "Great Vedaranyam Swamp". A mangrove species *Avicennia marina* is dominant in the lagoon followed by *Acanthus ilicifolius, Egiceras corniculatum, Excoecaria agallocha* and *Rhizopora mucronata*. Twenty-four sediment samples were collected from the lagoon during two seasons viz., pre-monsoon (June, 2006) and post-monsoon (Jan, 2007) and locations are shown in Fig. 11.1. The water depth of the lagoon ranges from 1.5 to 3.5 m. Due to the shallow nature of the lagoon and tidal factor, the movement of boat as per plan could not be done for field collection. Sediment and water samples were collected from all the 24 stations, the first sample was collected near the Koriyar river and eighth sample was collected near the Palk Straits.

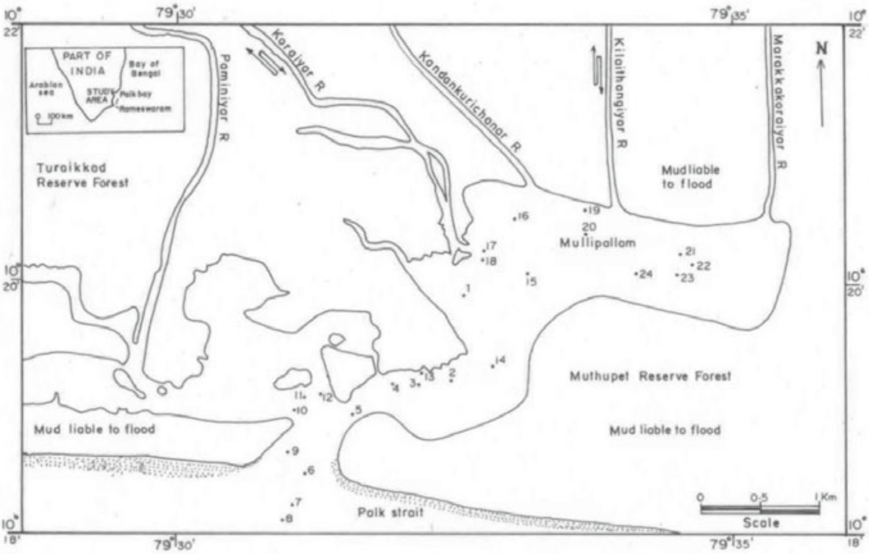

Fig. 11.1: Location map of the sampling stations in the Mullipallam lagoon area.

Sand-silt-clay ratios were determined and estimated by following the procedure of Krumbein and Pettijohn (1938). Organic matter was determined by titration method of Gaudette et al. (1974). Estimation of $CaCO_3$ was made by adopting the procedure proposed by Loring and Nota (1973). The standard titration method proposed by Knudsen (1901) has been followed to determine the salinity in the present study. Determination of dissolved oxygen was done spectrophotometrically (Duval et al., 1974).

RESULTS AND DISCUSSION

Systematic Paleontology

All the sediment samples were subjected to standard micropaleontological techniques and ostracoda fauna were recovered. Ostracod studies from the sediments collected from the lagoon have led to the recognition of 35 ostracod taxa belonging to 24 genera, 18 families, two superfamilies and two suborders of the order Podocopida (Table 11.1). *Neomonoceratina iniqua* is recorded in all the sediment samples studied. It outnumbered the entire ostracod population and represented by >90% of the total population in few samples (Hussain and Kalaiyarasi, 2010). *Hemicytheridea paiki* is represented second to *N. iniqua* in the study area. The classification proposed by Hartmann and Puri (1974) is followed.

Sediment, Water Characteristics and Standing Crop

The temperature of the bottom water was recorded from the built-in-thermometer. The temperature was slightly higher and ranges from 28.5 to 35.5°C (pre-monsoon) whereas it was recorded low during post-monsoon and ranges from 24.5 to 31.5°C. The maximum depth was recorded at stations 6, 7 and 8 (3.5 m) and minimum depth was at stations 20, 23 and 24 (1.0 m). Muthupet mangroves receive freshwater mostly during the northeast monsoon season from October to November. Around the mangrove areas dry spell is long, extending from February to September and corresponding to it, the average salinity to the mangrove water is also high during the dry period, ranging from 22.7 to 30.0 ppt (pre-monsoon) and low values are from 4.0 to 16.9 ppt (post-monsoon) (Table 11.2).

The dissolved oxygen content of water parameters of the study area is generally low. The DO ranges from 2 to 5.0% (pre-monsoon) and from 1.5 to 8.5% (post-monsoon). The percentage of DO content of post-monsoon is higher than pre-monsoon season, which may be due to freshwater influence in this monsoon. OM concentration varies from 0.57 to 4.31% during pre-monsoon and during post-monsoon it ranges from 2.01 to 6.5%. The content of calcium carbonate in the surface sediments of the study area is generally low and it varies between 1.0 and 2.3% in the pre-monsoon and during post-monsoon it ranges from 1.0 to 2.1% (Tables 11.3 and 11.4). The low values

Table 11.1: Taxonomic chart of the Ostracoda of the study area

Order	*Sub-order*	*Super family*	*Family*	*Genus*	*Species*
	Platy-copa		Cytherellidae	*Cytherelloidea*	*Cytherelloidea leroyi*
					C. sp.
Podocopida	Podocopa	Cytheracea	Cytheridae	*Hemicytheridea*	*Hemicytheridea bhatiai*
					H. paiki
					H.sp.aff..reticulata
				Neomonoceratina	*N.sp.cf. delicata*
					Neomonoceratina iniqua
					N.jaini
					N.porocostata
				Jankeijcythere	*Jankeijcythere mckenziei*
			Sinocytheridae	*Neosinocythere*	*Neosinocythere dekrooni*
			Leptocytheridae	*Cytherideidae*	*Callistocythere*
					Callistocythere flavidofusca intricatoides
				Tanella	*Tanella gracilis*
			Cytherettidae	*Miocyprideis*	*Miocyprideis spinulosa*
			Trachyleberidiae	*Stigmatocythere*	*Stigmatocythere indica*
				Keijella	*Keijella karwarensis*
					K. reticulata
					K. sp
				Basslerites	*Basslerites liebaui*
			Brachycytheridae	*Pterygocythereis*	*Pterygocythereis sp.*
			Hemicytheridae	*Mutilus*	*Mutilus pentoekensis*
				Caudites	*Caudites javana*
			Cytherettidae	*Neocytheretta*	*Neocytheretta murilineata*
					Neocytheretta sp.
			Loxoconchidae	*Loxoconcha*	*Loxoconcha gruendeli*
					L. megapora indica
			Cytheruridae	*Paijenborchellina*	*P. sp.*
			Xestoleberididae	*Xestoleberis*	*X. variegate*
			Paradoxo-stomatidae	*Paradoxostoma*	*Paradoxostoma bhatiai*
			Uncertain	*Kalingella*	*Kalingella mckenziei*
		Cytheracea	Cyprididae	*Cypridopsis*	*C. obesa*
			Ilyocyprididae	*Ilyocypris*	*Ilyocypris gibba*
					Ilyocypris bradyi
			Pontocyprididae	*Propontocypris*	*P. (Schedopontocypris) bengalensis*
			Candonidae	*Phlyctenophora*	*Phlyctenophora orientalis*

Table 11.2: Bottom water characters of pre-monsoon (2006) and post-monsoon (2007) in the lagoon

No. of sample	*Depth (mt)*	*Pre-monsoon (June, 2006)*			*Post-monsoon (Jan., 2007)*		
		Temp (°C)	*DO (ml/l)*	*Salinity (‰)*	*Temp (°C)*	*DO (ml/l)*	*Salinity (‰)*
1	1.5	29	4.5	26.3	25	5.04	8.7
2	2.5	29	4.7	26.3	29	5.02	5
3	2	28.5	5	23.3	28.5	5.02	4.2
4	2	29	3	22.7	29	7.05	4.2
5	1.5	30	4.7	26.9	30	8.5	5
6	3.5	30	4.7	30	25.5	4.6	14.4
7	3.5	30.5	4.9	28.8	30.5	5.6	16.9
8	3.5	30	3	27	30	6.3	15.9
9	3	31.5	4.7	22.7	31.5	3	12.4
10	2.5	31	3.2	26.7	31	3	9.01
11	2.5	35.5	2	26.2	25.5	8	10.01
12	2	31.5	3.5	27.7	25	3.1	11.6
13	2	31	4.2	28.2	25	3.1	8.5
14	2.5	31.5	3.3	26.7	24.5	7.7	8.7
15	2.5	31.5	3	27.7	31.5	7	5
16	2	31	2.5	28.8	31	6.9	6.5
17	2	31	4	27.7	31	7.2	9.5
18	1.5	30	2.5	26.7	29	5.8	8.3
19	2	29	3.2	28.2	29	8.2	5
20	1	29.5	3.3	29.4	29.5	3	4.2
21	1.5	29	3.7	29.6	29	4	4
22	1.5	30	3	28.8	30	2	7.3
23	1	31.5	4	24.9	31.5	1.5	4.2
24	1	30	4.7	27.1	30	2.6	8.9
Min	**1**	**28.5**	**2**	**22.7**	**24.5**	**1.5**	**4**
Max	**3.5**	**35.5**	**5**	**30**	**31.5**	**8.5**	**16.9**
Average	**2.11**	**30.55**	**3.70**	**26.96**	**28.75**	**5.12**	**8.39**

of $CaCO_3$ in the lagoon reflects on the sediments deposited through the freshwater and terrigenous environment.

Sand, silt and clay percentages were calculated using a combination of sieving and pipette procedure (Krumbein and Pettijohn, 1938) and sediment types were identified by adopting Trefethen's (1950) textural nomenclature. The surface sediments in the lagoon area are generally silt in nature and the average grain size distribution is as follows: sand 3.9%, silt 91.1%, clay 4.8% (pre-monsoon); sand 4.6%, silt 91.4%, clay 4.0% (post-monsoon). From the grain size distribution, it is observed that a low energy condition exists in the lagoon with more siltation mainly after post-monsoon period.

Table 11.3: Sedimentological characters in the lagoon sediment samples – pre-monsoon, 2006

No. of samples	*OM (%)*	*$CaCO_3$ (%)*	*Sand (%)*	*Silt (%)*	*Clay (%)*
1	1.01	2	5.5	90	4.5
2	2.01	2.1	6.2	89.3	4.5
3	2.05	2.3	3.1	93.7	3.2
4	2.17	2	3.1	93.4	3.5
5	2.08	1	2.4	93.1	4.5
6	2.02	1	2.4	93.1	4.5
7	2.02	1	2.5	92.3	5.2
8	1.01	1.1	3.1	92.4	4.5
9	0.57	1.1	3.1	92.4	4.5
10	3.04	1	5.1	92.6	2.3
11	3.01	1.3	2.4	92.6	5
12	2.01	1	7.2	87.3	5.5
13	2	1	4.1	90.4	5.5
14	1.07	1	3.2	90.8	6
15	3.04	2.1	3.2	90.8	6
16	2.03	1.1	2.5	92	5.5
17	2.01	1.1	2.5	92	5.5
18	2	2.1	4.1	90.9	5
19	2.08	2.1	7.3	86.2	6.5
20	4.31	2.3	4.3	90.7	5
21	4.01	1	5.2	89.7	5.1
22	1.07	1	3.4	91.5	5.1
23	1.71	2	3.4	91.5	5.1
24	1.72	1.2	3.5	91.2	5.3
Min	**0.57**	**1**	**2.4**	**86.2**	**2.3**
Max	**4.31**	**2.3**	**7.3**	**93.7**	**6.5**
Average	**2.11**	**1.46**	**3.94**	**91.14**	**4.85**

The abundantly occurring species *N. iniqua* and *H. paiki* might have been tried to adjust and accommodate in the only available silty substrate in the lagoon and the rest of the taxa could not sustain their population abundance in the silty sediment in the lagoon.

Seasonal variation of the living ostracod population size of all the 24 stations put together in the lagoon, ranges from 240 to 531 specimens, maximum population size during pre-monsoon and the minimum in post-monsoon. The total population of ostracoda of each season (all the 24 stations put together) ranges from 2391 to 5017, the maximum during pre-monsoon while the minimum has been witnessed during post monsoon. *Neomonoceratina iniqua* is recorded in all the sediment samples studied. The known ecology of this species is of epi-neritic to marginal marine

Table 11.4: Sedimentological characters in the lagoon sediment samples – post-monsoon, 2007

No. of samples	*OM (%)*	*$CaCO_3$ (%)*	*Sand (%)*	*Silt (%)*	*Clay (%)*
1	2.26	1.02	6.1	89.4	4.5
2	3.01	1.04	7.1	90.9	2
3	2.1	1.05	6.5	91.5	2
4	2.12	1.02	5	92.7	2.3
5	3.06	2.1	4.1	93.6	2.3
6	3.01	1.03	3.2	94.7	2.1
7	2.08	1.02	4.2	93.7	2.1
8	2.12	1.02	4.5	92	3.5
9	2.01	1	5	91.5	3.5
10	2.01	1.02	5.2	92.4	2.4
11	4.1	1.05	5.5	89.5	5
12	3.5	1.07	5	91.9	3.1
13	4.1	1.6	4.2	90.3	5.5
14	5.1	1.6	4.1	89.4	6.5
15	2.01	1.2	4.1	91.7	4.2
16	6.5	1.03	4.2	91.5	4.3
17	3.05	1	3.2	93.6	3
18	2.02	1	5.4	91.6	3
19	4.07	1	3.1	90.7	6.2
20	3.01	1.04	3.3	90.5	6.2
21	2.3	1.5	4.2	90.3	5.5
22	2.3	1.02	4.2	89.8	6
23	2.5	1.4	3.4	90.4	6
24	2.5	1.6	5.2	89.3	5.5
Min	**2.01**	**1**	**3.1**	**89.3**	**2**
Max	**6.5**	**2.1**	**7.1**	**94.7**	**6.5**
Average	**3.05**	**1.21**	**4.62**	**91.41**	**4.04**

distribution (Shyam Sunder et al., 2000; Zhao and Whatley, 1988, 1989). In the study area, it outnumbered the entire ostracod population and is represented by >90% of the total population in few samples. The standing crop of *N. iniqua* is counted in order to see its resistance against the environmental conditions existed in the lagoon. The living specimens of *N. iniqua* are found in all the samples. In the study area, *N. iniqua* was one of the very well represented species, with a maximum living population of 499 specimens (pre-monsoon) and minimum of 210 in post-monsoon. Total population size of this species observed was 6685 specimens, sharing 4752 in pre-monsoon and 1933 in post-monsoon (Hussain and Kalaiyarasi, 2010). Some species characteristic of brackish water such as *Hemicytheridea bhatiai, Jankeijcythere mackenziei, Loxoconcha megapora indica, Kalingella mckenzie* and

Neosinocuythere dekrooni occur more in the sample nos. 2, 3, 4, 5, 14, 15, 23 and 24. However, oligohaline taxa such as *Ilyocypris bradyi, I. gibba* and *Cypridopsis obesa* occur more in the sample nos. 16, 17, 18, 19, 20 and 21 in the lagoon, which is a freshwater dominant zone. Albeit, the occurrence of *Keijella reticulata, Miocyprideis spinulosa, Mutilus pentoekensis, Neocytheretta murilineata, N.* sp., *Neomonoceraqtina delicata, Cytherelloidea leroyi, C.* sp., *Xestoleberis variegata, Phlyctenophora orientalis* and *Stigamatocythere indica* in the lagoonal sediments may be due to the tidal influence. Based on the ostracod assemblage occurrence, the lagoon is divided into outer, middle and inner lagoonal environment.

Carapace Valve Ratio

The application of statistical aspects of ostracoda such as juveniles and adults; carapace and open valves; males and females; right and left valve; smooth and ornamented forms, etc., besides colour variation, pyritisation and predation, to interpret the environment of deposition and rate of deposition has attained importance these days. In the study area, the total ostracoda population during pre-monsoon is 5017 specimens of which closed carapace are 4709 and open valves are 308, whereas during post-monsoon the total ostracod specimens recovered are 2391, constituting 2346 closed carapaces and 45 open valves. Carapace valve ratio helps in knowing the comparative rate of sedimentation. In the study area, more number of closed carapaces occurs than open valves. Therefore, a very faster rate of sedimentation in the lagoon is inferred. The siltation is more during the NE monsoon due to the carrying of sediments by streams and distributaries of river Cauvery flowing in the lagoon. The high siltation rate is also reflected in the (C/V ratio) faunal population of ostracoda during both the seasons.

Predation

Predation can be stated as an interaction between two organisms which results in negative effects on the growth and survival of one of the populations. It can also be defined as a relationship between animals wherein one species eats another species. Predation is a more common phenomenon in a community of organisms of benthic habit of shallow water environment. It is one of the limiting factors that affect the abundance, distribution and individuals of species. The position, shape and dimension of the predatory drills found on ostracod carapaces can be utilized to interpret the environment of deposition and ecological implications. In the creek, single, double predation is noticed in *Hemicytheridea paiki* and multiple predation is noticed in *Neomonoceratina iniqua,* which shows more predatory activity is going on in the shallow nature of the lagoon (Figs 11.2a-e).

Fig. 11.2a: *Neomonoceratina iniqua* (Brady) – Right valve external view.

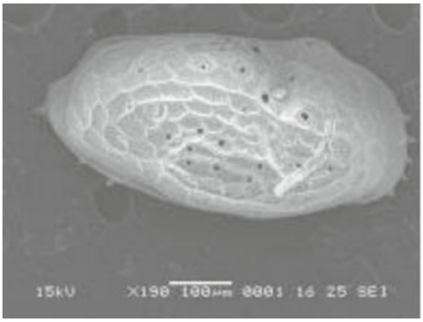

Fig. 11.2b: *Neomonoceratina iniqua* (Brady) – Multiple predation.

Fig. 11.2c: *Hemicytheridea paiki* Jain – Right valve external view.

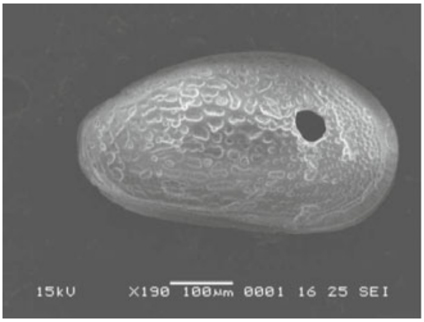

Fig. 11.2d: *Hemicytheridea paiki* Jain – Single predation.

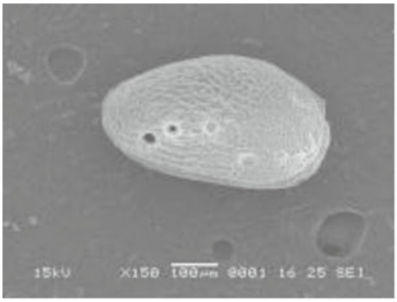

Fig. 11.2e: *Hemicytheridea paiki* Jain – Double predation.

CONCLUSION

Present study on Ostracod from the Mullipallam lagoon sediments have led to the recognition of 35 ostracod taxa belonging to 24 genera, 18 families, two superfamilies and two suborders of the order Podocopida. Among these, *N. iniqua* is the only species dominant and persistent (90% and above) in the entire population and followed by *H. paiki.* An analysis of sand, silt, clay ratio reveals a silty substrate, indicating a low energy environment where the fauna prefers to get accommodated. Ostracoda distribution in the sediment of the lagoon helps to demarcate the zones such as fresh water, brackish water and marine environment. Carapace-valve ratio indicates a faster rate of sedimentation in the Mullipallam lagoon. Presence of more dead ostracoda forms and less occurrence of living specimens also supports this observation. Due to high siltation from fresh water and terrestrial inputs, a progradational delta generates and the lagoon slowly shifts towards the sea. A fast geomorphological modifications are noticed in the Mullipallam lagoonal area which is highly vulnerable coast to tsunami and storm surges and also through the growth of mangrove vegetation. In the lagoon, double predation is noticed in *Hemicytheridea paiki* and multiple predation is noticed in *Neomonoceratina iniqua*. In the study area, almost all the ostracod specimens are light yellow and white in colour supporting the fact that the sediments are deposited under normal oxygenated environment.

In some environments, ostracod assemblages are dominated by a single taxon. In the study area also *N. iniqua* is a dominant and persistent taxon. This is often the case in biologically 'stressed' environments such as hypersaline waterbodies and intertidal settings. In the lagoon, *N. iniqua* appears tolerant to this stressed environmental condition and represents dominant in the entire ostracod assemblage. From the distribution of ostracod fauna; sedimentological and hydrographical parameters; ostracod carapace/valve ratio and predation, it is noticed that the lagoon is to be under stressed environment. This observation also supports the on-going growth of mud flats, shoreline changes (Selvaraj et al., 2005) and human induced interferences such as salt pan and agricultural activities etc. The abundance of single taxon in this type of environmental conditions may be used as a proxy for the interpretation of paleomicroenvironmental/paleolagoonal niche.

ACKNOWLEDGEMENTS

Authors are grateful to Dr. S.P. Mohan, Professor and Head, Department of Geology, University of Madras, for facilities and encouragement. Authors are also grateful to UGC for financial assistance (project No.31-192/2005 (SR), Dt. 31.03.2006) and to Department of Forest, Govt. of Tamil Nadu for permission for the collection of samples. We also thank Prof. T.Y.Naidu, Andhra University for his constructive review to improve the quality of the paper.

REFERENCES

Bentley, C. (1988). Podocopid ostracods of Brisbane water, near Sydney, south-eastern Australia. *In:* Evolutionary biology of ostracoda, its fundamentals and applications, developments in palaeontology and stratigraphy. Hanai, T., Ikeya, N. and Ishizaki, K. (eds). Elsevier Publishing Company, Kodansha, Tokyo.

Duval, W.S., Brockington, P.L, Von Melville, M.S. and Geen, G.B. (1974). Spectrometric determination of dissolved oxygen concentration in water. *Jour Fish Res Board of Canada*, **31:** 1529-1530.

Gaudette, R.E., Flight, W.R., Toner, L. and Folger, D.W. (1974). An inexpensive titration method for determination of organic carbon in recent sediments. *Jour Sed Petrol.*, **4:** 249-253.

Hartmann, G. and Puri, H.S. (1974). Summary of neontological and paleontological classification of ostracoda. *Mitteilungen Aus Dem Hamburgischen Zoologischen Museum Und Institude*, **70:** 7-73.

Hussain, S.M. and Kalaiyarasi, A. (2010). Distribution of *Neomonoceratina iniqua* in the sediments of Mullipallam creek, near Muthupet, Tamil Nadu, southeast coast of India: Ecological implications. *International Journal of Earth Sciences and Engineering*, **3(5)** (Special Issue): 23-35.

Knudsen, M. (1901). Hydrographical table. G.M. Manufacturing Co., New York.

Krumbein, W.C. and Pettijohn, F.J. (1938). Manual of Sedimentary Petrography. D. Appleton Century Co. Inc., New York.

Loring, D.H. and Nota, D.J.G. (1973). Morphology and sediments of the Gulf of St. Lawrence. *Jour Fish Res Board of Canada*, **182:** 147.

Puri, H.S. (1966). Ecologic and distribution of Recent Ostracoda. *In:* Proc. Symp. Crustacea, Pt. I, Mar Biol Assoc India, Mandapam, 457-495.

Sanjeev, R. and Subramanian, V. (2003). Land use/land cover changes in Ashtamudi wetland region of Kerala: A study using remote sensing and GIS. *Jour Geol Soc India*, **61:** 573-580.

Selvaraj, K., Ram Mohan, V., Jonathan, M.P. and Srinivasalu, S. (2005). Modification of a coastal environment: Vedaranyam wetland, southeast coast of India. *Jour Geol Soc India*, **66:** 535-538.

Shyam Sunder, V.V., Naidu, T.Y. and Varma, K.U. (2000). Salinity control on the distribution of Recent Ostracoda from the Goguleru Creek, east coast of India. *Bull ONGC*, **37(2):** 81-89.

Trefethen, J.M. (1950). Classification of sediments. *Amer Jour Sci.*, **248:** 55-62.

Yassini, I. and Jones, B.G. (1995). Foraminifera and Ostracoda from estuarine and shelf environments on the south-eastern coast of Australia. University of Wollongong Press, Wollongong, Australia.

Zhao, Q. and Whatley, R. (1988). The genus *Neomonoceratina* (Crustacea: Ostracoda) from the Cainozoic of the West Pacific Margins. *Acta Oceanologica Sinica*, **7(4):** 562-577.

Zhao, Q. and Whatley, R. (1989). Recent Podocopid Ostracoda of the Sedili River and Jason Bay, south-eastern Malay Peninsula. *Micropal.*, **35(2):** 168-187.

Zhao, Q., Wang, P. and Zhang, Q. (1985). Ostracoda in bottom sediments of the South China Sea, off Guangdong Province, China: Their taxonomy and distribution. *Mar Micropal China*, 296-317.

Part III

Coastal Dynamics

CHAPTER

12

Influence of Suspended Solid on in situ and ex situ Chlorophyll-*a*: A Case Study of Indian Sundarbans

Atanu Kumar Raha, Kakoli Banerjee[1], Susmita Das and Abhijit Mitra[1]

Directorate of Forest, Govt. of West Bengal, Aranya Bhawan, Salt Lake
Kolkata – 700098, India
[1]Department of Marine Science, University of Calcutta, Kolkata – 700019
West Bengal, India
abhijit_mitra@hotmail.com

INTRODUCTION

The Indian Sundarbans, at the apex of Bay of Bengal is noted for its rich taxonomic diversity, primary and secondary productivity (Mitra et al., 1992; Mitra et al., 1994). In the Indian Sundarbans, approximately 2069 sq. km of area is occupied by the tidal river system or estuaries, which finally end up in the Bay of Bengal. The seven main riverine estuaries from west to east (that contribute considerable sediment load in the aquatic sub-system) are listed in Table 12.1, along with their salient features. The significant increase of industrial and anthropogenic activities in the upstream zone of the Hooghly-Matla estuary in recent times has aggravated the problem related to suspended load (Mitra et al., 1992; Mitra et al., 1994). The presence of suspended solid has a regulatory influence on the phytoplankton community and primary productivity of the estuarine system. Satellite Remote Sensing can be used as a tool to monitor such influences. Qualitative study on suspended sediment content, coral reef and chlorophyll concentration along the Rameshwaram coast of Tamil Nadu have been carried out using Landsat TM data (Krishnamoorthy et al., 1992). Mapping of chlorophyll distribution using

J. Sundaresan et al. (eds.), *Climate Change and Island and Coastal Vulnerability*,
DOI 10.1007/978-94-007-6016-5_12, © 2013 Capital Publishing Company

Table 12.1: Important tidal rivers of Indian Sundarbans

Estuary	*Description*
Hooghly	• It forms the western border of Indian Sundarbans. • It is the main river of West Bengal and is a direct continuation of the River Ganges. • Most of the coastal industries of West Bengal are concentrated along the western bank of this river.
Muriganga	• It is a branch of the Hooghly River. • It flows along the east of Sagar Island, the largest island in the deltaic complex. • Unique mangrove vegetation is found along the bank of this river.
Saptamukhi	• It has its origin at Sultanpur. • It is connected with the Muriganga (Bartala) branch of the Hooghly River through Hatania-Duania canal.
Thakuran	• It begins near Jayanagar in South 24 Parganas and has a number of connections with the Saptamukhi. • It was connected in the earlier times with the Kolkata canal through the Kultali and the Piyali rivers, which exist today in a dying state.
Matla	• This river originates at the confluence of Bidyadhari, Khuratya and the Rampur Khal close to the town of Canning in 24 Parganas (South). • Matla is connected to Bidya and ultimately flows to the Bay of Bengal. The fresh water connection and discharge to this river has been lost in recent times. • Salinity of the river water is relatively high (in comparison to Hooghly or Muriganga) owing to fresh water cut-off from the upstream region.
Bidyadhari*	• This was flourishing branch of the Bhagirathi during the 15^{th} and 16^{th} century, but now serves only as a sewage and excess rainwater outlet from the city of Kolkata. • The river bed is completely silted and presently it is almost in dying condition.
Gosaba	• The waters of Matla and Harinbhanga (Raimangal) through a large number of canals form the estuary. • The estuary and its numerous creeks flow through the reserve forests.
Harinbhanga	• It is the eastern-most river in the Indian Sundarbans deltaic complex. • The Harinbhanga (also known as Ichamati and Raimangal) forms a natural demarcation between India and Bangladesh.

* Presently a dying estuary and not considered within the seven major types.

satellite sensors, especially the OCM (Ocean Colour Monitor) sensor combined with 'sea truth' measurements, has facilitated better understanding of the ocean productivity and also the exploration of the fishery resources. This has been achieved by considering two case study sites: Case I shallow coastal waters with high sediment concentration and case II is in deeper part of the coast with low sediment concentration. The photosynthetic pigments in phytoplankton absorb light strongly at particular wavelengths. The absorption maxima for chlorophyll-*a* are at 443 and 670 nm (Weeks, 1989; Morel and Gordon, 1984; Lin et al., 1984) have utilized more than one wavelength region from different parts of spectrum to obtain chlorophyll concentration from remotely sensed spectral data acquired over case II waters.

Previous investigations concerning the spectral composition of ocean colour have identified few sources governing water leaving radiance characteristics. These are mainly phytoplankton standing stock, associated biogenous and dissolved organic detritus, terrigenous particles and resuspended sediment and particulate and dissolved terrigenous or anthropogenic organic matter gelbstoff or yellow substance (Briacud and Sathyendranath, 1981; Gordon et al., 1980). Due to simultaneous influence of sediment and phytoplankton on the spectral signatures of case II waters, there is speculation among researchers that algorithms designed to extract chlorophyll-*a* concentrations from spectral data may be site and season specific (Briacud and Sathyendranath, 1981; Gordon and Morel, 1983). With this background we monitored 11 stations distributed in the aquatic phase of mangrove dominated Indian Sundarbans (both in the upstream and down-stream regions) during pre-monsoon 2005 and attempted to relate the in situ chlorophyll-*a* with the IRS P4 OCM data set. The objective of the present study is therefore to provide a regional distribution of chlorophyll-*a* in the aquatic sub-system of the Sundarban delta (Indian part) using Indian Remote Sensing Satellite IRS-P4 OCM data and validate the underlying algorithm in two different situations of suspended solid level in the said system.

MATERIALS AND METHODS

The Study Area

The Sundarban mangrove ecosystem covering about one million ha in the deltaic complex of the rivers Ganga, Brahmaputra and Meghna is shared between Bangladesh (62%) and India (38%) and is the world's largest coastal wetland. Enormous load of sediments carried by the rivers contribute to its expansion and dynamics. Station selection was primarily based on anthropogenic activities, mangrove floral richness and biomass.

The Indian Sundarbans (between 21°13′N and 22°40′N latitude and 88°03′E and 89°07′E longitude) is bordered by Bangladesh in the east, the Hooghly River (a continuation of the Ganges river) in the west, the Dampier and Hodges line in the north, and the Bay of Bengal in the south. The important morphotypes of deltaic Sundarbans include beaches, mud flats, coastal dunes, sand flats, estuaries, creeks, inlets and mangrove swamps (Chaudhuri and Chaudhury, 1972). The temperature is moderate due to its proximity to the Bay of Bengal in the south. Average annual maximum temperature is around 35°C. The summer (pre-monsoon) extends from the mid of March to mid-June, and the winter (post-monsoon) from mid-November to February. The monsoon usually sets in around the mid of June and lasts up to the mid of October. Rough weather with frequent cyclonic depressions occurs during mid-March to mid-September. Average annual rainfall is 1920 mm. Average humidity is about 82% and is more or less uniform throughout the year. Thirty-four true mangrove species and some 62 mangrove associated species have been documented in Indian Sundarbans, which is also the home ground of the Royal Bengal tigers (*Panthera tigris tigris*). This deltaic complex sustains 102 islands, only 48 of which are inhabited. The ecosystem is extremely prone to erosion, accretion, tidal surges and several natural disasters, which directly affect the top soil and the subsequent carbon density. The average tidal amplitude is around 3.0 m.

Chlorophyll Estimation (in situ and ex situ)

For in situ chlorophyll estimation, surface water samples (one litre) were collected at 11 sites (Table 12.2 and Fig. 12.1) using PVC water sampler along the Hooghly-Matla estuarine stretch, between 6 A.M and 1 P.M. on 03/03/2005 during IRS-P4 satellite overpass (Fig. 12.2). In situ chlorophyll measurement was done by following the spectrophotometric method as outlined in Strickland and Parsons (1972).

Table 12.2: Location of sampling stations

Zonation	*Station name and No. (as in map)*	*Station code*	*Geographical location*	
			Longitude (^0E)	*Latitude (^0N)*
High suspended solid region	Diamond Harbour (1)	HS1	88°11′35.05″	22°11′07.84″
	Kachuberia (2)	HS2	88°07′57.32″	21°52′27.99″
	Banstala (3)	HS3	88°10′44.55″	21°43′05.58″
	Sagar South (4)	HS4	88°03′06.17″	21°38′54.37″
	Frazergaunge (5)	HS5	88°15′15.63″	21°33′11.84″
Low suspended solid region	Chemaguri (6)	LS1	88°10′07.03″	21°39′58.15″
	Harinbari (7)	LS2	88° 04′52.98″	21°47′01.36″
	Sandheads (8)	LS3	88°04′56.02″	21°36′43.16″
	Lothian (9)	LS4	88°22′13.99″	21°39′01.58″
	Jharkhali (10)	LS5	88°41′47.25″	22°05′52.82″
	Netidhopani (11)	LS6	88°49′43.71″	21°54′16.33″

HS1-HS5 are the stations with high suspended solid (greater than 140 mg/l) and LS1-LS6 are the stations with low suspended solid (less than 140 mg/l)

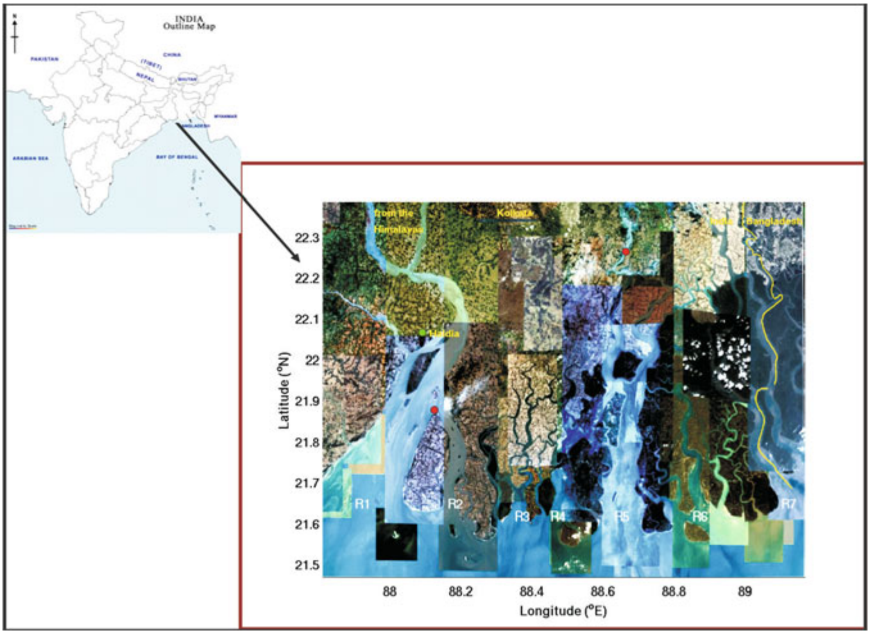

Fig. 12.1: Map showing the location of sampling stations. R1 to R7 are the seven rivers of Sundarbans starting from west to east, namely Hooghly, Mooriganga, Saptamukhi, Thakuran, Matla, Gosaba and Harinbhanga

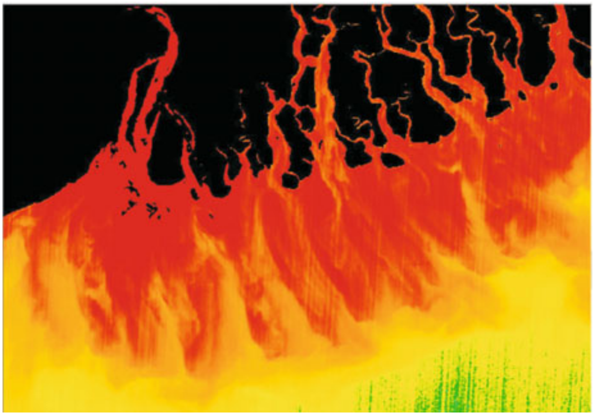

Fig. 12.2: Classified OCM data showing high (red), medium (yellow) and low (greenish) concentration of chlorophyll-*a* during March, 2005.

OCM data of NRSC, Hyderabad was registered for all the selected stations through GIS Cell of Directorate of Forests, Govt. of West Bengal. In the present study, OCM data have been processed for suspended particulate matter (SPM) and chlorophyll using Ocean Chlorophyll 2 (OC2) algorithms respectively from Oceansat-2 sensor data (Ramana et al., 2000; Raha, 2010).

Suspended Solid (SS) Estimation (in situ)

Suspended solid (in mg/l) for each of the 11 locations (as fixed with the help of GPS) was gravimetrically measured according to the method suggested in Strickland and Parsons (1972). Each sample was filtered through a pre-weighed Whatmann GF/F glass fibre filter paper. The filter was washed thrice to remove the salts adhered to that and dried in an oven at 75°C for 48 hours. Then it was reweighed using a digital balance.

Statistical Approach

We differentiated the selected stations into two categories (1) category A: stations with high suspended solid (greater than 140 mg/l) and (2) category B: stations with low suspended solids (less than 140 mg/l). Pearson correlation (*r*) values were computed through SYSTAT between in situ and ex situ data sets of chlorophyll-*a* for both the categories. Also the overall correlation between the ex situ and in situ data sets (considering all the 11 stations) were performed. This approach was adopted to understand the inter-relationship between both types of data sets under the influence of suspended solid.

RESULTS AND DISCUSSION

The use of remote sensing for mangrove mapping is well established by now (Aschbacher et al., 1995; Ramsey and Jensen, 1996; Green et al., 1998a; Green et al., 1998b; Sulong et al., 2002; Verheyden et al., 2002). Several attempts have been made in India in past to map the mangrove areas (Roy, 1989; Dwivedi et al., 1999; Kushwaha et al., 2000; Singh et al., 2004; Reddy et al., 2007). In marine and estuarine ecosystems the use of remote sensing has helped to understand aquatic productivity, pollution status, PFZ etc.

The oceanic waters have been classified based on spectral signatures. Case I waters tend to be oceanic in nature, while case II waters include coastal waters and estuaries. This classification is primarily due to phytoplankton and their detritus component's reflectance and absorbance (case I) from those waters wherein sediment and dissolved organic matter also exerts an influence on the spectral properties of water leaving radiance (case II). The normal range of chlorophyll-*a* concentration in case II waters (i.e., 0-100 μg/l) is usually different than that of case I waters (i.e., 0-10 μg/l). The higher chlorophyll-*a* concentrations of case II waters often produce measurable reflectance and absorbance in infrared wavelength regions weakly influenced by the lower chlorophyll concentration found in case I waters (Gower et al., 1984; Morel and Gorden et al., 1984).

In inland waters and case II coastal waters, the influence from suspended sediments and/or yellow substance originating from river outlets and bottom resuspension have impaired chlorophyll-*a* estimation (Moller-Sorensen et al., 1982; Verdin, 1985). Although, Landsat TM was originally designed for land observations, its potential use for chlorophyll estimation has been studied. Kim and Linebaugh (1965) found that TM data could be used to quantify chlorophyll-*a* in the range of 0.5 to 2.0 mg/m³.

Table 12.3 presents the ex situ and in situ data of chlorophyll-*a* in the selected stations in the present study area. Chlorophyll-*a* values measured for the water samples collected during high tide conditions have been utilized for the validation of the IRS P4 OCM data set. Pearson correlation (r) between in situ chlorophyll-*a* data and OCM derived chlorophyll-*a* data in the estuarine waters (Fig. 12.3) is 0.6775 ($p < 0.01$). The r values, however, varied significantly between the zones of high suspended solid (category A) and low suspended solid (category B). In stations 1, 2, 3, 4 and 5 (HS1–HS5), where

Table 12.3: In situ (sampled and analysed on 03.03.2005) and ex situ variables in the aquatic sub-system of Indian Sundarbans

Station	*In situ Chlorophyll-a*	*Ex situ Chlorophyll-a*	*In situ SS*	*Ex situ SS*
Diamond Harbour	2.88	1.68	153.8	1.61
Kachuberia	2.92	1.427	161.31	1.427
Banstala	2.73	1.457	170.05	1.462
Sagar South	2.74	1.52	141.49	1.407
Frazergaunge	2.77	1.412	149.8	1.497
Chemaguri	1.695	1.407	139.98	1.542
Harinbari	2.015	1.596	130.09	1.457
Sandheads	1.906	1.519	128.96	1.435
Lothian	1.565	1.328	120.78	1.323
Jharkhali	1.328	1.172	118.55	1.21
Netidhopani	1.303	1.162	115.76	1.162

'SS' denotes suspended solid

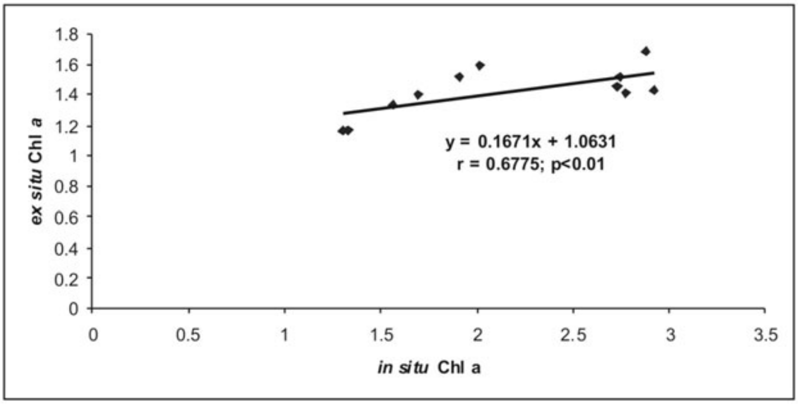

Fig. 12.3: Inter-relationship between in situ and ex situ data sets of chlorophyll-*a* (considering all the selected stations) during Mar, 2005 in the study area.

the suspended solid was 153.80 mg/l, 161.31 mg/l, 170.05 mg/l, 141.49 mg/l and 149.80 mg/l respectively, the *r* value was 0.2681 (Fig. 12.4). These are the stations in deltaic Sundarbans with intense industrialization, urbanization and fishing activities. It has also been stated by several workers that few areas of Indian Sundarban mangroves (particularly towards the inland side) are affected by the anthropogenic activities and conversion of mangroves to pisciculture was noticed as the main cause of disturbances (Nandy, 2009; Nandy et al., 2010). Such conversions accelerate the level of suspended solids in waters particularly during harvesting, water exchange and aquaculture pond preparation. In stations 6 to 11 (LS1–LS6), the human interference is low mostly because of their locations adjacent to reserve forests. The aquatic phase in these stations exhibited low suspended solid (category B) and the *r* value between the two types of data sets (Fig. 12.5) is significantly high ($r = 0.9993$, $p < 0.01$).

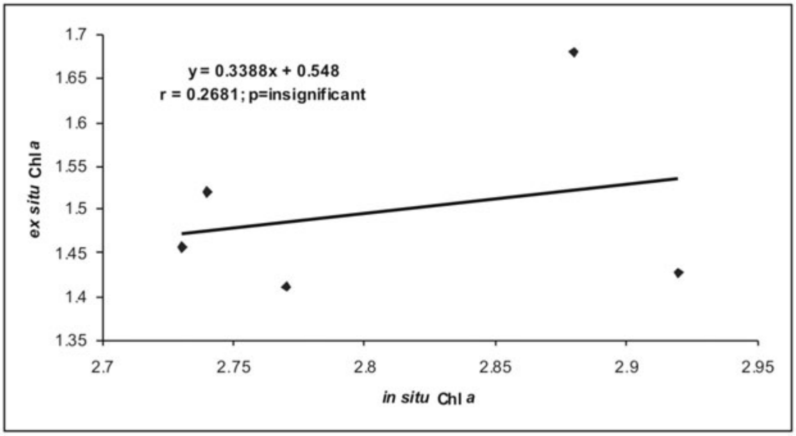

Fig. 12.4: Inter-relationship between in situ and ex situ data sets of chlorophyll-*a* (for suspended solid value of >140 mg/l) during Mar, 2005 in the study area.

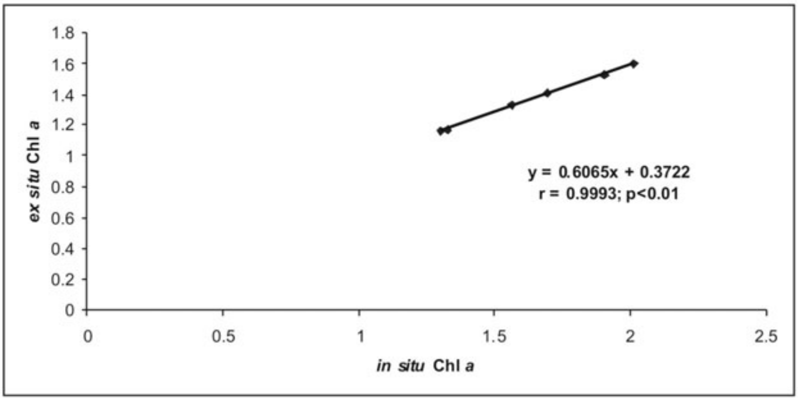

Fig. 12.5: Inter-relationship between in situ and ex situ data sets of chlorophyll-*a* (for suspended solid value of <140 mg/l) during Mar, 2005 in the study area.

We infer from our results that the algorithm developed for the retrieval of chlorophyll-*a* is not suited for waters with high suspended solid (in the framework of Indian Sundarbans) particularly in the region experiencing significant effect of industrialization, urbanization or erosion. Possible sources of interferences are bottom effects (Macko and Estep, 1984; Rundquist et al., 1995), the mixtures of organic (living or residual) and inorganic suspensions (Wetzel and Likens, 1979; Quibell, 1991; Dekker, 1993; Goodin et al., 1993; Han et al., 1994) generated from industries, agriculture, urban sewage and shrimp culture units. The present study depicts that algorithms designed to extract chlorophyll-*a* concentrations from spectral data acquired over case II waters need to be specific to meet the required near-shore situations and universal models are not possible to establish. Such specificity is particularly essential for systems like Indian Sundarbans, where significant spatial and temporal variations of suspended solid exist. The western part of Indian Sundarbans is primarily the zone of high suspended solid because of erosion and upstream discharge (that contribute huge quantum of silt) and industrial discharges from the city of Kolkata, Howrah and the newly developing Haldia complex (Mitra and Choudhury, 1993; Mitra, 1999; Mitra et al., 2009). The central and eastern Indian Sundarbans are, however, the zone of low suspended solid primarily because of the presence of mangroves that bind the soil particles with intricate root system and also due to absence of any industry in the region. We strongly recommend the development of region-specific algorithm for chlorophyll-*a* retrieval through satellite as the inter-relationship between ex situ and in situ chlorophyll-*a* has significantly changed in the present study area in varying level of suspended solid.

ACKNOWLEDGEMENTS

Authors thank the faculties of the Department of Marine Science and officials of West Bengal Forest Department for helping to collect and assemble the data. Also thank the research scholars of Ministry of Earth Sciences, Govt. of India who have helped during the collection and water analysis phase during 2005.

REFERENCES

Aschbacher, J., Ofren, R.S., Delsol, J.P., Suselo, T.B., Vibulsresth, S. and Charrupat, T. (1995). An integrated comparative approach to mangrove vegetation mapping using remote sensing and GIS technologies: Preliminary results. *Hydrobiol,* **295:** 285-294.

Briacud, A. and Sathyendranath (1981). Spectral signatures of substances responsible for the change in ocean colour. IPS Proc. Signature Spectral d'Objects en teledetection. Colloque International Avigon held at France from Sept. 8-11, 1981.

Chaudhuri, A.B. and Choudhury, A. (1994). Mangroves of the Sundarbans – India. (1st edn.), IUCN - The World Conservation Union, Bangladesh.

Dekker, A.G. (1993). Detectaion of optical water quality parameters for eutrophic water by high resolution remote sensing. Ph.D. Thesis. Vrige University, Amsterdam.

Dwivedi, R.S., Rao, B.R.M. and Bhattacharya, S. (1999). Mapping wetlands of Sundarban delta and its environs using ERS-1 SAR data. *Int J Remote Sens.,* **20:** 2235-2247.

Goodin, D.G., Han, L., Fraser, R.N., Rundquist, D.C., Stebbins, W.A. and Schalles, J.F. (1993). Analysis of suspended solids in water using remotely sensed high resolution derivative spectra. *Potogramm. Engg. Remote Sens*., **59:** 505-510.

Gordon, H.R. and Morel, A.Y. (1983). Remote Assesment of Ocean Colour for Interpretation of Satellite Visible Imagery: A Review of Lecture Notes on Coastal Estuarine Studies. No. 4 Springer-Verlag, New York.

Gordon, H.R., Clark, D.K., Mueller, J.L. and Hovis, W.A. (1980). Phytoplankton Pigments from the Nimbus 7 Coastal Zone Colour Scanner: Comparisons with Surface measurements. *Science,* **210:** 63-66.

Gower, J.F.R., Lin, S. and Borstad, G.A. (1984). The Information content of different optical spectral ranges from chlorophyll estimation in coastal waters. *Int. J. Remote Sens.,* **15:** 3707-3718.

Green, E.P., Clarke, C.D., Mumby, P.J., Edwards, A.J. and Ellis, A,C. (1998a). Remote sensing techniques for mangrove mapping. *Int J Remote Sens*., **19:** 935-956.

Green, E.P., Mumby, P.J., Ellis, A.C., Edwards, A.J. and Clarke, C.D. (1998b). The assessment of mangrove areas using high resolution multispectral airborne imagery. *J Coast Res*, **14:** 433-443.

Han, L., Rundqist, D.C., Liu, L.L., Fraser, R.N. and Schalles, J.F. (1994). The spectral response of algal chlorophyll in water with varying levels of suspended sediments. *Int. J. Remote Sens.,* **15:** 3707-3718.

Kim, H.H. and Linebaugh, G. (1985). Early evaluation of Thematic Mapper data for coastal process studies. *Advanced Space Res.*, **5(5):** 21-29.

Krishnamoorthy, R., Natisan, Usha, Ramachandran, S. and Natarajan, R. (1992). Qualitative remote sensing of suspended sediment content, coral reef and chlorophyll concentration in Gulf of Manner. *In:* Remote Sensing Application and Geographical Information Systems. I.V. Muralikrishna (ed.). Tata McGraw-Hill, New Delhi.

Kushwaha, S.P.S., Dwivedi, R.S. and Rao, B.R.M. (2000). Evaluation of various digital image processing techniques for detection of coastal wet lands using ERS-1 SAR data. *Int J Remote Sens.,* **21:** 565-579.

Lin, S., Borstad, G.A. and Gower, J.F.R. (1984). Remote Sensing of chlorophyll in the red spectral region. *In:* Remote Sensing of Shelf Sea Hydrodynamics. J.C.J. Nihoul (ed.). Elsevier Oceanography Series, New York, **38:** 317-337.

Macko, S.A. and Estep, M.L.F. (1984). Microbial alteration of stable nitrogen and carbon isotopic compositions of organic matter. *Org. Geochem.,* **6:** 787-790.

Mitra, A. (1998). Status of coastal pollution in West Bengal with special reference to heavy metals. *J. of Ind. Ocn. Studies*, **5(2):** 135-138.

Mitra, A. and Choudhury, A. (1993). Trace metals in macrobenthic molluscs of the Hooghly estuary, India. *Mar. Poll. Bull.UK*, **26(9):** 521-522.

Mitra, A., Banerjee, K., Sengupta, K. and Gangopadhyay, A. (2009). Pulse of climate change in Indian Sundarbans: A myth or reality. *Natl. Acad. Sci.Lett* , **32(1 and 2):** 1-7.

Mitra, A., Choudhury, A. and Yusuf, A.Z. (1992). Effects of heavy metals on benthic molluscan communities in Hooghly estuary. *Proceedings of the Zoological Society.*, **45:** 481-496.

Mitra, Abhijit, Trivedi, Subrata and Choudhury, Amalesh (1994). Inter-relationship between gross primary production and metal accumulation by *Crassostrea cucullata* in the Hooghly estuary. *Pollution Research.*, **13:** 391-394.

Moller-Sorensen, B., Sturm, B. and Tassan, S. (1982). Some results from experiments on remote sensing of water quality and oil pollution in the Meditteranean sea. *In:* Proc. 1st Thematic Conference, of the International Symposium on Remote Sensing of Environment, Remote Sensing of Arid and Semi-Arid Lands, held at Cairo, Egypt.

Morel, A.Y. and Gordon, H.R. (1984). Report of the working group on water colour. *Boundary-Layer Met.,* **18:** 343-355.

Nandy, S. (2009). Geospatial modeling of biological richness for conservation prioritization of Sundarban mangroves. Ph.D. Thesis. Forest Research Institute University, Dehradun.

Nandy, S. and Kushwaha, S.P.S. (2010). Geospatial modeling of Biological Richness in Sundarbans. *J. Indian Soc. Remote Sens.,* **38:** 431-440.

Quibell, G. (1991). The effect of suspended sediment reflectance from freshwater algae. *Int. J. of Remote Sens.*, **12:** 177-182.

Raha, A.K. (2010). Study of spectral signatures of Phytoplankton pigments using satellite based Remote Sensing and GIS in Indian Sunderbans wetland. Ph.D. Thesis, Jadavpur University, Kolkata.

Ramana, I.V., Rao, K.H., Rao, M.V., Choudhury, S.B. and Bhan, S.K. (2000). Data processing scheme for the retrieval of oceanic parameters using IRS-P4 OCM data. Proceedings of the 5th PORSEC-2000.

Ramsey, E.J. and Jensen, J.R. (1996). Remote sensing of mangrove wetlands: Relating canopy spectra to site-specific data. *Photogramm Engg Remote Sens.,* **62:** 939-948.

Reddy, C.S., Pattanaik, C. and Murthy, M.S.R. (2007). Assessment and monitoring of mangroves of Bhitarkanika Wildlife Sanctuary, Orissa, India using remote sensing and GIS. *Curr Sci,* **92:** 1409-1415.

Roy, P.S. (1989). Mangrove vegetation stratification using Salyut 7 photographs. *Geocarto Int*, **3:** 31-47.

Rundquist, D.C., Schalles, J.F. and Peake, J.S. (1995). The response of volume reflectance to manipulated algal concentrations above bright and dark bottoms at various depths in an experimental pool. *Geocarto Int.,* **10:** 5-14.

Singh, I.J., Singh, S.K., Kushwaha, S.P.S., Asutosh, S. and Singh, R.K. (2004). Assesment and monitoring of estuarine mangrove forests of Goa using satellite remote sensing. *J Indian Soc Remote Sens*., **32:** 167-174.

Strickland, J.D.H. and Parsons, T.R. (1972). A practical handbook of sea-water analysis (2nd edn.). *J. Fish. Res. Bd. Canada*, **167:** 311.

Sulong, I., Lokman, M.H., Tarmizi, K. and Ismail, A. (2002). Mangrove mapping using landsat imagery and aerial photographs: Kemaman District, Terrengannu, Malaysia. *In:* Dahdouh-Guebas, F. (ed.), Remote sensing and GIS in the sustainable Management of tropical Coastal Ecosystems. *Environment, Development and Sustainability*, **4(2):** 93-112.

Verdin, J.P. (1985). Monitoring water quality conditions in a large western reservoir with Landsat imagery. *Photogramm. Engg. and Remote Sens*., **51:** 343-353.

Verheyden, A., Dahdouh-Guebas, F., Thomaes, K., De Genst, W., Hettiarachchi, S. and Koedam, N. (2002). High-resolution vegetation data for mangrove research as obtained from aerial photography. *Environ Dev Sustain,* **4:** 113-133.

Weeks, A. (1989). Seasonal and Tidal cycles of suspended particulates in the Irish Sea. Ph.D Thesis, School of Ocean Sciences, University College of North Wales, Anglessy.

Wetzel, R.G. and Likens, G.E. (1979). Limnological Analyses. W.B. Saunders Company, Philadelphia.

CHAPTER

13

Climate and Sea Level Changes in a Holocene Bay Head Delta, Kerala, Southwest Coast of India

D. Padmalal, K.M. Nair[1], K.P.N. Kumaran[2], K. Sajan[3], S. Vishnu Mohan, K. Maya, V. Santhosh, S. Anooja and Ruta B. Limaye[2]

Centre for Earth Science Studies, Thiruvananthapuram - 695031 Kerala, India

[1]Sredha Scientific Charitable Society, Palayam Thiruvananthapuram – 695033, Kerala, India

[2]Palynology and Palaeoclimate Laboratory Agharkar Research Institute, Pune Maharashtra – 411004, India

[3]Department of Marine Geology and Geophysics School of Marine Sciences, Cochin University of Science and Technology Kochi – 682016, Kerala, India

drdpadmalal@gmail.com

INTRODUCTION

The Holocene epoch, all over the world, has witnessed exceptional climate and sea level changes. Although the south-west coast of India has a fairly thick deposit of Holocene sediments of 50-60 m in the South Kerala Sedimentary Basin (SKSB) and its adjoining coastal lowlands (see inset in Fig. 13.1), not much focus has been given to unfold its palaeo-climatic and palaeo-environmental potential till the beginning of the present century (Joseph and Thrivikramji, 2002; Nair and Padmalal, 2003; Nair et al., 2006; Kumaran

J. Sundaresan et al. (eds.), *Climate Change and Island and Coastal Vulnerability*, DOI 10.1007/978-94-007-6016-5_13, © 2013 Capital Publishing Company

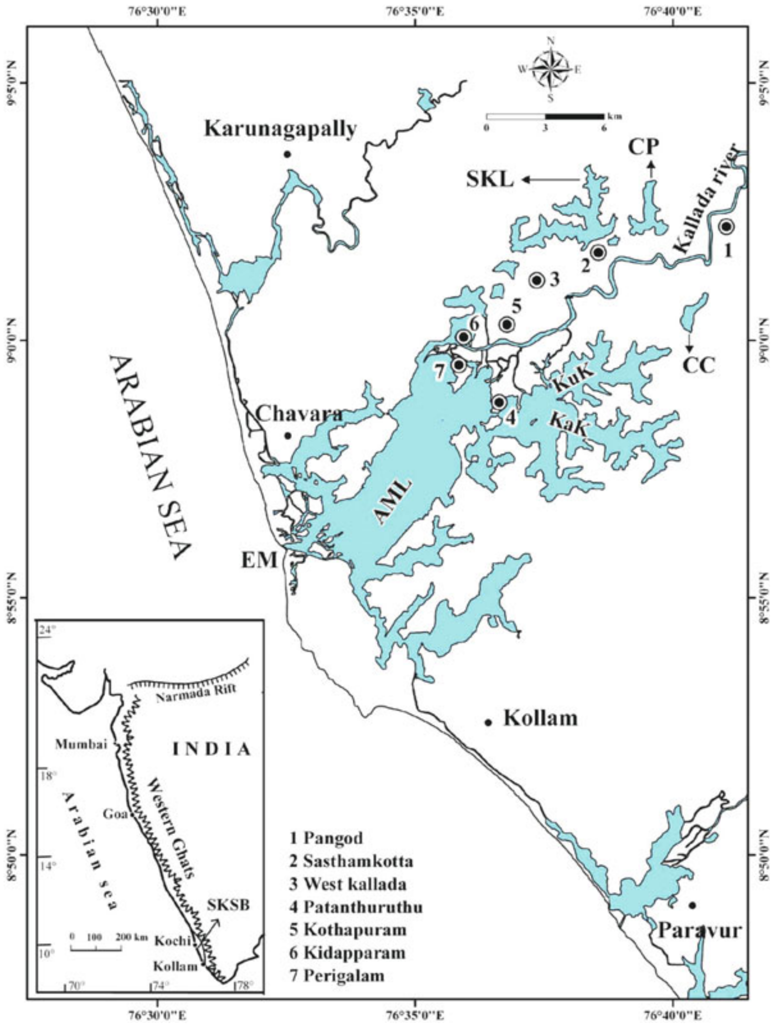

Fig. 13.1: Study area showing borehole locations.
AML: Ashtamudi lagoon; SKL: Sasthamkotta lake; CP: Chelupola; CC: Chittumala chira; Kuk: Kumbalattu *Kayal;* Kak: Kanjiramkottu Kayal; EM: Estuarine mouth.

et al., 2005; Limaye et al., 2007). South-west coast of India was affected significantly by sea level and climate changes which in turn had a strong bearing on human settlements/migration in the area. Recent advances in archaeological investigations in the Pattanam-Kodungallur stretch in Central Kerala (Shajan et al., 2004; Abraham, 2006) gave indications of shifts in human settlements in accordance with changing climates and/or sea level positions. Therefore, investigations on the Holocene deposits, that are profusely developed in the coastal lowlands of SKSB, are not only helpful in strengthening our understanding on palaeo-climate and sea level changes of the area but also useful in arriving information on how ancient human civilization responded to these millennia-scale geological events of the Holocene epoch.

Among the various sedimentary archives, deltas are one of the important environments that have a better preservation potential for climatic and sea level records. Delta is a discrete bulge of shoreline formed at a point where a river meets with a standing body of water. It occurs in a wide variety of sizes ranging from basin scale covering thousands of square kilometres to smaller components of depositional systems like lagoons and estuaries with a few square kilometres of aerial extent (Bhattacharya, 2003). Although the Indian subcontinent is endowed with many deltas of variable dimensions, the south-west coast is generally believed to be free of deltaic deposits because of the strong monsoon generated ocean currents, longshore drifts and sea waves. However, recent reports reveal the occurrence of delta in the river confluence zones of some of the medium sized rivers with the receiving coastal waters (Narayana et al., 2001). Here we report the occurrence of a Holocene bay head delta from the confluence of the River Kallada with the Ashtamudi lagoon, a coast perpendicular semi-enclosed basin in the Southern Kerala (south-west India). An attempt has also been made to unravel the palaeo-climatic and sea level changes in the Holocene epoch during which the delta has been built up at the head of the Ashtamudi lagoon.

STUDY AREA

The study area (Fig. 13.1) falls within the downstream side of Kallada river basin. It forms the northern part of Kollam district and extends from the coast to about 20 km inland. The area is bounded between latitudes 8°45′ -9°05′N and longitudes 76°25′-76°45′E and is generally undulating with low altitude hillocks and hill ranges of 10-40 m elevation interspaced by broad valleys and wetlands. Hillocks that bound the lake basins show moderate to steep slopes. Quaternary sediments occur in areas close to the Kallada river and are nearly flat or very gently sloping lands. Stratigraphically, the area is made up of three major lithological formations such as Archaean crystallines, Tertiary and Quaternary sedimentary sequences (Table 13.1). Archaean crystallines, represented by garnet-biotite gneisses, khondalites and charnockites, are dominant in the eastern and south-eastern parts of the Kallada basin (GSI, 1995). Only a part of the crystallines is seen in the mapped area (Fig. 13.2). Tertiary sediments are represented by Quilon and Warkalli Formations of Early Miocene age. Warkalli Formation is composed of sandstones and clay and seen exposed on the laterite hillocks surrounding the lakes. Quilon Formation, occurring below the Warkalli Formation, is represented by fossiliferrous limestone and sandy carbonaceous clays.

Table 13.1: Stratigraphic sequence of Kerala

Quaternary	Vembanad formation	Sands, clays, molluscan shell beds, riverine alluvium and floodplain deposits.
	Quilon formation	Limestone, marls, clays/ calcareous clays with marine and lagoonal fossils.
Tertiary	Vaikom formation	Sandstones with pebbles and gravel beds, clays and lignite and carbonaceous clay.
Mesozoic to Archaean	*Intrusives:* Veins of quartz, pegmatites, granites, granophyres, dolerite and gabbro.	
	Garnet sillimanite gneiss, hornblende-biotite gneiss, garnetbiotite gneiss, quartzo-feldspathic gneiss, charnockites, charnockite gneiss, etc.	

Modified after Najeeb, 1999.

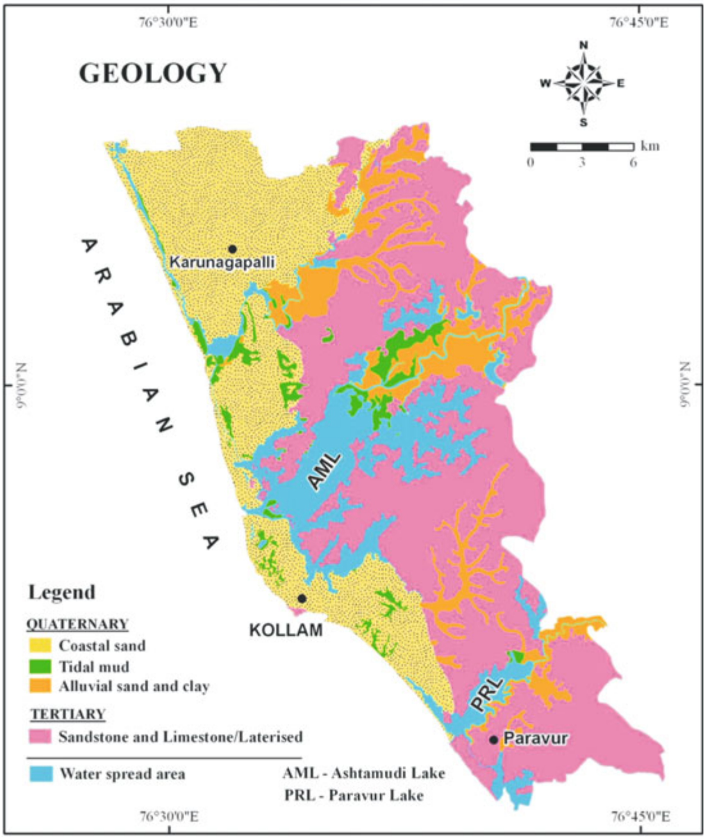

Fig. 13.2: Geological map of the study area (after GSI, 1995).

Quaternary deposits are represented by alluvial clays, sandy clays and peat on the south-eastern side of the lake.

MATERIALS AND METHODS

A detailed fieldwork was carried out in the Ashtamudi and Sasthamkotta lake basins as well as the downstream reaches of Kallada river. A total of seven undisturbed borehole cores were collected from the study area by rotary drilling (Fig. 13.1). Sediment samples were subjected to textural and heavy mineralogical studies following standard methods (Lewis, 1984; Mange and Maurer, 1992). Ternary diagram of Picard (1971) is used for the classification of sediments. Organic matter rich sediments from three selected borehole cores (BH1 from the upstream end, BH3 from the central zone and BH4 from one of the prograding downstream end) were subjected to palynological examinations. Samples for recovering palynomorphs were processed by conventional methods of separating organic walled microfossils from that of sediments (Traverse, 2007; Faegri and Iversen, 1989; Moore et al., 1991). Pollen, spores and Non Pollen Palynomorphs (NPP) were identified using the available database and published records (Limaye et al., 2007; Thanikaimoni et al., 1984; Thanikaimoni, 1987). Radiocarbon (C^{14}) dates of a few samples of subfossil wood and sediments at specific levels were determined at Birbal Sahni Institute of Palaeobotany, Lucknow (India) and these dates are non-calibrated ages. A few selected samples from the Pangod (BH1) and West Kallada borehole cores were subjected to stable isotopic estimations of carbon ($\delta^{13}C_{org}$) and nitrogen ($\delta^{15}N$) in Center for Tropical Marine Ecology (ZMT), Bremen (Germany) using a Finnigan Delta Plus Mass Spectrometer after high temperature combustion in a flash 1112 Elemental Analyser following standard procedures (Jennerjahn et al., 2004; Jennerjahn et al., 2008). The standard deviation of replicate measurements was 0.2% for both $\delta^{13}C_{org}$ and $\delta^{15}N$.

LITHOLOGY AND SEDIMENT TEXTURE

The sand, silt and clay contents and sediment types of the major sedimentary sequences of the borehole cores are depicted in Table 13.2. Lithological characteristics of borehole cores retrieved from the onland part of the Kallada Bay Head Delta are presented in Fig. 13.3. Borehole core BH1 collected from Pangod is composed of 6 m thick silt and clay dominated sediments followed by a light grey, medium to fine grained sand. The top 3 m thick portion of the upper part is yellowish brown and with substantially low content of organic carbon (0.12%). Contrary to this, the bottom greyish black portion registers markedly high content organic carbon (6.05%). Further, the bottom-most part of the layer is intervened by thin, often lenticular sand layers. Organic rich layer contains subfossil logs of wet ever green and semi

Table 13.2: Textural and geochemical characteristics of borehole sediments

Borehole/Location	*Depth(m)*	*Sand(%)*	*Silt(%)*	*Clay(%)*	*C_{org}(%)*	*C_{inorg}(%)*	*Sediment type*
Pangod (BH1)	0-3	21.62 - 46.70 (36.13)	17.74 - 34.39 (27.88)	22.63 - 46.95 (35.99)	0.02 - 0.22 (0.12)	0.23 - 0.48 (0.37)	Clayey and sandy mud
	3-4	5.67 - 32.08 (17.59)	50.96 - 63.84 (57.08)	16.95 - 37.90 (25.33)	6.05 - 6.05 (6.05)	0.06 - 0.06 (0.06)	Clayey and sandy silt
	4-5	31.33 - 59.33 (44.13)	23.41 - 42.53 (34.09)	16.33 - 27.41 (21.79)	2.05 - 7.04 (3.79)	0.12 - 0.47 (0.29)	Silty and sandy mud
	5-8.5	72.62 - 82.87 (77.37)	8.36 - 14.99 (11.82)	8.77 - 12.49 (10.85)	0.87 - 4.32 (2.85)	BDL	Silty sand and sand
Sasthamkotta (BH2)	0.75-3	8.78 - 21.38 (13.53)	27.94 - 32.66 (30.01)	50.68 - 59.81 (56.42)	0.15 - 0.28 (0.21)	BDL - 0.72 (0.35)	Silty clay
	3-10.5	84.40 - 94.31 (91.92)	3.42 - 12.29 (6.39)	0.30 - 3.31 (1.69)	0.15 - 1.9 (0.76)	BDL - 3.40 (0.65)	Sand
	10.5-11	20.83 - 20.83 (20.83)	44.86 - 44.86 (44.86)	34.31 - 34.31 (34.31)	7.17 - 7.17 (7.17)	3.91 - 3.91 (3.91)	Silty mud
	11-14	3.12 - 3.56 (3.34)	50.20 - 50.64 (50.42)	46.24 - 46.47 (46.36)	6.99 - 7.14 (7.07)	BDL - 4.12 (2.06)	Clayey silt
	14-18	6.40 - 10.87 (8.61)	34.28 - 40.18 (37.11)	51.21 - 59.14 (54.39)	7.41 - 7.76 (7.60)	BDL - 2.12 (0.62)	Silty clay
	18-19.5	36.65 - 43.71 (40.18)	5.35 - 5.59 (5.47)	50.86 - 57.55 (54.21)	0.21 - 0.29 (0.25)	BDL - 2.61 (1.31)	Sandy clay
	19.5-20	66.50 - 66.50 (66.50)	8.73 - 8.73 (8.73)	25.67 - 25.67 (25.67)	0.15 - 0.15 (0.15)	0.42 - 0.42 (0.42)	Clayey sand

(*Contd*)

Table 13.2: (*Contd*)

West Kallada (BH3)	0-10	80.61 - 95.02 (90.43)	2.68 - 14.08 (6.54)	1.72 - 5.31 (3.03)	0.23 - 0.73 (0.41)	0.72 - 0.74 (0.73)	Sand
	10-17	2.31 - 12.52 (5.73)	53.85 - 59.37 (56.03)	28.11 - 43.84 (38.24)	5.60 - 8.45 (6.77)	BDL - 0.37 (0.18)	Clayey silt
	17-18.5	9.26 - 9.26 (9.26)	46.05 - 46.05 (46.05)	44.69 - 44.69 (44.69)	5.69 - 5.69 (5.69)	BDL	Silty mud
	18.5-24	0.19 - 4.57 (2.48)	60.93 - 70.53 (64.38)	25.64 - 38.12 (33.14)	4.55 - 6.06 (5.21)	BDL	Clayey silt
	24-27	53.44 - 68.19 (60.82)	7.01 - 8.78 (7.89)	23.03 - 39.55 (31.29)	0.25 - 0.25 (0.25)	BDL	Clayey sand
Pattamthuruthu (BH4)	0-2	14.56 - 14.56 (14.56)	40.15 - 40.15 (40.15)	45.29 - 45.29 (45.29)	6.49 - 6.49 (6.49)	0.35 - 0.35 (0.35)	Clayey mud
	2-6	81.90 - 91.52 (85.07)	3.80 - 13.61 (9.34)	4.49 - 6.79 5.59	0.88 - 1.60 (1.29)	0.35 - 1.48 (0.58)	Sand
	6-14	5.62 - 38.25 (15.23)	26.40 - 48.74 (40.09)	23.46 - 56.26 (44.68)	4.44 - 7.29 (5.46)	0.12 - 2.29 (0.94)	Silty, sandy mud and silty clay
	14-15	7.29 - 89.10 (48.19)	6.05 - 40.36 (23.21)	4.85 - 52.36 (28.61)	1.31 - 5.65 (3.48)	0.12 - 0.75 (0.44)	Sand
Kothapuram (BH5)	0-1	16.47 - 16.47 (16.47)	50.74 - 50.74 (50.74)	32.80 - 32.80 (32.80)	10.06 - 10.06 (10.06)	0.75 - 0.75 (0.75)	Clayey silt
	1-6	83.94 - 88.06 (86.58)	5.41 - 9.61 (7.70)	2.33 - 7.30 (5.73)	0.13 - 2.90 (1.49)	BDL - 1.59 (0.52)	Sand

(*Contd*)

Table 13.2: (*Contd*)

Borehole/Location	*Depth(m)*	*Sand(%)*	*Silt(%)*	*Clay(%)*	*C_{org}(%)*	*C_{inorg}(%)*	*Sediment type*
Kidapparam (BH6)	0-2.5	15.47 - 45.04 (30.26)	23.78 - 40.31 (32.04)	31.18 - 44.22 (37.70)	1.62 - 2.82 (4.22)	BDL - 0.75 (0.36)	Sandy and clayey mud
	2.5-4.5	56.94 - 68.32 (63.06)	20.47 - 23.21 (22.30)	11.21 - 19.85 (14.65)	1.74 - 3.99 (3.19)	BDL - 0.12 (0.04)	Silty sand
	4.5-6	79.31 - 83.64 (81.48)	7.80 - 10.77 (9.29)	8.56 - 9.92 (9.24)	1.29 - 1.96 (1.63)	BDL - 0.12 (0.06)	Sand
Peringalam (BH7)	0-2	70.06 - 72.25 (71.16)	10.30 - 14.04 (12.17)	13.71 - 19.64 (16.68)	1.50 - 3.25 (2.38)	BDL	Clayey and silty sand
	2-5.5	51.18 - 81.97 (68.19)	10.14 - 25.41 (17.66)	7.79 - 23.41 (14.13)	1.45 - 4.13 (2.88)	BDL - 0.48 (0.18)	Sand and silty sand
	5.5-6	33.31 - 33.31 (33.31)	30.66 - 30.66 (30.66)	36.03 - 36.03 (36.03)	5.02 - 5.02 (5.02)	BDL	Clayey mud

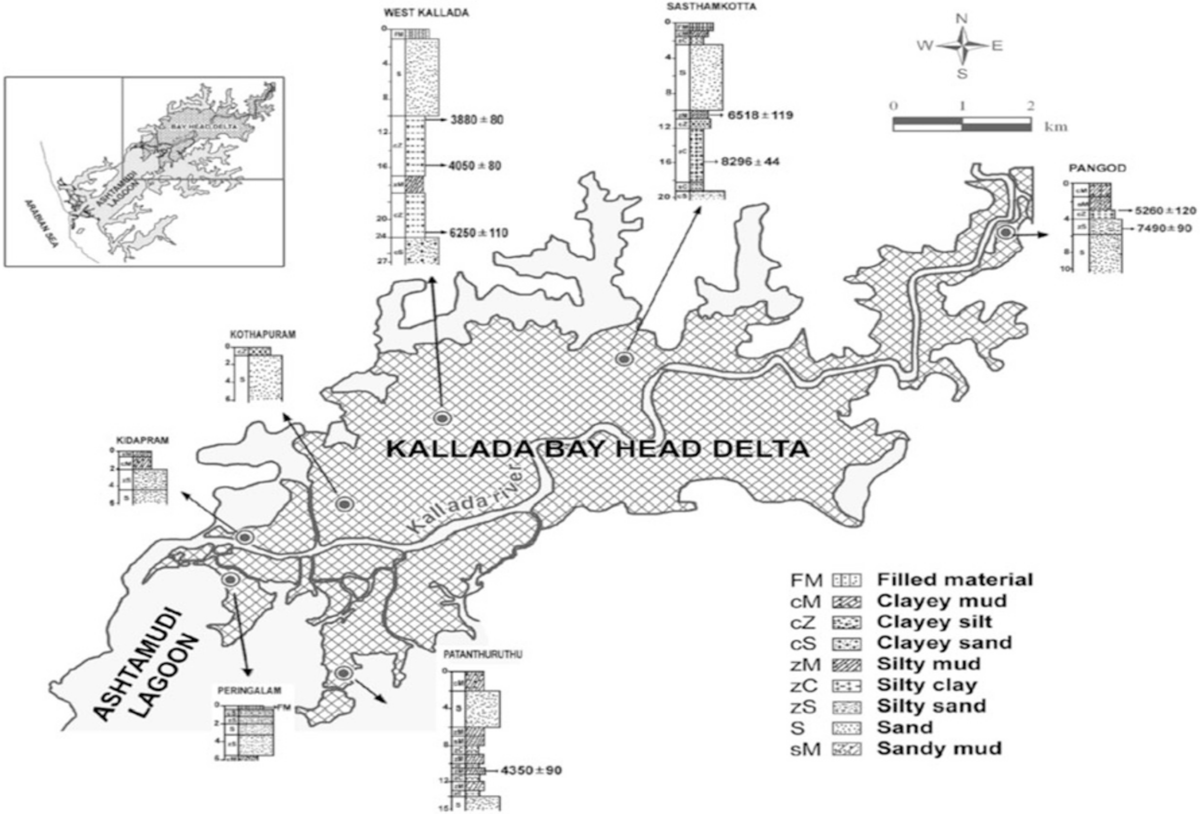

Fig. 13.3: The Kallada Bay Head Delta (KBHD) developed in the head of the Ashtamudi lagoon, showing the subsurface lithology and C^{14} ages. Depth of the borehole cores are given in metres.

ever green vegetation comprising *Dipterocarpus, Hopea, Shorea, Pterocarpus, Canarium, Artocarpus, Toona, Mangifera, Cullenia* and several unclassified plants (Kumaran and Nair, 2005). A wood sample collected at 3 m bgl is C^{14} dated 5260±120 Yrs BP. Interestingly, the C^{14} dates of a wood sample and the embedding sediment at 5 m bgl gave almost similar C^{14} ages of 7490±90 Yrs BP and 7480±80 Yrs BP, indicating quick burial of vegetative remains under sediments brought from the uplands.

The borehole BH2 (Sasthamkotta borehole) is 18 m long whose upper 3 m portion is similar to that of the borehole BH1 in its physico-chemical characteristics. It is followed successively by 7.5 m thick, light grey, medium to fine grained, poorly sorted sand and 8.5 m thick organic matter rich, stiff clay with occasional presence of gastropods (*Terrebra* sp) and pelecypods (*Paphia* sp). The entire sequence rests unconformably over a light grey, sand dominant layer often with yellowish brown patches. Sand in this layer is medium to fine grained, poorly sorted and devoid of any body fossils. Average organic carbon contents are 0.21% in the yellowish brown top layer, 0.76% in the sand, 7.36% in the mud/clay dominated sediments and 0.2% in the bottom grey clay. Two sediment samples collected at depths of 10.5 m bgl and 16 m bgl are C^{14} dated 6518 ± 119 Yrs BP and 8296 ± 44 Yrs BP, respectively.

The borehole BH3 is sited near West Kallada and has a length of 27 m. The borehole core begins with a light grey, coarse to fine grained, poorly sorted sand, which is followed downward by 16 m thick, greyish black, organic matter-rich, clayey silt with 6.77% of organic carbon. Lithounit is inter-bedded at 17-19 m level by a silty mud with almost similar megascopic properties as that of the clayey silt. Silty mud and the underlying clayey silt contain occasional presence of shell dusts indicating marine influence. The entire sequence lies unconformably over a greyish white, sand dominant layer with occasional yellowish brown patches. This layer could be correlated with the bottom layer of BH2. Organic carbon content is substantially higher in the middle clayey silt (5.89%) than that of the upper (0.41%) and lower (0.25%) sand dominated layers. The organic carbon rich layer at 10.5 m, 15.9 m and 25.5 m levels are C^{14}dated 3880±80 Yrs BP, 4050 ± 80 Yrs BP and 6250 ± 110 Yrs BP, respectively.

The 15.5 m long borehole core (BH4) recovered from the Pattamthuruthu is composed of silt and clay dominated sediments inter-layered at 2-6 m and 14-15 m levels by medium to fine grained sand dominated layers. Organic carbon-rich (5.98%), clay dominated sediment is embedded occasionally by calcareous nodular bodies (algal pisolites?) of different sizes and shapes. In thin section these nodular bodies exhibit occurrence of forams, spicules, plant remnants, detrial grains etc. A sediment sample at 11 m level is C^{14} 4350±90 Yrs BP.

The Kothapuram borehole core (BH5) is only 6 m long and made up essentially of two lithounits, an upper one metre thick greyish black, organic matter rich, clayey silt and lower coarse to medium grained, poorly sorted sand. Organic carbon content accounts for 10.06% in the upper clayey silt layer and 1.49% in the lower sand layer. Lithologically, the borehole core BH6, recovered from Kidapparam, is also similar to that of BH5, as it has organic-rich upper silt and clay apron and lower coarse to medium grained sand. Borehole core collected from Peringalam (BH7) is 5.8 m thick and composed of coarse to fine grained sand lying over a clayey mud. Organic carbon content accounts for 2.63% in the sand dominant layer and 5.02% in the mud dominated lower layer. The shallow borehole cores BH5-BH7 do not contain any visible presence of shells or shell dusts in their different lithounits.

PALYNOLOGY AND MICROPALAEONTOLOGY

Out of the seven borehole cores retrieved from the KBHD, those at Pangod (BH1), West Kallada (BH3) and Pattamthuruthu (BH4) are subjected to detailed palynological analysis. Palynological preparation of BH1 contains spores of *Glomus* sp and *Ceratopteris* sp and pollen of some wet evergreen plants like *Cullenia exarillata* and members of Euphorbiaceae indicating high precipitation and atmospheric humidity that prevailed during Early Holocene. Occurrence of dinoflagellates (*Tuberculodinium vancampoae, Spiniferites* sp, *Peridinium* sp etc.) indicates tidal influence during the period 8000-6000 Yrs BP. Like the BH1, the carbonaceous clay and silt-rich sediments at West Kallada (BH3) record occurrence of evergreen elements like *Cullenia exarillata,* fungal and pteridophytic spores, indicating heavy rainfall and atmospheric humidity. At the same time, occurrence of dinoflagellates and foraminiferal linings shows tidal influence in the region.

Top-most part of the borehole core BH3 does not exhibit any evidence of marine affinity (Fig. 13.4), rather a fresh water dominant environmental setting with anthropogenic pollution as revealed by the presence of Thecamoeba in the palynological preparation. The top-most part of the Pangod (BH1) and Sasthamkotta (BH2) borehole cores is subjected to chemical weathering under exposed conditions. Palynological preparation of BH4 (Pattamthuruthu borehole) shows highly fluctuating environmental condition during the deposition of sediments. Pteridophytic spores and pollen of *Cullenia exarillata* are recorded upto 6 m below ground level (bgl). Sediment below this level is devoid of any indication of terrestrial influence, rather a prominent tidal influence is noticed as indicated by the foraminiferal linings. This together with the occasional presence of calcerous nodules having 30-50% CaO, 5-8% MgO and 15-25% SiO_2/Al_2O_3 indicate quiet, dry climate during the depositional phase in the latter part of Middle Holocene.

$\delta^{13}C$ AND $\delta^{15}N$ ISOTOPES

Information on stable isotopes of carbon ($\delta^{13}C_{org}$) and nitrogen ($\delta^{15}N$) is used widely for tracking the sources and post-depositional changes of

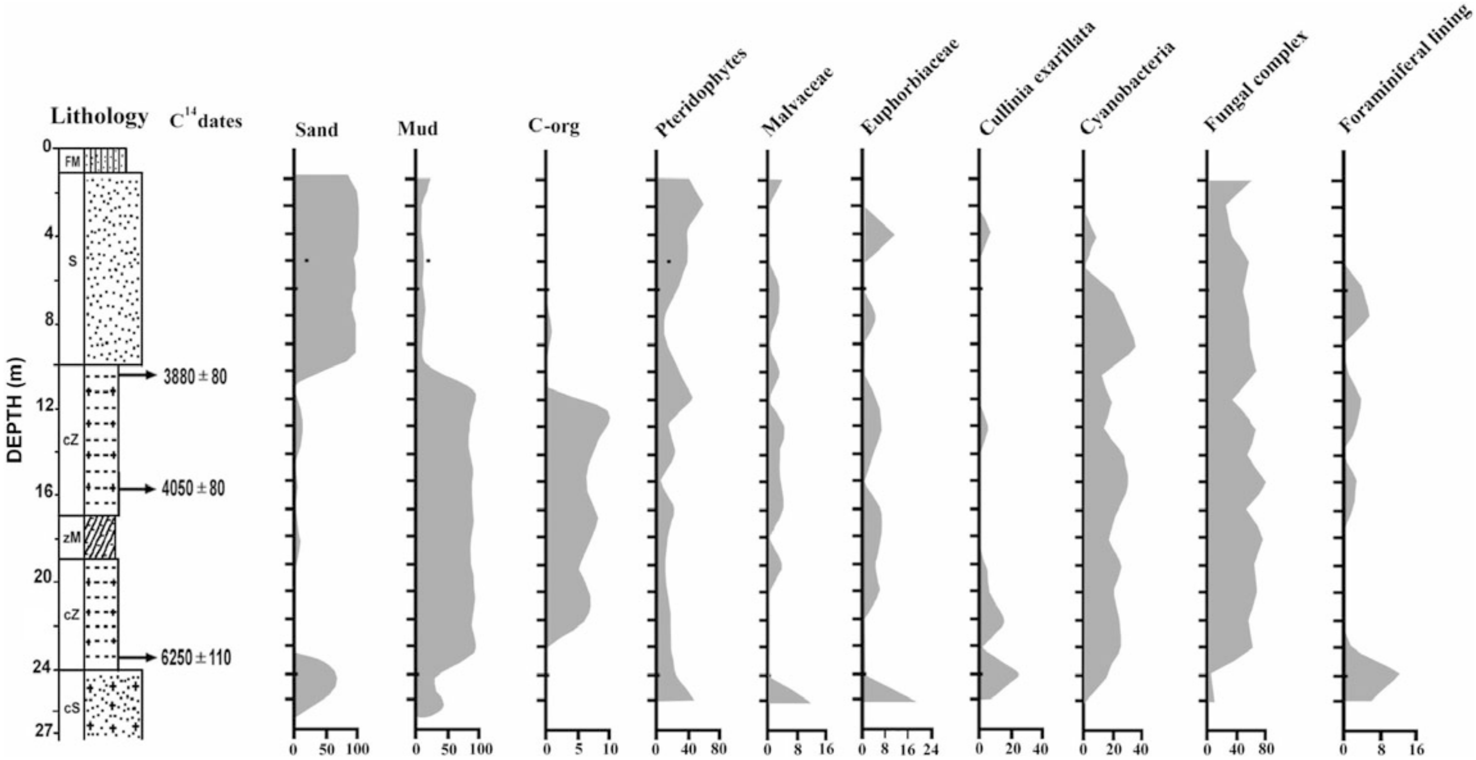

Fig. 13.4: Downcore variation of sand, mud and organic carbon along with palynological/mircro palaeontological contents in the Kallada borehole sediments. Values are given in percentages.

sediments/sedimentary rocks (Jennerjahn et al., 2004). In the present study, a total of eight samples (five from BH1 and three from BH3) was selected for $\delta^{13}C_{org}$ and $\delta^{15}N$ estimations and the results are given in Table 13.3. As seen from Fig. 13.5, it is evident that both these isotopes exhibit an increasing trend towards the top of the core. Although, the yellowish brown layer accounts for comparatively low concentration of organic carbon (0.12%) than that of the underlying carbonaceous clay (6.05%), the $\delta^{13}C_{org}$ shows an opposite trend indicating higher values towards surface (Fig. 13.5). This clearly indicates a gradual change in the depositional regime from terrestrial ($\delta^{13}C$ –28.17‰) to marine entity (–19.56‰; Fig. 13.5). It is now well understood that sediments of marine origin generally contain higher $\delta^{13}C_{org}$ values as a substantial proportion of it is evolved from marine phytoplankton having higher $\delta^{13}C_{org}$ values (Jennerjahn, 2004; Fischer, 1991).

The C^{14} age of upper-most part of the organic carbon rich layer, just below the yellowish brown silt and clay layer at 3 m bgl, is C^{14} dated 5260±120 Yrs BP. The low $\delta^{13}C_{org}$ values in the range of –28.17‰ to –26.88‰ shows that the organic input in the carbonaceous clay/peaty layer is from C3 plants that flourished in the hinterlands during Early Holocene. The $\delta^{15}N$ values vary from 3.92‰ to 8.85‰ with the highest values recorded for the top yellowish brown layer. The $\delta^{13}C_{org}$ and $\delta^{15}N$ values of the West Kallada borehole core (BH3) were –27.6‰ to –28.88‰ and 2.5‰ to 3.26‰, respectively. This clearly indicates that the West Kallada site was under lagoonal condition during Middle Holocene and received sediments from the hinterlands dominated by the C3 plants. Comparatively lower $\delta^{15}N$ value in the layer also points to the degree of preservation of organic matter derived mainly from terrigenous sources.

Table 13.3: Sand, mud, organic carbon and nitrogen contents in the sediments of Pangod borehole core along with the concentration of $\delta^{15}N$ and $\delta^{13}C_{org}$

Depth (m)	*Sand (‰)*	*Mud (%)*	*C_{org} (%)*	*Nitrogen (%)*	*$\delta^{15}N$ (%)*	*$\delta^{13}C_{org}$ (%)*
0.25	21.62	78.38	0.22	0.61	8.85	–19.56
0.75	25.28	74.72	0.15			
1.25	30.75	69.25	0.08			
1.75	43.55	56.45		0.26	7.4	–23.84
2.25	40.6	59.4	0.02			
2.75	46.7	53.3	0.07			
3.1	44.39	55.61	0.15			
3.35	5.67	94.33		0.21	4.79	–26.88
3.55	32.08	67.92		4.42	4	–27.79
3.85	15.02	84.98	6.05			
4.15	31.33	68.67		4.65	3.92	–28.17

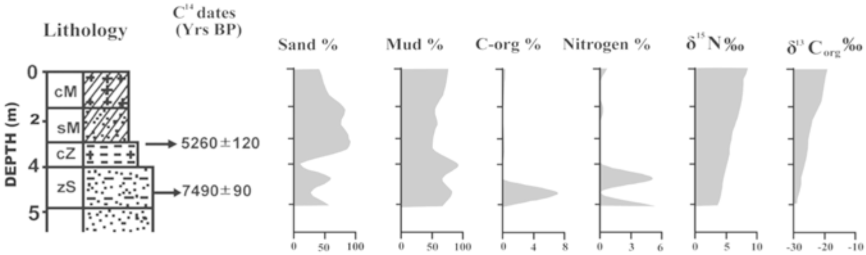

Fig. 13.5: Downcore variation of sand, mud, C_{org}, δ^{15} N and δ^{13} C_{org} contents in the Pangod borehole core.

DISCUSSION

Holocene Evolution of Kallada Bay Head Delta (KBHD)

The coastal lands of the Kallada river basin, comprising an inter-lacing network of water bodies and fluvial channels, have evolved through complex interactions of climatic and sea level processes that affected the coast during the Holocene epoch (Nair et al., 2010). In the post-glacial period, the Ashtamudi lagoon was a semi-enclosed drowned channel with about 12 branches (arms). The formation of a bay head delta in the upper part of the lagoon began in Early Holocene, as evidenced from the C^{14} age (8296±44 Yrs BP) of the Sasthamkotta borehole core (BH2). Heavy influx of terrigenous materials under the rising spells of sea levels in Early Holocene was not only responsible for the deposition of sediments in the upper end that has later evolved into the KBHD, but also responsible for the quick burial of the riparian vegetation in the area. Sea level rise has continued even in the beginning of Middle Holocene, an event that affected many parts of the tropical and subtropical coasts (Amorosi, 1999; Coe, 2002).

Over the last 5000 years, the Bay Head Delta has prograded further seaward filling up almost half of the Ashtamudi lagoon leaving some of its prominent upper arms into discrete wetland bodies like Chittumalachira, Chelupola and Sasthamkotta fresh water lake. Progradation of the KBHD and the landward development of a flood tide delta – the Ashtamudi Flood Tide Delta (AFTD) – near the estuarine mouth have resulted in the formation of a Central Basin (CB) with mud dominated sediments within the Ashtamudi lagoon (Fig. 13.6). Progradation of KBHD has slowed down considerably in the last 3-4 decades due to depletion of sediment supply from the hinterlands because of (1) trapping of sediments by the Thenmala dam in the highlands of the Kallada river basin and (2) uncontrolled instream sand and clay mining for building constructions. It is unfortunate to note that these anthropogenic processes have hindered the making of a new fresh water body – perhaps one of the largest of its kind in the west coast of India, in the place of the present Kumbalattu *kayal*-Kanjirakkottu *kayal* twin aquatic system (see Fig. 13.1) of the Kallada basin.

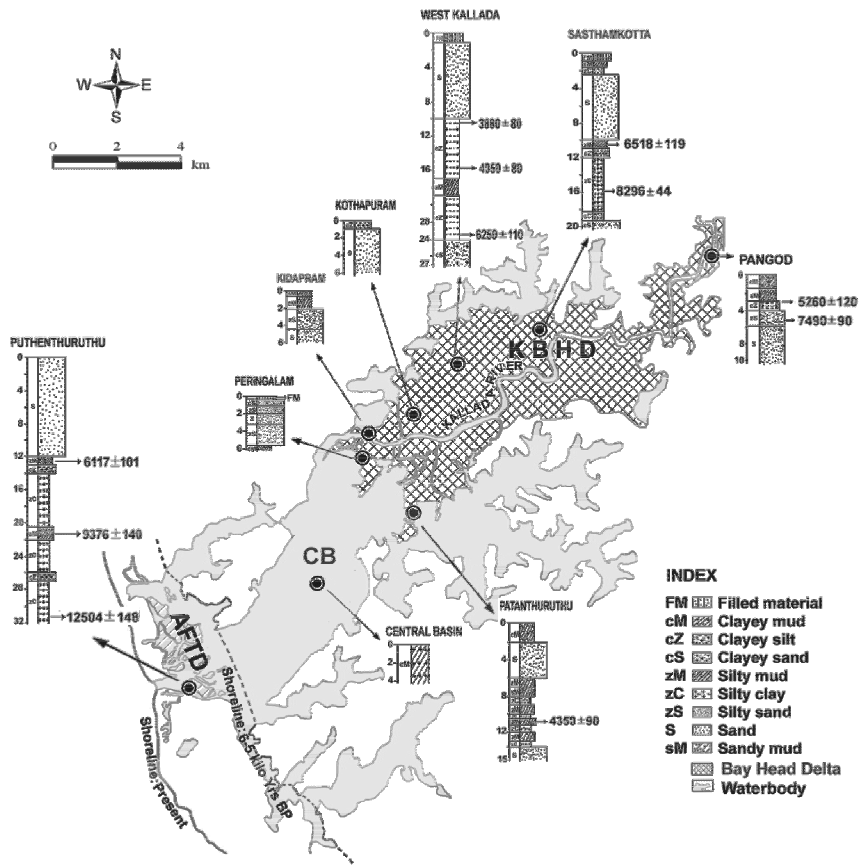

Fig. 13.6: The Kallada Bay Head Delta (KBHD) developed in the head of the Ashtamudi lagoon. Note the shoreline positions of 6-5 kilo Yrs BP and the present. AFTD: Ashtamudi flood tide delta; CB: Central basin.

Evidences of Climatic and Sea Level Changes

The sedimentary sequences as revealed by the borehole cores collected from the onland part of the KBHD register a fairly complete record of climatic and sea level changes to which the south-west coast has been subjected during Holocene epoch. As the transgression progressed in the Early Holocene, the salt water affected area of the Ashtamudi lagoon expanded further inland. Maximum sea level rise at 6000-5000 Yrs BP was responsible for the formation of silt and clay-rich top sediments of the Pangod (BH1) and Sasthamkotta (BH2) borehole cores. At this time, shoreline should have been migrated 3-4 kilometres eastwards with respect to the present coast line (Fig. 13.6), a feature also reported earlier by Nair (1996). Thereafter, the strandline system has prograded seaward and, dunes and marshes developed in the regressive phase which is characterised by substantially reduced rainfall as compared to that of the Early Holocene. The abundance of fossil/subfossil logs and heavy accumulation of sediments as revealed by the quick burial of vegetative remains mentioned earlier are some of the direct evidences of the Holocene Climatic Optimum (Nair and Kumaran, 2006; Nair et al., 2009) that the Kerala coast witnessed. Sea level lowering in the Middle Holocene might have exposed many elevated areas in the uplands of the bay head delta for sub-aerial weathering/chemical alteration. The iron bearing minerals get oxidized imparting yellowish brown colour to the sediments. Degradation of surface sediments is also reflected in the elevated $\delta^{15}N$ levels which according to Jennerjahn et al. (2004) have resulted from preferential consumption of lighter isotopes and subsequent enrichment of heavier $\delta^{15}N$ isotope in the layer. The phase was marked in the Pattamthuruthu borehole core in the form of calcareous nodules embedded within clayey sediments and also in its palynological preparations. Dry spell in the regressive phase of the Middle Holocene is followed by a wet spell with heavy input of terrigenous sediments, which was responsible for further development/growth of the Kallada Bay Head Delta in the Late Holocene.

SUMMARY AND CONCLUSIONS

The sedimentological, palynological, geochemical and stable isotopic studies ($\delta^{13}C$ and $\delta^{15}N$) of a few borehole cores collected from the onland part of the Kallada Bay Head Delta (KBDH) reveal highly varied climatic and sea level conditions during its developments. Radiocarbon dates obtained at various levels show that Early Holocene witnessed heavy rainfall and was responsible for the high influx of terrigenous sediments under a rising spell of sea level. This was responsible for the fast deposition of sediments in the river mouth areas. Similarity in the ages of a wood sample (7490±90 Yrs BP) in the Pangod borehole core (BH1) and the embedding sediments (7480±80 Yrs BP) at 5 m bgl supports the phenomena. This was followed by a regressive phase in the Middle Holocene with comparatively low rainfall and a dry spell at around 5000-4000 Yrs BP. The yellowish brown colouration of the surface layer in borehole cores BH1 (Pangod borehole) and BH2 (Sasthamkotta borehole) might have formed during this period due to oxidation of iron containing minerals under subaerial conditions. The enhanced level of δ^{15} N isotope in the surface sediments as compared to the lower organic rich layers points to degradation and preferential consumption of lighter isotopes and subsequent enrichment of heavier $\delta^{15}N$. After the dry spell, the KBHD has prograded further seaward filling up almost half of the pre-Ashtamudi lagoon leaving some of its prominent arms into discrete wetlands like Chittumalchira, Chelupola and Sasthamkotta lake.

ACKNOWLEDGEMENTS

Authors thank Centre for Earth Science Studies (CESS), Thiruvananthapuram for financial support under the PLAN 254 Scheme for carrying out this work. Thanks are also due to Dr. C.M. Nautiyal, Scientist F for C^{14} dates and Dr. K. Soman, former Head, Resource Analysis Division, CESS and Professor (Dr.) V. Ittekkot and Dr. Tim C. Jennerjahn, ZMT, Bremen (Germany) for stable isotopic estimation. DP, VMS, MK, SV and AS thank the Director, CESS for facilities, encouragement and support. KPNK and RBL thank Director, ARI, Pune for permission to publish the paper. KS thanks CUSAT for facilities.

REFERENCES

Abraham, S.A. (2006). Structuring an intensive surface survey: Strategies for investigating the early historic port site of Pattanam, Kerala. *Adharam*, **1:** 8-32.

Amorosi, A., Colalorgo, M.L., Pasini, G. and Preti, D. (1999). Sedimentary response to Late Quaternary sea-level changes in the Romagna coastal plain (Northern Italy). *Sedimentology*, **46:** 99-121.

Bhattacharya, J. (2003). Deltas and estuaries. *In:* Encyclopedia of sediments and sedimentary rocks. G.V. Middleton (ed.). Kluwer Academic Publishers.

Coe, A.L. (2002). The sedimentary record of sea-level changes. Cambridge University Press, Cambridge.

Faegri, K. and Iversen, J. (1989). Textbook of Pollen Analysis. John Wiley and Sons, Chichester.

Fischer, G. (1991). Stable carbon isotope ratios of plankton carbon and sinking of organic matter from the Atlantic sector of the Southern Ocean. *Mar. Chem.*, **135:** 581-596.

GSI (1995). Geological and mineralogical map of Kerala. Geological Survey of India, Calcutta.

Jennerjahn, T.C., Ittekkot, V., Arz, H.W., Berling, H., Patzold, J. and Wefer, G. (2004). Asynchronous terrestrial and marine signals of climate change during Henrich events. *Sci.*, **306:** 2236-2239.

Jennerjahn, T.C., Soman, K., Ittekkot, V., Nordhans, I., Sooraj, S., Priya, R.S. and Lahajnar, N. (2008). Effect of landuse on the biogeochemistry of dissolved nutrients and suspended sedimentary organic matter in the tropical Kallada river and Ashtamudi estuary, Kerala, India. *Biogeochemistry*, **90:** 29-47.

Joseph, S. and Thrivikramji, K.P. (2002). Kayals of Kerala coastal land and implication to Quaternary sea level changes. *Geol. Soc. India*, Memoir **49:** 51-64.

Kumaran, K.P.N. and Nair, K.M. (2005). Palaeoclimatic signatures in fossil woods and sub fossil logs of Kerala, Southwestern India. *Pages News*, **13:** 15-17.

Kumaran, K.P.N., Nair, K.M., Shindikar, M., Limaye, R.B. and Padmalal, D. (2005). Stratigraphical and palynological appraisal of the Late Quaternary mangrove deposits of the West Coast of India. *Quat. Res.*, **64:** 418-431.

Lewis, D.W. (1984). Practical Sedimentology. Hutchinson and Ross Publishing Company, Pennsylvania.

Limaye, R.B., Kumaran, K.P.N., Nair, K.M. and Padmalal, D. (2007). Non-pollen palynomorphs (NPP) as potential palaeoenvironmental indicators in the Late Quaternary sediments of West Coast of India. *Curr. Sci.*, **92:** 1370-1382.

Mange, M.A. and Maurer, H.F.W. (1992). Heavy minerals in colour. Chapman and Hall, New York.

Moore, P.D., Webb, J.A. and Collinson, M.E. (1991). Pollen Analysis. Blackwell Scientific Publication, Oxford.

Nair, K.K. (1996). Geomorphology and evolution of the coastal plain of Kerala. Geological Survey of India. Special Publication No. 40.

Nair, K.M. and Padmalal, D. (2003). Quaternary sea level oscillations, geological and geomorphological evolution of South Kerala Sedimentary Basin. PCR, ESS/23/VES/6/98, Report Submitted to DST, GoI.

Nair, K.M. and Kumaran, K.P.N. (2006). Effects of Holocene climatic and sea level changes on ecology, vegetation and landforms in coastal Kerala. PCR Submitted to Kerala State Council for Science, Technology and Environment (No. 56/2004/KSCSTE), GoK.

Nair, K.M., Kumaran, K.P.N. and Padmalal, D. (2009). Tectonic and hydrologic control on Late Pleistocene-Holocene landforms, Paleoforest and non-forest vegetation, Southern Kerala. PCR Submitted to Kerala State Council for Science, Technology and Environment, GoK.

Nair, K.M., Padmalal, D. and Kumaran, K.P.N. (2006). Quaternary geology of South Kerala sedimentary basin – An outline. *J. Geol. Soc. India*, **67:** 165-179.

Nair, K.M., Padmalal, D., Kumaran, K.P.N., Sreeja, R., Limaye, R.B. and Sreenivas, R. (2010). Late Quaternary evolution of Ashtamudi-Sasthamkotta lake systems of Kerala, Southwest India. *J. Asian Earth Sci.*, **37:** 361-372.

Narayana, A.C., Priju, C.P. and Chakrabarti, A. (2001). Identification of a Palaeodelta near the mouth of Periyar river in Central Kerala. *J. Geol. Soc. India*, **57:** 545-547.

Picard, M.D. (1971). Classification of fine-grained sedimentary rocks. *J. Sediment. Petrol.*, **41:** 179-195.

Shajan, K.P., Selvakumar, V. and Cheriyan, P.J. (2004). Locating the ancient Port of Muziris: Fresh findings from Pattanam. *J. Roman Archaeol.*, **17:** 312-320.

Thanikaimoni, G., Caratini, C., Venkatachala, B.S., Ramanujam, C.G.K. and Kar, R.K. (1984). Selected Tertiary angiosperm pollen from India and their relationship with African Tertiary pollen. *Travaux de la section scienti.que et Technique*, **19:** 1-93.

Thanikaimoni, G. (1987). Mangrove palynology. *Travaux de la section scienti.que et Technique*, **24:** 1-100.

Traverse, A. (2007). Palaeopalynology. Springer, The Netherlands.

CHAPTER

14

Role of Sea Level Rise on the Groundwater Quality in Coastal Areas of Sri Lanka

Ranjana U.K. Piyadasa, K.D.N. Weerasinghe[1], J.A.Liyanage[2] and L.M.J.R. Wijayawardhana[1]

Department of Geography, University of Colombo
Colombo, Sri Lanka
[1]Department of Agricultural Engineering
University of Ruhuna, Sri Lanka
[2]Department of Chemistry, University of Kelaniya
Kelaniya, Sri Lanka
ranjana@geo.cmb.ac.lk

INTRODUCTION

Coastal areas are among the world's most productive but ecologically fragile regions. Coastal groundwater is a dynamic and replaceable resource. Ground water is the largest source of fresh water available on earth, which is exploited to satisfy domestic, agriculture and industrial purposes. Ground water plays a significant role in the overall circulation of water through the hydrologic cycle. It is always considered as a readily available and safe source of water for domestic, agricultural and industrial use (Bear, 1979; Gavich et al., 1980). Groundwater will be less directly and more slowly impacted by climate change as compared to surface water, but in coastal areas ground water will be directly affected by sea level rise. Sea level rise would directly affect the coastal river basin areas and increase saline water intrusion to the coastal areas of Sri Lanka. Sea water intrusion in coastal areas of Sri Lanka cause serious problems to various sectors of natural and anthropogenic environments.

J. Sundaresan et al. (eds.), *Climate Change and Island and Coastal Vulnerability*,
DOI 10.1007/978-94-007-6016-5_14, © 2013 Capital Publishing Company

Rainfall is the principal natural source of groundwater recharge in Sri Lanka. Quantification of rate of this natural recharge and quality of water is a prerequisite for optional development and management of ground water resources. Most of the people of coastal regions of Sri Lanka depend on groundwater for drinking and domestic purpose. However, fresh water availability in these wells especially in coastal and shallow water table areas is rapidly declining. Coastal aquifers of southern Sri Lanka experience severe degradation of water quality due to various anthropogenic activities. Coastal groundwater resource was contaminated by the December 26th tsunami and the majority of wells used for drinking water became salty and unusable (Piyadasa, 2004). Studies in Matara district indicated that heavy rain spells had no impact on the change of groundwater quality in some locations (Piyadasa et al., 2006). However in some locations quality of ground water has gradually improved. Increment of electrical conductivity after precipitation is associated with dissolving accumulated salt in the unsaturated (aeration) zone, with the downward flux. Hence present study was conducted with the objective to investigate the water quality dynamics in the Matara coastal and inland areas and its distribution with atmospheric precipitation.

MATERIAL AND METHOD

The study was conducted in the Matara town area which is bound by latitudes 5°56′37″ and 5°57′36″ N and longitudes 80° 32′ and 80°33′12″E (Fig. 14.1). Matara is situated 150 km south to Colombo, the capital of Sri Lanka. Study area is relatively flat and gently seaward sloping. Elevation and topographic relief generally increases towards inland from the coastal line. Matara district falls within the DL3 agro-ecological region which is defined as an area where 75% of the annual rainfall exceeds 580 mm. North-western region of

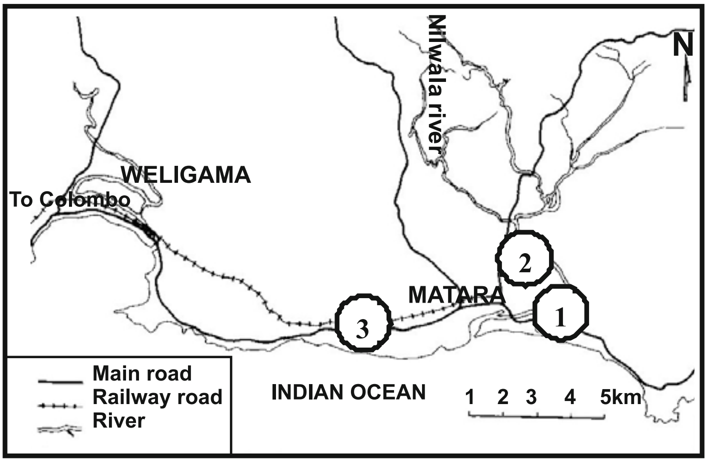

Fig. 14.1: Matara town area and selected monitoring sites.

study area receives an annual average of 1000 to 1250 mm range and the annual rainfall for Matara is 1167 mm. Study area receives rainfall from both southwest monsoon (April-May to Aug-September "*Yala season*") and the north-west monsoon (October-December to March-April "*Maha season*").

Precambrian metamorphic hard rock covered by quaternary sedimentary deposits is dominant in the study area (Cooray, 1984). The top unconfined alluvium aquifer is distributed in the Nilwala river area. In general, the aquifer consists of calcified sand and sandstone is dominant. Top quaternary sandy aquifer and the surface soils of the coastal margin of Matara town area are mostly permeable due to the sandy condition. Hydro-geological conditions are very favourable for saltwater intrusion; therefore, along the coastal belt, alluvial and coastal sand deposits are dominating and forming higher-yielding local aquifers.

A network of 66 dug wells distributed over the Matara town area was selected for the present study. Dug wells were distributed in approx 9 km^2 area within the Matara city. Three sites on the Matara coast were selected for the monitoring programme: (1) Sandwich area in between Nilwala river and sea; (2) countryside of the Matara town and Nilwala river bank area; and (3) Tsunami affected coastal area very close to the sea. Dug wells in each sites were selected maintaining equal distance between two wells which was generally 50-100 m. Continuous monitoring of the water levels in each well have been conducted in the end of 2^{nd} week of each month from December 2006 to May 2007. Groundwater monitoring conducted with respect to electrical conductivity (EC), total dissolved solids (TDS), salinity (SAL) and pH were measured using portable EC/pH meters. Rainfall data were obtained from the nearest meteorological station located in study area (maintained by Agriculture Department, Matara, Sri Lanka).

RESULTS AND DISCUSSIONS

Majority of the dug wells examined are shallow in a 1-6 m depth range (Table 14.1). However, more than 75% of the total wells had a depth of 2-4 m. Dug wells of the coastal belt and the wells sandwiched between the coastal line and the Nilwala river and tsunami affected coastal area are very close to sea. They are very shallow, at a 1-3 m depth range. Dug wells constructed in Nilwala river basin area, in the countryside of the Matara town, are very shallow. These well are constructed in alluvial sand deposit.

As per the diameter, most wells were in a 1-1.5 m range (Table 14.2). From the depth diameter classes, it is evident that seawater intrusion to the aquifer through the inundation of wells may cause little damage. However, infiltration and percolation through the top sandy soil may have a more contribution of seawater into the coastal aquifer. Submergence and flooding during the tsunami may have also caused a deposition of salts on the unsaturated zones of the soils which may have subsequently leached down to the saturated zone.

Table 14.1: Depth of the wells in the study area

Depth of the dug wells	*No. of wells*
0-1	2
1-2	3
2-3	25
3-4	27
4-5	5
> 5	4

Table 14.2: Diameter of the wells in the study area

Diameter of the dug wells	*No. of wells*
0-0.5	1
0.5-1.0	28
1.0-1.5	25
1.5-2.0	8
2.0-2.5	3
> 2.5	1

Electrical conductivity (EC) of the Matara town area is in the range of 316 to 1980 µSiemens/cm (Fig. 14.2). Ground water in 69% of the dug wells are within the acceptable level of the drinking water quality. In 21% of the wells EC levels are exceeding the World Health Organisation (WHO) standard for drinking water quality (WHO EC standard for drinking water quality is below 1000 µSiemens/cm).

In case of the pH level of the unconfined aquifer in coastal areas of Matara town, most of the wells observed acceptable range of drinking water standards as per the WHO guidelines. The pH levels in the study area is in the range of 6 to 8. But about 8% of monitoring wells recorded pH level above 8 (Fig. 14.3). The observed EC and pH values of the Matara town area revealed that ground water is a reliable source for drinking and other domestic purposes.

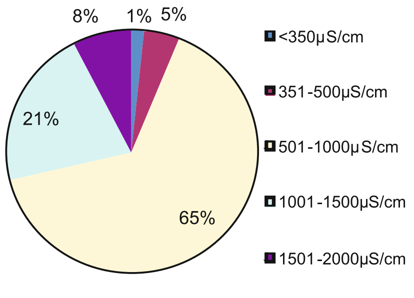

Fig. 14.2: EC distribution in shallow dug wells water in Matara town area.

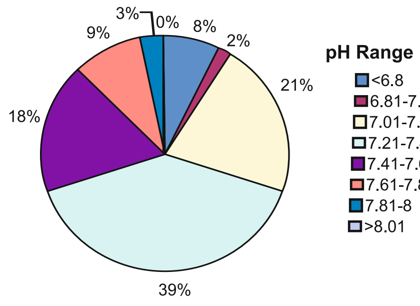

Fig. 14.3: Groundwater pH distribution in Matara town area.

Average EC variation in all monitoring wells was in the range of 703 to 1109 µS/cm but maximum number of EC values were in between 1278 to 1980 µS/cm (Table 14.3). Site 2 is located in countryside of the Matara town and Nilwala river bank area. During the dry periods, tidal saline water intrusion traverses in the upstream direction through the river. With the lowering of the river water level in dry months tidal water tends to flow into the country along the course of the Nilwala river. The seas around Sri Lanka are micro-tidal by world standards. The tidal range is within 75 cm at spring tide and 25 cm at neap tide (Panaboke, 1996).

Groundwater EC distribution in site 2 varies from 491 to 1075 mS/cm (Table 14.3). Due to salinity intrusion in the river, southern part of the area EC values exceed the 1000 mS/cm. Most of the Nilwala basin area remains within the accepted Sri Lankan standards for drinking purposes (1500 mS/cm). EC values are high near the river and it reduces with the increase of distance from the river.

Precipitation is one of the most important factors that is linked to groundwater regime in the study area. Graphs were prepared to compare rainfall with EC and pH. It demonstrates that due to increase of rainfall unconfined groundwater level increases and with a decrease in rainfall the unconfined groundwater level decreases.

Groundwater quality in site 3 observed high average EC values (1109 µS/cm) in comparison with other two sites. The site 3 wells are located in the coastal belt and in the affected region of Asian tsunami in 2004. Earlier studies immediately after the tsunami showed that the groundwater resources were seriously damaged by saline water intrusion upto 1.5 km from the coast line in the aquifers in southern Sri Lanka (Piyadasa, 2005). Consequently EC values increased up to 7000 µS/cm in some wells near the coastline and with the subsequent precipitation EC values decreased marginally. Significant changes in EC of the groundwater appears with precipitation as depicted in Fig. 14.4. In location 3 high EC values (1500 µS/cm) received close to the sea and those wells are directly affected by tsunami. The high precipitation (265 mm) in January 2007 resulted in significant increase in EC values in the following month. It's associated with low recharge of fresh water from inland area and the salinity intrusion progressing towards coastal aquifers.

Table 14.3: Statistics of EC values in monitoring sites 1, 2 and 3

Monitoring sites	*Average EC (µS/cm)*	*Maximum EC (µS/cm)*	*Minimum EC (µS/cm)*
Sandwich area in between Nilwala river and sea (site 1)	703	1278	316
Countryside of the Matara town and Nilwala river bank area (site 2)	698	1075	491
Tsunami affected coastal area very close to the sea (site 3)	1109	1980	579

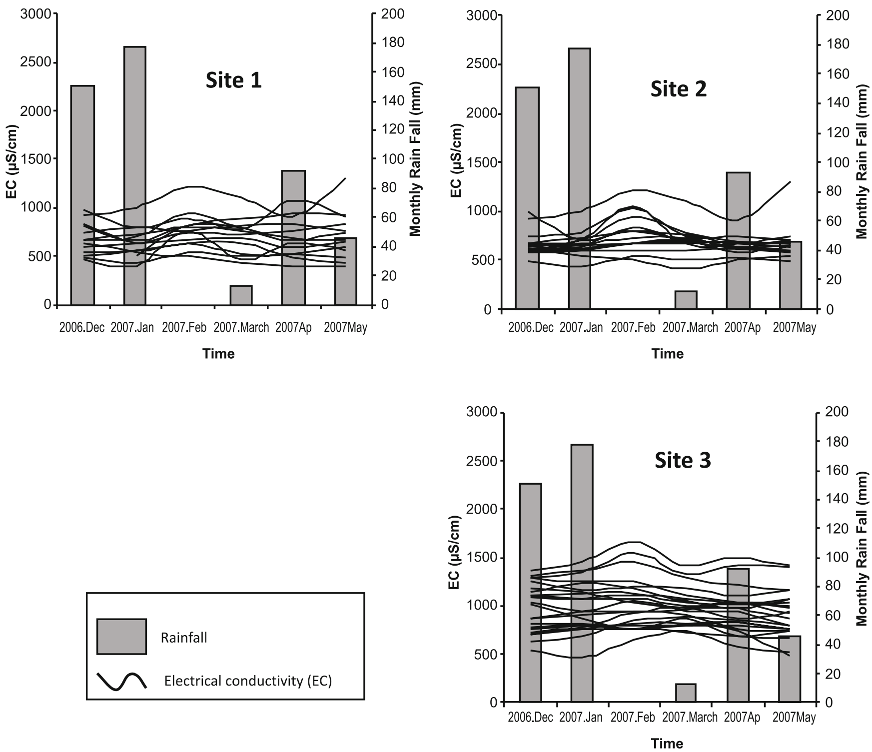

Fig. 14.4: Electrical conductivity changes with respect to time in the three study sites.

Averages of EC values for other two locations were 703 µS/cm and 698 µS/cm. Because of this it can be concluded that the unconfined aquifer of the studied area is deficient of good quality water and it cannot be used for drinking purposes except one well which is located in cluster 3 area. The graphs were used to illustrate the relationship between atmospheric precipitation, electrical conductivity and pH level separately for each of the three clusters during the study period (Figs 14.4 and 14.5).

The pH values are not changing significantly throughout the monitoring period and changes are in the range of 6 to 8. Therefore, there is an existing intimate relation between atmospheric precipitation and unconfined groundwater level in the quaternary aquifer.

CONCLUSIONS

In the study area EC and pH of the groundwater resources are identified to be static and lie below WHO and Sri Lankan standards for drinking water, and as such it is a reliable source to meet the water demands of the population. But in the cluster one where dug wells are located in close proximity to

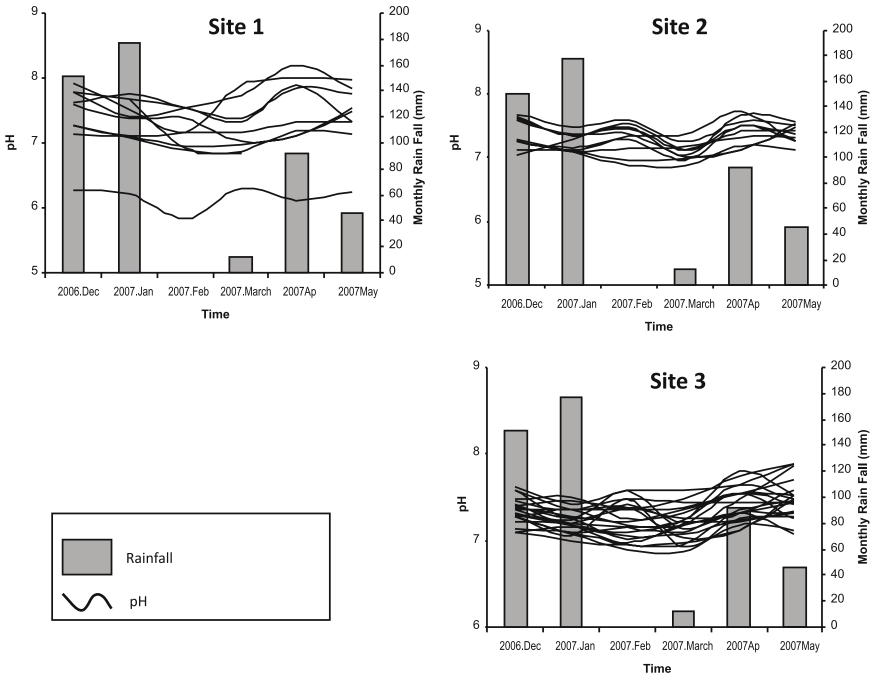

Fig. 14.5: pH changes within the three cluster areas.

coastal areas, EC values are relevantly high. It shows that sea level rise directly affect the river basin areas and increase sea water intrusion in the coastal areas. Regime of unconfined quaternary aquifer groundwater level is intimately related to atmospheric precipitation. characteristic of the hydrograph elucidates that the recharge of unconfined groundwater in quaternary aquifer takes place during the rainy period.

ACKNOWLEDGEMENT

Authors acknowledge the financial assistance from National Science Foundation. Authors wish to acknowledge the work of G. Gamage, Chathura Weerasinghe, Ruwan Sampath, Moreau Yoann (France) and Dupin Maxime (France) for their active involvement with the research programme on groundwater study in Tsunami affected areas of the Southern coastal belt.

REFERENCES

Bear, J. (1979). Hydraulics of groundwater. McGraw-Hill, New York.

Cooray, P.G. (1984). The Geology of Sri Lanka. National Museum of Sri Lanka Publication, Colombo.

Gavich, E.K., Lysbewa, A.A. and Semionowa, A.A. (1980). Practical Problems in Hydrogeology. Headra, Moscow.

Weerasinghe, K.D.N., Piyadasa, R.U.K., Kariyawasam, I.S., Pushpitha, N.P.G., Vithana, S.B., Kumara, D.S.E., Wijayawardhana, L.M.J.R., Schwinn, P., Gruber, M., Maier, M. and Maier D. (2006). Well water quality in tsunami affected areas and their purification by reverse osmosis – A case study, after the tsunami rehabilitation in Sri Lanka. Mosaic Books, New Delhi, India.

Manfred Domroes (2006). Tsunami Catastrophe in Sri Lanka – Its Dimension, Relief and Rehabilitation. Mosaic Books, New Delhi, India.

Panaboke, C.R. (1996). Our Engineering Technology. The Open University Review of Engineering Technology, **2(1):** 17-19.

Panabokke, C.R. and Perera, A.P.G.R.L. (2005). Groundwater Resources of Sri Lanka. Water Resources Board, Colombo. Sri Lanka.

Piyadasa, R.U.K., Weerasinghe, K.D.N., Harsha Kumara, P.W. and Maier, D. (2006). Groundwater distribution and quality characteristics in the right bank of Nilwala ganga (Badulla oya and Kirama oya basins), Sri Lanka. Third National Symposium on Geo-Informatics.

Piyadasa, Ranjana U.K., Weerasinghe, K.D.N. and Liyanage, Janitha A. (2006). Impact of Tsunami wave on the groundwater quality of the Weligama bay, Southern Sri Lanka, After the tsunami rehabilitation in Sri Lanka. Mosaic Books, New Delhi.

CHAPTER

15

Mangrove Responses to Climate Change along the Southwestern Coast of India during Holocene: Evidence from Palynology and Geochronology

K.P.N. Kumaran, Ruta B. Limaye and D. Padmalal[1]

Palynology and Palaeoclimate Laboratory, Palaeobiology Group
Agharkar Research Institute, Pune – 411004, Maharashtra, India
[1]Centre for Earth Science Studies, Thiruvanthapuram 695031, India
kpnkumaran@hotmail.com

INTRODUCTION

Mangrove vegetation is an important component of the coastal ecosystem and is associated with near-shore marine habitat in the tropics and subtropics of the world. Indian mangrove vegetation covers about 6749 km^2 along the 7516 km long coast line, including Island territories (Mandal and Naskar, 2008). The distribution of mangrove areas along the Indian coast is influenced by physical forces such as geomorphology, climate, tidal amplitude and duration and quantity of freshwater inflow (Selvam, 2003). In fact, the geomorphic setting of the mangroves of east coast of India is different from that of the west coast (Ahmed, 1972). The coastal strip of west coast is narrow, and steep in slope as compared to the gentle slope of east coast. Though there are large number of small rivers bringing enormous quantity of sediment to the Arabian Sea along the west coast, deltas are not developed, possibly due to the high-energy conditions of the coast. This topographic set up gives a contrasting pattern of mangrove vegetation in India. Accordingly,

J. Sundaresan et al. (eds.), *Climate Change and Island and Coastal Vulnerability*,
DOI 10.1007/978-94-007-6016-5_15, © 2013 Capital Publishing Company

the mangrove wetlands of west coast are small, less diverse and less complicated in tidal creek network, while the east coast has larger mangrove wetlands with high species diversity. Besides, beach morphological changes along the west coast are controlled by the southwest monsoon. Therefore it is interesting to ascertain the consequences of mangroves in response to climate changes along the Kerala coast, southwestern India using the sedimentary archives of the coastal plains.

Kerala with a coastal line of about 560 km and 41 rivers emptying into the Lakshadweep Sea, was once very rich in mangrove formations, perhaps next only to Sunderbans, extending to more than 700 sq. km (Yesodharan, 2007). Palynological data of the Warkalli Formation revealed that the Kerala coast had a luxuriant mangrove cover in the Neogene when the palaeogeographic position and palaeoceanographic conditions were favourable for better mangrove vegetation (Kumaran et al., 1995, 2005, 2010; Ramanujam, 1995). However, the mangrove area in the State has shrunken considerably to about 1095 ha and mangrove vegetation is now confined largely to river mouths and tidal creeks (Kurien et al., 1994). Radhakrishnan et al. (2006) showed that mangrove vegetation in four northern districts of Kerala – Kasargod, Kannur, Kozhikode and Malappuram – is approximately 3500 ha, which represents about 83 per cent of mangrove cover in the State. Further, the present peculiar geomorphology of the estuarine area of Kerala, because of heavy sand mining from the rivers, poses problems for the natural regeneration of mangroves (Sunil Kumar, 2002). In view of the alarming trend of the decline and further degradation of mangrove cover during the past few thousand years in this part of India it would be worthwhile to address the aspects of environmental and climate changes that lead to the depletion of this major component of the coastal ecosystem for a better appraisal using the subsurface sediments of the Kerala basin.

Mangrove pollen preserved in the swamp sediments represents a product of geosphere and biosphere interactions along tropical coastlines and as such pollen signatures are found to be potential biomarkers for studying the past history of mangroves and palaeoecology (Blasco, 1984; Kumaran, 1991). As the mangrove vegetation comprises fairly large sized trees and shrubs, producing abundance of pollen, their chances of being preserved in the sediments are remarkable. The high rates of production, unique nature of the wall due to sporopollenin and the prevailing favourable environmental conditions enhance the abundance and preservation of pollen grains in mangroves and sediments of the tropical deltas and estuaries.

The establishment of correlation between species diversity and extent of mangrove ecosystem over time thus appears to be the most important contribution that palynology can make to the understanding of contemporary mangrove ecosystems, their structure and dynamics. Since the vegetation is directly affected by the climatic, geographical and geological changes, palynological studies may reveal the past extent of mangroves and also changes of environmental conditions over time. Being the major component of the ecosystem, the mangrove vegetation has a considerable role in regulating the hydrodynamic processes and as such it has tremendous influence on sediment accumulation. The differential rainfall rates along the west coast as well as the freshwater discharge through the rivers have important implications in the deposition of sediments in the mangrove swamps. Considering the uniqueness and the sensitivity of the specialized ecosystem, the pollen signatures preserved in mangrove sediments provide the palaeoclimatic signatures as they occupy the interface between the marine and terrestrial environments.

MATERIALS AND METHODS

The materials used for the present study are subsurface samples obtained from four boreholes from the wetlands of South Kerala Sedimentary Basin (SKSB): Panavally (76° 21′ 28″ E – 9° 47′ 45″ N) and Kumarakam (76° 26′ 0″ E – 9° 37′ 0° N) associated with the Vembanad Lake while Ayiramthengu (76° 29′ 0″ E – 9° 6′ 30″ N) in the southern part of the Kayamkulam Lake and West Kallada (76° 37′ 30″ E – 9° 1′ 15″ N in the over bank area of Ashtamudi Estuary (Fig. 15.1). Panavally borehole site is in the silica sand belt within Alappuzha district and the area is occupied by dense settlement with mixed tree crops. Kumarakam borehole is in a wetland used earlier for paddy cultivation, whereas Ayiramthengu location is in the over-bank area of Trivandrum-Shornur canal (the earlier backwater transport channel) that forms part of the Kayamkulam Lake. The area at present is blanketed with patches of mangroves and mangrove associates. The West Kallada borehole site lies in a wetland connecting one of the arms of the Ashtamudi estuary which is earlier used for paddy cultivation. The borehole samples were retrieved from continuous and uncontaminated mechanized augur rig cores. The bore holes drilled vary from 26.0 m to 45.0 m depth by Static Penetration Test (SPT). The advantage of obtaining samples by this method is that they are uncontaminated material and further the samples can be extracted from the barrel.

Details of lithologs, stratigraphy, sediment description and radiocarbon ages of the studied profiles are given in Fig. 15.2. Samples were processed depending upon the lithology using conventional palynological techniques (Faegri and Iversen, 1989; Moore et al., 1991; Traverse, 2007). These involve mechanical separation, chemical digestion, and concentration of organic materials and permanent preparation of slides for microscopic observations. Besides, additional methods have been improvised from time to time, depending upon requirements in order to get the maximum organic matter using palynological techniques. Photomicrographs were taken by Canon Powershot digital camera. Pollen spores and non-pollen Palynomorphs (NPP) were identified using the available database and published records (Thanikaimoni, 1987; Thanikaimoni et al., 1984; Nayar, 1990; Tissot et al.,

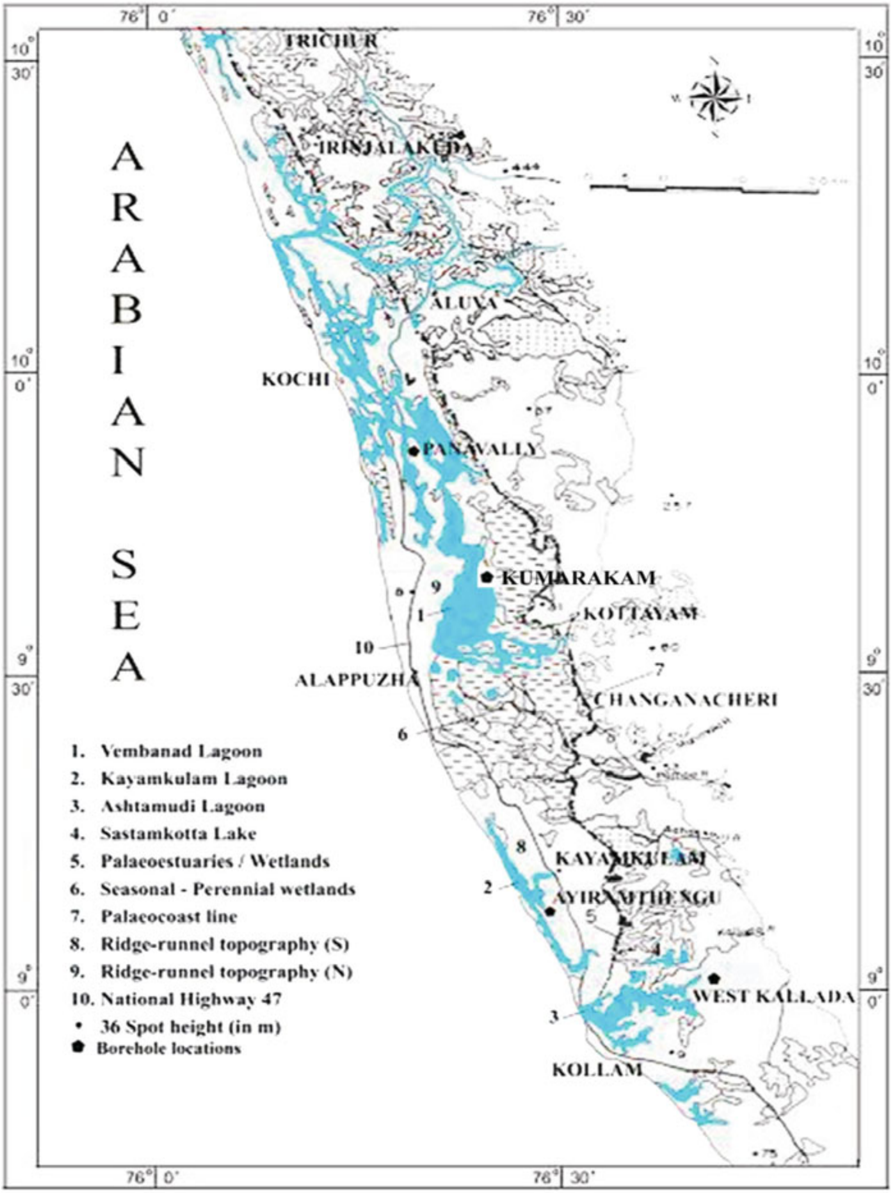

Fig. 15.1: Location map of bore holes of South Kerala Basin (modified after Limaye et al., 2010).

1994; Limaye, 2004; Limaye et al., 2007). Quantitative palynological analysis and pollen profiles of selected boreholes were prepared using Sigmaplot software. Radiocarbon (^{14}C) dates of a few samples of subfossil wood and organic matter-rich sediments at specific levels were determined at Birbal Sahni Institute of Palaeobotany, Lucknow (India).

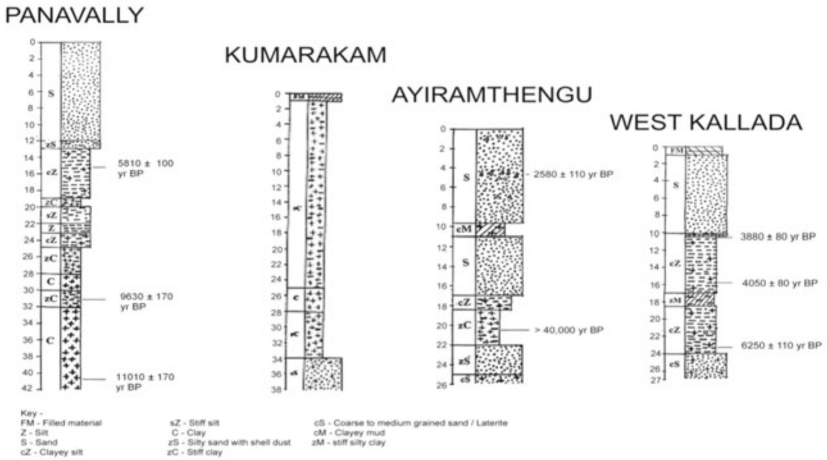

Fig. 15.2: Lithologs, stratigraphy and radiocarbon ages of selected sites.

RESULTS

Four boreholes from South Kerala Sedimentary Basin (Panavally, Kumarakam, Ayiramthengu and West Kallada) were analysed for palynological observations. The samples have been subjected to palynological analysis to ascertain ecological and palaeoenvironmental aspects. Depthwise analysis of boreholes and their results have been provided in Tables 15.1-15.4. The Panavally borehole has yielded abundance of organic matter right from 42.0 m depth to 3.40 m. However, pollen signatures of mangrove associates (Malvaceae) are confined to a narrow interval between 25.0 m and 21.0 m and falls within the Middle Holocene limit. Heavy accumulation of terrestrial vegetation represented by *Cullenia exarillata* and Euphorbiaceae along with foraminiferal linings, foram tests and dinoflagellates suggests heavy precipitation and higher sea level were prevailing very well at Panavally (Fig. 15.3; Table 15.1).

The 45.0 m Kumarakam borehole has a considerable thickness of mangrove facies as indicated by pollen of mangrove associate (Malvaceae). This interval is in between 33.0 m and 10.0 m and is dominated by black clays. It seems that the sediments were deposited in a calm and brackish lagoonal environment having abundant mangrove vegetation. However, the absence of pollen signatures beyond 8.0 m and further up in the profile indicates that the mangroves declined due to change in environmental conditions (Table 15.2).

The Ayiramthengu borehole has three levels of mangrove signatures as indicated by Malvaceae pollen and salt glands. The older signatures are within the Late Pleistocene while the Holocene interval is probably within Early Holocene and Middle Holocene. Here too decline of mangrove facies

Table 15.1: Palynological analysis of Panavally borehole

Sr. No.	*Depth in metres*	*Lithology*	*Observations*	*Remarks*
1	3.4–3.5	Coffee brown sand with mica particles	Few pteridophytic spores and fungal spores found to be present. Transparent mica particles abundant with few charcoal remains.	Moist conditions with evidence of fire in the past
2	11.9–12.0	Clayey sand of grey colour	Foram test and foram linings are found to be abundant. Pteridophytic spores of *Pteris* are common. *Rivularia* and Dinoflagellates, Palm pollen and charcoal are also found in the assemblage.	Marine environment with terrestrial input
3	12.9–13.0	Greyish green stiff clay with packets of shells	*Botryococcus* dominant of different type. *Rivularia*, foram linings, diatoms – *Buddulphia*, *Triceratium*, etc., silicoflagellates, Pteridophytic spores, Euphorbiaceae pollen few.	Lacustrine environment with fresh water input (Indicator of hydrological change)
4	13.9 – 14.0	Greyish green stiff clay with packets of shells	*Botryococcus* comparatively lower than previous level. Diatoms - *Melosira, Triceratium, Actinocyclus marylandicus*, *Coscinodiscus* etc. Foram test, Foram linings, Dinoflagellates few.	Marine environment
5	15.4	Greyish green stiff clay with packets of shells	Foram tests dominant, Diatoms – *Triceratium, Cocconeis, Thalassiosira*, Rivularia – few, charcoal, sheath with few structures, pteridophytic spores and silicoflagellates.	Marine environment with fresh water input
6	15.9 – 16.0	Greyish green stiff clay with packets of shells	Pteridophytic spores, silicoflagellates, Diatoms – *Coscinodiscus, Thalassiosira, Triceratium*, *Rivularia*, charcoal scarcely present. Dinoflagellates like *Peridinium, Spiniferites* are found. Foraminiferal linings are also present.	Marine environment with fresh water input

(*Contd.*)

Table 15.1: (*Contd.*)

7	18.9–19.8	Greyish green stiff clay with packets of shells	Rivularia dominant, Phytoplankton, foram lining, Diatoms – *Coscinodiscus/Thalassiosira*, *Triceratium*, *Navicula* are found to be present. Fungal fruiting bodies, fungal spore – *Cirrenalia, Glomus* and *Meliolinites* are common. Dinoflagellates – Spiniferites and Peridinium types are present.	Phosphate eutrophication of water bodies with some kind of marine input; disappearance of mangroves
8	19.9–20.0	Greyish green stiff clay with packets of shells	Foram test dominant. Pteridophytic spores, Rivularia, Diatoms few and Dinoflagellate cysts are present.	Facies change and decline mangrove ecosystem. Higher influx of fresh water along with marine affinity
9	22.0	Silty clay	Foram test – *Brizalino* sp and *Elphidium* sp dominant, foram linings and stellate structures few. Mangrove associate (Malvaceae pollen)	Prevalence of estuarine environment and higher influx of fresh water
10	22.7–22.8	Stiff greyish green clay with pockets of sand/shells	Type of Botryococcus is dominant. Rivularia dominant. Foram test and foraminiferal linings are few. Other associated elements in the assemblage are Meliola – fungal element, Dinoflagellates – Spiniferites, Pediastrum, Bacteriastrum and charcoal with Gramineae type of stomata. Mangrove associate (Malvaceae pollen)	Mangrove environment with fresh water to brackish water input. Indicator of hydrological change
11	22.9–23.0	Stiff greyish green clay with pockets of sand/shells	*Rivularia* dominant, dino-flagellate - *Peridinum*, cuticle present perhaps of fern type, palm pollen, phytoplankton, *Meliola* is also present. *Pediastrum* few than previous levels. Mangrove associate (Malvaceae pollen)	Prevalence of estuarine environment and higher influx of fresh water; Phosphate eutrophication of water bodies with terrestrial input

(*Contd.*)

Table 15.1: (*Contd.*)

Sr. No.	*Depth in metres*	*Lithology*	*Observations*	*Remarks*
12	24.4–24.5	Stiff greyish green clay with pockets of sand/shells	Sponge spicules common. *Rivularia* is dominant. Fungal fruiting bodies, germlings and *Meliola* found to be present. Palm pollen, *Staurastrum*, Foraminiferal lining also found to be present. Dinoflagellate cyst – Peridinium present. Mangrove associate (Malvaceae pollen)	Estuarine environment with heavy input of fresh water along with higher sea level
13	27.9–28.0	Stiff greyish green clay with pockets of sand/shells	Foram test present, linings few, invertebrates scale, *Pediastrum* present in low concentration than the previous level. Pteridophytic spores few – *Ceratopteris, Peridinium* type of dinocyst and *Bacteriastrum* present	Marine environment with fresh to brackish water environment
14	31.2	Stiff greyish green clay with pockets of sand/shells	*Triceratium* – Diatom palm pollen, *Staurastrum*, Triporate grain, dinoflagellate, pterido-phytic spores, charcoal and few Rivularia represent assemblage at this level.	Terrestrial environment with freshwater input
15	31.4–31.5	Stiff greyish green clay with pockets of sand/shells	*Rivularia* dominant. Bacteriastrum, sponge spicule, charcoal with gramineae stomata, dinoflagellates – Spiniferites and Peridinium more dominant. Pediastrum present, Meliola and charcoal more dominant.	Freshwater environment with some marine input
16	34.9–35.0	Stiff greyish green clay with pockets of sand/shells	Foram test common, mite remains seen, *Pediastrum* and pollen tetrad found to be present.	Marine environment with some temperature change
17	40.8	Stiff greyish green clay with pockets of sand/shells	*Ceratopteris*, pteridophytic spores, cuticles with stomata, fungal complex – fruiting bodies, spores – Lirasporites, Glomus, rotifers, salt glands – *Heliospermopsis*. Sponge spicules, Dinoflagellate cyst, Invertebrate scales are also found to be present.	Fresh water environment with marine affinity
18	40.9–41.0	Stiff greyish green clay with pockets of sand/shells	Foram linings dominant. *Rivularia*, *Ceratopteris*, *Pediastrum*, *Lirasporites* (fungal spore) are also found.	Marine affinity

Table 15.2: Palynological analysis of Kumarakam borehole

Sr. No.	*Depth in metres*	*Palynological observation*	*Remarks*
1	2.00 (grey colour mud)	Structural terrestrial remains, fungal complex and cyanobacteria.	Terrestrial fresh water environment
2	4.00 (grey colour mud)	Dominance of foraminiferal linings, presence of cyanobacteria, dinoflagellate, sponge spicule and fungal complex, presence of microscopic charcoal.	Marine environment
3	6.00 (grey colour mud)	Dominance of foraminiferal linings along with structural terrestrial remains and microscopic charcoal. Presence of fungal complex, cyanobacteria, dinoflagellate, leaf cuticle, sponge spicule, less number of pollen.	Marine environment
4	8.00 (grey colour mud)	This sample is dominated by cyanobacteria and foraminiferal linings. Presence of dinoflagellate, fungal complex, pollen, sponge spicule and insect part. Presence of *Ceratopteris* spore and microscopic charcoal.	As marine forms are dominating the sample, presence of *Ceratopteris* spores indicate influx of fresh water into marine water
5	10.00 (grey colour mud)	Rich in the structural terrestrial remains, dominance of fungal complex along with various types of diatom and cyanobacteria, presence and dominance of pollen (Malvaceae) grain. Marine forms like foraminiferal lining, radiolarians (?), sponge spicule. Presence of *Ceratopteris* spore. Presence of grass cuticle and microscopic charcoal.	Terrestrial fresh water environment with influx of marine water. There is dominance of the fungal complex indicating high humidity and heavy rainfall.
6	12.00 (grey colour mud)	Dominance of the fungal complex along with structural terrestrial remains, microscopic charcoal and cyanobacteria. Marine form such as foraminiferal lining, dinoflagellate and sponge spicule. Presence of insect part, pollen, *Ceratopteris* spore.	Terrestrial fresh water environment with marine influence. Dominance of fungal complex indicates high humidity and heavy rainfall
7	14.00 (grey colour mud)	Dominance of the fungal complex along with the Cyanobacteria. Presence of structural terrestrial remain, leaf cuticle and pollen. Marine forms such a foraminiferal lining, scolecodonts, sponge spicule and insect part.	Terrestrial fresh water environment with slight influence of marine water. High humidity and heavy rainfall.

(*Contd.*)

Table 15.2: (*Contd.*)

Sr. No.	*Depth in metres*	*Palynological observation*	*Remarks*
8	16.00 (grey colour mud)	Rich in the organic matter, dominance of fungal complex, pollen and structural terrestrial remains, microscopic charcoal along with cyanobacteria. Marine forms such as foram iniferal lining, dinoflagellate, scolecodonts, and sponge spicules. Presence of leaf cuticle (f), *Ceratopteris* spore.	Terrestrial fresh water environment with marine influence.
9	18.00 (grey colour mud)	This sample is dominated by structural terrestrial remains, microscopic charcoal, along with oil forming algae *Botryococcus* (lacustrine environment). There is presence of scoleocodonts, fungal complex, and pollen.	More fresh water but slight marine influence.
10	20.00 (grey colour mud)	Dominance of structural terrestrial remains, microscopic charcoal along with pollen, fungal complex and cyanobacteria. Marine forms such as dinoflagellate, *Bacteriastrum* and sponge spicule is present; *Ceratopteris* spores seen.	Terrestrial fresh water environment with marine influence.
11	22.00 (grey colour mud)	Dominance of pollen along with structural terrestrial remains, fungal complex. Presence of diatom, grass leaf cuticle, spore and cyanobacteria but the number is very less. *Complete absence of marine forms.	Terrestrial fresh water environment.
12	24.00 (grey colour mud)	Dominated by structural terrestrial remains, presence of *Ceratopteris* spore, pollen, fungal complex. Presence of *Bacteriastrum*, foraminiferal lining (less number), sponge spicule, cyanobacteria but number is very less. Presence of microscopic charcoal.	Terrestrial fresh water environment with marine influence.
13	27.00 (grey colour mud)	This sample is dominated by sponge spicule and diatom along with structural terrestrial remain and pollen. Presence of grass cuticle, foraminiferal lining. Presence of *Ceratopteris* spore. Less number of fungal complex.	Marine environment with influx of fresh water.

(*Contd.*)

Table 15.2: (*Contd.*)

14	30.00 (grey colour hard mud with clay particles)	Structural terrestrial remains, microscopic charcoal dominant. Presence of the fungal complex (dominant), diatom, Cyanobacteria, *Bacteriastrum* and sponge spicule.	Dominant fresh water facies with marine influence.
15	33.00 (grey colour mud)	Dominated by structural terrestrial remains, microscopic charcoal along with fungal complex, pollen, cyanobacteria and diatom. Presence of fern leaf cuticle and other type of cuticles, **presence of Malvaceae pollen.** Marine form such as foraminiferal lining, dinoflagellate and insect part. Few pteridophytic spore.	Terrestrial fresh water environment with marine influence.
16	39.00 (grey colour orange hard mud)	Dominance of the sponge spicule. Presence of *Bacteriastrum*, dinocyst and fungal complex, presence of grass cuticle, grass spikelet, pteridophytic spore (less in number) and microscopic charcoal	Marine environment.
17	42.00 (grey colour yellow orange mud)	Dominance of sponge spicule along with structural terrestrial remains, marine forms such as *Bacteriastrum* is present. Presence of pollen, pteridophytic spore and microscopic charcoal.	Marine environment.
18	45.00 (yellow orange clay)	This sample is dominated by fern leaf cuticle, pollen, *Ceratopteris* spore, pollen along with structural terrestrial remains. Presence of microscopic charcoal and *Bacteriastrum.*	Fresh water environment (dominated by fresh water facies).

Table 15.3: Palynological analysis of Ayiramthengu borehole

Sr. No.	*Depth in metres*	*Lithology*	*Observations*	*Remarks*
1	0.9–1.0	Yellowish sand with mica.	Foram linings are abundant. *Ceratopteris* and other pteridophytic spores present. Thecamoeba and Discoaster seen.	Marine facies with fresh water influx; facies change towards fresh water indicated by *Ceratopteris* and also level of pollution due to Thecamoeba.
2	9.9–10	Yellowish brown sand with mica	Pteridophytic spores abundant. This is followed by the Thecamoeba and Discoasters few. Presence of *Cullenia* pollen and tricolpate pollen grain.	Suggestive of stressed terrestrial environment with slight marine influence and the same time rainfall seems to be fair at this level.
3	10.4–10.5	Yellowish brown – black clay hard	Pteridophytic spores few followed by the camoebians. Foram linings are few. *Meliolites* found to be present. Malvaceae pollen few (Mangrove associate).	Decline of mangrove facies; Precipitation and strong terrestrial input indicate wet conditions and higher atmospheric pressure at this level.
4	13–14	Grey black sand	*Ceratopteris* spores dominant. Rivularia follows this. Foram linings and test few. Dinoflagellate cyst, Thecamoeba, charcoal fragments, fruiting bodies, hyphae also found. Malvaceae (mangrove associate).	Transitional facies (mangroves) along with fresh water flood plain and eventual exposure of wetland for considerable period with occasional tidal inputs.
5	17.9–18	Greyish green coloured clay	*Rivularia* few but more than foram linings. Malvaceae pollen, *Ceratopteris* spores few. Thecamoeba, dinoflagellate cyst also present. Gramineae pollen found. Relatively less salt glands.	Decline of mangrove facies and change is indicated here as the brackish water getting more influence of tidal waves.

(*Contd.*)

Table 15.3: (*Contd.*)

6	18.5	Grey clay	Pteridophytic spores –*Pteris, Ceratopteris* abundant. This is followed by *Cullenia* pollen. Few foram linings and fungal fruiting bodies found to be present. *Rivularia* forms also present Euphorbiaceae pollen also seen.	Dominant fresh water facies. However, tidal influence seen by the presence of foram linings. Strong terrestrial and presence of evergreen taxa indicative of good rainfall and wet climate.
7	18.9–19	Grey clay	*Ceratopteris* spore dominant along with other kind of spores (Pteridophytic). Few fungal fruiting bodies found to be present. Foram linings few. *Rivularia* also found to be present. Dinoflagellates present. Fungal spores few. Salt glands (mangroves)	Estuarine condition; Humic conditions and prevalence of wet climate.
8	20.4–20.5	Black clay	Pteridophytic spores dominant. *Rivularia* few, dinoflagellates few. Presence of salt gland, charcoal. Foram lining of different type showing constriction in between two lobes. Dinoflagellates few. *Ceratopteris* spores dominant. Salt glands (mangroves).	Estuarine condition; Humic conditions and prevalence of wet climate.
9	22.9–23	Brown mud	Organic material without any known type of microfossil.	Less sedimentation and low input either from terrestrial/aquatic sources. Quiescent period? Dry/Arid conditions may be also inferred here but needs careful analysis.
10	25.5	Brown hard mud layer	Thecamoeba present. Malvaceae pollen (mangrove associate). Pteridophytic spores, Discoasters few.	Prevalence of mangrove facies; Fresh water facies are prevalent and may be exposed for a considerable period of time.

Table 15.4: Palynological analysis of West Kallada borehole

Sr. No.	*Depth in metres*	*Sediment characters*	*Palynological observation*	*Remarks*
1	1.9–2.0	Filled material with coarse to medium grained sand.	*Glomus*, but *Rivularia* absent	Low organic input, erosional features
2	4.4–4.5	Coarse to medium grained sand.	Presence of Thecamoeba, no cyanobacteria	Stressed/ contamination/pollution type environment, fresh water organic rich
3	5.9–6.0	Coarse to medium grained sand.	Cyanobacteria	Exclusively fresh water influence. Decline of mangroves.
4	7.4–7.5	Coarse to medium grained sand.	Organic matter relatively poor, no cyanobacteria, marine influence less. Malvaceae (Mangrove associate)	Mangrove facies continues in stressed environment.
5	8.0–9.0	Coarse to medium grained sand with pyrite nodules/granules.	Heavy terrestrial organic input but marine influence persists. Malvaceae (Mangrove associate)	Mangrove facies continues; Heavy rainfall and freshwater Influx.
6	9.4–9.5	Pyrite nodules/granules clay organic rich.	Marine influence clearly indicated by foram linings and dinoflagellates, Cyanobacteria few. Malvaceae (Mangrove associate)	Mangrove facies continues; Marine facies dominant.
7	10.5	Black clays dominant, silts with less sand.	*Arthrodesmus convergens* (Desmidiaceae) dominant; abundance of fungal spores and fruiting bodies along with *Glomus* sp; cyanobacteria (*Rivularia* sp.); trichomes abundant; pteridophytic spores, *Veryhachium* sp. scarce. Malvaceae (Mangrove associate).	Abundance of desmids indicates facies changes and the presence of few types of plankton relates to slight marine affinity. Erosional activity may be due to *Glomus*. Cyanobacteria dominance is suggestive of fresh water marsh/ wetland system; Mangrove ecosystem gradually alters
8	10.9–11.0	Black clays dominant, silts with less sand.	Heavy input of terrestrial organic matter (occasional foram linings) Malvaceae (Mangrove associate)	Mangrove facies continues; High precipitation.

(*Contd.*)

Table 15.4: (*Contd.*)

9	12.9–13.0	Black clays dominant, silts with less sand.	Organic rich mainly terrestrial. Malvaceae (Mangrove associate)	Mangrove facies continues; High precipitation.
10	13.9–14.0	Black clays dominant, silts with less sand.	Organic rich mainly from terrestrial – (*Cullenia* many). Malvaceae (Mangrove associate)	Mangrove facies continues; Probably heavy rainfall.
11	14.9–15.0	Black clays dominant, silts with less sand.	*Glomus*, fungi abundant, terrestrial input. Malvaceae (Mangrove associate)	Mangrove facies continues but erosional features.
12	15.9	Clay and silt are almost equal with less sand.	*Arthrodesmus convergens* (Desmidiaceae) dominant; abundance of fungal spores and fruiting bodies; cyanobacteria (*Rivularia* sp.) dominant; pteridophytic spores, pollen grains, scolecodonts, foram linings and charcoal few. Malvaceae (Mangrove associate)	More or less wetland ecosystem and terrestrial input suggestive of fresh water. Marine influence as indicated by few linings and foram tests.
13	15.9–16.0	Black clays dominant, silts with less sand.	Fungi dominate, *Rivularia*. Malvaceae (Mangrove associate)	Estuarine and mangrove facies; High humidity.
14	16.9–17.0	Black clays dominant, silts with less sand.	Fungal dominant, pteridophytic spores, *Lirasporites*. *Sonneratia* pollen few; Malvaceae (Mangrove associate)	Estuarine and mangrove facies. High humidity.
15	18.9–19.0	Black clays dominant, silts with less sand.	Fungi dominate and a few pteridophytic spores; *Sonneratia* pollen few; Malvaceae (Mangrove associate)	Estuarine and mangrove facies.
16	19.9–20.0	Black clays dominant, silts with less sand.	Fungi more and a few *Rivularia*. Malvaceae (Mangrove associate)	Estuarine facies; High humidity.
17	20.9– 21.0	Black clays dominant, silts with less sand.	Marine influence (foram linings), scolecodonts, pollen few (less organic). Malvaceae (Mangrove associate)	Estuarine facies with less fresh water.

(*Contd.*)

Table 15.4: (*Contd.*)

Sr. No.	*Depth in metres*	*Sediment characters*	*Palynological observation*	*Remarks*
18	22.9– 23.0	Black clays dominant, silts with less sand.	*Cullenia* (pollen), *Rivularia* (cyanobacteria), charcoal, *Lirasporites*, grass cuticles, Pteridophytic spores, fungal spores (organic rich). Mangrove elements (salt glands); Malvaceae (Mangrove associate)	High rainfall and freshwater dominance within mangrove facies
19	23.5	Silt dominant over clay and sand very less.	Fungal spores and fruiting bodies dominant; cyanobacteria abundant. Gramineae cuticles represented in the form of charcoal dominant; Pteridophytic spores and *Cullenia* pollen few; Foram linings are few. Mangrove elements few.	Prevalence of freshwater swamp environment along with mangrove facies
20	26.1–26.2	Greyish white sandy clay with patches of limonite.	Dominance of desmids. Few foram linings and mangrove elements (*Sonneratia*) observed.	Change in facies from marine/ estuarine to fresh water; Mangrove facies
21	26.3–26.4	Greyish white sandy clay with patches of limonite.	Presence of *Tuberculodinium vancampoae* and *Cullenia*	Shallow marine elements and high rainfall indicators.

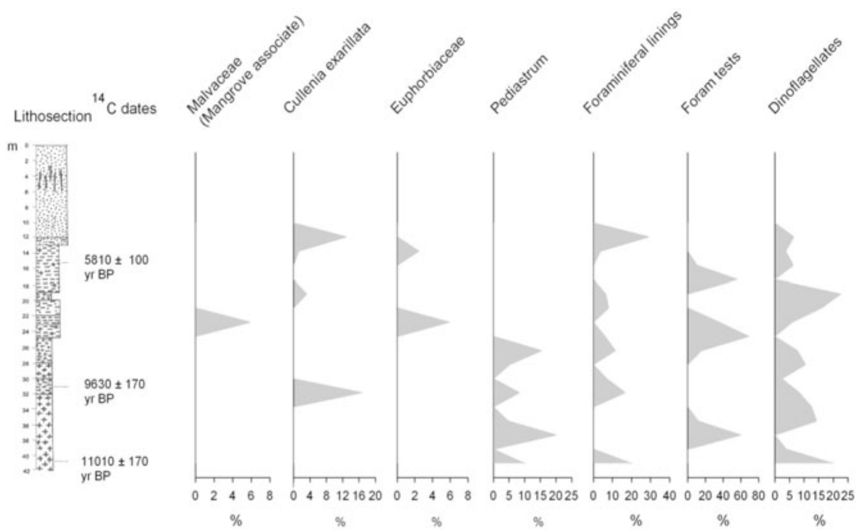

Fig. 15.3: Pollen and other microfossil spectrum of Panavally.

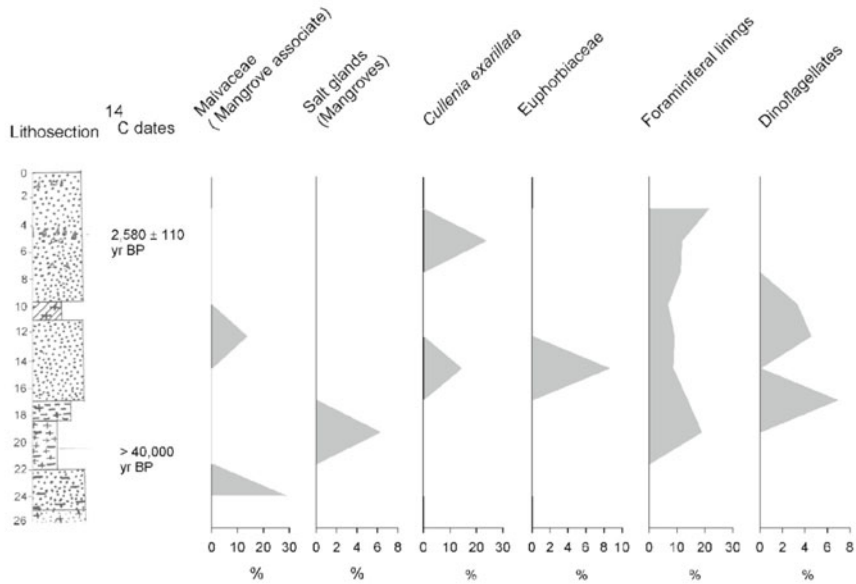

Fig. 15.4: Pollen and other microfossil spectrum of Ayiramthengu.

has been observed in the Late Holocene despite there having been heavy downpour as well as marine influence to this region until Late Holocene. The pollen spectrum reveals pollen signatures of terrestrial vegetation and marine elements of foraminiferal linings and dinoflagellates (Fig. 15.4; Table 15.3).

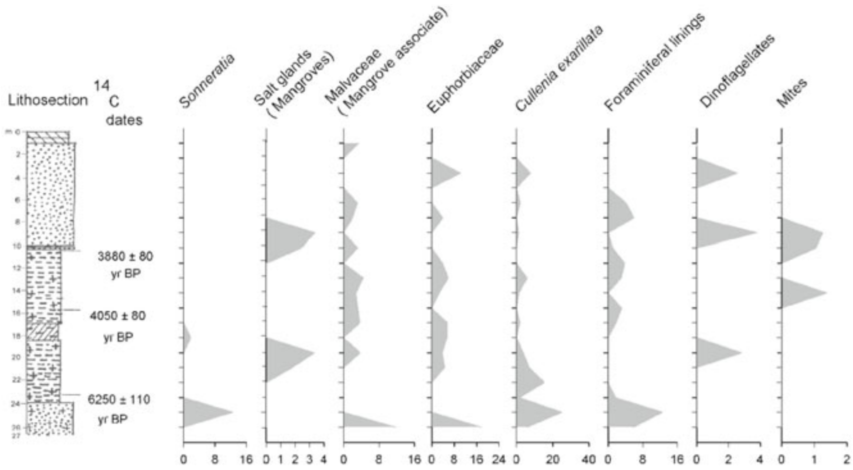

Fig. 15.5: Pollen and other microfossil spectrum of West Kallada.

The West Kallada profile has been found to be the best for mangrove development along the southwestern coast of India as pollen signatures of both mangroves as well as mangrove associates are observed from well dated Holocene sequence of 6250 ± 110 yrs BP to 3880 ± 80 yrs BP and even in the younger sediments. The Mid-Holocene is characterized by both *Sonneratia* and mangrove associates. However, there seems to be a facies change until 5000 yrs BP or so as *Sonneratia* reappeared again towards 4000 yrs BP and its decline towards Late Holocene. As compared to other profiles, mangrove associates are well represented even in the Late Holocene. Marine influence to West Kallada even towards Late Holocene continued as foraminiferal linings and dinoflagellates do occur throughout the profile with intermittent aberrations. Another important palynological observation is the abundance of palynomorphs of terrestrial vegetation (*Cullenia exarillata* and Euphorbiaceae) due to heavy discharge of freshwater influx into the West Kallada area. The occurrence of mites at an interval of 12.0-9.0 m (3880 ± 80 yrs BP) recalls rise in temperature and prevalence of arid climate despite frequent supply of fresh water to this region (Fig. 15.5; Table 15.4).

DISCUSSION

The mangroves along Kerala coast had a relatively long geological history as their pollen signatures are recorded in the Neogene and Pleistocene sediments (Kumaran et al., 2005, 2010). However, their occurrence and diversity in the Holocene and Recent sediments are sparse due to response and decline as a result of environmental and climate change related to hydrodynamics of the coastal region (Nair et al., 2009). Further, the geomorphological changes as a result of neotectonic activities (Nair et al., 2009) have affected the topography of the Kerala coast considerably and thereby the mangrove habitats have been greatly reduced. As of now, there is no typical mangrove location, comparable to the environmental set up seen in other parts of India. However, the mangroves are confined to very small pockets on the bank of estuaries. The longest mangrove patch is found in Kumarakam, about a kilometre in length, along the bank of the Vembanad Lake. While studying the tropical paleoecology and paleoclimate of the coastal plains of Kerala the authors have come across the past signatures of mangrove vegetation in well dated subsurface sequence associated with three most important wetlands, Vembanad Lake, Kayamkulam Lake and Ashtamudi estuary and accordingly an attempt is made to address how the mangroves responded to the changing scenarios of climate and environment in the southwestern part of India.

Out of the four studied profiles only one sample of Ayiramthengu (20.4-20.5 m) has been found to be of Late Pleistocene (>40,000 yrs BP) showing the mangrove signatures while the others are of mainly Middle Holocene age. The occurrence of Late Pleistocene is debatable as these older sediments may be of reworked Warkalli sediments having the limitations of ^{14}C dating. Otherwise all the four borehole samples belong to Holocene. The Panavally and Kumarakam boreholes represent locations associated with the Vembanad Lake which has still a better mangrove cover. However, in Panavally pollen signatures of mangrove associates (Malvaceae) are confined only to a narrow interval between 25.0 m and 21.0 m and fall within the Middle Holocene limit (~5000 yrs BP) and is linked to a stabilized sea level of the Holocene and a conducive environment for mangrove development. Prior to this (11010 ± 170 yrs BP to 5000 yrs BP), the area received heavy freshwater influx as indicated by abundance of *Pediastrum* and a higher sea level (Foraminiferal linings, foram tests and dinoflagellates) which did not allow the development of mangroves in this region. The higher terrestrial input from erosion, as a result of heavy rainfall during the Holocene Climate Optimum (HCO), must have carried heavy load of substrate to the region which also had a negative impact for mangrove development. Kumarakam borehole has a considerable thickness (33.0 m and 10.0 m) of mangrove facies as indicated by pollen of mangrove associate (Malvaceae). Though the sediments are not dated, it seems that the sediments were deposited in a calm and brackish lagoonal environment having abundant mangrove vegetation probably during the Mid-Holocene (Kumaran et al., 2008). Though mangrove vegetation continues to grow in Kumarakom, the absence of pollen signatures of mangroves beyond 8.0 m and further up in the profile indicates that the mangroves declined due to environmental changes (Fig. 15.4).

The Ayiramthengu borehole is located on the eastern bank of Kayamkulam Lake. As of now, the area is surrounded by luxuriant growth of mangroves and mangrove associates. Though the older signatures are found within the

Late Pleistocene (? Neogene of Warkalli), mangrove development and establishment seems to be during the Middle Holocene. The abundance of *Cullenia exarillata* and Euphorbiaceae of terrestrial vegetation and marine microfossils (foraminiferal linings and dinoflagellates) indicate heavy downpour and higher sea level in this region and these extreme conditions might too have contributed to decline of mangrove facies towards Late Holocene.

Of all the four profiles, the West Kallada profile displays the best scenario of mangrove development along the southwestern coast of India as pollen signatures of both mangroves as well as mangrove associates are observed from well dated Holocene sequence of 6250 ± 110 yrs BP to 3880 ± 80 yrs BP and even in the younger sediments. The significant aspect is the development and reoccurrence of *Sonneratia* and other mangroves (salt glands) during the Middle Holocene. Further, throughout the profile, pollen signatures of mangrove associates have been recorded except for a short interval in Middle Holocene and towards the Late Holocene. It seems that this area appears to be developing towards a delta habitat (Padmalal et al., in this volume) which is good for mangrove development as the prevailing environmental conditions have been favourable right from Middle Holocene to Recent (Fig. 15.5).

The studied mangrove profiles of Kerala coast are found to be of Mid-Holocene in general as a result of the prevailing paleogeographic position and paleoceanographic conditions. Such Mid-Holocene mangrove development is attributed to a stabilized sea level of global significance. Pollen and geochronological data reveal that the Kerala coast had a better, stable and luxuriant mangrove cover until Middle Holocene especially in West Kallada region as observed in Konkan coast and also in West Bengal basin (Limaye and Kumaran, 2012; Hait and Behling, 2009). The West Kallada region near the confluence of Kallada River with the Ashtamudi estuary is gradually converting into a delta which eventually forms an excellent mangrove habitat in course of time. This area still appears to enjoy conditions similar to that of Mid-Holocene and as such it has excellent potential for the rehabilitation of mangroves in south-western India.

ACKNOWLEDGEMENTS

K.P.N. Kumaran thanks Council of Scientific and Industrial Research, New Delhi for providing financial support [24 (0275)/05/EMR-II] and Dr. D.R. Ranade, Officiating Director, ARI, Pune for facilities and encouragement. R.B. Limaye acknowledges the Department of Science and Technology for granting DST-Fast Track Young Scientist Scheme (SR/FTP/ES-38/2006) and SRA of CSIR. D. Padmalal thanks the Director, CESS, Thiruvananthapuram for his kind permission for publication.

REFERENCES

Ahmed, E. (1972). Coastal geomorphology of India. Hindustan Publishing Corporation, New Delhi.

Blasco, F. (1984). Climatic factors and the biology of mangrove plants. *In:* Mangrove ecosystem: Research methods (edited by S.C. Snedaker and J.G. Snedaker). UNESCO, Paris.

Faegri, K. and Iversen, J. (1989). Textbook of Pollen Analysis. John Wiley and Sons, Chichester.

Hait, A.K. and Behling, H. (2009). Holocene mangrove and coastal environmental changes in the western Ganga-Brahmaputra delta, India. *Veg. Hist. and Archaeobot.*, **18:** 159-169.

Kumaran, K.P.N. (1991). Importance of Palynology in Mangrove ecosystems. Proceedings of the symposium on Significance of Mangroves. Maharashtra Association for the Cultivation of Science Research Institute, Pune.

Kumaran, K.P.N., Nair, K.M., Shindikar, M.R., Limaye, Ruta B. and Padmalal, D. (2005). Stratigraphical and palynological appraisal of the Late Quaternary mangrove deposits of west coast of India. *Quat. Res.*, **64:** 418-431.

Kumaran, K.P.N., Padmalal, D. and Nair, K.M. (2008). Late Quaternary environmental changes in the coastal plains of Southern Kerala, southwest India. Project Completion Report, Council of Scientific and Industrial Research, New Delhi.

Kumaran, K.P.N., Punekar, S.A. and Limaye, R.B. (2010). Palaeoclimate and phytogeographical appraisal of Neogene pollen record from India. *J. Palynol.*, **46:** 315-330.

Kumaran, K.P.N., Soman, K., Kamble, C.V. and Joseph, A. (1995). Palynofloral analysis of sections from Bharathi and Kundara mines of Kerala Basin: Palaeocological and tectonic perspective. *Curr. Sci.*, **69:** 1023-1027.

Kurien, N., Samsuddin, M., Ramchandran, K.K. and Salim, M.B. (1994). Resource evaluation using remote sensing for aquaculture site selection. A case study. Proc. of sixth Kerala Sci. Cong.

Limaye, R.B., Kumaran, K.P.N., Nair, K.M. and Padmalal, D. (2007). Non-pollen palynomorphs (NPP) as potential palaeoenvironmental indicators in the Late Quaternary sediments of west coast of India. *Curr. Sci.*, **92:** 1370-1382.

Limaye, Ruta B., Kumaran, K.P.N., Nair, K.M. and Padmalal, D. (2010). Cyanobacteria as potential biomarkers of hydrological changes in the Late Quaternary sediments of South Kerala Sedimentary Basin, India. *Quat. Int.*, **213:** 79-90.

Limaye, R.B. and Kumaran, K.P.N. (2012). Mangrove vegetation responses to Holocene climate change along Konkan coast of south-western India. *Quat. Int.*, **263:** 114-128.

Limaye, R.B. (2004). Contribution to Palaeopalynology and Palaeoecology of the coastal deposits of Maharashtra, India. Ph.D. Thesis, University of Pune, India.

Mandal, R.N. and Naskar, K.R. (2008). Diversity and classification of Indian mangroves: A review. *Trop. Ecol.*, **49:** 131-146.

Moore, P.D., Webb, J.A. and Collinson, M.E. (1991). Pollen Analysis. Blackwell Scientific, Oxford.

Nair, K.M., Kumaran, K.P.N. and Padmalal, D. (2009). Tectonic and hydrologic control on Late Pleistocene-Holocene landforms palaeoforest and non-forest vegetation, Southern Kerala. Project Completion Report, Kerala State Council for Science Technology and Environment, Thiruvananthapuram.

Nayar, T.S. (1990). Pollen flora of Maharashtra state, India. Today and Tomorrow Printers and Publishers, New Delhi.

Radhakrishnan, C., Gopi, K.C. and Palot, M.J. (2006). Mangroves and their faunal associates in Kerala, India. *Rec. Zool. Surv, India, Occ. Paper*, **246:** 1-81.

Ramanujam, C.G.K. (1995). Tertiary floristic complexes of Southern India – A critical appraisal. *Geophytol.*, **25:** 1-14.

Selvam, V. (2003). Environmental classification of mangrove wetlands of India. *Curr. Sci*, **84:** 757-765.

Sunil Kumar, R. (2002). Status of mangroves in Kerala: The degraded ecosystem urgently needs conservation and management strategies for their development. Proceedings of the National Seminar on Marine and coastal ecosystems: Coral and mangrove problems and management strategies. J.K. Patterson Edward, A. Murgan and Jamila Patterson (eds), SDMRI Res. Publ. 2.

Thanikaimoni, G., Caratini, C., Venkatachala, B.S., Ramanujam, C.G.K. and Kar, R.K. (1984). Selected Tertiary Angiosperm pollens from India and their relationship with African Tertiary pollen. *Trav. Sci. Sec. Tech.*, Institute of French Pondicherry, **19:** 93.

Thanikaimoni, G. (1987). Mangrove palynology. Institute of French Pondicherry. *Trav. Sci. Sec. Tech.*, **24:** 1-100.

Tissot, C.H., Chikhi, H. and Nayar, T.S. (1994). Pollen of wet evergreen forests of the Western Ghats of India. Institute of French Pondicherry, **35:** 1-133.

Traverse, A. (2007). Palaeopalynology (second ed.). Springer, Dordrecht, The Netherlands.

Yesodharan, E.P. (2007). State of the environment report of Kerala, IV. KSCSTE, Government of Kerala.

CHAPTER

16

Predicted Recurrence of Coral Bleaching Events along Lakshadweep Reef Region

M. Hussain Ali, B. Jasper[1] and E. Vivekanandan[1]

Cenduit India Services, Prestige Nebula, Bengaluru – 560001, India
[1]Central Marine Fisheries Research Institute, Dr Salim Ali Road
Kochi – 682018, India
surfhussain@gmail.com

INTRODUCTION

Coral bleaching is by far the most damaging event in coral reefs and is currently viewed as a major threat to the long-term health of coral reef communities. Although there are certainly many other factors (fishing, outbreaks of coral diseases and predators, sedimentation and nutrient inputs) (Sebens, 1994; Jackson, 1997; Wilkinson, 1999), coral bleaching is currently viewed as a major agent of change in coral reef communities (Brown, 1997; Hoegh-Guldberg, 1999) and the rise in sea surface temperature causes stress, which leads to the expulsion of symbiotic zooxanthellae by the corals (Jokiel and Coles, 1990). Evidence of sea surface temperature warming has been found throughout much of the tropics, especially in the northern hemisphere (Strong et al., 2000). While decadal increases in temperature of this magnitude may seem small at first glance, such increases become very significant for corals living close to their thermal limits in oceans where the background temperatures are steadily rising over time (William et al., 2001). A combination of elevated seawater temperature and exposure duration induces coral bleaching and can be used to predict coral bleaching with great certainty (Toscano et al., 2000).

J. Sundaresan et al. (eds.), *Climate Change and Island and Coastal Vulnerability*,
DOI 10.1007/978-94-007-6016-5_16, © 2013 Capital Publishing Company

Coral bleaching at small local scales (10-1000 m^2) has been reported for almost a century (Yonge and Nichols, 1931). Bleaching at larger geographical scales, however, is a relative new phenomenon. Indian reefs have experienced 29 widespread bleaching events since reported during the year 1989 (Vivekanandan, 2008). During the year 1998 and 2002 these events were intense (Arthur, 2000; Rajasurya et al., 2002; Rajasurya et al., 2004). Two indices of warm season sea surface temperature are found in the Indian reef regions where intense bleaching occurred during 1998 and 2002 (Arthur, 2000; Kumaraguru et al., 2003). The 1997-1998 El Nino Southern Oscillation events, that elevated sea surface temperatures of tropical oceans by more than 3°C, was one of the most extreme ENSO events in recent history (Arthur, 2000). The hypothesis is that the corals and other reef organisms might be the first to show adverse effects of global warming (Jokiel and Coles, 1990; Glynn, 1996; Goreau and Hayes, 1994). Even marginal increases might push an organism over its physiological limits (Jokiel and Coles, 1990).

Timing and recovery from the massive coral mortality on ocean reefs and how frequently rising SSTs will cause repeat mortalities are issues of practical urgency for many countries because of the high value of reefs to shoreline protection, biodiversity, protein supply and tourism (Wilkinson et al., 1999). Present study provides a unique environmental gradient by examining the relationships between environmental variation, climate change, and adaptation and its consequences for biodiversity and ecological functions with regard to Lakshadweep coral reef regions. The frequency of mass coral bleaching and the increase in thermal tolerance necessary to ensure long-term survival for coral reefs along Lakshadweep to future scenario is assessed in the present study. This paper provides a dataset of Sea Surface Temperature (SST) for five locations of Lakshadweep reef region (Fig. 16.1). Though

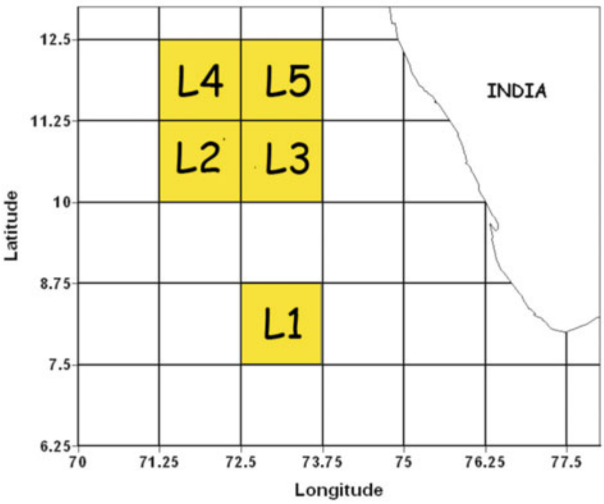

Fig. 16.1: Map showing the study location along Lakshadweep reef region.

exact SST values remain unattainable in forecasting for a specific year and site, the probability approach has revealed valuable and interesting patterns in this region, as it has in others (Sheppard, 2003; Sheppard, 2004).

MATERIAL AND METHODS

The SST compilation is derived from satellite (historical) and forecast SST series. Forecast SSTs were seamlessly blended onto historical SST data (Sheppard, 2003). In the absence of continuous real time data, the United States National Oceanic and Atmospheric Administration, National Environmental Satellite Data and Information Service (NOAA/NESDIS) images are the most useful and accurate means of gaining a comprehensive data on the SST anomaly in the Indian seas (Arthur, 2000). For the historical data, monthly SST data for the years 1985-2008 around the study sites were obtained from NOAA/NASA Oceans Pathfinder SST project (Vasquez and Kilpatrick, 1998). It consists of all pixel product of monthly SST derived from the 5-channel Advanced Very High Resolution Radiometers (AVHRR) on board the NOAA polar orbiting satellites (http://podaac.jpl.nasa.gov). This was combined with the simulated monthly surface 'skin' temperature from 2000 to 2099 from simulation of the UKMO HadCM3 model for each study site, under the SRES A2 scenario conducted from the third IPCC assessment (Cubasch et al., 2001). The SRES future emissions scenarios were designed to reflect different paths of future economic development and energy use (Nakicenovic, 2000). The SRES A2 emission scenario is commonly used for 'business as usual' impact studies, projecting a 3ºC increase by 2100. This scenario has played a central role in the 3rd IPCC assessment (Cubasch et al., 2001) and is commonly used in climate impact studies (Parry, 2004). The surface 'skin' temperature from GCMs is the closest proxy for the satellite-derived SST and has been employed in previous coral bleaching studies (Hoegh-Guldberg, 1999; Sheppard, 2003). The historical data set has a resolution of 0.045 × 0.045 degree latitude and longitude, while the HadCM3 data has a larger grid of 1.25 × 1.25 degrees. For both historical data and forecast data, the cells encompassing each study site were used.

Forecast data (SST) from climate models rarely flow seamlessly from historical series. The errors in forecast seasonal amplitude further prevent accurate estimation of when lethal mortalities might occur (Sheppard, 2003). Construction of seamless monthly series from 1985 to 2099 needs two treatments. First transformation is to adjust each forecast data series by the mean difference in values in the overlapping data between two datasets (N = 100 months). This helps to vertically adjust by the mean monthly differences between the two series. Second transformation scales the annual variation of each forecast data series to match that of each site's historical data. Scaling of annual variation to match that of the historical set by substitution of the standard deviation of the historical data set's residuals in place of the forecast data set's residuals is done. This provides a SST monthly data set from 1985 to 2099 without any disjunction or jump and has same seasonal amplitude in the annual range where they overlap. The intention is to provide data series for two study regions along Lakshadweep reef region that are dominated by the temperature sensitive corals. Transformation for forecast data series was done using Excel package.

RESULTS AND DISCUSSION

The Hovmoller graph (Fig. 16.2) for the period 1985-2008 for the latitudinal range from 8º to 13ºN helps to identify the recent stress that reefs were experiencing along the Lakshadweep reef region. Monthly longitude-averaged (78º to 80ºE) temperature values are plotted for every 9-km resolution falling in the latitudinal range as mentioned above. The y-axis represents time in months starting from 1985-2008 (N = 280 months). Clearly the 1997-1998 and 2002 years show an abnormal increase in temperature. As the time increases, temperature rises and it is evident that cooler months are becoming warmer and the latitudinal effect also plays a key role for reefs experiencing thermal stress.

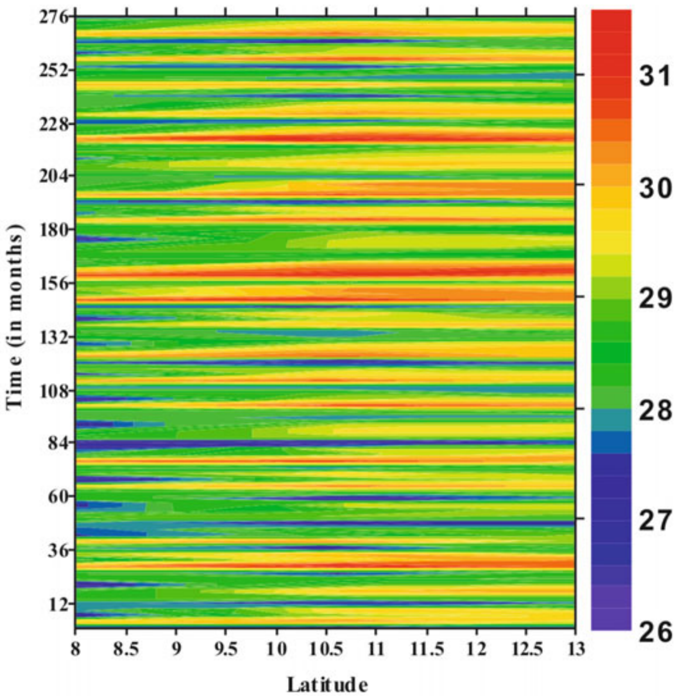

Fig. 16.2: Hovmoller graph showing the warmest years (1998 and 2002) of Lakshadweep reef region. The axes latitude (x-axis) and longitude averaged over time (y-axis) corresponding to 1985-2008.

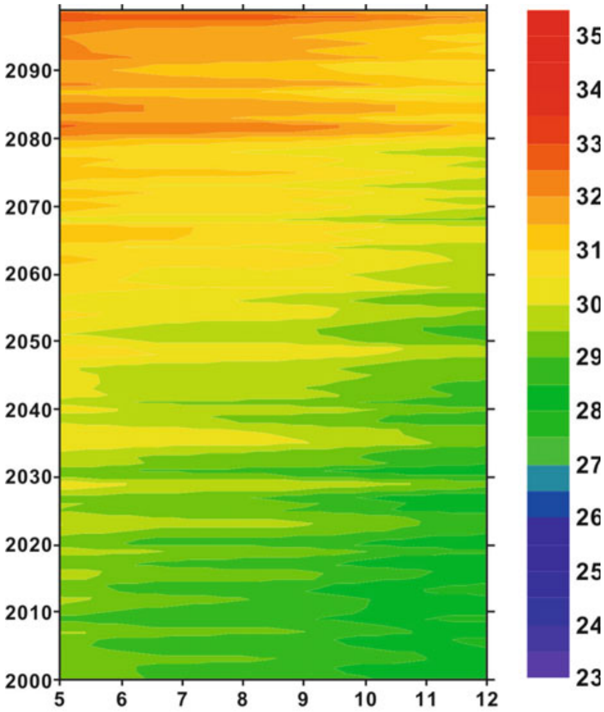

Fig. 16.3: Hovmoller graph showing the warming behaviour for the forecast data series HadCM3 SRES A2 model. The axes latitude (x-axis) and longitude averaged over time (y-axis) corresponding to 2000-2099.

Similarly, the Hovmoller graph for HadCM3 forecast data series shows how temperature increases over time along with latitudinal variation with longitude averaged. SRES A2 model was used and clearly it (Fig. 16.3) shows three different time periods when temperature changes significantly, mainly after 2020, 2050 and 2080. The *X* values help to study the latitudinal variation and Y values correspond to time from 2000-2099. The *X* values range from 5ºN to 12ºN to better understand the variation in warming. It is also visible that there will be a different behavioural pattern in temperature during second half of the century.

Projected Thermal Stress and Frequency of Coral Bleaching

The predicted rise becomes marked for all the sites and continues increasingly throughout the present century. Probability of repeat critical SSTs can be determined (Figs 16.4, 16.5, 16.6) from each site. Mortality in 1998 was triggered by SST rise lasting as short as the warmest month, although warming lasted three months in many areas (Wilkinson, 1999; Hoegh-Guldberg, 1999). It is not yet known exactly how much warming triggers bleaching leading to

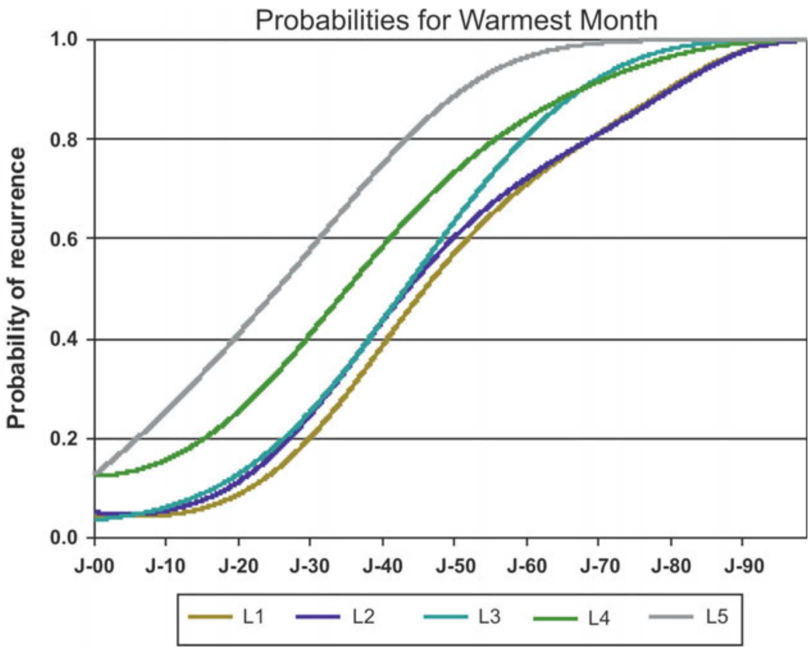

Fig. 16.4: The probability of recurrence for warmest month.

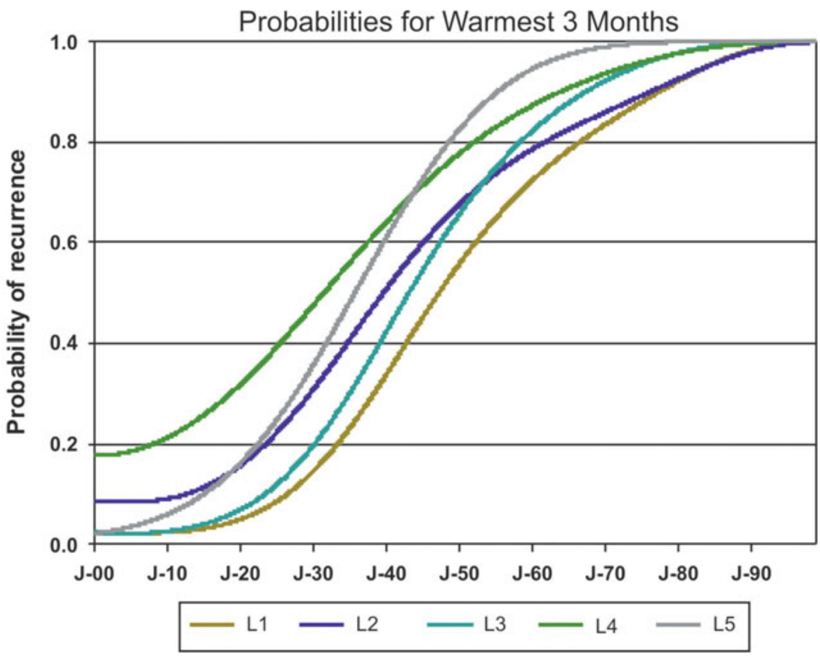

Fig. 16.5: The probability of recurrence for warmest three months.

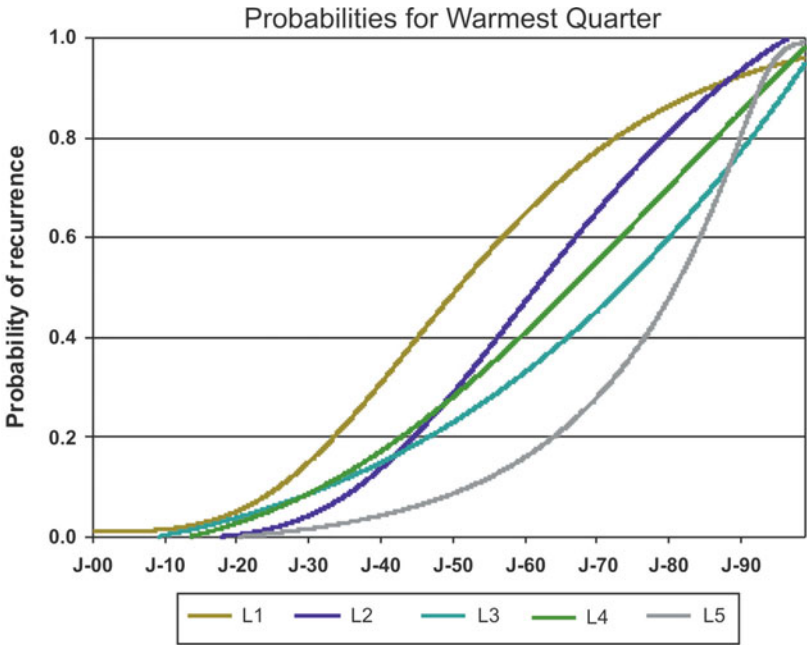

Fig. 16.6: The probability of recurrence for warmest quarter.

Table 16.1: 'Extinction date' values for Lakshadweep reef region based on climate model analyzed ($p = 0.2$)

Location	*Warmest month date*	*Warmest 3 months date*	*Warmest quarter date*
L1	2030	2034	2035
L2	2028	2023	2045
L3	2026	2030	2045
L4	2015	####	2042
L5	####	2023	2062

Cells with ### in a date column indicate the probability curves have crossed the desired value already.

mortality. The peak temperature which occurred in the 1998 El Nino was lethal to more than 90% of shallow corals, chosen to calculate the probability of warmest months, reaching this particular SST value as time progresses (Sheppard, 2003), along with warmest three months and warmest quarter. The curves integrate: the absolute SST at a site, its rate of rise and the temperature that was lethal to more than 90% of the shallow corals in 1998, which is a function of acclimation. Table 16.1 shows the date when temperature is expected to reach the peak 1998 values with a probability of 0.2, for the SRES A2 scenario for all the study regions.

The patterns are clear. Figs 16.4 to 16.6 show the probability recurrence for study regions for warmest three months and warmest quarter reaching the lethal temperature over time. The massive damage to coral reefs which already has occurred (Hoegh-Guldberg, 1999; Hughes et al., 2003) means that even in areas where conservation measures have been strong, reef recovery has been limited or absent. This clearly shows that warming is already present or may soon have an inhibiting effect on recovery of reefs; an important significance especially where up current areas, which are relied upon for supply of new recruits, are more affected by temperature stress than the recipient site, or are affected sooner (Sheppard and Rioja-Nieto, 2005). Site L5 and Site L4 have already reached the warmest month and warmest 3-month dates respectively. For the warmest month and warmest 3-month date, all sites expect to reach the thermal stress within the next two decades.

Required Adaptation to Increased Thermal Stress

The degradation of coral reefs is expected to increase in the coming decades. The increasing threat to coral reefs from rising temperatures and other interacting factors emanates a growing interest in identifying reefs that maintain high coral cover, biodiversity, and ecological functioning (McClanahan et al., 2007). This concept of resilience, addressing the capacity of ecosystems to recover and regenerate following major ecological disturbances, is increasingly becoming a main focus in ecological and resource management research (Hughes et al., 2005; Hooper, 2005).

To determine the increase in thermal tolerance required to ensure bleaching occurs only once every 10 ($p = 0.02$) years in the projected climates under SRES A2 model, iterations were performed at 0.05°C increase in threshold temperature accumulate for the study regions, until the frequency of bleaching events in a given decade reduced to the desired level. The 10-year return intervals is selected here based on a variety of evidence for the average time required for full recovery of coral cover after a bleaching or disturbance event (Done, 1999; Connell et al., 1997). The decades of 2030s and 2050s are used as possible benchmarks because all the reef sites experience thermal stress either annually or biannually during this period.

CONCLUSION

The results indicate that the thermal tolerance for corals need to increase substantially as mentioned in Table 16.2, to ensure that low-intensity bleaching events do not occur more than once every 10 years. Though the analysis shows substantial variation between the reef sites, it predicts that fastest adaptation will be required at the rate of 0.7°C to 1.5°C for reefs to experience thermal stress once ($p = 0.2$) every 10 years in 2050-2059 and adaptation rate of up to 0.65°C with 2030 as deadline. The required rate of thermal adaptation for sites at higher latitude is more compared to other sites. Present

Table 16.2: Required rate of thermal adaptation to limit bleaching recurrence for the warmest month

What-if scenario	*Study site*				
	L1	*L2*	*L3*	*L4*	*L5*
Thermal adaptation required to limit bleaching recurrence to once every 5 or 10 years (by the 2030-2039)	0-0.35	0.1-0.45	0.10-0.35	0.45-0.80	0.65-0.95
Thermal adaptation required to limit bleaching recurrence to once every 5 or 10 years (by the 2050-2059)	0.7-0.95	0.85-1.10	0.70-1.00	1.10-1.40	1.30-1.65

study suggests the increase in thermal tolerance required to ensure significant time for coral reef recovery between bleaching events is at least 0.2 to 0.3°C per decade in all the study sites, using either the 2030s or the 2050s as a deadline (Donner et al., 2005). Present study elucidates that SST will be increasingly important in the Lakshadweep, and the present data compilation may assist in determining, and forecasting, both the magnitude, dates and regional locations of such effects.

REFERENCES

Arthur, R. (2000). Coral bleaching and mortality in three Indian reef regions during an El Nino southern oscillation event. *Curr. Sci.*, **79(12):** 1723-1729.

Brown, B.E. (1997). Coral Bleaching: causes and consequences. *Coral Reefs*, **16:** S129-S138.

Connell, J.H., Hughes, T.P. and Wallace, C.C. (1997). A 30-year study of coral abundance, recruitment, and disturbance at several scales in space and time. *Ecological Monographs*, **67:** 461-488.

Cubasch, U., Meehl, G.A., Boer, G.J. et al. (2001). Projections of future climate change. *In:* Climate Change 2001: The Scientific Basis (eds Houghton, J.T. et al.). Cambridge University Press, New York.

Done, T.J. (1999). Coral community adaptability to environmental change at the scales of regions, reefs and reef zones. *American Zoologist*, **39:** 66-79.

Donner, S.D., Skirving, W.J., Little, C.M., Oppenheimer, M. and Hoegh-Guldberg, O.V.E. (2005). Global assessment of coral bleaching and required rates of adaptation under climate change. *Global Change Biology*, **11:** 2251-2265.

Glynn, P.W. (1996). Coral reef bleaching: facts, hypotheses and implications. *Global Change Biology*, **2:** 495-509.

Goreau, T.J. and Hayes, R.L. (1994). Coral Bleaching and Ocean 'Hot Spots'. AMBIO, **23:** 176-180.

Hoegh-Guldberg, O.V.E. (1999). Climate change, coral bleaching and the future of the world's coral reefs. *Marine and Freshwater Research*, **50:** 839-866.

Hooper, D.U. et al. (2005). Effects of biodiversity on ecosystem functioning: A consensus of current knowledge. *Ecological Monographs*, **75:** 3-35.

Hughes, T.P., Bellwood, D.R., Folke, C., Steneck, R.S. and Wilson, J. (2005). New paradigms for supporting the resilience of marine ecosystems. *Trends in Ecology and Evolution*, **20:** 380-386.

Hughes, T.P. et al. (2003). Climate change, coral bleaching and the resilience of coral reefs. *Science*, **301:** 929-933.

Jackson, J.B.C. (1997). Reefs since Columbus. *Coral Reefs*, **16:** S23-S32.

Jokiel, P.L. and Coles, S.L. (1990). Response of Hawaiian and other Indo–Pacific reef corals to elevated temperatures. *Coral Reefs*, **8:** 155-161.

Kumaraguru, A.K., Jayakumar, K. and Ramakritinan, C.M. (2003). Coral bleaching 2002 in the Palk Bay, southeast coast of India. *Current Science*, **85(12):** 1787-1793.

McClanahan, T.R., Ateweberhan, M., Ruiz Sebastian, C., Graham, N.A.J., Wilson, S.K., Bruggemann, J.H. and Guillaume, M.M.M. (2007). Predictability of coral bleaching from synoptic satellite and in situ temperature observations. *Coral Reefs*, 10.1007/s00338-006-0193-7.

Nakicenovic, N., Davidson, O., Davis, G. et al. (2000). IPCC Special Report on Emissions Scenarios, Intergovernmental Panel on Climate Change. Available at: http://www.grida.no/climate/ipcc/emission/

Parry, M.L., Rosenzweig, C., Iglesias, A., Livermore, M. and Fischer, G. (2004). Effects of climate change on global food production under SRES emissions and socio-economic scenarios. *Global Environmental Change – Human Policy Dimensions*, **14:** 53-67.

Rajasurya, A., Zahir, H., Venkataraman, K., Islam, Z. and Tamelander, T. (2004). Status of coral reefs of south Asia: Bangladesh, Chagos, India, Maldives and Sri Lanka. G.C.R.M.N. Report. *Aust. Inst. Mar. Sci.*, 213-234.

Rajasurya, A., Venkataraman, K., Muley, E.V., Zahir, H. and Cattermonl, B. (2002). Status of coral reefs in south Asia: Bangladesh, India, Maldives, Sri Lanka. G.C.R.M.N. Report. *Aust. Inst. Mar. Sci.*, 101-121.

Sebens, K.P. (1994). Biodiversity of Coral Reefs: What we are losing and why? *American Zoologist*, **34:** 115-133.

Sheppard, C.R.C. (2003). Predicted recurrences of mass coral mortality in the Indian Ocean. *Nature*, **425:** 294-297.

Sheppard, C.R.C. (2004). Sea surface temperature 1871-2099 in 14 cells around the United Kingdom. *Mar. Pollut. Bull.*, **49:** 12-16.

Sheppard, C. and Rioja-Nieto, R. (2005). Sea surface temperature 1887-2099 in 38 cells in the Caribbean region. *Marine Environmental Research*, **60:** 389-396.

Strong, A.E., Gjovig, K.K. and Kearns, E. (2000). Sea Surface Temperature Signals from Satellites – An Update. *Geophys. Res. Lett.*, **27(11):** 1667-1670.

Toscano, M.A., Liu, G., Guch, I.C., Casey, K.S., Strong, A.E. and Meyer, J.E. (2000). Improved prediction of coral bleaching using high resolution hot spot anomaly mapping. *Proc. IX International Coral Reef Symp., Bali*, **2:** 1143-1148.

Vasquez, J., Perry, K. and Kilpatrick, K. (1998). NOAA/NASA AVHRR Oceans

Pathfinder Sea Surface Temperature Data Set User's Reference Manual Version 4.0. JPL Publication D-14070. Available online at http://podaac.jpl.nasa.gov/

Vivekanandan, E., Hussain Ali, M., Jasper, B. and Rajagopalan, M. (2008). Thermal thresholds for coral bleaching in Indian seas. *Journal of Marine Biological Association of India*, **50(2):** 209-214.

Wilkinson, C. (1999). Global and local threats to coral reef functioning and existence: Review and predictions. *Marine and Freshwater Research*, **50:** 867-878.

Wilkinson, C., Linden, O., Cesar, H., Hodgson, G., Rubens, J. and Strong, A.E. (1999). Ecological and socioeconomic impacts of 1998 coral mortality in the Indian Ocean: An ENSO impact and a warning of future change. *AMBIO*, **26:** 188-196.

William, K.F., Barbara, E.B., Mark, E.W. and Richard, P.D. (2001). Coral bleaching: interpretation of thermal tolerance limits and thermal thresholds in tropical corals. *Coral reefs*, **20:** 51-65.

Yonge, C.M. and Nichols, A.G. (1931). Studies on the physiology of corals: V. The effect of starvation in light and in darkness on the relationship between corals and zooxanthellae. Scientific Report of the Great Barrier Reef Expedition, **1:** 177-211.

Part IV

Livelihood Options

CHAPTER

17

Hatchery Production of Marine Ornamental Fishes: An Alternate Livelihood Option for the Island Community at Lakshadweep

K.V. Dhaneesh, R. Vinoth, Swagat Ghosh, M. Gopi, T.T. Ajith Kumar and T. Balasubramanian

Centre of Advanced Study in Marine Biology, Faculty of Marine Sciences
Annamalai University, Parangipettai – 608502, Tamil Nadu
tt_ajith@yahoo.co.in

INTRODUCTION

The hobby of marine ornamental fish keeping is more valuable as aquarium keeping has become more popular and more hobbyists are interested in this lucrative trade. The export value of ornamental fishes has increased 10 times higher from 0.9 to 9 million US $ and continues to reach almost 29 million US $ in 2007 (Tissera, 2010). A total of 1471 marine ornamental fish species are traded globally and among them only 25% are bred in captivity and out of that, only 21 species are commercially produced. The most commonly traded marine fish belong to the family Pomacentridae, which accounted for 43% (Collette et al., 2003; Madhu et al., 2010). About 400 species belonging to 175 genera coming under 50 reef families are found in the Indian seas. To preserve the delicate reef ecosystem, many studies have been carried out to develop breeding and rearing methods for marine ornamentals which are essential for the development of sustainable ornamental aquaculture (Ajith and Balasubramanian, 2009; Ajith et al., 2010; Dhaneesh et al., 2011).

The increasing demand of marine ornamental fishes due to the recent developments in aquarium keeping has resulted in over exploitation of natural

J. Sundaresan et al. (eds.), *Climate Change and Island and Coastal Vulnerability*,
DOI 10.1007/978-94-007-6016-5_17, © 2013 Capital Publishing Company

stock and consequent destruction of reef areas (Alava and Gomes, 1989). The indiscriminate methods of harvest followed can damage the coral ecosystem, which provides the microhabitat requirement for different species of reef associated organisms. Hence, the only option to meet the demand of marine ornamental fishes and to restore the wild population is their hatchery production. By developing and transferring the breeding technology of marine ornamental fishes to the coastal people as their livelihood, will lead to reduction of over-exploitation and pressure on popular species and can save the fragile coral reef ecosystem from degradation. Considering this, the present study was conducted to develop a hatchery technology for clownfish *Amphiprion nigripes* and damselfishes *Chromis viridis* and *Dascyllus aruanus* for sustainable aquarium trade.

MATERIALS AND METHODS

Study Area

Agatti Island lies (Lat. 10°51′ N; Lon. 72°11′ E) on the Lakshadweep archipelago in the Arabian Sea and it is India's one of the four coral reef regions and only one that has atoll.

Broodstock Development

Matured clownfish *A. nigripes* [total length (TL) 70-80 mm; *n* = 20], damselfish *Chromis viridis* (TL, 50-60 mm, *n* = 10), *Dascyllus aruanus* (TL, 50-60 mm, *n* = 10) and sea anemone *Heteractis magnifica* (*n* = 12) were collected from 1-2 m depth from the west side of the island by skin diving during low tide using gill net and scoop nets. Clownfish and sea anemone were accommodated in the same tank and damselfishes were accommodated in two separate fibre glass tanks (capacity, 2000 litre) for a month. After pair formation, 10 pairs of *A. nigripes* (TL, 75-85 mm) were transferred to individual ash coloured rectangular fibre glass tanks (capacity, 1000 litre) with host anemone and white ceramic tile, dead coral pieces and live rocks were provided as substratum for egg laying (Figs 17.1 and 17.2). Among the three substratums, the fish mostly preferred the ceramic tile for egg deposition.

The green damsel *Chromis viridis* (*n* = 5) and humbug damsel *Dascyllus aruanus* (*n* = 5) were also transferred to individual white inner coloured circular fibre glass tanks (capacity, 1000 litre) and, earthen pot and ceramic tile were provided as substratum for egg laying (Figs 17.3 and 17.4). The tanks were provided with individual locally made underwater biological filter. The photoperiod was maintained at 12 h light (0700-1900 h): 12 h dark (1900-0700 h) using fluorescent bulb with light intensity of 600-900 lux. Fishes were fed with tuna eggs, boiled meat of fish and clam five times per day (08:00, 10:00, 12:00, 14:00 and 16:00 h). Excreta and remnant food

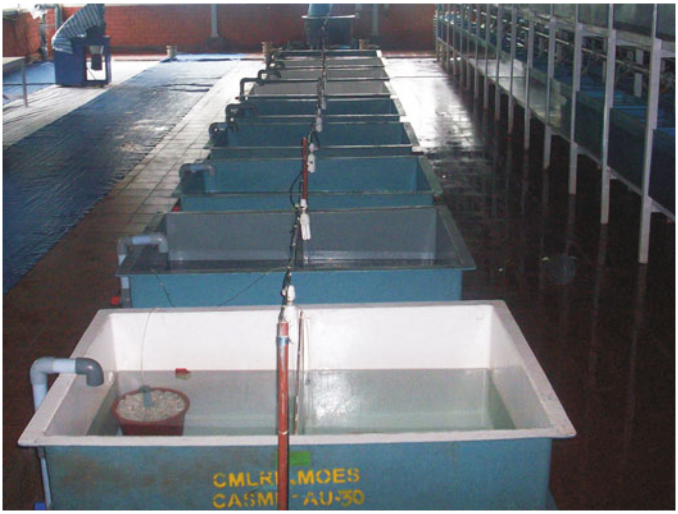

Fig. 17.1: Broodstock rearing setup of *A. nigripes* which is accommodated with sea anemone in fibre glass tanks.

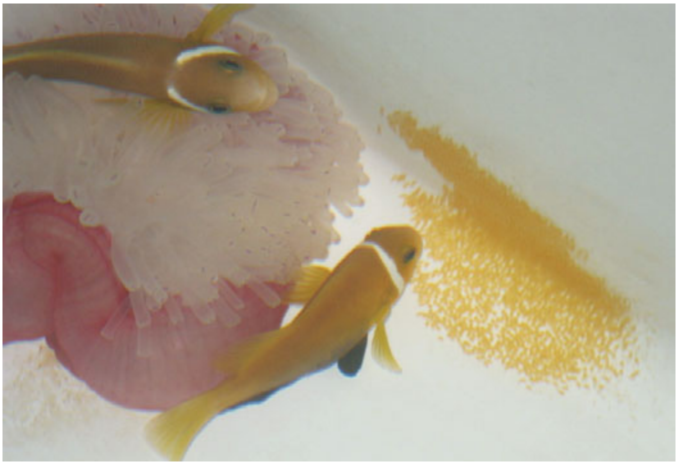

Fig. 17.2: *A. nigripes* with newly laid eggs.

particles were siphoned out an hour after feeding. Water used in the brooder tank was U.V. irradiated and then passed through a cartridge filter. Water quality parameters in the tanks were maintained at optimum levels (temperature 28 ± 1°C, salinity 34 ± 1 ‰, pH 8 ± 0.2 and dissolved oxygen 6.8 ± 0.3 mg l^{-1}). Once a week, 50% water was exchanged in the tanks. The batch fecundity was estimated by counting the eggs in 1 cm^2 and then multiplying with the total area of deposition (Satheesh, 2002).

Fig. 17.3: Green damsel *C. viridis.*

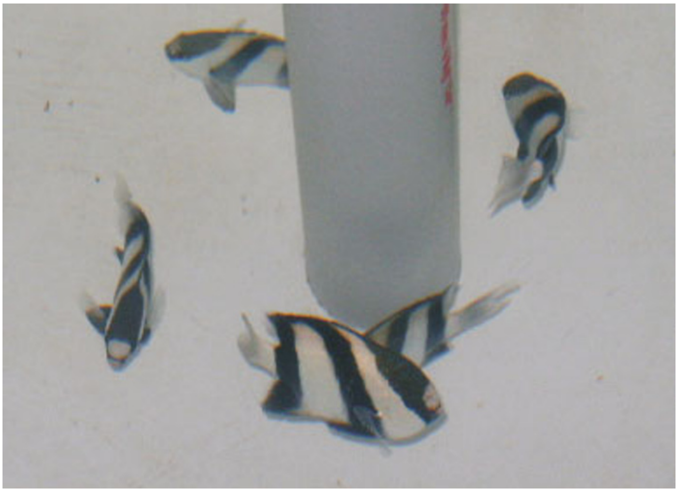

Fig. 17.4: Humbug damsel *D. aruanus*.

Live Feed Culture

The stock culture of microalgae and rotifer were brought from the Centre of Advanced Study in Marine Biology, Annamalai University, Tamil Nadu. The algal stock culture of *Nannochloropsis salina* was maintained using F2 medium under laboratory condition (temperature 25 ºC, salinity 34 ± 1 ‰ and pH 8.3 ± 0.2). The photoperiod was maintained as 12 h light: 12 h dark with a light intensity of 4000 lux. The same was enhanced to outdoor mass culture (Batch culture) in white circular fibre glass tanks (capacity, 1000 litre) with commercial fertilizers like ammonium sulphate, super phosphate and urea in 10:1:1 ratio for 100 litre. The outdoor mass culture of rotifer *Brachionus plicatilis* was raised in 1000 litre translucent tanks by feeding with microalgae. *Artemia* cysts (Supreme Plus, USA) were hatched out in separate 200 litre black circular fibre glass tank with vigorous aeration, which was illuminated by a 100 W bulb for 24 h.

Larval Rearing

Amphiprion nigripes

The hatching occurred after sunset (178 h after spawning) and the hatched out larvae were gently collected with a beaker and transferred to 100 litre oval shaped white fibre glass tanks. The tanks were stocked at three larvae l^{-1} of water. Water quality parameters were monitored daily (temperature 27 ± 1°C, salinity 34 ± 1‰, pH 8 ± 0.2 and the dissolved oxygen 7.0 ± 0.2 mg l^{-1}). A 12 h photoperiod was provided at an intensity of 600 lux (12 light – 12 dark).

Chromis Viridis and Dascyllus Aruanus

Both species of damsels laid oval shaped transparent eggs on the substratum provided in the tanks (Figs 17.5 and 17.6). The substratum with egg clutch were transferred to previously set fibre glass larval rearing tanks containing seawater, on the evening of the 3rd day after spawning. A gentle air flow was created near the egg clutch by placing an air stone under the substratum. The eggs hatched out to larvae at night time after 3-4th day of incubation. The water quality was maintained at the same level as in parent tanks.

Fig. 17.5: Eggs of damsel fishes spawned on the earthen pots.

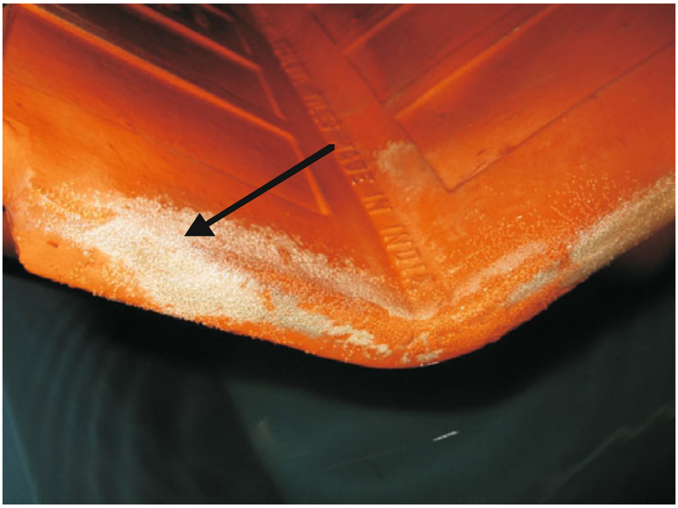

Fig. 17.6: Eggs of damsel fishes spawned on the ceramic tile.

RESULTS

Spawning

Clownfish *A. nigripes* started spawning within two months of rearing in the spawning tank. Spawning mostly occurred during morning hours (09:00-12:00 h). The females started to lay capsule shaped eggs on the cleaned substratum mostly in oval patch and the male subsequently shed milt and fertilized the eggs. The spawning lasted upto 45 to 60 minutes with an approximate fecundity of 300-800 eggs per spawning. The embryonic development was illustrated in Figs 17.7 a-h. The periodicity of spawning ranged between 9 and 21 days.

The capsule shaped orange eggs were attached to the substratum and measured 2.0-2.3 mm length and 1.0-1.2 mm width (Figs 17.8 a-d and 17.9 a-d). During the incubation period, males played major role in parental care which involves fanning and mouthing the eggs. The incubation period lasts 7-9 days depending upon the surrounding water temperature. On the day of hatching, the egg capsule became very thin and transparent which underwent a series of colour changes from orange, black and finally to silvery during incubation.

The damsels started to lay eggs after four months of rearing in the spawning tank. Before spawning, the parents actively clean the substratum using their mouth and fins. Spawning occurred in morning hours. During spawning, the female attached the eggs on the cleaned substratum, which were immediately fertilized by the male and the batch fecundity was 1500-2500 eggs. The eggs were oval shaped and measures 1.2-1.4 mm length and 0.6 mm width.

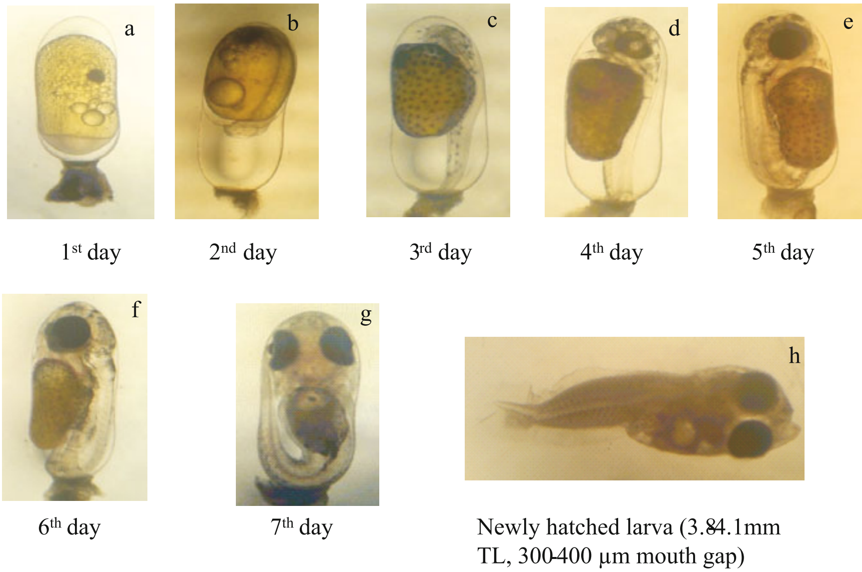

Fig. 17.7 a-h: Embryonic developmental stages and newly hatched larva of *A. nigripes.*

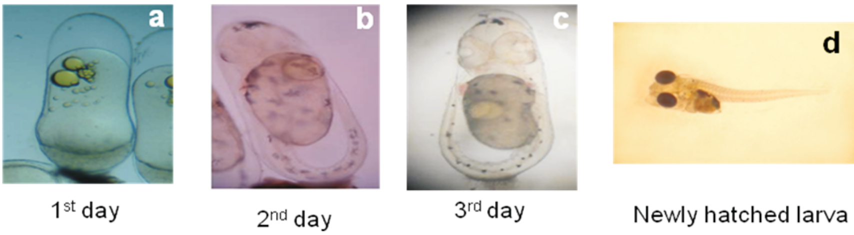

Fig. 17.8 a-d: Embryonic developmental stages and newly hatched larva of Green damsel *C. viridis*.

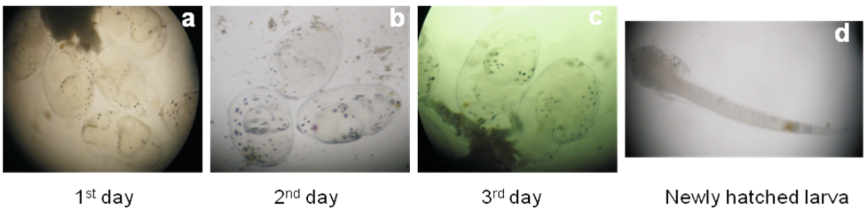

Fig. 17.9 a-d: Embryonic developmental stages and newly hatched larva of Humbug damsel *D. aruanus*.

Larval Rearing

The newly hatched larvae (TL, 3.8-4.1 mm) of clownfish were primarily floating and were collected and transferred into larval rearing tanks at a density of three larvae per litre. Rotifers (*B. plicatilis*) enriched with algae

(*N. salina*) were added to the larval tanks at a density of 6-8 rotifers ml^{-1} as the initial feed thrice daily (10:00, 13:00 and 16:00 h) for the first 10 days. The rotifers were substituted with freshly hatched *Artemia* nauplii at a density of 3-5 nos. ml^{-1} from 11^{th} day of hatch. Boiled and finely chopped clam meat was fed to the juveniles from 25^{th} day of hatch. Gentle aeration was provided to maintain optimum level of dissolved oxygen and to achieve homogeneous distribution of the added live feed. The tank bottom was cleaned and 10% of the tank water was replaced daily without disturbing the fry. Water quality parameters were monitored daily and 12 h photoperiod was provided with an intensity of 600 lux (12 h light - 12 h dark). The larvae got parent colouration by 15-16 days after hatching. For the first two weeks the larvae were pelagic, but gradually moved to the bottom during metamorphosis (Fig. 17.10).

The newly hatched larvae of both species of damselfish have 2.4-2.5 mm total length and at third day they have 40 µ mouth gap. Microalgae (*N. salina*) along with plankton collected from wild (10-20 no ml^{-1}) were gently added to circular larval rearing tanks (100 litre). Up to 20 days post hatch, the larvae were fed with algae enriched wild plankton (nauplii of copepod, Sagitta, Mysis, Ostracod and Zoea). After 20 days, freshly hatched *Artemia* nauplii were supplemented (3-5 nauplii ml^{-1}). The larvae attained parent colouration between 25 and 30 days after hatch and were 20-21 mm length (Figs 17.11 and 17.12).

Fig. 17.10: One month old juveniles of *A. nigripes* associated with sea anemone *H. magnifica.*

Technology Transfer to Islanders

Through transfer of the breeding technology developed for these marine ornamental fishes to the public for their livelihood, the stress associated with

Fig. 17.11: Metamorphosed juveniles of *C. viridis*.

Fig. 17.12: Metamorphosed juveniles of *D. aruanus*.

the over-exploitation of fishes from the wild habitat can be reduced and the islanders can be made capable of earning additional income. The technology developed by the Centre of Advanced Studies in Marine Biology, Annamalai University with the financial support of Centre for Marine Living Resources and Ecology (MoES), Kochi has been geared up to transfer to the recognized progressive islanders of Agatti through training programmes. This will facilitate to set up backyard hatcheries through funding by National Fisheries

Development Board, Hyderabad with 50% subsidy as a livelihood development and so conserve the coral reef fauna from degradation.

DISCUSSION

Many studies have already been carried out with the aim of developing breeding and rearing methodology for marine aquarium ornamentals which are in demand for the trade (Madhu et al., 2010; Dhaneesh et al., 2011; Satheesh, 2002; Gopakumar et al., 2002). The main key factor for successful larviculture of marine ornamental fishes depends chiefly on the appropriate size and nutritional quality of live feeds. Among the marine ornamental fishes, the first success was achieved in the breeding and seed production of clownfishes, as their larviculture protocols are comparatively easy (Hoff, 1996). There are many reports on the successful breeding and larval rearing of clownfishes and damselfishes from different parts of the world using seawater or estuarine water (Ajith and Balasubramanian, 2009; Dhaneesh et al., 2011; Gopakumar et al., 2002; Gopakumar and Santhoshi, 2007). However, the present study is one of the first successful attempts on broodstock development, breeding and larval rearing of clownfish *A. nigripes* and two damselfishes *Chromis viridis* and *Dascyllus aruanus* in Lakshadweep. Water quality requirements, nutrition, feeding and appropriate photoperiod that influences the successful hatchery production of these species have been standardized in this study.

Approximately 10-20% of larval (clownfish) mortality was observed during 1st and 2nd days after hatching and it was unavoidable. This mortality may be due to the stress and injury caused during larval transfer from the parent tank to the larval rearing tank and due to difficulties of the larvae in accepting the first feed. Mortalities were also observed during weaning the larvae from rotifer to *Artemia* feed regime. In case of damselfish larva, the mortality was approximately 30-40% during the initial days which was largely due to the problems experienced in the initial feeding activities. It was also observed that ingested un-hatched *Artemia* cysts blocked the digestive tract of larvae and interfered with the normal digestive process.

The shape of Pomacentrid fish eggs was varying from oval to capsule shaped in different species (Moyer and Nakazono, 1978; Pathiyasevee, 1994). Hoff (1996) reported that the length of clownfish eggs ranged from 2.0 to 2.4 mm. The eggs of *Amphiprion chrysopterus* was measured as 2.4 × 0.9 mm (Allen, 1980), *A. ocellaris* was 1.5-3 mm × 0.8-1.84 mm (Madhu et al., 2006), *Premnas biaculeatus* was 2.8-3.5 mm × 1.1-1.7 mm (Madhu et al., 2006), *A. percula* was 2.0-2.3 mm × 1.0-1.2 mm (Dhaneesh et al., 2009) and *A. nigripes* was 2.0-2.3 mm × 1.0-1.2 mm (present study). In the present study, in *A. nigripes* metamorphosis was completed within 15-17 days. This duration was within the range of days reported in earlier works with other species of clownfish. Madhu et al. (2006) recorded the completion of metamorphosis of *A. ocellaris* in 9-10 days; 12-15 days in *A. sebae* (Ignatius et al., 2001); 11-12 days in *Premnas biaculeatus* (Madhu et al., 2006) and 12-15 days in *A. chrysogaster* (Gopakumar et al., 2001).

A number of studies have shown that the inclusion of copepods nauplii in the early larval diet significally improved the survival and growth of groupers (Doi et al., 1997; Toledo et al., 1999) and snappers (Singhagraiwan and Doi, 1993; Doi et al., 1997; Schipp et al., 1999). Copepods have also been employed for the larviculture of the halibut *Hippoglossus hippoglossus*, turbot *Scophthalmus maximus*, cod *Gadus morhua*, sea bream *Archoargus rhomboidalis*, bay anchovy *Anchova mitchilli* and lined sole *Achirus lineatus* (Phelps et al., 2005). Similarly, in the present study, the damselfish larvae were initially fed with wild collected plankton mainly containing copepods which resulted in much better eventual survival rate. The small sized first naupliar stages of the copepods and the availability of different sizes of nauplii during the initial phase of larviculture had facilitated and sustained the first exogenous feeding of the larvae (Gopakumar et al., 2009).

CONCLUSION

The present study unveiled the breeding and larviculture of clownfish *A. nigripes*, green damsel *C. viridis* and humbug damsel *D. aruanus* under captive condition at Agatti Island, Lakshadweep. The larvae of clownfish and damselfishes showed good survival when they fed with rotifer *Brachionus plicatilis* and wild collected plankton (majority copepods) enriched with microalgae *Nannochloropsis salina*. The simple technology developed through this study can be adopted by the islanders for their supplementary livelihood option in the way of producing marine ornamental fish juveniles for export. In addition it will lead to reduce the destructive fishing practices followed in the wild and thereby can conserve and protect the fragile reef ecosystem.

ACKNOWLEDGEMENTS

Authors are thankful to the authorities of Annamalai University for the facilities and the Centre for Marine Living Resources and Ecology (Ministry of Earth Sciences), Kochi for financial assistance.

REFERENCES

Ajith Kumar, T.T. and Balasubramanian, T. (2009). Broodstock development, spawning and larval rearing of the false clownfish, *Amphiprion ocellaris* in captivity using estuarine water. *Curr. Sci.*, **97(10):** 1483-1486.

Ajith Kumar, T.T., Subodh Kant Setu, Murugesan, P. and Balasubramanian, T. (2010). Studies on captive breeding and larval rearing of clownfish *Amphiprion sebae* (Bleeker, 1853) using estuarine water. *Indian J. Mar. Sci.*, **39(1):** 114-119.

Alava, V.R. and Gomes, L.A.O. (1989). Breeding marine aquarium animals: The anemone fish. *Naga* (The ICLARM Quarterly), **12:** 12-13.

Allen, G.R. (1980). Anemonefishes of the world: Species, care and breeding. Aquarium Systems Mentor, Ohio.

Collette, W., Taylor, M., Green, E. and Razak, T. (2003). From ocean to aquarium: A global trade in marine ornamental species. UNEP world conservation and monitoring centre (WCMC), 1-64.

Dhaneesh, K.V., Ajith Kumar, T.T. and Shunmugaraj, T. (2009). Embryonic Development of Percula Clownfish, *Amphiprion percula* (Lacepede, 1802). *Middle-East J. Sci. Res.*, **4(2):** 84-89.

Dhaneesh, K.V., Nanthini Devi, K., Ajith Kumar, T.T., Balasubramanian, T. and Kapila Tissera (2012). Breeding, embryonic development and salinity tolerance of Skunk clownfish *Amphiprion akallopisos*. *Journal of King Saud University - Science*, **24(3):** 201-209.

Doi, M., Ohno, A., Taki, Y., Singhagraiwan, T. and Kohno, H. (1997b). Nauplii of the calanoid copepod *Acartia sinjiensis* as an initial food organism for larval red snapper, *Lutjanus argentimaculatus. Suisanzoshou*, **45:** 31-40.

Doi, M., Toledo, J.D., Golex, M.S.N., De los Santos, M. and Ohno, A. (1997a). Preliminary investigation of feeding performance of larvae of early red–spotted grouper, *Epinephelus coioides*, reared with mixed zooplankton. *Hydrobiologia*, **358:** 259-263.

Gopakumar, G., Rani Mary George and Jasmine, S. (2001). Hatchery production of the clown fish *Amphiprion chrysogaster*. *In:* Perspective in Mariculture (ed.) N.G. Menon and P.P. Pillai. The Marine Biological Association of India.

Gopakumar, G. and Santhoshi, I. (2007). Use of copepods as live feed for larviculture of damselfishes. Asian Fisheries Forum, Kochi. Abstract AQP 050.

Gopakumar, G., Santhoshi, I. and Ramamurthy, N. (2009). Breeding and larviculture of the sapphire devil damsel *Chrysiptera cyanea. J. Mar. Biol. Ass. India*, **51(2):** 130-136.

Gopakumar, G., Sreeraj, G., Ajith Kumar, T.T., Sukumaran, T.T., Raju, B., Unnikrishnan, C., Hillary, P. and. Benziger, V.P. (2002). Breeding and larval rearing of three species of damselfishes (Family Pomacentridae). *Mar. Fish. Infor. Serv. T. and E.*, **171:** 3-5.

Hoff, F.H. (1996). Conditioning, Spawning and Rearing of Fish with Emphasis on Marine Clown Fish. *Aqua. Consult*, 1-211.

Ignatius, B., Rathore, G., Jagdis, I., Kandasami, D. and Victor, A.C.C. (2001). Spawning and larval rearing technique for tropical clownfish *Amphiprion sebae* under captive conditions. *J. Aqua. Trop.*, **16(3):** 241-249.

Madhu, K., Rema Madhu and Gopakumar, G. (2010). Breeding technology developed in marine ornamental fishes under captivity in India. *In:* Ornamentals Kerala-2010, Dept. of Fisheries, Govt. of Kerala.

Madhu, K., Rema Madhu, Gopakumar, G., Sasidharan, C.S. and Venugopalan, K.M. (2006b). Breeding, larval rearing and seed production of maroon clown *Premnas biaculeatus* under captive conditions. *Mar. Fish. Infor. Serv. T. and E.*, **190**.

Madhu, K., Rema Madhu, Krishnan, L., Sasidharan, C.S. and Venugopalan, K.M. (2006a). Spawning and larval rearing of *Amphiprion ocellaris* under captive conditions. *Mar. Fish. Infor. Serv. T. and E.*, **188**.

Moyer, J.T. and Nakazono, A. (1978). Protandrous hermaphroditsm in six species of the anemone fish genus Amphiprion in Japan. *Jap. J. Icthyol.*, **25:** 101-106.

Pathiyasevee, U. (1994). Egg-laying behaviour and growth of false clown anemonefish, *Amphiprion ocellaris* (Cuvier, 1830). National Institute of Coastal Aquaculture, Department of Fisheries, Bangkok, Thailand.

Phelps, P.R., Gede, S., Sumiarsa, Emily, E.L., Hsiang-Pin Lang, Komarey Kao Moss and Allen, D.D. (2005). Intensive and extensive production techniques to provide copepod nauplii for feeding larval red snapper *Lutjanus campechanus. In:* Copepods in Aquaculture. Cheng-Sheng Lee, Patricia, J.O. and Nancy H. Marcus (Blackwell Publishing, USA) 2005, pp. 115-168.

Satheesh, J.M. (2002). Biology of the clownfish, Amphiprion sebae (Bleeker) from Gulf of Mannar (South east coast of India). Ph. D. thesis, Annamalai University, India.

Schipp, G.R., Bosmans, J.M.P. and Marshall, A.J. (1999). A method for hatchery cultivation of tropical Calanoid copepods, *Acartia* spp. *Aquaculture*, **174:** 81-88.

Singhagraiwan, T. and Doi, M. (1993). Induced spawning and larval rearing of the red snapper, *Lutjanus argentimaculatus* at the Eastern Marine Fisheries Development Centre. *Thai. Mar. Fish. Res. Bull.*, **4:** 45-57.

Tissera, K. (2010). Global trade in ornamental fishes. *In:* Ornamentals Kerala-2010. Dept. of Fisheries, Govt. of Kerala.

Toledo, J.D., Golex, M.S., Doi, M. and Ohno, A. (1999). Use of copepod nauplii during early feeding stage of grouper *Epinephelus coioides. Fish. Sci.*, **65:** 390-397.

CHAPTER

18

Living in Harmony with Nature: Complication of Climate Change and Governance

H.A. Karl

Antioch University New England
Keene, New Hampshire, USA
hkarl@comcast.net

INTRODUCTION

Climate change, a coupled natural and human system, is perhaps the greatest challenge facing society as it is global, but it will affect regions and localities in different ways. Anthropogenic activities have altered the natural climate system. Changing climate alters human activities. This feedback loop is non-linear and effects are amplified in unknown ways that may lead to unexpected tipping points both in global climate and viability of society. We must find ways, and soon, to adapt to changing climate to sustain social systems. Human systems are coupled to, and indeed dependent upon, natural systems; we need to conduct climate change research that integrates studies of both systems. *And we need to apply what we learn about these systems to decisions that get made*.

Climate change is a wicked problem—a class of problems that cannot be solved by technology and science alone because they have a human dimension (Rittel and Weber, 1973; Brown et al., 2010). Coupled natural and human systems, by this definition, present wicked problems. Almost all environmental problems are wicked and climate change is the perfect storm of a wicked problem (Karl et al., 2011). Wicked problems are considered intractable. It is suggested they are only intractable if one expects a discrete and one-time

J. Sundaresan et al. (eds.), *Climate Change and Island and Coastal Vulnerability*,
DOI 10.1007/978-94-007-6016-5_18, © 2013 Capital Publishing Company

solution. The nature of a wicked problem is constantly changing through time, because both natural and human systems are dynamic. Thus, one cannot approach solving a wicked problem with a solution in mind. There is no solution and in this sense the problem is intractable. But that does not mean it cannot be dealt with. We might define "the solution" in a different way. The solution is one of altering and adjusting decisions in response to the changing problem. In other words we need to find ways to adapt to the ever-emerging properties of changing climate.

Whereas this paper focusses on the United States, it has implications for other societies and cultures striving to adapt to changing climate. During the last decade, societies have begun to embrace not only mitigation but also adaptation as strategies to cope with global warming. And now adaptation is considered by most to include mitigation measures.

International accords and national policies, although necessary, are insufficient for effective adaptation to climate change. Adaptation is local and requires community planning and grass roots movements. My premise is that collective action across and that integrates all scales and levels of governance and society is needed to address the impacts of climate change to achieve sustainable societies and ecosystems. An essential and critical part of this premise is the imperative of representing the wide range of interests, insights, knowledge, and experience that resides in a highly diverse society. Disadvantaged groups and communities are being disproportionately affected by the impacts of climate change (for example, submergence of the Sundarbans and Pacific island nations, the effects of Hurricane Katrina, etc.). These groups and communities must be included in developing adaptation strategies for society to survive changing climate. Many reports and guides on adaptation to climate change recommend public involvement. We must develop a truly participatory, collaborative process that combines deliberation with analysis in an inclusive process; it must become a way of thinking and doing that infuses our current governance and decision-making processes and helps to guide their evolution and foster new institutional arrangements, and it must grow from the grass roots up and be supported from the top down.

In modern western culture, the question of whether humans can live in harmony with nature has been debated since at least the contrasting philosophies of the 17th century English philosopher Thomas Hobbes and the 18th century French philosopher Jean-Jacques Rousseau. Essentially Hobbes viewed competitiveness and violence as the innate tendency of humans, whereas Rousseau saw human nature as largely benevolent and good. An extension of Hobbes' view is that humans are in competition with nature, whereas Rousseau believed humans could live in harmony with nature. The "cynical" and "idealistic" view of human nature may be considered end-members of the human relationship with the environment.

CONCEPTUAL MODELS OF ENVIRONMENTAL POLICY

These contrasting philosophies to this day influence and shape distinctly different approaches to environmental policy and climate change. In the late 1960s and early 1970s several environmental protection laws, including the Clean Air Act of 1970, the Clean Water Act of 1972, and Endangered Species Act of 1973, were enacted in the United States. These unprecedented laws were a response to the environmental crisis of the 1960s that was symbolized by Cleveland's contaminated Cuyahoga River catching fire. The National Environmental Policy Act (NEPA)—the foundation of modern American environmental policy—was enacted in 1969.

The purpose of NEPA is "to foster and promote the general welfare, to create and maintain conditions under which man and nature can exist in productive harmony, and fulfill the social, economic, and other requirements of present and future generations of Americans."[1] In effect, NEPA aspires to achieve reconciliation or balance or harmony among three systems: natural (ecological) systems, social systems, and economic systems. Moreover, it mandates, among other directives, that all federal agencies should "utilize a systematic, interdisciplinary approach which will ensure the *integrated use* of the natural and social sciences and the environmental design arts in planning and in decisionmaking which may have an impact on man's environment" and "…insure that presently unquantified *environmental amenities and values* may be given appropriate consideration in decision-making along with economic and technical considerations"[2] (emphasis added).

Many subsequent reports and environmental initiatives have also aimed to achieve the aspirations set forth in NEPA. Yet, environmental policy continues to fall short of achieving productive harmony (Karl et al., 2012).

Contrasting Conceptual Models

The following discussion is excerpted from the first chapter of Karl et al. (2012).

> Productive harmony is most often interpreted to imply an equal status among the three systems. However, one worldview puts economic systems and societies they support on a higher plane than ecological systems, whereas another worldview elevates ecological systems. These opposing worldviews generate conflict, which often results in dysfunction, because the antagonists on one side presume robust economies are attained at the expense of ecosystem health (despoiling the environment) and those on the other side believe aggressive environmental protection and ecosystem restoration are not compatible with strong (profitable) economies. Some actions to reduce environmental impacts do carry costs, and most production and consumption activities have some

[1] http://ceq.hss.doe.gov/nepa/regs/nepa/nepaeqia.htm; Section 101.
[2] http://ceq.hss.doe.gov/nepa/regs/nepa/nepaeqia.htm; Section 102.

environmental impacts. However, pursuit of economic and environmental benefits need not be a zero-sum contest. Such a framework presents an unnecessary dichotomy. Adherence to it causes polarization and stalemate. The potential tensions between economic actions and environmental protection, when managed well, can transform into a creative tension that can lead to breakthrough solutions—the harmony among ecological, economic, and social systems envisioned in the National Environmental Policy Act. ….

… The conventional conception of productive harmony among the three systems is that each system occupies the corner of a triangle or some other trilogy analogy (Fig. 18.1). Productive harmony, or sustainability, is achieved at the centre of the triangle, which seldom occurs in practice. There are various paths and combinations to reach the harmonious centre, yet these paths often require trade-offs that can possibly (and often do) result in deadlock. Theoretically, productive harmony could be achieved at numerous points along these paths through compromise. But compromise is difficult to achieve, particularly where mistrust flourishes and, where decision making remains framed within the triangle of competing systems, there is no way to think outside the "box."

.Figure 18.1 is a representation of the traditional way of thinking of harmony among ecological systems, social systems, and economic systems. The dots with crosses represent a few of the infinite combinations within the circle among the three systems. This is a static model, with movement only possible within the bounds of the triangle, with sustainability essentially conceived as a series of different tradeoffs.

Another way to visualize productive harmony is to look at sustainability as a house (Fig. 18.2). In this conceptual model, Dynamic Productive Harmony, ecological systems are the foundation of the house and the heating, plumbing, electrical, and water systems (infrastructure) of the house; social systems are the

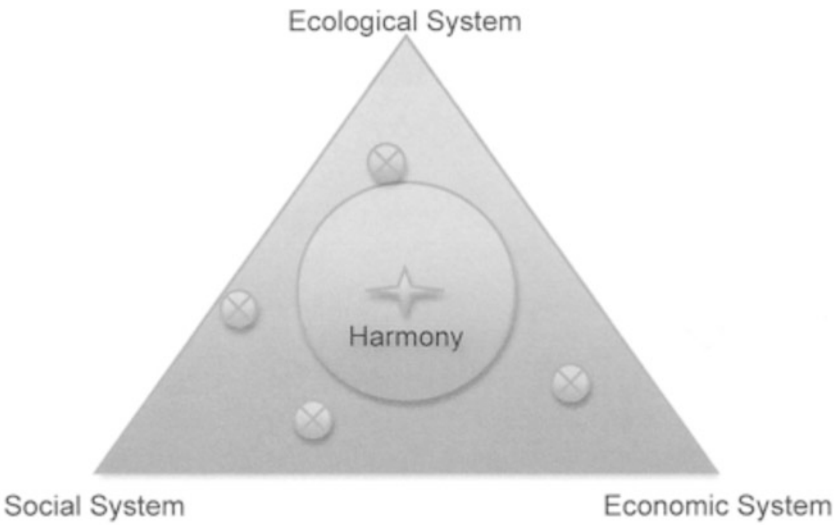

Fig. 18.1: Static productive harmony model.

Source: Karl et al. (2012), Springer.

living spaces (superstructure); and economic systems are the flows of goods and services such as food and fuel into the house to service the living spaces.[3] The engines (ecosystem services) for the infrastructure are housed in the basement, the structural foundation of the house. The environment is the overall framework of the house that shelters all. A deteriorating framework exposes everything within the house to the weather, with degradation or even, ruination resulting. Similarly, if the foundation is faulty or allowed to deteriorate, the superstructure and flow of goods and services will eventually deteriorate. Indeed, if the foundation has been neglected, a nicely painted house may provide a false sense of security. The house must be constantly maintained (a continuing process) to stay in good repair. Given a strong foundation, the house can be remodelled and enlarged—breaking out of the original "box." The architect (scientist/engineer), general contractor (policy maker/economic actors), subcontractors (natural resource managers/land use planners), and owner (citizen/community) together

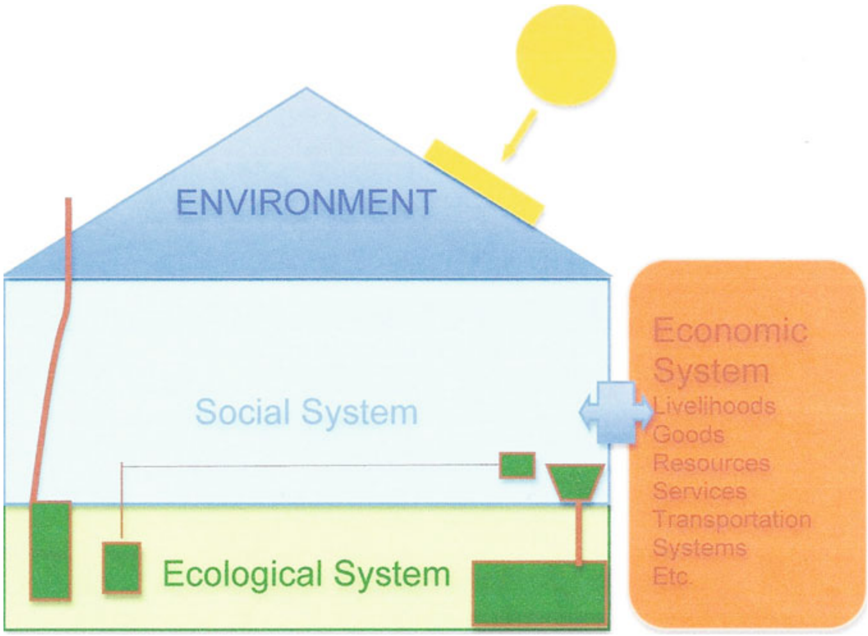

Fig. 18.2: Dynamic productive harmony model.
Source: Karl et al. (2012), Springer.

[3] Ecological systems are both foundations and infrastructure. Using ecosystems in an ecosystem services framework is often about replacing "gray" infrastructure—levees, wastewater treatment plants, etc.—with "green" infrastructure i.e. coastal sea marshes, wetlands, etc. Economic systems are not really just matters of "static" infrastructure i.e. bridges, roads, airports, etc. As systems, economies are highly dynamic contexts through which people exchange goods and services, allocate scarce resources, etc.

can create something new to fit the growing needs of the family (society/nation).[4]

Figure 18.2 is a conceptual model where the ecological system is the foundation and infrastructure for robust social systems and strong economic systems. Sustainability is not possible without a healthy ecosystem. This is a dynamic model reflecting the complex and complicated dynamics of coupled natural and human systems. The "house" needs constant upkeep and if the needs of the family (society) change it can be expanded and remodelled. It is a dynamic, process-oriented model. Sustainability is attainable as an outcome of continual decision-making processes.

The distinction between these conceptual models is critical as they represent two fundamentally different approaches to restoring and sustaining lands and setting environmental policy. Following the first conceptual model, policy tends to move toward compromise among the three systems by seeking the centre of the triangle, equating harmony as balance, but generally requiring tradeoffs among systems. Trade-offs are presumed at the expense of one system over another. In the second, policy focusses on sound construction and preservation of the foundation and the overall decision framework to sustain and preserve the superstructure, infrastructure and resource flows. Trade-offs may still be necessary in this model. However, value can be added by "remodelling" mitigating trade-offs. Others have described this intersection of environmental, economic and social values as achieving "triple bottom line" or win-win-win outcomes.

Fundamentally these models represent value dynamics at play; it is believed that decisions at their core are based on values. The set of values are essentially the same in both. However, individual values are weighted differently in the decision-making process under each conceptual model. For example, often under the Static Productive Harmony Model power and wealth seem to be the dominant values that influence the decision outcome; these are associated with politics and economics, respectively. Whereas in the Dynamic Productive Harmony Model, for instance, enlightenment and respect would be weighted more heavily in the decision-making process (ideally a participatory, collaborative process) and have a greater role in shaping the outcome. Note that no value judgement about the "goodness" or "badness" of different values is being made here. It is said that under the different conceptual models, the same values would be weighted differently and, consequently, the resultant outcome under each model given the same situation or issue could be different.

NEW INSTITUTIONS AND DECISION-MAKING PROCESSES

Will the existing institutional and governance arrangements give us the information we need to respond in a timely and effective manner to the risks

[4] Anyone who has built a house knows that there is constant negotiation and tension among the architect, contractor, subcontractors and owner. When tension is managed well, a superior house is built.

associated with climate change, and more generally, formulate policy guided by the Dynamic Productive Harmony Model? A recent 2009 National Research Council (NRC) report (2009) "Informing Decisions in a Changing Climate" states explicitly that our current institutions and decision-making processes are not adequate to deal with changing climate. The report asserts, "Decision makers…need new kinds of information, as well as new ways of thinking, new decision processes, and sometimes new institutions to function effectively in the context of ongoing climate change." It discusses aspects of these elements that include that scientists should address user's needs, problems should be tackled by interdisciplinary and multidisciplinary workforces (that include social scientists and engineers), institutions should cooperate across boundaries, enhanced interdisciplinary programmes for graduate students, opportunities for graduate students and researchers to engage in applied research, and develop ongoing forums for collaborative problem solving with citizens. Many of the concepts and applications described in the report have been described in earlier reports, books, and papers. And consider the language in NEPA. Does it not presage that above?

The following is excerpted from an internal Massachusetts Institute of Technology proposal (Susskind and Karl, 2007) to the U.S. Geological Survey:

> In the 1995 report, *Science, Policy, and the Coast—Improving Decisionmaking,* the National Research Council (NRC) stated
>
> > more effort is needed in the interpretation of fundamental science results for use in policymaking. Perhaps the most effective means of such integration is by … scientists who are engaged in both fundamental research and policy-relevant scientific activities, although such individuals are a rarity. They are able to extend the results of more applied, and often more descriptive, research by bringing in the understanding of processes resulting from fundamental research.
>
> Neal Lane in his 2006 *Science* editorial, "Alarm Bells Should Help Us Refocus," develops the NRC perspective further, stating that to meet the challenges of a rapidly changing world that we must engage "… the nation's top social scientists, including policy experts, to work in collaboration with scientists and engineers from many fields and diverse institutions on multidisciplinary research efforts that address large but well-defined national and global problems."
>
> To increase the number of scientists with these capabilities, the NRC has encouraged institutions of higher learning to "improve the cross-disciplinary training of natural and social scientists … and [to create] "programs of training for 'science translators'." Science translator training programs "should include exposure to the natural and social sciences, policy development and implementation, and conflict management and communication skills." Recent experiences with collaborative research illustrates that science can be a "community-building tool" that brings together diverse individuals and organizations, creating credibility and agreement around policy outcomes.
>
> To help ensure that good science is given its due in public policy making, appropriate forums and collaborative procedures, particularly at the local or

> community level, are needed to bring experts, public officials, environmental advocates, business interests, and the general public together to take account of scientific input, local knowledge, as well as the relevant values and interests of the stakeholders involved. This is widely recognized to be the case; the NRC report, *Science, Policy, and the Coast* suggests that "the scientific community could help improve the application of appropriate scientific information to … management problems by developing consensus-forming processes that support credible analyses for use to policymaking."
>
> More than a decade ago, in her Presidential Address to the Annual Meeting of the American Association for the Advancement of Science, Jane Lubchenco asserted, "Urgent and unprecedented environmental and social changes challenge scientists to define a new social contract." Under this contract, scientists are expected not only to do the best possible science but also to produce "something useful." She recognized that "new and unmet needs of society include more comprehensive information, understanding, and technologies for society to move toward a sustainable biosphere." She challenged scientists to meet these requirements. Lubchenco's challenge has been issued repeatedly over the past decade.

Why have not the recommendations made in the above reports and others been widely accepted and become routine practices? Researchers and practitioners should focus on answering this question to help foster substantive change.

Adaptation to Climate Change and Sustainability

There is great uncertainty regarding the risks associated with climate change, especially at local and regional (as opposed to continental and global) scales; hence, we must develop flexible and adaptive strategies to mitigate and manage their impacts.

Most reports on adaptation to climate change agree that adaptation is local. For example, "Because impacts of and vulnerabilities to climate change vary greatly across regions and sectors, adaptation decisions are fundamentally place-based…. Local governments should develop and implement climate change adaptation plans pursuant to national climate change adaptation strategy in consultation with the broad range of stakeholders in their communities" (National Research Council, 2010). A contradiction is seen in the above on two accounts.

First, if adaptation is place-based, why should local adaptation plans be developed and implemented "pursuant to national" policy? Consider what we know about the best practices of stakeholder participatory collaborative processes. Each place has different physical and cultural characteristics, which ought to be taken into account when developing and implementing a climate change adaptation strategy. National strategies cannot be that specific for place-based adaptation; they can, however, provide general guidelines. Consider three US coastal and port cities: New York City, Boston and Miami.

Let's consider only their physical location (and not cultural differences) and only one effect of climate change that of rising sea level and increasing storm surge. New York City and Boston are in the northeast and about 300 km apart. Yet, the impact of climate change will be different for each. With rising sea level, the lower elevations of both cities will be submerged and storm surges will cause frequent flooding of higher elevations. It is within the realm of possibility to build a sea wall completely around the island of Manhattan, which is the world's financial hub and the home to global organizations such as the United Nations, to protect these institutions and other highly valued infrastructure. Other adaptation strategies would likely be necessary for the other boroughs that might include abandonment and migration. Boston, on the other hand, is not an island. Although surge barriers might be constructed, it might not be possible to isolate and protect areas of Boston deemed critical and essential as it would Manhattan, one of five New York City boroughs. Engineering adaptations might not be effective for Miami at all. It is built on porous and permeable limestone and beach sand unlike New York City and Boston that, while portions of each are built on fill, are largely underlain by impermeable bedrock. For Miami adapting to climate change might require relocation of large parts of the city. The above scenarios are driven by economic and technical considerations. Recall, however, the language in NEPA to "…insure that presently unquantified environmental amenities and values may be given appropriate consideration in decisionmaking along with economic and technical considerations."

So, second, let's consider the role of a place's culture, environmental amenities, and values—components of the social system—with respect to developing and implementing climate change adaptation strategies. Even if the scientific evidence shows that an area that has been severely impacted will very likely be impacted as severely or worse again, people who live in the area may decide to rebuild and continue living there; this was the case in certain districts in New Orleans after Hurricane Katrina. The NRC report (2010) above states that adaptation plans should be developed by local government "in consultation with the broad range of stakeholders in their communities." What does this mean? Often "consultation" means that a plan has already been developed by a government agency and is presented to citizens for comment at a public meeting. The public usually has a limited time to comment at the meeting often as short as two minutes per person. In the United States, Daniels and Walker (2001) characterized this form of consultation as the "Three-'I' Model: inform, invite, and ignore," because usually the public comments are not substantively included in the final plan. A more participatory consultation process is that of establishing a citizen committee that functions as an advisory committee in the government decision-making process. This approach was used by Boston in developing its climate change adaptation plan (Karl et al., 2012). However, this approach is still not a true participatory approach where citizens make decisions as equal partners with government, which will be addressed in the subsection *New Process*.

In the discussion above, two end members—economic and social systems—of the Static Productive Harmony Model (Fig. 18.1) have been briefly touched upon. For the sake of discussion let us say that in the United States "trajectories and solutions of harmony" are generally contained in the lower one-third of the triangle between social and economic systems and weighted toward the economic end member. Yet, if we strive to live in harmony with nature, it would seem that "trajectories and solutions" of harmony need to move toward the top of the triangle and the ecological systems end member, because "…healthy ecosystems are the foundation for thriving communities and dynamic economies" (Karl et al., 2012). This has not been achievable in the four decades since enactment of NEPA even though many sustainability and environmental initiatives have encouraged it as well. Perhaps it is not even possible if environmental policy continues to be influenced conceptually by the static model and is formulated within current institutions and governance regimes.

Whereas it may not be possible or desirable to relocate many existing cities and communities as they are impacted by the effects of changing climate, as part of strategic planning to adapt to changing climate, for people that will be forced to migrate and relocate, it might be possible and desirable to plan and develop new communities based on the conceptual principles of the Dynamic Productive Harmony Model (Fig. 18.2). Ecovillages might serve as one model. Avelino and Kunze[2] state:

> The ecovillage movement emerged in the 1980s/90s in response to ecological and social challenges in modern societies. The definition that ecovillages most often use to describe themselves is "a human-scale, full-featured settlement, in which human activities are harmlessly integrated into the natural world, in a way that is supportive of healthy human development and can be successfully continued into the indefinite future" (Gilman, 1991). A more recent definition of ecovillages is: "private citizens' initiatives in which the communitarian impulse is of central importance, that are seeking to win back some measure of control over community resources, that have strong shared values and that act as centres of research, demonstration and (in most cases) training" (Dawson, 2006).

Currently a type of ecovillage, called Khajuraho Eco Business City, is being planned in the Indian state of Madhya Pradesh. "The purpose of the Khajuraho Eco Business City is to be the motor for the multicultural and sustainable social, economic and ecological development of the city and the (regional) community" (de Rooij et al.). This experiment is a concept of co-learning between East and West and North and South and the outcome will not be known for several years. Ecocities may provide an alternative approach to sustainability. Planning for ecocities would require collaboration among a range of stakeholders that include citizens, planners, scientists and government officials.

New Process

There is a distinction between "consultation" and "collaboration" when considering community and citizen engagement in a process. Yet, the two are often conflated in usage. Similarly, there is a distinction between "involvement" and "participation." These also are often used interchangeably. Consultation does not imply that the recommendations of those consulted will be acted upon. Involvement does not necessarily mean full and equal participation. Collaboration and participation, on the other hand, imply a higher, more equal, and more active level of engagement among actors.

The consultative processes (public hearing and advisory committee) described above are two of a spectrum of participation processes. What is meant by an active, equal, and inclusive community participation process is a consensus-seeking decision process that includes a broad range of stakeholders each of whom has an equal role (Susskind et al., 1999). To be effective so that the decisions of the group are implemented, those agencies authorized by statue and law to make and implement the decision must be represented and meet regularly with the group. In this process, it is important to understand that the group does not usurp the authority of the decision-making agency or agencies. In a well-designed process, the agency agrees to implement the consensus decision of the group instead of making a unilateral decision. This is a critical distinction that is often misunderstood by agencies. There are well-defined best practices for developing and managing a consensus seeking process (Susskind et al., 1999). One critical factor is that the actors around the table must be self-selecting. This is done through an impartial stakeholder assessment. The stakeholder assessment will also determine if a collaborative process is even appropriate. The selection of a representative stakeholder group is not a trivial matter and there are a number of complicating factors that must be taken into account. In large metropolitan complexes, for example, one complicating factor is cultural differences between neighbourhoods (Karl et al., 2012) as well as social and environmental justice concerns.

Indeed, a consensus-seeking process seems to be among the new decision-making processes called for by the NRC (2009) and others. The report describes a decision support process that combines "participatory deliberation with expert analysis in an iterative process." In effect they have described a consensus-seeking process with a joint fact finding element (Ehrmann and Stinson, 1999; Andrews, 2002; Karl et al., 2007). This is not a new process, yet it is not tried and implemented as often as it could be. Many people are not aware of it and to them it is new.

New Information

Among the new information that the NRC report (2009) urges is developing "…the science of climate change *response*, as a complement to the science of climate change *processes*. … Also, needed are contributions from a wide range of the disciplines including behavioral and social science disciplines….” Unless “…decision support processes … take priority over information products…” the products are unlikely to be used by decision makers. This is in accord with the discussion in the previous subsection.

As documented herein, this type of information and research is not new. That it continues to be the subject of new reports underscores the fact that multi-disciplinary research that includes the social and behavioural sciences is rare, and, rarer yet is the use of products of this research in collaborative or other decision-making processes.

Equally as rare is the integration of local, indigenous, or experiential knowledge with scientific knowledge. Collaborative, multidisciplinary and interdisciplinary processes should take into account these forms of information.

New Thinking

It should be apparent that to tackle the wicked problem of adapting to changing climate, a more holistic way of thinking is necessary. In the past very few graduate schools trained scientists to think broadly across disciplines. Scientists, for the most part, continue to be trained to focus narrowly on a discipline. To do so is necessary to make fundamental advances in a particular discipline or field. It is not being suggested abandoning reductionist science. It is suggested that a new class of professional be trained to think holistically and to learn how to synthesize diverse intelligence and information (Susskind and Karl, 2007). These professionals would have a strong grounding in a discipline or field, but would engage in an integrated, multi-disciplinary course of study.

There are many barriers to conducting integrated, multi-disciplinary research and training students to think holistically. Foremost among these is the strong disciplinary nature of academic departments. Others include the reward structure for research scientists and the tenure system for academic faculty (both of which emphasize achieving excellence in a discipline or field), the paucity of funding for interdisciplinary research, and the under-appreciation for such skills among decision makers.

New Institutions

Overcoming the barriers to support new information and new thinking will require bridging gaps and developing new institutions. Holling and Chambers (1973) stated this almost forty years ago: “Wherever we look there are gaps – gaps between methods, disciplines and institutions.”

A core question and area of action research: What will the new institutions look like to bridge these gaps?

As stated earlier, my premise is that collective action across and that integrates all scales and levels of governance and society is needed to address the impacts of climate change to achieve sustainable societies and ecosystems. Therefore, the new institutions need to function cooperatively and support collaborative process approaches.

Because developing the professionals to staff these institutions is critical, universities and colleges should establish programmes to train students in interdisciplinary (Clark et al., 2011), transdisciplinary (Klein et al., 2001), and collaborative processes (Susskind et al., 1999) approaches so that they build the capacity to think critically, holistically, and collectively to solve problems. These programmes must have students working in collaborative teams on a problem (Susskind and Karl, 2009). The nature of the problem will shape the questions to be asked, the intelligence to be gathered, who will gather it, and what approach and process will be used. Universities and colleges that have such a programme should make it widely known and take care to distinguish it from typical environment studies programmes (Walton, 2007). The U.S. Geological Survey and the Massachusetts Institute of Technology developed such a programme—MIT-USGS Science Impact Collaborative (MUSIC)—housed in MIT's Department of Urban Studies and Planning.[5] The administrators of these programmes might reflect on whether the course content and structure is in accord with that recommended by the NRC for "science translators" and strategies for "integrating knowledge, education, and actions for a better world" as articulated by Clark et al. (2011). Course curricula should also evolve to meet the continual challenges brought about by emerging properties of coupled natural and human systems. In this regard, academic faculty should interact more with practitioners and citizens. Universities and colleges should be strongly integrated into their communities.

Owing to length restraints, it is not possible to discuss thoroughly the various forms of new institutions that are emerging during a period of transition and evolution in responding to the interactions between human and natural systems in a changing climate. For a synopsis and pertinent references, the reader is referred to Scarlett (2012) and Karl et al. (2012) and the social-ecological, political science, and social science literature.

What these new institutions and governance regimes have in common is a structure and operating principle based on coordination, cooperation and collaboration among institutional entities and individual actors. These institutional arrangements could include public-private partnerships, commissions consisting of several government agencies that cooperate to act as a single entity, and local stewardship groups that consist of diverse stakeholders using a consensus-seeking decision process. Also, these institutions ought to give more weight to values such as enlightenment, respect and well-being to balance better the often dominant values of power and wealth in typical decision-making processes.

---

[5] http://web.mit.edu/dusp/epp/music/; USGS ended its participation in the programme in 2010. MUSIC is continued by MIT as Science Impact Collaborative.

Kania and Cramer (2011) describe a promising form of institutional arrangement, called collective impact. “Shifting from isolated impact to collective impact is not merely a matter of encouraging more collaboration or public-private partnerships. It requires a systematic approach to social impact that focusses on the relationship between organizations and the progress toward shared objectives. And it requires the *creation of a new set* (emphasis added) of nonprofit management organizations that have the skills and resources to assemble and coordinate the specific elements necessary for collective action to succeed.”

We are in a period of transition globally and societies have the opportunity to shape the institutions that will enable more effective and durable decisions with respect to the environment and adaptation to climate change.

SCALE

The processes and institutions described above will need to take into account and operate over different spatial and temporal scales. The processes of climate change have global impacts and operate over long (hundreds of years to geologic) time scales. Yet, adaptation to climate change is local and policy is formulated and planning done on short time scales (months to years). The new institutions will need to reconcile these differences in scale between natural processes and decision-making processes.

Do we have the time to develop these institutions? Climate is changing rapidly as manifested by rising global temperature, rising global sea level, and increasing local extreme weather events that include flooding and drought. Not only will it take time to develop institutions that function collaboratively, it will take time *to build the trust* among individuals and between the institutions so that they can function at all. Trust takes years to build among those that have different points of view and it is a constant challenge to keep it. Yet, once developed, often impasses are broken and new ideas sprout that enable creative solutions to what before were unsolvable problems.

For the most part societies on a global scale have been sufficiently resilient to absorb the impacts of natural disturbances and human activity. However, as Holling and Chambers (1973) point out “resilience is not infinite” and “…three hundred years of ignoring these limits has left us with a baggage of approaches and solutions that are only admirable as instruments for resolving fragments of problems.”

SUMMARY AND CONCLUSIONS

Environmental crises, exacerbated by climate change, are occurring worldwide with greater frequency and more intensity. International accords and national plans outlining strategies to mitigate the effects of and adapt to changing climate have been developed over the past decade. These are insufficient and have had little effect in meeting the challenges of a rapidly changing climate. Climate adaptation is local and local planning is necessary to implement the recommendations of the international and national plans. Current institutions, legal frameworks, and decision processes were developed during a stable climate. These may not be adequate to deal with changing climate, which is now the new normal. New institutions will need to reconcile the difference in scale (spatial and temporal) between natural processes of climate change and governance processes.

Climate change is not a scientific problem—it is a political and social problem. Human behaviour and values are essential elements in developing policies and plans for adapting to climate change. Consequently, societies need new institutions and decision processes that integrate scientific, political, and social information to formulate more durable and equitable climate change policies and environmental policies in general. Whereas lawmakers like to claim that environmental decisions are based on the best science, with rare exception[6] this assertion is largely a myth (Karl et al., 2007). Decisions are based on values. Often lawmakers cannot agree on the science and it becomes a source of conflict and consequent inaction. And, even when there is agreement about the science, political, economic and social factors often take precedence in decisions that get made.

Because there is a diversity of worldviews and values held by individuals and societies, herein it is suggested that processes that enable collective action should be built into new institutions. Any form of coordination, cooperation and collaboration takes longer and is more difficult than unilateral decision-making, regulatory and law-making processes. And, in fact, it may not be appropriate for all situations. However, there are well known procedures to determine if some form of collaborative process is possible and best practices for managing such processes.

Conflict can be a creative force when managed well and trust is built; when not managed well, particularly in a context of mistrust, it is destructive. Societies need to harness, and concentrate through new institutions, the wisdom and power represented by a diverse citizenry to tackle the wicked problem of climate change.

ACKNOWLEDGEMENTS

Concepts discussed herein were refined over the course of numerous conversations with colleagues and friends Charles Curtin (Antioch University New England), Mike Flaxman (MIT and Geoadaptive), Paul Kirshen (Battelle Institute), Lynn Scarlett (Resources for the Future and former Deputy Secretary U.S. Department of the Interior), and Juan Carlos Vargas-Moreno (Geoadaptive).

[6] One exception was the decision by the U.S. Department of the Interior to list the polar bear as a threatened species.

REFERENCES

Andrews, C.J. (2002). Humble analysis: The practice of joint fact finding. Praeger, London and Westport, CT.

Avelino, F. and Kunze, I. (In press). Ecovillages: Intentional communities on sustainable living. Beliefs and Values: Understanding the Global Implications of Human Nature. *In:* de Rooij, A. (ed.), Global knowledge cities: Twins of communities, one rich one poor, co-learning on practices and theories of connectivity and multiplicity. International Beliefs and Values Institute. http://www.springerpub.com/product/19420617#.TlZaKXNq1U0.

Brown, V.A., Harris, J.A. and Russell, J.Y. (2010). Tackling wicked problems through the interdisciplinary imagination. Earthscan, Washington, DC/London.

Clark, S.G., Rutherford, M.B., Auer, M., Cherney, D.N., Wallace, R.L., Mattson, D.J., Clark, D.A., Foote, L., Krogman, N., Wilshusen, P. and Steelman, T. (2011a). College and university environmental programs as a policy problem (Part 1): Integrating knowledge, education, and action for a better world? *Environmental Management*, **47:** 701-715.

Clark, S.G., Rutherford, M.B., Auer, M., Cherney, D.N., Wallace, R.L., Mattson, D.J., Clark, D.A., Foote, L., Krogman, N., Wilshusen, P. and Steelman, T. (2011b). College and university environmental programs as a policy problem (Part 2): Strategies for improvement. *Environmental Management*, **47:** 716-726.

Clark, S.G., Steen-Adams, M.M., Pfirman, S. and Wallace, R.L. (2011a). Professional development of interdisciplinary environmental scholars. *J. Environ. Stud. Sci.,* **6:** 99-113.

Curtin, Charles (2005). Complexity, conservation, and culture in Mexico/U.S. Borderlands. Natural Resources as Community Assets: Lessons from Two Continents. Chapter 9, pp. 237-258.

Daniels, S.E. and Walker, G.B. (2001). Working through environmental conflict. Praeger, Westport, Connecticut and London.

Dawson, Jonathan (2007). Ecovillages achieve lowest-ever Ecological Footprint results. *Global Ecovillage Network Europe News* (winter 2006/07).

de Rooij, A., Matta, C., van Rooizen, M. Karl, H.A. and Mishra, J. (2011). The Global Knowledge Cities Concept: Local-Global Solution to Social, Economic and Ecological Crises. *Beliefs and Values,* **3(1):** 147-162.

Ehrmann, J.R. and Stinson, B.L. (1999). Joint fact-finding and the use of technical experts. *In:* L. Susskind, S. McKearnan and Thomas-Larmer, J. (eds), The Consensus Building Handbook. Sage Publications, Thousand Oaks.

Gilman, R. (1991). The Ecovillage Challenge. *In:* In Context, No.1/1991.

Holling, C.S. and Chambers, A.D. (1973). Resource science: The nurture of an infant. *Bioscience*, **23:** 13-20.

http://www.context.org/ICLIB/IC29/Gilman1.htm 03.01.09

Kania, J. and Kramer, M. (2011). Collective impact. *Stanford Social Innovation Review*, Winter **2011:** 36-41.

Karl, H.A., Curtin, C., Scarlett, L. and Hopkins, W. (2011). Adapting to climate change—A wicked problem. *In:* I. Linkov and T.S. Bridges (eds), Climate: global change and local adaptation, NATO Science for Peace and Security Series C: Environmental Security, Springer Science+Business Media, B.V.

Karl, H.A., Scarlett, L., Vargas-Moreno, J.C. and Flaxman, M. (2012). Restoring Lands - Coordinating Science, Politics and Action: Complexities of Climate and Governance. Springer Science + Business Media, Dordrecht, The Netherlands.

Karl, H.A., Scarlett, P.L., Kirshen, P., Dell, R., Ibrahim, H., Kuhl, L., Mosher, T., Navarro, B., Rising, M. and Towery, N. (2012). Adapting to climate change: exploring the role of the neighborhood. *In:* Karl, H.A., Scarlett, L., Vargas-Moreno, J.C. and Flaxman, M. (eds). Springer Science + Business Media, Dordrecht, The Netherlands.

Karl, H.A., Susskind, L.E. and Wallace, K.H. (2007). A dialogue, not a diatribe—Effective integration of science and policy through joint fact finding. *Environment*, **49:** 20-34.

Klein, Julia Thomas, Grossenbacher-Mansuy, Walter, Haberti, Rudof, Scholz, Bill, Alain, Scholz, Roland W. and Welti, Mythra (eds) (2001). Transdisciplinarity—Joint problem solving among science, technology, and society: An effective way for managing complexity. Birhhauser Verlag, Basel, Boston, Berlin.

Lane, N. (2006). Alarm bells should help us refocus. *Science,* **312:** 1847.

Lubchenco, J. (1998). Entering the century of the environment: A new social contract for science. *Science*, **299:** 491-497.

National Research Council (2010). Adapting to the impacts of climate change. The National Academies Press, Washington, D.C.

National Research Council (2009). Informing decisions in a changing climate. The National Academies Press, Washington, D.C.

National Research Council (1995). Science, policy, and the coast: Improving decisionmaking. The National Academies Press, Washington, D.C.

Rittel, H. and Weber, M. (1973). Dilemmas in a general theory of planning. *Policy Sci*., **4:** 155-169.

Scarlett, L. (2012). Transcending boundaries: The emergence of conservation networks. *In:* Karl, H.A., Scarlett, L., Vargas-Moreno, J.C. and Flaxman, M. (eds). Springer Science + Business Media, Dordrecht, The Netherlands.

Susskind, L. and Karl, H. (2007). Proposal: request for multi-year support for the MIT-USGS Science Impact Collaborative (MUSIC). A field-based internship program to train science impact coordinators. Working Paper Massachusetts Institute of Technology, submitted to U.S. Geological Survey.

Susskind, L. and Karl, H. (2009). The Best of MUSIC. MIT Working Paper, Environmental Policy and Planning Group, MIT-USGS Science Impact Collaborative (MUSIC), http://web.mit.edu/dusp/epp/music/pdf/Best-of-Music-2009.pdf; http://web.mit.edu/dusp/epp/music/

Susskind, L., McKearnan, S. and Thomas-Larmer, J. (eds) (1999). The Consensus Building Handbook. Sage Publications, Thousand Oaks.

Walton, Abigail Abrash (2007). Conservation through different lenses: Reflection, responsibility, and the politics of participation in conservation advocacy. *Environmental Management*, **45:** 19-25.

Index

^{13}C 79, 80
^{18}O 79, 80, 82, 83, 84
2A12 33, 34
3B42 V6 33, 35
Acclimatization 141, 245
Adaptation 141, 148, 151
Adaptation strategies 267, 274
Agro ecological region 210
Air-sea level fluxes 53, 55, 58, 59, 62
Alappuzha 219
Algal overgrowth 124
Ambient 142
Amino acids 155
AMS (Accelerator Mass Spectrometry) 23
AMSI 35
Anatomical 141, 143, 144, 148, 150, 151
Anthropogenic 179, 186
Anthropogenic activities 115, 121, 123
Anthropogenic environments 209
Anticyclonal atmosphereic circulation 55
Aquaculture 186
Arabian Gulf 114
Arabian Sea 217
Archaeancrystallines 193
Artificial reefs 108
ASCII 33
Ashtamudi 194, 219, 235, 236
Ashtamudi Flood Tide Delta (AFTD) 204
Ashtamudi lagoon 193, 204, 205
Assimilation 146
Atmosphere tele connection 38
Atmosphere 31, 32, 40, 43
Atmospheric precipitation 214, 215
Augur rig 219
Automated area computation 117
AVHRR 54, 58, 241
AWiFS 117
Ayiramthengu 219, 221, 235

Bacterial count 137
Benthic 154
Benthic cyanobacteria 137
Biochemical 154, 155, 157, 158, 159
Biological and ecological parameters 79
Biomarkers 218
Biomass 155, 181
Birbal Sahni Institute of Palaeobotany 195
Boreholes 195, 200, 201
Broodstock development 254, 262
Buoys 54

C3 Species 142
C4 Species 142
Calcified sand 211
Carapace 173
Carbohydrate 155, 157, 158, 159, 160, 161, 162
Carbon dioxide exchange 139

J. Sundaresan et al. (eds.), *Climate Change and Island and Coastal Vulnerability*,
DOI 10.1007/978-94-007-6016-5, © 2013 Capital Publishing Company

Carbonate 23
Carcinoscorpius rotundicauda 128
Castanea sativa 141
Center for Tropical Marine Ecology (ZMT) 195
Centre for Advance Studies in Marine Biology 261
Chlorophyll 184, 185, 187
Chlorophyll-*a* 130
Chlorophyll-*b* 132
Clean Air Act 268
Clean Water Act 268
Climate change 4, 32, 38, 39, 40, 101, 102, 104-106, 114, 141, 142, 151, 164, 217, 218, 266-268, 273-275, 277-280
Climate-relevant gases 126
Climatology 54, 64, 69
Cloud formation 32
Cloud liquid water 31, 32, 33, 34, 40, 43, 50
Cloud models 33
Cloud physics 32
CMAP 6, 7, 9, 10
COADS 54
Coastal aquifer 210
Coastal dunes 181
Coastal ecosystem 217
Coastal groundwater 209
Coastal lowlands 191, 192
Collective impact 279
Colonization 124
Community participation 276
Community planning 267
Conceptual model 269, 271
Consultative processes 276
Continental shelf 166
Convective rain 33, 39, 43, 45, 49
Coral bleaching 32, 239, 240, 243
Coral farming 107
Coral Park programme 107
Coral reef ecosystem 75, 106, 107, 114, 239, 246, 247, 253, 254
Creeks 181
Cross-dating 78
CRU 10, 11, 12, 13, 15
Cuticle 148, 149
Cyclones 32, 38
Dead zones 104
Debris 156, 193
Diatom 130
Dinoflagellates 201, 221, 233, 234
Disdrometer 33
Dissolved nutrient concentration 130
Dissolved organic matter 184
Dissolved oxygen 136, 255, 260
Domestic waste 155
Drought 142
Dug wells 211
Dynamic Productive Harmony Model 269, 271

Ecological systems 268-270
Ecosystem 114
Ecosystem restoration 268
Ecosystem services 270
Ecovillage 275
EDTA 23
Effluents 155
Egg capsules 258
Egiceras corniculatum 167
Electrical conductivity 211, 212, 214
El-Nino 38
El Nino southern oscillation, ENSO 79, 240
Emissivity 31
Energetic monsoon 60
Enhancement algorithms 118
Enriched 141, 142
Environmental amenities 268
Environmental policies 268
Epidermal 142, 143, 145, 148
Epiphytes 156
ERSST 54, 63, 68, 69, 72
Estuaries 179
Estuarine 166, 181, 182
Eukaryotic 127
Excoecaria agallocha 167

False colour composites 118
FFT 63, 68
Foraminifera 221, 233, 234
Fresh water 156
Frond 143
f-test 34
Fucoxanthin 130

GCM 241
Geochronology 217, 236
Geolocation 34
Geomorphology 217, 218
Glacial-interglacial cycle 21, 25, 26
Global Circulation Model (GCM) 4, 6, 7, 8, 9, 15, 16
Global circulation 31
Global warming 40
Glycine max 141
GNIP 82
Grassroot development 267
Gravity sedimentation 128
Greenhouse gases 4
Ground truth 35
Guard cells 146
Gulf of Mexico 103

HadCM3 241, 243
HadRM3P 5, 6, 10-13, 15
Harbour 154
Hatchery production 253
HDF 33
Herbarium 157
High-altitude doppler ardar 33
Hillocks 193
Holocene 22-27, 191-193, 201, 203-206, 217, 221, 233-236
Holocene climate optimum (HCO) 235
Horizontal resolution 54
Hovmoller graph 242, 243
Hurricanes 32, 38
Hybrids 145, 147, 148, 149, 151
Hydrodynamic 219
Hydrograph 215
Hydrography 55
Hypersaline 175
Hypodermis cell 150

Ice cores 78
ICOADS 54, 62
IMD 33, 35, 38, 40, 50
India 217
Indian Sundarbans 179
Indian peninsular 53
International accords 267
Intertidal settings 175
Intertidal zones 155, 156
IPCC 241
IRMS 89, 90
Irrigation 143
ISMR 95
Isotopic record 79

JOFURO 55, 58

Kallada 193, 194, 200, 201, 203, 204, 206, 219, 221, 234, 236
Kallada Bay Head Delta 201, 204-206
Kannur 218
Kasargod 218
Kayamkulam 219, 235
Kerala 218, 234, 235
Kidapparam 201
Kollam 193
Kothapuram 200
Kozhikode 218
Kumarakam 219, 221, 235

Lacustrine 222
Lagoon 168, 170, 173
Lakshadweep Sea 218, 240, 242, 247
Land-ocean boundary 139
La-Nino 38
Larval hatching 257
Larval rearing 257, 259
Larviculture 262
Latent heat 31, 32-34, 43, 45, 49, 50
Lignin 148
Lipid 155, 157-162
LISS III 117
Lithologs 219
Little Ice Age 94
Long wave radiation 55

Macro algae 123
Malappuram 218
Mangrove 32, 106-108, 127, 156, 180, 181, 217, 218, 221, 234-236
Marine Science 187
Mass spectrometer 195
MBrendel method 88
Mesophyll cells 142
Metaxylem 148, 149, 150
Meterological 31
Microfossils 166, 195

Micronutrients 104
Microwave imager (TMI) 32, 34
Modulated 3
Morphotypes 181
Muddy creaks 155

NASA 54, 241
National Environmental Policy Act 268, 269, 272
National policies 267
Natural catastrophes 125
NCEP 54, 55, 58
NE monsoon 84
Nektonic 154
Neogene 218, 234, 236
NESDIS 241
Nitrate 128
Nitrogen-fixing cyanobacteria 104
NOAA 35, 54, 58, 241
Northeasterly 55

Ocean dynamics 53, 55, 61
Offshore 60
OI 54
Oil refinery 155
Oil spill 154, 155, 163, 164
Organic carbon 195, 200, 201
Ornamental aquaculture 253
Ornamental fishery 253, 262
Ornamental organism 32
Ostracods 166-168, 170, 173, 175
Oxygenated environment 175

Palaeoclimate 166, 191-193, 219
Palaeoecology 218
Palaeo-environmental potential 191
Paleomonsoon 22, 26, 27
Paleoproductivity 22, 27
Palisade parenchyma 141
Palynological 195, 201, 206
Palynology/palynological 217-221
Palynomorphs 219, 234
Panavally 219, 221, 235
Pattanam-Kodungallur 192
Pentadal oscillations 64
Perceptible water 31, 32, 34, 40, 43, 45, 49, 50
Perennial species 142
Peridinin 130
pH 133, 136
Phosphate 128
Photomicrographs 219
Photoperiod 256, 257, 260
Photosynthetic rate 144
Physicochemical parameters 127
Physiological 141, 148
Phytoplankton 104, 126, 179, 181
Phytoplankton diversity 127
Pico-eukaryotes 139
Picophytoplankton 137
Pigment analysis 130
Pixel 33
Planktonic 154
Pleistocene 221, 234-236
Podocopida 168
Pollen 218-221, 233, 234, 236
Pollution 155
Polyhaline 135
Pre cambrian metamorphic rock 211
Precipitation 3, 13
PRECIS 4, 5, 9-13, 15
Predation 173
Productive harmony 268, 269
Protein 155, 157-162
Public-private partnership 278
Pylotypes 138
Pyritisation 173

Quarternary aquifer 215
Quaternary sediments 193, 194, 211
Quilon 193

Radar-AMeDAS 33
Radiation budget 31
Radiocarbon (C^{14}) 195, 200, 204, 206, 219, 220
Reflectance 184
Relative humidity 143
Resilience 246
Resolution 143
Resourcesat-1 115
Rhizopora mucronato 167

Safranin 144
Salinity 133, 166, 211, 255
Salt water intrusion 32
Sand flats 181

Sandstone 211
Sasthamkotta 195
Satellite sensed 53, 54, 58
Saturated zone 211
Sea level rise 32, 274
Sea levels 106
Sea surface temperature (SST) 32, 53-55, 59, 60, 62-64, 67, 69, 70, 240-243, 245, 247
Sea water 156
Sea water intrusion 211
Seaward sloping 210
Seaweeds 154-159, 163
Sediment deposition 123
Seedlings 142-151
Shortwave radiation 55
Shrimp culture 187
Silicate 128
Skin temperature 241
SOC 54, 55, 58
Socio-economic condition 32
Soil erosion 32
Solar radiation 32
South Kerala Sedimentary Basin (SKSB) 191, 192
Southeast trade wind 55
Southeasterly 55
Southwest monsoon 53, 218
Spawning 258
Spectophotometric 182
Spectrometer 168, 182
Speleothems 78
Sporopollenin 218
SRES A2 241, 243, 245, 246
SSMI 35
SST anomalies 53, 69
Stakeholder assessment 276
Static penetration test (SPT) 219
Static Productive harmony Model 271, 272
Stomatal 141-148, 151
Stratiform rain 33, 39, 43, 45, 49
Stratigraphy 219
Stresses 141
Subfossil 220
Subsidiary cells 146
Subtropical Indian ocean 22
Suess effect 80
Sundarban mangrove 181, 186, 187
Sunderbans 127, 218
Superstructure 270
Surface flag 33
Surface water temperature 133
Sustainability 271, 273
Sustainable aquaculture 254
South west (SW) monsoon 84

Technology transfer 260
Temporal dynamics 124
Temporal gradient 138
Terrigenous 204
Tertiary sediments 193
Thermal stress 243, 246
Tidal amplitude 182
Tidal saline water 213
Tidal surges 182
Tolerance 142
Topographic relief 210
Total dissolved salts 211
Tree-rings 78
Trivandrum-Shornur 219
TRMM 32-35, 43
Tropical isotope dendrochronology 92
Tsunami 106, 175, 213
Turbulent mixing 60

UKMO 241
Underwater biological filters 254
Upwelling 60
Urbanisation 186

Vembanad 219, 235
Vermicompost 143
VSMOW 90

Warkalli 193, 218, 235, 236
Warkalli formation 193
Water potential 148
Water quality 108
Water vapour 31
Weather system 31
Western ghats 94

Xylem 148

Zooxanthellae 239